STUDIES ON IDENTIFICATION OF ANIMAL SPECIES BASED ON MORPHOLOGY, FT-IR SPECTROSCOPY AND MOLECULAR METHODS

SHAMBHULINGAPPA, Y. BADDI.

DEPARTMENT OF VETERINARY ANATOMY AND HISTOLOGY
VETERINARY COLLEGE, BANGALORE
KARNATAKA VETERINARY, ANIMAL AND FISHERIES
SCIENCES UNIVERSITY, BIDAR

APRIL, 2014

STUDIES ON IDENTIFICATION OF ANIMAL SPECIES BASED ON MORPHOLOGY, FT-IR SPECTROSCOPY AND MOLECULAR METHODS

Thesis submitted to the

KARNATAKA VETERINARY, ANIMAL AND FISHERIES SCIENCES UNIVERSITY, BIDAR

in partial fulfilment of the requirements
for the award of the degree of

DOCTOR OF PHILOSOPHY

in

VETERINARY ANATOMY AND HISTOLOGY

By

SHAMBHULINGAPPA, Y. BADDI.

DEPARTMENT OF VETERINARY ANATOMY AND HISTOLOGY
VETERINARY COLLEGE, BANGALORE
KARNATAKA VETERINARY, ANIMAL AND FISHERIES SCIENCES UNIVERSITY, BIDAR

APRIL, 2014

KARNATAKA VETERINARY, ANIMAL AND FISHERIES SCIENCES UNIVERSITY, BIDAR

DEPARTMENT OF VETERINARY ANATOMY AND HISTOLOGY
VETERINARY COLLEGE, BANGALORE

CERTIFICATE

This is to certify that the thesis entitled **"STUDIES ON IDENTIFICATION OF ANIMAL SPECIES BASED ON MORPHOLOGY, FT-IR SPECTROSCOPY AND MOLECULAR METHODS"** submitted by **Mr. SHAMBHULINGAPPA, Y. BADDI, I.D. No. DVHK 1122** in partial fulfilment of the requirements for the award of **DOCTOR OF PHILOSOPHY** in **VETERINARY ANATOMY AND HISTOLOGY** of the Karnataka Veterinary, Animal and Fisheries Sciences University, Bidar is a record of bonafide research work carried out by him during the period of his study in this University under my guidance and supervision, and the thesis has not previously formed the basis for the award of any degree, diploma, associate ship, fellowship or other similar titles.

Bangalore,
APRIL, 2014

Dr. R.V. Prasad
Major Advisor

Approved by:

Chairman : _____
(Dr. R.V. Prasad)

Nominated External Examiner : _____
(Dr. P.L. Dhande)

Members : 1. _____
(Dr. K.V. Jamuna)

2. _____
(Dr. M. Narayana Bhat)

3. _____
(Dr. C. S. Nagaraja)

4. _____
(Dr. H.D. Narayana swamy)

5. _____
(Dr. Jagadeesh. S.Sanganal)

"Extinction is forever,

endangered means, we still have time

but

don't make them history"

- Alesander & Amaya Rocks

Dedicated to

My father shri. Yallappa Baddi

My mother Late. Smt. Shankramma

&

all wild animals those extinct and extanct

ACKNOWLEDGEMENT

I sincerely express my profound sense of gratitude and indebtedness to the Chairman of my Advisory Committee ***Dr. R.V. Prasad,*** *Dean, Shivamogga Veterinary College, for his excellent supervision, inspiring guidance, valuable suggestions, timely advice, constant encouragement, immense patience and affectionate dealing throughout the period of my research.*

I wish to place on record my sincere gratitude and indebtedness to ***Dr. K.V. Jamuna****, Professor & Head Department of Anatomy, Veterinary College, Hebbal, Bangalore, member of my Advisory Committee for her invaluable guidance, constructive criticism, concrete suggestions, co-operation and magnanimity without which this work would not have been undertaken.*

I am grateful to ***Dr. M. Narayana Bhat****. Professor and Head, Department of TVCC, Hassan Veterinary College, for his enthusiasm in filling me up with critical suggestions and technical guidance as a Member of my Advisory Committee.*

I am deeply indebted to ***Dr. C. S. Nagaraja****, Principal Scientist, AICRP Veterinary College, Bangalore, member of Advisory Committee for the help, advice and encouragement I constantly received during the course of study.*

I would like to express my heart-felt and profound gratitude to member of my Advisory Committee ***Dr. H.D. Narayanswamy****, Professor, Department of Pathology, for permitting me to work in his laboratory for PCR related work. I also thank* ***Dr. Krishnaveni, N., Ms. Deepa, Ms. Ghanavi and Ms. Shruthi & Mr. Pracheth (IISc)*** *and all the staff members of the pathology lab for the cooperation rendered.*

I am grateful to ***Dr. Jagadeesh. S. Sanganal****, Associate Professor and Head, Department of Pharmacology and Toxicology, for his enthusiasm in filling me up with critical suggestions and technical guidance as a Member of my Advisory Committee.*

A special mention of thanks to ***Dr. Ramkrishna, V.*** *and* ***Dr. Thandavamurthy****, contract teachers and* ***Mr. Narayana Gowda****, Rtrd. Sr.Lab technician, for their help in technical guidance and valuable suggestions.*

I express my heartfelt thanks to ***Mr. Avinash Bhat*** *lab technician &* ***Dr. Venkanna****, Department of Veterinary Pharmacology, Veterinary College, Bangalore, for their valuable suggestions for FTIR Spectroscopy during the study.*

I consider it would be incomplete without extending my hearty thanks to ***Dr. S. M. Byre Gowda,*** *Joint Director,* ***Dr. Purushotham, K, M (SRF) and Mr. Naveen (JRF), Ms. Devamma, Ms. Kumuda,*** *IAH and VB, Hebbal, for their help in molecular research work.*

I owe my sincere thanks to ***Principal Chief Conservator of Forests (wildlife),*** *and wild life warden, Karnataka, Bangalore, for their permission to collect wild animal samples from various National Parks and Zoos of Karnataka.*

I wish to express my special thanks to ***Department of Animal husbandry & Veterinary Services, Govt. of Karnataka*** *for giving me permission for PhD study.*

I express my whole hearted thanks to ***Dr. Chettiyappa, Dr. Arun Sha (SOS), Dr. Sujay, Dr. Manjunath, Dr. Hemalatha, Ms. Nandini*** *& staff of Bhannerghatta National Park, Bangalore.* ***Mr. Ravi*** *(Executive Director),* ***Dr. Suresh*** *(Assistant Director),* ***Dr. Prashanth, Dr. Kshama, Mahadev Swamy*** *& staff of Mysore Zoo, for their timely help and support during my research work. My sincere thanks to field Veterinarians* ***Dr. Prayag****,* ***Dr. Manikanta and Dr. Pavithra*** *for their help and support during my research work.*

My sincere thanks to my fellow colleague, ***Dr. Dhoolappa, Dr. Ganga Naik, Dr. Lakshmishree, Dr. Nagaraju, Dr. Rajani, Dr. Sathosh Kumar C.N, Dr. Mahesh Kadgi, Dr. Premkumar, Dr. Gururaj, Dr. Nagappa, Dr. Rudresh, Dr. Naveen, Dr. Jayashree, Dr. Nithin Prabhu, Dr. Yalagoud, Dr. Manjunath, S.S, Dr. Anjan, Dr. Kavitha Rani, Dr. Vetri, Dr. Deepak, Dr. Ramesh, Dr. Avinash, to my juniors Dr. Manjunatha K., Dr. Shridevu, Dr. Ravi, Dr. Madhu. D, Dr. Pavanashri, Dr. Sindhu, Dr. Navya, Dr. Sathish, Dr. Ravishankar, Dr. Shriranga, Dr. Puttaraju, Dr. Ramya, Dr. Darshan, Dr. Divya,*** *for their generous help and co-operation during my study.*

I also thank my loving friends, ***Drs. Shridhar B.G, Divya.V, Hemannagowda, Nagesh, Sunil Patil, Raji.S.S, Banuprakash.A.R, Sowmya, Praveen P C and Ramesh Pattar,*** *for their support and help during my study.*

I wish to express my special thanks to ***Mr. Pradeep*** *lab technician Department of Veterinary anatomy and histology and* ***Mr. Narayanappa, Mrs. Girijamma*** *and* ***Mr. Sadappa*** *supporting staff of Department of Veterinary Anatomy and Histology, Veterinary College Bangalore-24 for their timely help.*

I am extremely grateful to my father ***Yallapa. Baddi****, brother* ***Dr. Ajay*** *and* ***sister-in-law Sangeetha, nephew Mr. Chirayush, Dr. Shambhulinga. Bankolli, Dr. Deepak and staff of Chirayush Children's Hospital, Tilak nagar, Shivamogga. Also to Dr. Srikanth Konapur, Dr. Mahesh Baddi, Dr. Ramesh, Dr. Balu, Dr. Srivijay, and Dr. Suresh,*** *my brother in law* ***Manjunath.Burli****, sister* ***Maheshwari &*** *niece* ***Sahithya*** *and* ***jelly,*** *whose love and affection has always been a source of inspiration to me.*

Last but not least, I am immensely thankful to those who have directly or indirectly helped me in my work.

Place: Bangalore

Date: 16.08.2014 ***(SHAMBHULINGAPPA, Y. BADDI.)***

CONTENTS

LIST OF PLATES

LIST OF FIGURES

LIST OF TABLES

ABBREVIATION

HATR	Horizontal Attenuated Total Reflection
FTIR	Fourier Transforms InfraRed
ATR	Attenuated Total Reflection
%	Percentage
PCA	Priciple Componant Analysis
DRIFT	Diffuse Reflectance Infrared Fourier Transform
SF	Splittig Factor
LDA	Linear Discriminant Analysis
CVA	Canonical Variate Analysis
CLS	Classical Least Square
ILS	Inverse Least Square
PCR	Principal Componant Regression
PLS	Partial Least Square
µg	: microgram
µl	: microlitre
AFLP	: amplified fragment length polymorphism
APD	: average percentage difference
ASO	: allele specific oligonucleotide
bp	: base pair
DMSO	: dimethyl sulfoxide
DNA	: deoxy ribonucleic acid
dNTP	: deoxy ribonucleoside triphosphate
EDTA	: ethylene diamine tetraacetic acid
g	: gram
kb	: kilo base
KCl	: potassium chloride
MAPD	: mean average percentage difference
mg	: milligram
MHC	: major histocompatibility complex
ml	: milliliter
µmol	: micro moles
Mol	: molar
mM	: milli molar
ng	: nano gram
OD	: optical density
pmol	: pico moles
PCR	: polymerase chain reaction
PCR- RFLP	: polymerase chain reaction – restriction fragment length polymorphism
PD	: percentage difference

RAPD	: random amplified polymorphic DNA
RBC	: red blood cells
RFLP	: restriction fragment length polymorphism
rpm	: revolutions per minute
SDS	: sodium dodecyl sulphate
SNP	: single nucleotide polymorphism
TBE	: tris- boric acid – EDTA
TE	: tris- EDTA
Tris- HCl	: tris – hydrochloride
UV	: ultra violet
VNTR	: variable number of tandem repeats
HEPA	: high efficiency particulate air
WPSI	Wild Life Protection Society of India
WII	Wild Life Institute of India

Introduction

I. INTRODUCTION

In 2008, the most comprehensive assessment of the world's mammals has confirmed an extinction crisis, with almost one in four at risk of disappearing forever, according to the IUCN Red List of Threatened Species (IUCN 2008). The IUCN Red List of Threatened Species (Version 2011.1) shows that at least 1136 of the 5487 mammal species on earth are known to be threatened with extinction (IUCN, 2011). According to the IUCN at least 76 mammal species and 7 mammal subspecies have become extinct since the year 1500 (IUCN 2010; IUCN 2011). However, the real situation could be much worse, as 836 mammal species are listed as Data Deficient (IUCN 2010; IUCN 2011). As information improves, more mammals may well prove to be in danger of extinction or already extinct (IUCN 2008). A recent study (Velho *et al.,* 2012) observed that hunting was reported in 23 out of the 28 states and 7 Union Territories of India. Among the 350 mammal species, 114 are reported to be hunted in India.

The gaur (*Bos gaurus*), is also called Indian bison, the largest and tallest species of wild cattle and are in danger of extinction, because people are hunting them for meat, horns for decorative items and internal organs for traditional medicinal purposes (Menon and Vivek, 2009). The number of wild gaurs decreased drastically due to the loss of suitable habitat hunting or hybridization with domestic cattle (National Research Council, 1983). Gaurs were once distributed throughout the forested tracts of India and South Nepal, east of Vietnam and south of Malaya but today they are confined to just over a hundred existing and 27 proposed protected areas in India (Sankar *et al.*,2013). The species is listed under the IUCN Red List as vulnerable and according to Indian Wildlife

Protection Act (1972) it is an endangered animal as per Schedule – I and also it is included in Appendix I of the Conservation on International trade in Endangered Species of Wild Fauna and Flora (CITES) and categorized as vulnerable by the International Union for Conservation of Nature and Natural Resources (IUCN) (IUCN Red List of Threatened Species; Mallon, 2008). The black buck (*Antelope cervicapra)* is one of 26 species of mammals, which have been declared endangered and is the only living species of the genus Antelope (Nowak, 1999). Poaching and habitat destruction has seriously affected the population of the Black Bucks. It is usually hunted for its skin, flesh and also for sports. As its range has decreased sharply during the 20th century, it has been classified as near threatened by IUCN since 2003 (IUCN Red List of Threatened Species). During the 18^{th} century to first half of the 20th centuries, blackbucks were the most hunted wild animal all over India. The nilgai (*Boselaphus tragocamelus*) has become extinct in Bangladesh, it is the only member of genus *Boselaphus* and the main threat to this species is the loss of habitat due to deforestation and human population growth (Nowak, 1999). Half of the top 20 countries for numbers of threatened species are in Asia. Habitat loss affecting over 2000 mammal species, is the greatest threat globally (Nikunj and Nishith, 2011). Southern India, one of the last strongholds of the endangered Asian elephant (*Elephas maximus*), harbours about one-fifth of the global population (Vidya *et al.*, 2005). Prior to 1989, conservationist estimates that about 70,000 elephants may have been killed annually for their tusk by ivory poachers in Africa (Charles, 2009). The wild boar tusks are collected as trophies by hunters and regularly displayed at trophy exhibitions (Miles and Grigson,1990).

India was once home to many cheetahs, but the last of them was killed in 1947. It was declared extinct in 1952. The last physical evidence of the Asiatic cheetah in India was three shot by the Maharajah of Surguja in 1947 in eastern Uttar Pradesh. With the death of the last remaining population of the Asiatic cheetah in India, the species was declared extinct in India; it is the only animal in recorded history to become extinct from India due to unnatural causes (Anindo, 2009). Trapping of large numbers of adult Indian cheetahs, who had already learned hunting skills from wild mothers, for assisting in royal hunts is said to be another major cause of the species rapid decline in India as they were never bred in captivity with only one record of a litter ever (Travel India Guide, 2012). The Cheetah (*Acinonyx jubatus*) is a large feline (family Felidae, subfamily Felinae) inhabiting most of Africa and parts of the Middle East. It is the only extant member of the genus *Acinonyx*. As the world's last Asiatic cheetah population in Iran is currently classified as critically endangered, with an estimated total of below 100.

In Arunachal Pradesh, hunting is a widespread cultural practice that has probably led to low wildlife abundance (Hilaluddin *et al*., 2005). In certain tracts in India like those inhabited by the Bishnois there is a rich tradition of protecting wildlife and its habitats.

Wildlife crime is a growing problem in a number of countries including South Africa, India and some other parts of the world where there is presence of rich flora and fauna. It includes live animal trafficking and illegal poaching for both meat and trophies. Fraudulent mislabeling of game meat products is increasing due to the large profit margin and monitoring this is a difficult process (Fajardo *et al.*, 2010). Another market which has increased the rate of wildlife crime is the use of animal parts such as rhinoceros horns and

elephant tusks in the making of traditional medicines, jewellery and ornaments (Greg, 2004; Humphreys & Smith 2011).

For many wildlife crime investigations it is necessary to identify the species involved to determine whether a crime has taken place. Some of the methods includes like physical inspections, gross morphology, histology, Toxicological analysis, DNA analysis and FT-IR Spectroscopy analysis.

Artifacts constructed from elephant and giraffe tail hairs are often encountered in museum collections and in the modern wildlife trade. The most common examples include tail-hair bracelets, necklaces, rings and flywhisks used by indigenous people throughout Africa and parts of Southeast Asia. Proper identification of these keratinous fibers is of interest to museum conservators, since various plastics and botanical fibers are often used as substitute materials. Rigorous methods for identifying elephant and giraffe hairs are also of interest to law enforcement officials, who monitor the illegal trade in endangered and threatened species (Espinoza *et al.*, 2008).

In the last two decades, several DNA based techniques have been developed to characterize the living creatures. Random Amplified Polymorphic DNA (RAPD) is one such technique which is based on amplification of genomic DNA by PCR using random sequence oligonucleotide primers (Williams *et al.*, 1990). The main advantage of this technique is that, it can identify and type a large number of genetic markers quickly and is cost effective.

Species identification has many applications including forensics, speciation and the monitoring of illegal animal and animal product trade (Fajardo, 2010). For this

reason, it is necessary to have a standard identification system in place. This system would need to efficiently identify a number of different species from various sample types including hair, blood and tissue which are often degraded. The process would need to be fast, highly sensitive, cost effective and allow for high throughput.

The arrangement of hair follicles in the domestic animals such as cattle, sheep, goat, dog and cat and wild carnivores such as Bengal tiger, leopard, lion and sloth bear have been described and indicated that they have species specific arrangement of hair follicles (Dellman and Brown, 1981; Nagaraju, 2012; Shambhulingappa *et al*., 2013). Review of literature has not shown any detail on the architecture of hair follicle in wild herbivore and carnivore animals studied.

FTIR spectroscopy has become a powerful tool for investigation of the three-dimensional structure of various biomolecules such as proteins, nucleic acids and lipids (Jackson and Manisch, 1993). There are only a few reports on the applications of FT-IR spectroscopic imaging to forensic science (Tahtouh *et al.,* 2005). Biological systems, including lipids, proteins, peptides, biomembranes, nucleic acids, animal tissues, microbial cells, plants and clinical samples, have all been successfully studied by using infrared spectroscopy. This technique has been employed for a number of decades for the characterization of isolated biological molecules, particularly proteins and lipids. However, the last decade has seen a rapid rise in the number of studies of more complex systems, such as diseased tissues. Microscopic techniques, combined with other sophisticated analytical methods, allow for complex samples of micron size to be investigated.

Being able to identify not only trace materials at a crime scene, but also to link specific people to specific acts via the detection of exogenous substances left in their hands, ATR-FT-IR spectroscopic imaging shows the potential to significantly enhance the amount of information needed in the prevention and investigation of drug abuse (Camilla *et al*., 2006). Vibrational spectroscopy in the mid-infrared (IR) region can provide molecular structure information about mineralized and non-mineralized connective tissues (Carden and Morris 2000).

The present study is taken up for histological studies on the original skin of wild herbivores such as *Bos gaurus* (Indian bison or gaur), *Antilope cervicapra* (Black buck), *Boselaphus tragocamelus* (Nilgai), *Elephas maximus* (Asian elephant), *Loxodonta africana* (African elephant), *Sus scrofa afinis* (Wild boar) and *Acinonyx jubatus* (Cheetah). FTIR spectroscopy study on hairs of these animals along with *Rusa unicolor* (Sambar), *Canis lupus pallipes* (Indian gray wolf) and *Melursus ursinus* (Sloth bear), hooves of Indian bison, Black buck and Nilgai and tusk of African elephant. Further, DNA analysis (RAPD-PCR) of Indian bison, Black buck, Nilgai, Wild boar, Sloth bear, Cheetah and *Bos primigenius* (Cattle) was used for comparison.

Keeping this background in view, the present study was undertaken with the following objectives.

1. To study the morphology of animal specimens for their species identification.
2. FT-IR Spectral analysis of animal specimens for their species identification.
3. DNA Analysis of the animal specimens for their species identification.
4. Evaluation of the above methods from the point of identification of the animal species.

Review of Literature

II. REVIEW OF LITERATURE

2.1 HISTOLOGY

2.1.1 Epidermis:

The epidermis was the outermost layer of the skin and was a keratinized stratified squamous epithelium (Evans and Christensen 1967; Trautmann and Fiebiger 1957; Delmann and Brown 1981; Bacha and Bacha 1990). The surface was smooth or irreguler and Evans and Christensen (1967) observed scale like folds forming depressions into which hair follicles invaginate and occassionally knob-like enlargements; the epidermal papillae interrupted the pattern of scale-like folds in the skin of carnivores. Generally the epidermis is four layered with additional stratum lucidum observed only in thick epidermis of digital pads, teat and planum nasale (Delmann and Brown, 1981; Bacha and Bacha, 1990; Sar and calhoun, 1966). The thickness of the epidermis varies with the location. In regions where there is a heavy protection coat of hair, the epidermis is thin. In nonhairy skin, such as that of mucocutaneous junction, the epidermis is thicker (Delmann and Brown 1981). The stratum basale, stratum spinosum, stratum granulosum and stratum corneum are constantly present (Delmann and Brown 1981; Bacha and Bacha 1990) and stratum granulosum contained basophilic keratohyaline granules in their cytoplasm. In structures with hard keratin such as hooves and claws, stratum granulosum and stratum lucidum are absent with often sloughing off of the dead keratinized cells from the surface (Bacha and Bacha 1990). Strickland and Calhoun (1963) reported that the integument of cat revealed a decreased skin thickness dorsal to ventral on the trunk and proximal to distal on the limbs. Bhayani *et al.* (1995) found that in lion, the total thickness of epidermis of the skin was maximum in neck region and minimum in lower

abdomen. Lloyd and Garthwaite (1982) observed that in the canine, the epidermis of skin was composed of three to six cell layers.

Saxena *et al*. (1994) observed that the skin and dermal thickness of cattle increased with age and the cuticle thickness was not significantly affected by age. The absence of significant difference in thickness of epidermis in various age groups indicated that the number of cell layers constituted epidermis remained constant irrespective of age groups.

Yu *et al*. (2010) recorded all epidermal layers in the skin of Bama miniature pig, such as stratum corneum, stratum lucidum, stratum granulosum, stratum spinosum, and stratum basale. Kozlowski and Calhoun (1969) reported that in sheep, Keratohyalin granules characterized the stratum granulosum and melanocytes were seen amongst the stratum basale. Talukdar *et al*. (1972) found that the epidermis consisted of four layers in the horse viz., stratum basale, stratum spinosum, stratum granulosum and stratum corneum. The stratum lucidum was absent. Keratohyalin granules and dendritic melanocytes were seen in the stratum spinosum and stratum basale respectively. Follicular folds were observed below the openings of sebaceous glands which showed the corrugations of the inner root sheath of hair follicle.

Sharma and Bharadwaj (1993) observed that in yak, the thickest skin occurred in the ventral side of neck. The dorsum of the trunk was thicker than the ventral, and the lateral side of limbs showed thicker skin than the medial side. Atlee *et al.* (1997) noted that in llama, the epidermis was comprised of dead stratum corneum which also included stratum lucidum and the viable epidermal layers viz., stratum basale, stratum spinosum

and stratum granulosum. Rete ridges were present in most hairless areas and in the haired areas near mucocutaneous junctions.

Baba *et al.* (1998) observed that in chotanagpuri sheep, the palpebral epidermis comprised of four layers viz., stratum basale, stratum spinosum, stratum granulosum and stratum corneum. The Stratum lucidum was absent. Dellmann and Eurell (1998) stated that in domestic animals, both hairy and non-hairy skin consisted of stratum basale, stratum spinosum, stratum granulosum and stratum corneum. The stratum lucidum was found between the stratum granulosum and corneum only in non-hairy regions such as planum nasale, foot pads, teat etc.

Bhattacharya *et al*. (2003a) reported that in buffalo, the epidermis consisted of stratified squamous epithelium and was found to be deep, black and dense in appearance in non-descriptive buffalo. The stratum corneum consisted of dead cells without having any cellular architecture and was thicker in the neck region. The stratum granulosum containing several layers of flattened cells was present only in the neck region. The stratum lucidum was absent in all the regions. The stratum lucidum was also found to be absent in American goats (Sar and Calhoun, 1966), Black Bengal goats (Gayen *et al.*, 1989), Decani sheep (Mandage *et al*., 2003) and also in Osmanabadi goats (Kapadnis and Bhosle, 2004).

The epidermis of one humped camel was comprised of a relatively thin stratified squamous epithelium and stratum corneum was extremely flat (Pfeiffier *et al*., 2006). The stratum granulosum and stratum lucidum was absent in rabbit (Yagci *et al*., 2006).

More *et al*. (2007) observed that the skin of spotted deer was lined by stratified squamous epithelium with abundant hair follicles. Cells were arranged in three to four layers. The hair follicles were associated with branched tubular sebaceous glands were connected with hair follicles.

Nagaraju, (2012) opined that the epidermis of the spotted deer (Axis axis) consisted of only three layers namely stratum corneum, stratum granulosum and stratum basale. The stratum corneum consisted of smooth, thin epithelial layer. The stratum lucidum and stratum spinosum layers were not observed and there was stratum granulosum with round shaped single cell layer with very thin basement membrane. There was distinct separation of epidermis and dermis, which consists of loose connective tissue.

Gaykee *et al.* (2008) found that the epidermis of skin of wild pig consisted of 15-20 layers. However, Bacha and Bacha (2000) reported only three to four layers of cells of epidermis in domestic pig.

Sumena *et al.* (2010) observed in yorkshire pigs that the papillary layer was thickest in the snout region and thinnest in the ventral neck region. The papillary layer conformed to the contour of the stratum basale of the epidermis. It was protruded into the epidermis at certain intervals, giving rise to dermal papillae. There was no clear demarcation between the papillary and reticular layer. The papillary layer was made up of more of collagen fibers. The fine fibers of the papillary layer interdigitated into the stratum basale and dermal papillae was highly vascular. The papillary dermis formed primary ridges corresponding to the epidermal ridges. The primary dermal ridge was

again divided into secondary dermal ridges or dermal papillae by the vete pegs. These were numerous, tall and often branched.

Stratum basale

The stratum basale consisted of single layer of cuboidal to columnar cells in the epidermis of llama (Atlee *et al*., 1997), Deccani sheep (Mandage *et al*., 2003), Osmanabadi goats (Kapadnis and Bhosle, 2004), ferret (Martin *et al*., 2007) and Red Kandhari cows (Hole *et al*., 2008a).

Stratum spinosum

Banks (1993) described that the stratum spinosum layer contained light staining cells that flattened towards the surface and had intercellular bridges in domestic animals. Atlee *et al.* (1997) stated that the stratum spinosum was made up of one to three layers in the skin of llama. However, Mandage *et al.* (2003) reported that the stratum spinosum presented four to five layers of cuboidal cells with spherical nuclei in the skin of Deccani sheep. However, these cells were reported as Langerhans cells or clear cells by Dellmann and Eurell, (1998) in domestic animals. The clear cells in stratum spinosum were observed in Black Bengal goats (Gayen *et al*., 1989) and in Osmanabadi goats (Kapadnis and Bhosle, 2004).

Gaykee *et al*. (2008) found that the stratum spinosum of the skin of wild pig was arranged in 10-12 layers of cells in which lightly stained nuclei and cytoplasm were observed. Hole *et al.* (2008a) observed that the stratum spinosum consisted of four to five layers of polyhedral cells with rounded nuclei in Red Kandhari cows.

Stratum granulosum

Singh *et al.* (1975) found that the stratum granulosum was absent in the paralumbar skin of Indian buffalo calf. Atlee *et al.* (1997) observed that the stratum granulosum of llama skin was composed of single layer of thin flattened cells with compressed nuclei and had small basophilic keratohyalin granules. The stratum granulosum consisted of several layers of flattened cells which were parallel to the epidermal-dermal junction possessing keratohyalin granules in the skin of domestic animals (Dellmann and Eurell, 1998). Mandage *et al*. (2003) in Deccani sheep and in Osmanabadi goats (Kapadnis and Bhosle, 2004) reported that the stratum granulosum consisted of single layer of elongated cells.

Gaykee *et al.* (2008) and Hole *et al*. (2008a) observed that the stratum granulosum was arranged in a single layer with abundant cytoplasmic keratohyalin granules in the skin of wild pig and Red Kandhari cows respectively.

Stratum corneum

The stratum corneum consisted of about 30 cell layers in cattle (Lloyd *et al*., 1979) and four to five layers in Osmanabadi goats (Kapadnis and Bhosle, 2004). Banks (1993) stated that in domestic animals, the stratum corneum was composed of several layers of non-nucleated cornified cells, peripheral cells became dead and were constantly sloughed off as scales.

Atlee *et al.* (1997) noted that the stratum corneum of llama skin had a basketweave appearance, but regional variation existed as mucocutaneous junctions had thin while footpads had thick stratum corneum.

Mugale and Bhosle (2002) observed that stratum corneum was thinner in young Deoni cattle and increased in thickness with the advancement of age. Bhattacharya *et al.* (2003a) reported that the stratum corneum consisted of dead cells in non-descriptive buffalo.

The skin of cattle (*Bos indicus*) showed all five layers namely stratum basale, stratum granulosum, stratum spinosum, stratum lucidum and stratum corneum. The stratum corneum was prominent, nuclei were absent. The stratum lucidum was a shiny, translucent, homogenous layer. The stratum granulosum consisted of three layers of round shaped cells containing keratohyaline granules. The stratum spinosum consisted of oval shaped nuclei with four to six cell layers. The stratum basale contained single layer of columnar cells (Nagaraju, 2012).

2.1.2 Dermis

In Bama miniature papillary and reticular layers were recorded in the dermis of skin (Yu *et al*., 2010). The epidermal interpapillary pegs and dermal papillae fitted together well to form a tight junction that was irregular at the epidermal–dermal interface. Many superficial venules and arteriolar plexuses were distributed around the boundary between the papillary and reticular layers. The dermis contained a variable amount of fat as well as collagen and elastic fibers. Elastic fibers, which often were intertwined with collagen fibers, primarily were located in the papillary dermis and surrounding vessels. These characteristics of the skin of Bama minipigs resembled those of human skin. In addition, the Langerhans cells, fibroblasts, vascular endothelial cells and mast cells of adult pigs did not display any marked differences from those in human skin.

Talukdar *et al*. (1972) found that in horses, the dermis consisted of two well demarcated layers; the superficial or papillary layer containing fine, loosely arranged collagen fibres and the deep or reticular layer with organized compact collagenous fiber bundles. An extensive network of elastic and reticular fibers were seen throughout the dermis, but was more prominent in the superficial layer.

Mowafy and Cassens (1975) noticed that in pig, the dermis was composed mainly of coarse collagen fibres oriented both perpendicular and parallel to the surface. Elastic fibres were found in the entire dermis but were concentrated around the hair follicles and in the papillary layer around the interpapillary pegs.

Meyer *et al*. (1981) reported that in pig, the thicker elastic fibres predominated in the deeper reticular layer of dermis than the papillary layer and around the pilosebaceous units. Meyer *et al*. (1982) found that in different body regions of wild boars, domestic pigs and miniature pigs, the bulk of the dermis is dominated by a massive three dimensional network of collagen fibres and fibre bundles, which crossed each other in two main directions. Several smaller fibre bundles passed through the network in various other directions in a densely interwoven fibre pattern.

Meyer *et al.* (1994) studied the hairy skin of important domesticated mammals (12 species) with scanning electron microscopy, transmission electron microscopy, laser scanning microscopy, and several light microscopical methods, to obtain more information about three-dimensional elastic fibre arrangement. It was obvious that there was a basic construction scheme of the elastic fibre meshwork as present in the upper and mid-dermis, with special regard to the size, number, and grouping of hair follicles. In the

densely-haired species, in particular, a typical elastic mat with horizontal fibres were formed. In many of the sparsely-haired animals, the upper and mid-dermis showed a sponge-like elastic system. In the massive, collagen-rich skin of large species, the lower two thirds of the dermis without hair follicles only possessed a loosely-structured elastic network, but thick elastic sheets were found at the border zone with the hypodermis. Specific features appeared with regard to the type of mechanical strain exerted, different body regions and varying hair follicle density or as connected with the anchoring of the hair follicle complex, blood vessels and nerves.

Atlee *et al*. (1997) noted that in llama, the thickest dermis was present on the dorsal aspect of neck and ventral areas presented a much thinner dermis.

Dellmann and Eurell (1998) described that in the skin of domestic animals; the dermis was divided into a superficial (papillary) layer and a deep (reticular) layer without a clear line of demarcation and was composed of collagen, elastic and reticular connective tissue fibers. Moreover, hair follicles, sweat and sebaceous glands, blood and lymph vessels and nerves were embedded throughout the dermis. The reticular layer was thicker and consisted of denser connective tissue than the papillary layer. The connective tissue cells were fewer in the deep layers of the dermis.

Kapadnis and Bhosle (2004) observed that in Osmanabadi goats, the meshwork of dermis consisted of felt work of collagen, elastic and reticular fibres. The elastic fibres were found predominantly at both ends of arrector pili muscle, associated with the hair follicles and sweat glands.

Bhayani *et al.* (2005) reported that in sheep, the elastic fibres were found to be more prominent in papillary layer of dermis as compared to reticular layer. Kapadnis *et al*. (2005) reported that in goat, the dermis of skin in neck region consisted of feltwork of collagen, elastic, reticular fibers, sweet glands, sebaceous glands, hair follicles and arrector pili muscles. The collagen fibres were fine, loosely arranged and irregularly distributed in the papillary layer and were thick and densely arranged in the reticular layer. The elastic fibres were rare and finely branched in the papillary layer and arranged perpendicular to the skin surface. The reticular fibers were abundant in the dermo-epidermal junction, around the sweat glands, sebaceous glands and walls of the blood vessels and in the capsule of hair follicle.

Monte *et al*. (2005) showed that the skin of goat had a thicker thermostatic layer (papillary layer) with a greater density of follicles and glands at 180 days. The reticular layer developed with age. Archana *et al*. (2006) found that the papillary layer comprised of loose areolar connective tissue with fibroblasts, mast cells, melanocytes, macrophages and lymphocytes in the skin of Indian crested porcupine. The reticular layer was composed of dense areolar connective tissue. The nerve endings were found at the junction of papillary layer and reticular layer.

Mandage *et al*. (2006) observed that the dermis of the skin in loin region of Deccani sheep presented an upper papillary layer and a deep reticular layer without clear cut demarcation between these layers. The collagen fibres were found to be thin, running parallel to the epidermis in papillary layer but running horizontal to oblique direction to epidermis in reticular layer. The elastic fibres were found in horizontal, vertical and oblique directions to epidermis in reticular layer. The reticular fibres in the papillary layer

were found to be arranged in horizontal directions where as in reticular layer, they were arranged vertically. In one humped camel numerous capillaries as well as small arteries and veins were observed throughout the dermis (Pfeiffier *et al*., 2006).

Hole *et al*. (2007b) found that in Red Kandhari cows, the dermis was enmeshed with collagen, elastic and reticular fibres. The collagen fibres were thick, coarse and irregularly distributed in the dorsal, lateral and ventral aspects of thorax region and were arranged parallel to the skin surface and formed a close attachment of dermis to the epidermis. These fibres were loosely arranged in papillary layer but dense arrangement of large bundles of collagen fibres were observed in the reticular layer of the dermis. The elastic fibres were arranged perpendicular to the skin surface and were finely branched in the papillary layer than the reticular layer of dermis. They were abundant in the dermo-epidermal junction, around sweat and sebaceous glands and wall of the blood vessels. Martin *et al*. (2007) noted that in Ferret skin, the dermis was comprised of irregular collagenous tissue with a few dermal papillae.

Nagaraju (2012) opined that in spotted deer, the sebaceous glands surrounded the primary hair follicle. There was sparse distribution of collagen fibers. The sweat glands were located at the junction of dermis and hypodermis which were merocrine simple tubular glands. The interfollicular spaces were predominantly occupied by the elastic tissues. There were elastic fibers surrounding the hair follicle and sebaceous glands. The dermal connective tissue was occupied by abundant elastic fibers. The arrector pili muscle distribution was scanty, reticular fibers were present in the dermis of the skin but present only at the basement membrane. The nerve fibers were penetrating and encircling

the primary hair follicle and secondary hair follicles. The sweat glands were predominantly innervated than the sebaceous glands.

Trautmann and Fiebiger (1957) described that the most superficial layers of the dermis were condensed into a feltwork of delicate reticular fibers with an admixture of fibroelastic elements. The remainder of the corium consisted of bundles of collagen fibers, and some elastic fibers joined the collagenous bundles, while others form fine networks, especially in the more superficial layers of the corium (as in the ox, sheep, and dog). In the papillary layer the fine collagenous bundles were densely interwoven.The stratum reticulare was not sharply marked off from the stratum papillare. The latter was the deeper and heavier layer of the corium. Here the fiber bundles were interwoven mainly in a horizontal plane. The thickness of the skin varies with age, sex, species, and body region. The ox has the thickest skin, while it was thinnest in sheep.

Sar and Calhoun (1966) stated that in the dermis there was no sharp distinction between papillary and reticular layers in most of the body regions, as the layers blended with each other without demarcation. The collagenous fibers of the superficial layer of the dermis were fine, loosely arranged, and irregularly distributed. These fibers were thick and densely arranged in the reticular layer. The elastic fibers were abundant in young goats. They were most numerous in the neck and thoracic region, but were scarce in interdigital skin and junctions of hoof and horn with skin.

According to Evans and Christensen (1967) the dermis under the epidermal papillae was composed of very fine, closely packed connective tissue fibers which extended under the thickened epidermis to form the papilla. The dermal-epidermal junction

of the hairy skin was normally thrown up into folds which were paralleled the surface. The hair follicles, sweat and sebaceous glands, blood and lymph vessels and nerves were embedded at various levels throughout the dermis and was generally divided into a superficial (papillary) layer that blends into a deep (reticular) layer without a clear line of demarcation.

The superficial layer of dermis was wider in horse and cattle skin than in that of carnivores where in it encompasses the hair follicles and adjacent sweat glands. The deep layer of the dermis was much more coarse and dense than the superficial layer, and contained large bundles of collagen fibers aligned parallel to the surface (Delmann and Brown 1981; Bacha and Bacha 1990).

Evans and Christensen (1967) stated that apocrine sweat glands were found mainly in connection with hair follicles. The secretory parts of the glandular tubules were situated in the dermal and subcutaneous layers of the skin. The sebaceous glands secreted by holocrine mode and distributed over the integument in connection with the hair follicles, they are largest along the dorsal part of the neck, back, and tail, particularly in the specialized tail gland area.

Evans and Christensen (1967) observed that the individual follicle and hair bulb of the cover-hair or guard-hair was larger and penetrated more deeply in to the subcutaneous tissue than those of the satellite or subsidiary hairs. The canine hair follicle could be defined as a pilosebaceous –arrector muscle complex. The sebaceous glands of the individual hair follicles bunched together in clusters and sometimes fused.

Bhayani *et al*. (1995) reported that the skin of lion was similar to that of dog with compound hair follicles. The depth of hair follicle was more in the lower abdomen and less in the thorax region in adult lion. The hair follicles were situated deep in the reticular layer. Delmann and Brown (1981) observed that errector pili muscles contracted during cold to cause the hair to bristle and air spaces were formed in the medulla of hair serving as insulators.

Trautmann and Fiebiger (1957), described in man and other primates that the merocrine tubular glands (sweat glands) were distributed over the entire skin surface, while the apocrine glands are restricted to a few areas, such as the axilla. In domestic animals, on the other hand, the apocrine glands make up the great majority of tubular skin glands. In the sheep, pig, cat, and horse the secretory tubule was wound up, whereas in the ox, goat, and dog it was serpentine. The poorly developed glands of the cat were present only in a few body areas (oral region, anus, lower jaw, and foot pads). The tubular glands of the dog vary greatly in diameter. Although they were distributed over the entire body, they do not function visibly under normal conditions.

Sar and Calhoun (1966) found that the sebaceous glands were simple or branced alveolar glands distributed throughout all body area in goat. With few exceptions, the glands were associted with hair follicles and opened into follicular lumen through a duct below the opening of the duct.

2.1.3 Hair follicle distribution

Jenkinson and Nay (1972), found variations in diameter and length of hair follicle and there were no secondary hair follicles in the skin of European cattle. Bhayani *et al*.

(1995) reported that the skin of lion was similar to that of dog with compound hair follicles. The depth of hair follicles was more in the lower abdomen and less in the thorax region in adult lion. The hair follicles were situated deep in the reticular layer.

Atlee *et al.* (1997) noticed that in llama skin, both simple and compound hair follicles were present. The dorsal and lateral aspects of the body presented high density of hair follicles and were oriented at a sharp oblique angle. The compound hair follicles consisted of one or two primary hair follicles surrounded by multiple smaller secondary follicles.

Raheem and Al-Hety (1997), opined that the primary follicles were arranged in trios, duos or as solitary follicles in Iraqi goats. The secondary follicles were smaller and shorter than the primary follicles. They accompanied the primary follicles and comprised a high percentage of the total follicles. Some secondary follicles opened independently on the skin surface, but others shared an opening with primary follicles.

Mehta (2002), observed that in Murrah buffalo and ox, the hair follicle unit consisted of the bulb of the hair and sebaceous gland, arrector pili muscle and a single sweat gland. Kapadnis *et al.* (2004) observed that in goat skin, the primary hair follicles were arranged in groups of three, which were associated with three to five secondary hair follicles. The secondary hair follicles were located deep in the dermis and associated with sebaceous glands only.

Archana *et al.* (2006) found that the reticular layer of skin of Indian crested porcupine showed the presence of hair follicles. Gaykee *et al.* (2008) reported three or four hair follicles in one group which were connected with arrector pili muscle on one

side or at some places both sides in wild pig. The hair follicles were surrounded by dense connective tissue.

Abdul-Raheem *et al.* (2009) studied the skin of native buffalo to detect the value of hair density in different regions of the body. The hair follicles were characterized by variable sizes and their indefinite grouping arrangement, although some doublets or triplets groups were detected in some regions.

Delman and Brown (1981) described hair follicles into several types. A primary hair follicle was one of large diameter, which was deep rooted in the dermis, and was usually associated with sebaceous and sweat glands and arrector muscle . A secondary follicle was smaller in diameter than a primary follicle, and the root was near the surface. It may present a sebaceous gland but lacked a sweat gland and an arrector muscle. Those follicles with only one hair emerging to the surface were called single or simple follicles. The compound follicles have several hairs emerging from a single opening on the surface of the skin. Each hair of the compound follicle has its own papilla and root sheath. At the level of the sebaceous gland opening, the follicles fuse to form a single external follicular orifice.

Delman and Brown (1981) identified in horses and cattle single hair follicles distributed evenly. The bovine skin was well supplied with sweat and scent glands and these are lacking only in the skin of the teats and interdigital spaces. There were also a considerable number of sebaceous glands with independent openings. The secreting sweat glands were very wide (60-100 µm) and often only slightly undulating but not coiled (Nickel *et al.*, 1981).

Bhayani *et al.* (1999) found that sweat glands were tubular in shape in the skin of hyaena and depth of sweat gland was maximum in the mid-side and minimum in the lower abdomen with significant regional differences.

Delman and Brown (1981), observed in pigs, single follicles grouped in clusters of two to four follicles, with three being most common. This cluster was usually surrounded by dense connective tissue.In case of goat the primary follicles occur in a groups of three, with three to six secondary follicles associated with each group. In sheep the hair-growing regions contained mostly single follicles, whereas the densely covered wool-growing regions presented large numbers of compound follicles. The typical follicle cluster contained three primary follicles and a number of secondary follicles. In dog compound follicle consisted of a single, long, primary hair and a group of smaller secondary under hairs. As many as 15 hairs may emerge from a single opening in the skin. The compound follicles occured in clusters of three, with the center one slightly larger. The arrangement of the follicles in the cat consisted of a single, large, primary (guard) hair follicle surrounded by clusters of two to five compound follicles. In each compound follicle there are 3 coarse primary hairs and 6 to 12 fine or secondary hairs.

Nickel *et al.* (1981) stated that the skin of the goat is considerably thinner than that of the ox but it was thicker, tougher and more elastic than that of the sheep.

Further they explained that the skin of the sheep was thinner than that of the goat. In adult animals its average thickness was 2.5 mm. The hair follicles of sheep occured in groups which contained both primary and secondary hair follicles. The primary hair follicles presented both sebaceous and tubular sweat glands as well as muscles while the

secondary follicles only showed sebaceous glands. The sweat glands of sheep were twisted but their ends were not coiled. The complement of sebaceous glands remained constant throughout the animal's life while the sweat glands increased in number with age.

Bacha and Bacha (1990), described single (simple) hair follicles evenly distributed in the skin of horses and ruminants and occured in groups of three in pigs. In carnivores most of the follicles were compound follicles. Each compound follicle was formed from a single primary follicle and several secondary follicles . The follicles united at the level of the openings of the sebaceous glands, forming a common follicle, which extended from the point of union to the skin surface.

Nagaraju (2012) reported that the primary hair follicles associated with two to three secondary hair follicles and these columns of hair follicles were arranged in a parallel fashion to each other in skin of spotted deer. Again in cattle, he opined that the distribution of hair follicle was species specific arranged in a single row of primary hair follicles.

Shambhulingappa *et al.* (2013) opined that circumferential arrangement of hair follicle bundles appear to be a characteristic of the leopard skin. Further, within each bundle single primary hair follicle was surrounded by groups of secondary follicles. Each group follicle consisted of 6-8 fine secondary follicles interspersed by fine connective tissue fibers. In Bengal tiger skin, a hair follicle bundle consisting of a primary hair follicle located at one end underneath which 6-8 secondary hair follicles were observed and dense irregular connective tissue separated the individual hair follicles with profusely

distributed sebaceous glands in both primary and secondary hair follicles. The arrangement of hair follicles in lion resembled that of the cat but it differed from it by the presence of smaller primary hair follicles in the surrounding clusters of compound follicles. The shape of the surrounding compound follicles varied and did not follow any specific shape. The sweat glands were evenly distributed in the hair follicle bundles between primary and secondary hair follicles, the apocrine sweat glands coiled in nature were observed around the clusters of hair follicles in the dermis. The sloth bear skin showed sparsely distributed hair follicle bundles, surrounded by connective tissue and were elliptical in out line. Each hair follicle bundle consisted of 3-4 primary hair follicles only. There were no secondary hair follicles associated with it (Shambhulingappa *et al.,* 2013).

2.1.4 Sweat gland

Goswami *et al.* (1994) observed that in camel, the simple coiled tubular sweat glands associated with primary hair follicles and rarely with secondary hair follicles throughout the hairy skin areas except the upper lip, the lower lip and the nostrils. The sweat glands were comparatively deeply embedded in the dermis on the dorsal aspect of the body. The duct of the sweat gland opened in a pilosebaceous canal just before the emergence of the hair shaft.

Bhayani *et al.* (1995) found that the sweat glands were longer and saccular in skin of lion. The length and diameter of sweat glands were maximum in leg region and minimum in lower abdomen. Atlee *et al.* (1997) opined that in llama, the glandular portion of sweat gland was tubular and usually coiled. The myoepithelial cells were present between the secretory epithelium and basement membrane. The sweat gland duct

was either coiled or straight and consisted of two or three layers of squamous or cuboidal cells.

Bhayani *et al*. (1999) found that sweat glands were tubular in shape in the skin of hyaena and depth of sweat gland was maximum in the mid-side and minimum in the lower abdomen with significant regional differences. Archana *et al*. (2006) observed that the skin of Indian crested porcupine lacked the sweat glands. Nagaraju (2012) observed the coiled tubular sweat glands in cattle, spotted deer and goat.

2.1.5 Sebaceous glands

Barari *et al*. (1994) opined that in yaks, the glands were round to oval, rectangular, triangular or irregular in shape and might be single, bilobed, multilobed and branched in different areas of skin.

Sharma *et al.* (1996) reported that in yaks, the sebaceous glands were associated with small hair follicles. Mugale and Bhosle (2001b), observed that the sebaceous glands were located in the papillary layer of the dermis in Deoni cattle. The glands were multilobulated and simple to branched alveolar type. They also found that the secretory cells were of squamous type with centrally placed nuclei. Almost two sebaceous glands were associated with one hair follicle.

Mandage *et al.* (2003) reported that the sebaceous glands in the loin region of the Deccani sheep were simple to branched alveolar type placed around the wool follicles and the narrow glandular duct opened into wool follicles. Hole *et al.* (2007a) observed that in Red Kandhari cows, the sebaceous glands were multilobulated, simple to branched alveolar type and situated in the papillary layer of dermis surrounding the hair follicle.

Almost two sebaceous glands were associated with one hair follicle. The secretory cells were squamous type with centrally placed nuclei.

2.1.6 Arrector pili muscle

Banks (1993) and Dellmann and Eurell (1998) reported that in the skin of domestic animals, bundles of smooth muscle fibers grouped together to form the arrector pili muscle. The arrector pili muscle was inserted in the connective tissue sheath of the hair follicles in one end and its other end was attached to the papillary dermis above. Sharma *et al.* (1996) found that the arrector pili muscles were associated only with a few deeply seated large hair follicles in the skin of yak. Pfeiffier *et al.* (2006) stated that arrector pili muscles were frequently observed in association with hair follicles in one humped camel. Zade *et al.* (2007) observed that the arrector pili muscle was arranged obliquely in dermis associated with primary wool follicles in sheep and around hair bulb in goat.

2.1.7 Melanocytes

Chandra and Bhardwaj (1969), found that in buffaloes, the maximum concentration of pigmented granules occurred in stratum basale which gradually declined towards stratum corneum. The pigmented granules blackened in silver preparations and were seen as concentrated nuclear cappings in the supranuclear zone of the cells of stratum basale and stratum spinosum.

Dimond and Montagna (1975) reported that the skin of Giraffe was deeply pigmented. The epidermis, pillary canals and the outer cell layer of the apocrine duct were richly melanized. The melanotic dendritic cells were frequently seen in the sebaceous glands,

the entire length of the external root sheath and the secretory tubules of the apocrine glands.

Dellman and Eurell (1998) observed that in domestic animals, the melanocytes were located in the basal layer of the epidermis. They also occur in the external root sheath and hair matrix of hair follicles, in the sweat gland ducts and in sebaceous glands. The cytoplasm was clear except for pigment containing ovoid granules, which were referred to as melanosomes and the nucleus was spherical.

Mugale and Bhosle (2001a), found that in Deoni cattle, the melanin pigments were brown to dark black in colour in stratum basale and stratum spinosum of epidermis. The melanin pigments were found to increase with the advancement of age. The concentration of melanin granules decreased from stratum basale to stratum corneum.

Mehta (2002) observed that melanin pigment was quite intense in skin of dorsal surface, moderate in the lateral surface and least in ventral surface in buffalo and ox.

2.2 FTIR spectroscopy

FTIR spectroscopy is a vibrational spectroscopic technique that can be used to optically probe the molecular changes associated with biological tissues. The method is employed to find more conservative ways of analysis to measure characteristics within molecules that would allow accurate and precise assignment of the functional groups, bonding types, and molecular conformations. The spectral bands in vibrational spectra are molecule specific and provide direct information about the biochemical composition.

Fourier transform infrared spectroscopy (FT-IR) is an analytical tool that ,when used in examining hard biological tissues, stands out for its robustness, easy of sample preparation, simplicity of operation and the ability to make structure elucidations (Rintoul *et al*., 1998*;* Lyman *et al.,* 2001). FTIR has been applied in such diverse fields as forensic fiber identification (Kirkbridge and Tungol,1999) and bacterial species identification (Timmins *et al.,* 1998).

Discriminant analysis (also known as linear discriminant analysis or canonical variates analysis) of vibrational spectra (Raman or infrared) has been successfully used to extend the limitation inherent in vibrational data examples includes forensic identification of finger nails versus toenails (Widjaja and Seah 2006) and fiber blends (Espinoza *et al.,* 2006).

Espinoza *et al*. (2007) have analyzed the sea turtles and bovidae keratin artifacts using DRIFT spectroscopy and discriminant analysis is a statistical tool which are used in the forensic identification.

Discriminant analysis is a multivariate statistical method that assists in the classification of data into distinct groups. Discriminant analysis of spectral data has been comprehensively reviewed by Enlow *et al*. (2005). The rationale of discriminant analysis in the present situation was to establish discriminant functions from known keratin standards (i.e., Bovidae versus Cheloniidae) and then use the discriminant function to classify keratin materials of uncertain origin. The software (TQ Analyst™) compiles an average spectrum from the known standards, and then each sample is assigned a

numerical score based on the deviation from the calculated spectrum. These numerical scores are then plotted to provide a graphical representation.

A considerably wide field of medical and biological studies has been covered by spectroscopic methods in recent years. It is strongly believed that in studies related to spectroscopic techniques, both the reliable experimental procedure and characterization of spectral peak positions and their assignment along with accurate peak detection and definition are of crucial importance. Although a number of scientists have used different techniques, it seems that there is a marked similarity in their spectral interpretation of comparable areas in their collected spectra (Movasaghi. *et al.*, 2008).

FTIR spectroscopy is a vibrational spectroscopic technique that can be used to optically probe the molecular changes associated with biological tissues. The method is employed to find more conservative ways of analysis to measure characteristics within molicules that would allow accurate and precise assignment of the functional groups, bonding types, and molecular conformations. Spectral bands in vibrational spectra are molecule specific and provide direct information about the biochemical composition.

2.2.1 Spectra

Early infrared instruments recorded percentage transmittance over a linear wavelength range. It is now unusual to use wavelength for routine samples and the wave number scale is commonly used. The output from the instrument is referred to as a spectrum. Most commercial instruments present a spectrum with the wave number decreasing from left to right. The infrared spectrum can be divided into three main regions: the far infrared (<400 cm^{-1}), the mid-infrared (4000–400 cm^{-1}) and the near-

infrared (13000–4000 cm^{-1}). Many infrared applications employ the mid-infrared region, but the near- and far-infrared regions also provide important information about certain materials. Generally, there are less infrared bands in the 4000–1800 cm^{-1} region with many bands between 1800 and 400 cm^{-1}. Sometimes, the scale is changed so that the region between 4000 and 1800 cm^{-1} is contracted and the region between 1800 and 400 cm^{-1} is expanded to emphasize features of interest. The ordinate scale may be presented in % transmittance with 100% at the top of the spectrum. It is commonplace to have a choice of absorbance or transmittance as a measure of band intensity, the relationship between these two quantities transmittance spectra. It almost comes down to personal preference which of the two modes to use, but the transmittance is traditionally used for spectral interpretation, while absorbance is used for quantitative work (Stuart, 2004).

2.2.2 Attenuated Total Reflectance Spectroscopy

Attenuated total reflectance (ATR) spectroscopy utilizes the phenomenon of total internal reflection .A beam of radiation entering a crystal will undergo total internal reflection when the angle of incidence at the interface between the sample and crystal is greater than the critical angle, where the latter is a function of the refractive indices of the two surfaces. The beam penetrates a fraction of a wavelength beyond the reflecting surface and when a material that selectively absorbs radiation is in close contact with the reflecting surface, the beam loses energy at the wavelength where the material absorbs. The resultant attenuated radiation is measured and plotted as a function of wavelength by the spectrometer and gives rise to the absorption spectral characteristics of the sample (Stuart, 2004).

2.2.3 Spectral Analysis

Once an infrared spectrum has been recorded, the next stage of this experimental technique is interpretation. Fortunately, spectrum interpretation is simplified by the fact that the bands that appear can usually be assigned to particular parts of a molecule, producing what are known as group frequencies. The characteristic group frequencies observed in the mid-infrared region is discussed.

The materials were analysed using computerized system of Fourier Transform Infrared Spectroscopy. A bulk analysis data were collected and converted from an interference pattern to a spectrum. The absorption of various infrared light wavelengths by the material was measured. The intensity of the infrared beam was measured before and after it interacted with the sample, as a function of the light frequency which is expressed in reciprocal wave length, termed wave numbers (cm–1). FTIR enabled us to measure weak signals with high precision.

2.2.4 Mid-Infrared Region

The mid-infrared spectrum (4000–400 cm^{-1}) can be approximately divided into four regions and the nature of a group frequency may generally be determined by the region in which it is located. The regions are generalized as follows: the X–H stretching region (4000–2500 cm^{-1}), the triple-bond region (2500–2000 cm^{-1}), the double-bond region (2000–1500 cm^{-1}) and the fingerprint region (1500–600 cm^{-1}). The fundamental vibrations in the 4000–2500 cm^{-1} region are generally due to O–H, C–H and N–H stretching. O–H stretching produces a broad band that occurs in the range 3700–3600 cm^{-1}. By comparison, N–H stretching is usually observed between 3400 and 3300 cm^{-1}.

This absorption is generally much sharper than O–H stretching and may, therefore, be differentiated. C–H stretching bands from aliphatic compounds occur in the range 3000–2850 cm^{-1}. If the C–H bond is adjacent to a double bond or aromatic ring, the C–H stretching wave number increases and absorbs between 3100 and 3000 cm^{-1}. Triple-bond stretching absorptions fall in the 2500–2000 cm^{-1} regions because of the high force constants of the bonds. C≡C bonds absorb between 2300 and 2050 cm^{-1}, while the nitrile group (C≡N) occurs between 2300 and 2200 cm^{-1}. These groups may be distinguished since C≡C stretching is normally very weak, while C≡N stretching is of medium intensity. These are the most common absorptions in this region, but you may come across some X–H stretching absorptions (Stuart, 2004).

These absorptions usually occur near 2400 and 2200 cm^{-1}, respectively. The principal bands in the 2000–1500 cm^{-1} region are due to C=C and C=O stretching. Carbonyl stretching is one of the easiest absorptions to recognize in an infrared spectrum. It is usually the most intense band in the spectrum and depending on the type of C=O bond, occurs in the 1830–1650 cm^{-1} region. Note also that metal carbonyls may absorb above 2000 cm^{-1}. C=C stretching is much weaker and occurs at around 1650 cm^{-1}, but this band is often absent for symmetry or dipole moment reasons. C=N stretching also occurs in this region and is usually stronger (Stuart, 2004).

It has been assumed so far that each band in an infrared spectrum can be assigned to a particular deformation of the molecule, the movement of a group of atoms, or the bending or stretching of a particular bond. This is possible for many bands, particularly stretching vibrations of multiple bonds that are ‘well behaved’. However, many vibrations are not so well behaved and may vary by hundreds of wave numbers, even for

similar molecules. This applies to most bending and skeletal vibrations, which absorb in the 1500–650 cm^{-1} regions, for which small steric or electronic effects in the molecule lead to large shifts. A spectrum of a molecule may have a hundred or more absorption bands present, but there is no need to assign the vast majority. The spectrum can be regarded as a 'fingerprint' of the molecule and so this region is referred to as the fingerprint region (Stuart, 2004).

2.2.5 Derivatives

Spectra may also be differentiated. A single absorption peak have first and second derivative. The benefits of derivative techniques are twofold. Resolution is enhanced in the first derivative since changes in the gradient are examined. The second derivative gives a negative peak for each band and shoulder in the absorption spectrum

2.2.6 Biological Applications

In biological materials, the standard building blocks such as proteins, lipids, nucleic acids, and carbohydrates have unique chemical structures and thus distinctive infrared spectra. Therefore, FTIR can provide a spectrum that is structure-specific through probes the vibrational modes of molecules. In applications requiring qualitative and quantitative analysis, the potential of IR spectroscopy to identify chemical components via finger printing analysis of their vibrational spectrum is unsurpassed (Shi-Ying *et al.*, 2014).

2.2.7 Chemometric analysis of FTIR spectra

The improvement in technology associated with spectroscopy has led to the expansion of quantitative and qualitative infrared spectroscopy. The application of

statistical methods to the analysis of experimental data is known as Chemo metric analysis (Stuart.2004). The most commonly used analytical methods in infrared spectroscopy are classical least square (CLS), inverse least square (ILS), partial least square (PLS) and principal component regression (PCR).

There are two major types of pattern recognition methods. The methods like principle component analysis (PCA) and cluster analysis do not use information related to predefined classes of objects are classified under unsupervised pattern recognition method. On the other hand method like linear discriminant analysis requires a priori information. On the set of samples that is used for classification purpose and it is placed in the category of supervised pattern recognition method (Ballabio and Todeschini, 2009).

2.2.8 Keratin biochemistry

Keratins (including hairs) are a broad class of fibrous proteins (Lehninger 1982), which has been divided into 2 major classes, termed α-keratins and β-keratins. An intrinsic difference in vertebrate keratins is that mammals (including elephants and giraffes) produce only α-keratins, while reptiles and birds produce both α-keratins and β-keratins (Alexander & Parakkal 1969; Marshall *et al*., 1991; Fraser & Parry 1996 and Alibardi 2003a,b,c). The morphological structures and biochemistry of keratin have been systematically described (Lehninger 1982, Marshall *et al*., 1991), whereas Alibardi (2003a, 2003b, 2003c) has reviewed the selective advantage of inheriting α-keratins vs. β-keratins genes.

Elliott (1956) reported that for the folded form the amide I band occurs at 1655cm-1 and the amide II band occurs at 1540cm-1, whereas for the extended form the corresponding bands are at 1630 and 1520 cm-1 respectively. The possibility that differences between folded and extended polypeptide chain conformations could be detected by infrared spectroscopy was first shown by Elliott & Ambrose (1950). Subsequent studies on synthetic polypeptides (Ambrose & Elliott, 1951a*;* Elliott, 1953) and on fibrous proteins (Ambrose & Elliott, 1951b; Elliott, 1956) have established this fact.

Alexander and parakkal (1969) and Marshal *et al.* (1991) have reported an intrinsic difference in vertebrate keratins was that mammals including elephants and giraffe produce only alpha keratins while reptiles and birds produce both alpha and beta keratins.

Lehninger (1982) described the keratins including hairs into a broad class of fibrous protein, which has been divided into two major classes' alpha keratins and beta keratins.

Solomon *et al.* (1986) described that alpha keratins are characterized by a helical structure whereas beta keratins have a beta pleated structure, either form of keratinization produces extremely hard keratin (sea turtle shell scutes, horn sheath, hoof ungus,claw angus) which provide external protection to mammals and reptiles.

Griebenow *et al.* (1992) reported that the spectra of wool fiber which displayed the characteristic absorption bands of proteins at $1630cm^{-1}$ (amide I) $1515cm^{-1}$ (amide II) and $1230cm^{-1}$ (amide III). Amide I primarily a C=O stretching vibration while amide II

and amide III are heavily mixed vibrational modes. In particular, amide III results from N-H bending and C-N stretching vibrations. Amide III is a very complex range resulting from in phase combination of C-N stretching and N-H in plane bending with some contribution from C-C stretching and C=O bending vibrations. Amide I, II and III are very important bands because from their position and shape information about protein structure and conformation can be derived. In fact hydrogen bonding steric situation and environment properties is known to influence the frequencies of the amide vibrations. However, amide II and III are vibrational modes and correlation between bands shape and the structure of proteins may become rather questionable. For this, it has been decided to study the shifts and shape of amide I.

Gallagher *et al.* (1992) studied FTIR spectroscopy which provides information about the secondary structure content of proteins, unlike X-ray crystallography and NMR spectroscopy which provide information about the tertiary structure. FTIR spectroscopy works by shining infrared radiation on a sample and seeing which wavelengths of radiation in the infrared region of the spectrum are absorbed by the sample. Each compound has a characteristic set of absorption bands in its infrared spectrum. Characteristic bands found in the infrared spectra of proteins and polypeptides include the Amide I and Amide II. These arise from the amide bonds that link the amino acids.

The absorption associated with the Amide I band leads to stretching vibrations of the C=O bond of the amide, absorption associated with the Amide II band leads primarily to bending vibrations of the N—H bond .Because both the C=O and the N—H bonds are involved in the hydrogen bonding that takes place between the different elements of secondary structure, the locations of both the Amide I and Amide II bands are sensitive to

the secondary structure content of a protein. Studies with proteins of known structure have been used to correlate systematically the shape of the Amide I band to secondary structure content. The Amide II band, though sensitive to secondary structure content, is not as good a predictor for quantitating the secondary structure of proteins. One difficulty with analyzing the Amide I band for secondary structure is that the shifts in the Amide I band are small compared to the intrinsic width of the band. Instead of a series of nicely resolved peaks for each type of secondary structure, one broad lumpy peak is observed several numerical methods are used to increase the apparent resolution of the Amide I band so that estimates can be made of the secondary structure content (Gallagher *et al.*, 1992)

Rintoul *et al*. (1998) and Lyman *et al*. (2001) used HATR-FTIR in examining hard biological tissues, which stands out for its robustness, ease of sample preparation, simplicity of operation and the ability to make structural elucidations. The resolving power of FT–IR has been applied in such diverse fields as forensic fiber identification (Kirkbride and Tungol, 1999) and bacterial species identification (Timmins *et al.*, 1998). Discriminant analysis (also known as linear discriminant analysis or canonical variates analysis) of vibrational spectra (Raman or infrared) has been successfully used to extend the limitation inherent in vibrational data. Examples include confirmation of edible oils and fats (Baeten and Aparicio, 2000), bacterial taxonomy (Amiel *et al*., 2001), sub-typing of nylon polymers (Enlow *et al*., 2005), the forensic characterization of printer toners (Egan *et al*., 2003), geographical sourcing of medicinal plants (Dharmaraj *et al*., 2006), forensic identification of fingernails versus toenails (Widjaja and Seah, 2006) and the forensic identification of fiber blends (Espinoza *et al*., 2006).

Alibardi (2000a, 2003b, 2003c) has revived the selective advantage of inheriting alpha keratins verses beta keratins.

Pielesz *et al*. (2000) studied the identification of structural changes in the keratin of wool fibre with an azo dye using Raman and Fourier transform Infrared spectroscopy methods. They found changes were observed in the region of Amides I and II and the fingerprint region. For FT-Raman Spectroscopy, changes were observed in the region of S–S bonds, tyrosine and methionine regions and the fingerprint region (1100–900 cm^{-1}). The percentage of share of particular conformational forms of keratin (α-helix, disordered, β-sheet) was observed. the amide I mode was resolved into three Gauss-shaped bands corresponding to α-helix (1654 cm^{-1}), β-sheet (1680 cm^{-1}) and undefined (1667 cm^{-1}) structure .The phenylalanine peak at 1003 cm^{-1} was chosen as a reference band. A frequently compared FT-IR measured region is the 1650–1550 cm^{-1} range, i.e. the region of Amide I and Amide II vibrations.

For the untreated sample a clear band of the a-helical structure, a disordered structure, is visible, for vibrations of both Amide I (1652 cm^{-1}) and Amide II (1541 cm^{-1}).

Panayioutou (2004) described the spectral analysis of cat fur, parrot feather, human hair, horse hair, cow hair, sheep wool and dog hair by using FTIR spectroscopy followed by chemometrics analysis. She stated that amide A and amide B were found in the 3300-3050 cm^{-1}. Spectral features in these regions are assigned to the stretching modes of the C-H lipid alkyl chains. The methyl (CH_3) assignment and symmetric modes are observed at 2955cm^{-1} and 2933cm^{-1} respectively and methylene (CH_2) asymmetric and symmetric modes at 2875 cm^{-1} and 2855cm^{-1}.

The wave number region between 1700-1500cm^{-1} contained the most intensive feature in the IR spectra arising from the –CONH grouping, predominantly from protein structure such as amide I and amide II band at 1657cm^{-1} and 1537cm^{-1} respectively. The region in between 1200-400cm^{-1} contains one of the most important bands, which was attributed to the cystic acid vibration at 1040cm^{-1}.

Movasaghi *et al.* (2008) studied the biochemical compounds (lipids, proteins, nucleic acids) and the chemical structure of these compounds can be evaluated using peak frequencies at 2956 cm^{-1} (asymmetric stretching vibration of CH_3 of acyl chains), 2922 cm^{-1} (asymmetric stretching vibration of CH_2 of acyl chains), 2874 cm^{-1} (symmetric stretching vibration of CH_3 of acyl chains), 2852 cm^{-1} (Symmetric stretching vibration of CH_2 of acyl chains), and 1600–1800 cm^{-1} (C=O stretching).

The specifications of protein contents of biological samples can also be understood from 1717 cm^{-1} (amide I, arising from C=O stretching vibration), 1500–600 cm^{-1} (amide II, N-H bending vibration coupled to C-N stretching), and 1220–1350 cm^{-1} (amide III, C-N stretching and N-H in plane bending, often with significant contributions from CH_2 wagging vibrations). The peaks related to nucleic acids were as follows: 1717 cm^{-1}(C=O stretching vibration of purine base), 1666 cm-1 (C=O stretching vibration of pyrimidinic base), and 1220–1240 cm21 (asymmetric PO_2 ^{2} stretching), 1117 cm^{-1} (C-O stretching vibration of C-OH group of ribose), 1040–100 cm^{-1}

Jalkanen *et al*. (1991) used vibrational spectroscopy to study protein and DNA structure, hydration, and binding of bimolecular, as a combined theoretical and experimental approach. The system studied systematically was the amino acids, peptides,

and a variety of small molecules. The goal was to interpret the experimentally measured vibrational spectra for these molecules to the greatest extent possible and to understand the structure, function, and electronic properties of these molecules in their various environments. It was also believed that the application of different spectroscopic methods to biophysical and environmental assays is expanding, and therefore a true understanding of the phenomenon from a rigorous theoretical basis is required.

Fabian (2000) and Bandekar (1992) have described the infrared spectra of proteins exhibit absorption bands associated with their characteristic amide group. In-plane modes were due to C=O stretching, C–N stretching, N–H stretching and O–C–N bending, while an out-of-plane mode is due to C–N torsion. The characteristic bands of the amide groups of protein chains are similar to the absorption bands exhibited by secondary amides in general, and are labeled as amide bands. There are nine such bands, called amide A, amide B and amides I–VII, in order of decreasing wave number.

The amide II band represents mainly (60%) N–H bending, with some C–N stretching (40%) and it is possible to split the amide II band into components depending on the secondary structure of the protein. The position of the amide II band is sensitive to deuteration, shifting from around 1550 cm^{-1} to a wave number of 1450 cm^{-1}. The amide II band of the deuterated protein overlaps with the H–O–D bending vibration, so making it difficult to obtain information about the conformation of this band. However, the remainder of the amide II band at 1550 cm^{-1} may provide information about the accessibility of solvent to the polypeptide backbone (Fabian, 2000; Bandekar**,** 1992)

Hydrophobic environments or tightly ordered structures, such as α-helices or β-sheets, reduce the chance of exchange of the amide N–H proton. The most useful infrared band for the analysis of the secondary structure of proteins in aqueous media is the amide I band, occurring between approximately 1700 and 1600 cm^{-1} (Barth, 2000). The amide I band represents 80% of the C=O stretching vibration of the amide group coupled to the in-plane N–H bending and C–N stretching modes.

The exact wave number of this vibration depends on the nature of hydrogen bonding involving the C=O and N–H groups and this is determined by the particular secondary structure adopted by the protein being considered. Proteins generally contain a variety of domains containing polypeptide fragments in different conformations. As a consequence, the observed amide I band is usually a complex composite, consisting of a number of overlapping component bands representing helices, β-structures, turns and random structures.

Frazier (2005) stated that hawk bill scutes were typically thicker than those of other sea turtle species and is more conducive to use as a raw material source. Green sea turtles raised in captivity with high protein diets have produced relatively thick scutes that could be used in the same manner as hawk bill scutes.

Paris *et al*. (2005) used attenuated total reflectance infrared spectroscopy to differentiate hard keratin (tortoise shell and horn) from natural synthetic imitation (galalith or bakelite) though they analyzed only artifacts and did not compare their results with vouchered specimens of original species.

Espinoza *et al.* (2006) studied broad range of sea turtle and bovidae keratins using diffuse reflectance infrared Fourier transform spectroscopy (DRIFT) combined with discriminant analysis. They analyzed the absorption of the amide I, amide II and amide III peaks occurring over a broad range. The amide II moiety of the spectrum showed an intense absorption at 1516 cm^{-1}, which is characteristic of β-keratins in reptilian origin. In the Cheloniidae family, the 1516 cm^{-1} absorption was present in all individuals tested but, surprisingly, this peak was also present in the bovidae sampled. Conversely, the amide II absorption at 1543 cm^{-1} has been described as diagnostic for α-keratins, and thus mammals. However, they reported that it was present in the bovidae tested, when analyzing the keratin, the higher resolution of Raman spectroscopy allows one to differentiate between the 1543 cm^{-1} and 1516 cm^{-1} absorptions.

Mathematical post processing of the spectra employing discriminant analysis provided a useful statistical tool to differentiate tortoise shell from bovid horn keratin. All keratin standards used in their study were correctly classified with the discriminant analysis. A resulting performance index of 95.7% shows that DRIFTS, combined with discriminant analysis, is a powerful quantitative technique for distinguishing sea turtle and bovid keratins commonly encountered in museum collections and the modern wildlife trade.

Renata *et al.* (2006) used the modern technology of Fourier Transform Infrared Spectroscopy (FTIR) for textile fiber constitution and sometimes the former colors identification. The comparison of various wool fibers in FTIR spectra showed the possibility of distinguishing some animal breed wool fibers and even fibers colors. The difference in natural white and black wool fiber's spectra was obvious, the sharper

inclination and deflection for black wool spectrum in the frequencies region from 2900 cm^{-1} to 2400 cm^{-1} is noticed. The black wool spectrum has no visible peak at 3100 cm^{-1} meanwhile in the case of white wool spectrum the peak in the similar frequency zone is obvious.

In the case of Cameroon sheep wool the frequencies region was from 3500 cm^{-1} to 2850 cm^{-1} and from 1700 cm^{-1} to 1050 cm^{-1}. The analogous investigations were carried out with flax, hemp, nettle cellulose fibers and cellulose archaeological fabric. It is known that cellulose fibers are more vulnerable under than protein fibers. So the analysis contains a lot of discrepancies as well. Flax, hemp and nettle fiber's spectra have a rise peak in the frequencies about 3000 cm^{-1} and a descent peak in the frequencies about 2900 cm^{-1}. In case of archaeological textile the frequencies region was from 3200 cm^{-1} to 2600 cm^{-1} and the spectrum gradually rises (no well-defined peaks were obtained). Peak presence in archaeological textile spectrum in the frequencies region about 1700 cm^{-1}, 1650 cm^{-1} and 900 cm^{-1} showed similarity to flax fiber, but in the frequencies regions 1700 cm^{-1}, and from 1300 cm^{-1} to 1000 cm^{-1} showed similarity to nettle fiber.

Espinoza *et al.* (2007) investigated the utility of horizontal-attenuated total-reflection Fourier transform infrared (HATR FTIR) spectroscopy for the analysis and identification of tail hair of reputed elephant and giraffe origin, commonly used to manufacture indigenous artifacts (e.g. bracelets, earrings, finger rings, etc.) in the wildlife trade. They described a prominent peak at 1032 cm^{-1}, seen extensively in proboscidean standards and absent in giraffe samples. This absorption appears to be related to surface

cystine oxides and suggests that cysteic acid is one of the compounds useful for distinguishing elephant and giraffe hairs.

An examination of the second order derivative of the proboscidean spectra revealed that cysteic acid stretching [SO] at 1040 cm^{-1} and 1170 cm^{-1}) was present in the African and Asian elephant samples, which was absent in the giraffe hairs. While spectral libraries are helpful in determining the material class represented by suspected hair artifacts (i.e. keratin vs. plastic vs. botanical), mathematical post-processing of the spectra employing discriminant analysis provided a more useful statistical tool for differentiating elephant and giraffe hairs than relying on visual inspection of spectral peaks alone. A resulting performance index of 91.8% showed that HATR FTIR, combined with discriminant analysis is a reliable tool for differentiating elephant hairs from giraffe hairs (Stuart, 2004).

According to Edward and Batrick (2002) vibrational spectroscopy is applicable to a wide range of physical evidence. Because polymers are so common, they frequently play an evidentiary role in criminal cases. Polymeric materials such as fibers, paints and adhesive tapes are frequently analyzed to identify characteristic information regarding their composition. Physical and chemical information on these materials is stored in computer databases to help determine the manufacturer or, supplier, or simply to discriminate between many similar samples of material. The material was heavily filled with calcite ($CaCO_3$), identified by the intense, broad C–O antisymmetric stretch near 1450 cm1, and narrow out-of-plane and in-plane bends near 880 and 710 cm^{-1} respectively.

The IR spectrum clearly shows the resin binder features. The N–H stretch near 3350 cm^{-1}, the C–H stretches near 3000 cm^{-1}, the C=O stretch near 1730 cm^{-1}, the C–N stretch near 1540 cm^{-1}, and the typical C–O envelope from 1300 to 1000 cm^{-1} are observed in the IR. Of particular interest to paint analysis are any contributions by pigments. The weak, broad band at 868 cm^{-1} appears to be contributed by chrome yellow, as shown in the reference spectrum. However, because of the band's comparatively low intensity and lack of detail in the paint spectrum, it would be difficult to positively identify chrome yellow by this method alone (Stuart, 2004).

The peaks labeled at 659, 425 and 357 cm^{-1} are rutile,(a crystal form of titanium dioxide) is the Raman spectrum of the yellow auto paint. The major peaks at 843 and 365 cm^{-1} match up with the Raman spectrum of chrome yellow Peaks at 611 and 446 cm^{-1} are contributed by rutile, as shown in an atypical duct tape backing spectrum containing calcium carbonate (calcite). The calcite filler has a lattice band21 near 315 cm^{-1} that would not have been observed without the extended frequency range capabilities. The C–O asymmetric stretching band near 1450 cm^{-1} underlies the C–H bending band near 1460 cm^{-1}. The C–O out-of-plane bend can be observed near 880 cm^{-1}(Stuart, 2004).

Shengqing *et al*. (2011) have made work on identification of Rhinoceros horn and its substitutes by using FTIR spectroscopy. The chemical components of rhinoceros horn are made up of amino acids, cholesterol, taurine, hexosamine, phospholipids, and so on (Wang and paliwal, 2007)

Amino acid: 1650 cm^{-1} belongs to C=O stretching vibration; 3050 cm^{-1} belongs to N-H stretching vibration. Cholesterol: 3270 cm^{-1} belongs to O-H stretching vibration;

1540 cm^{-1} belongs to C=C stretching vibration. Taurine: 1116 cm^{-1} belongs to S=O asymmetric stretching vibration; 1040 cm^{-1} belongs to S=O symmetric stretching vibration; 881 cm^{-1} belongs to S-O stretching vibration. Hexosamine: 1733 cm^{-1} belongs to C=O stretching vibration. Phospholipids: 2355, 2300 cm^{-1} belongs to P-H stretching vibration; 1240 cm^{-1} double peaks belong to P=O stretching vibration. Other saturated hydrocarbons: 2920 cm^{-1} belongs to C-H asymmetric stretching vibration; 2850 cm^{-1} belongs to C-H symmetric stretching vibration; 1450 cm^{-1} belongs to C-H bending vibration.

The absorption peaks of the cattle horn's infrared spectrum at 2907 cm^{-1}, 2850 cm^{-1}, 1446 cm^{-1} were obviously weaker than those of the rhinoceros horn, which are respectively C-H asymmetric stretching, C-H symmetric stretching vibration and C-H bending vibration. And the weaker absorption peak intensity means the content of saturation hydrocarbon was lower. The cattle horn's infrared spectrum has only one absorption peak at 2350 cm^{-1}, yet the rhinoceros horn's infrared spectrum has two absorption peaks, which was P-H stretching vibration region of phospholipids; And the absorption peak intensity at1076 $cm^{-1}$of cattle horn is weaker obviously than that of rhinoceros horn, which is the S=O stretching vibration. Furthermore, there was no C=O stretching vibration absorption peaks of hexosamine at 1733 $cm^{-1}$and no S-O stretching vibration peak of taurine at 881 cm-1 in the cattle horn's infrared spectrum (Stuart, 2004).

In the yak horn's infrared spectrum, compared to that of rhinoceros horn, there were out-of-plane bending N-H vibration at 634 cm^{-1} of amino acid and NC=O symmetric stretching vibration at 1583 cm^{-1} of amino acids, and there was no P-H stretching vibration absorption peaks of phospholipids at 2350 cm^{-1} and no S-O stretching

vibration absorption peaks of taurine at 881 cm^{-1}. The absorption peaks of the goat horn's infrared spectrum at 2920 cm^{-1}, 2850 cm^{-1}, 2450 cm^{-1} were obviously weaker than those of the rhinoceros horn, which are respectively C-H asymmetric stretching, C-H symmetric stretching vibration and C-H bending vibration.

This explains the saturated hydrocarbon content of the goat horn is less as compared to the rhinoceros horn's infrared spectrum, there was no P-H stretching vibration absorption peaks of phospholipids at 2350 cm^{-1}, no C=O stretching vibration absorption peaks of hexosamine at 1733 cm^{-1} and no S-O stretching vibration absorption peaks of taurine at 881 cm^{-1} in the goat horn's infrared spectrum.

Akhtar and Edwards, (1997) recorded, the FT-Raman spectra of mammalian and avian keratotic biopolymers including bull's horn, cat's claw, bird's feather quill, pheasant's beak and compared with the hard keratinous tissue, human nail and callus. Although there were similarities in all the spectra, particularly in the ν (CH) stretching region, the 1450–1100 cm(su−1) region exhibited some differences ascribed to intramolecular skeletal backbone conformational changes. Of particular significance for human, mammalian and avian samples in the 1000–400 cm^{-1} wavenumber region were differences in the structurally important ν(SS) and ν(CS) bands, near 500 cm^{-1} and 630 cm^{-1}, respectively. The amide I and III modes near 1650 and 1250 cm^{-1} respectively, demonstrate that the mammalian keratins studied exist predominantly in the α-helical conformation, whereas the avian keratins adopt the β-sheet structure as the dominant conformation.

Paris *et al.* (2005) used attenuated total reflection infrared spectroscopy (ATR–FTIR) to differentiate hard keratins (tortoiseshell and horn) from natural synthetic imitations (galalith or bakelite), though they analysed only artifacts and did not compare their results with vouchered specimens of known species origin. Edwards *et al*. (1998) differentiated horn and turtle keratin with Raman spectroscopy, though their sample sizes were relatively small.

2.2.9 Ivory: Morphology and internal structure

The word "ivory" was traditionally applied only to the tusks of elephants. However, the chemical structure of the teeth and tusks of mammals is the same regardless of the species of origin, and the trade in certain teeth and tusks other than elephant is well established and widespread. Therefore, "ivory" can correctly be used to describe any mammalian tooth or tusk of commercial interest. Teeth and tusks have the same origins. Teeth are specialized structures adapted for food mastication. Tusks, which are extremely large teeth projecting beyond the lips, have evolved from teeth and give certain species an evolutionary advantage. The teeth of most mammals consist of a root, a neck and a crown (Banerjee, and Bortolaso, 2004)

Tusk consists of a root and the tusk proper. Teeth and tusks have the same physical structures: pulp cavity, dentine, cementum and enamel. The innermost area is the pulp cavity. The pulp cavity is an empty space within the tooth that conforms to the shape of the pulp. Elephant and mammoth tusk ivory comes from the two modified upper incisors of extant and extinct members of the same order (Proboscides). The tusks of an elephant are deeply implanted into the long cylindrical sockets which are located in the bones in the anterior portion of its upper jaw. The tusk of an elephant has three distinct

regions: pulp cavity in the centre, dentine in the middle and cementum in the outmost border. Odontoblastic cells line the pulp cavity and are responsible for the production of dentine. Dentine is the main component of ivory, forms a layer of consistent thickness around the pulp cavity and comprises the bulk of the tusk. Dentine is a mineralized tissue with an organic matrix of collagenous proteins. The inorganic component of dentine is dahllite, a phosphate mineral. Dentine contains a microscopic structure called dentinal tubules which are micro-canals that radiate outward through the dentine from the pulp cavity to the exterior of the cementum border. These canals have different configurations in different ivories and their diameter ranges between 0.8 and 2.2 microns. Their length is dictated by the radius of the tusk. The three dimensional configuration of the dental tubules is under genetic control and is therefore a characteristic unique to the order. The configurations of the dental tubules are observed on the polished cross sections of elephant tusks and are called Schreger line.

Banerjee *et al.* (2008) carried out the spectral analysis of the crystallinity of carbonate hydroxyapatite, the mineral composing mammoth ivory, can be measured by evaluating its splitting factor (SF). SF is based on the increasing separation of the FTIR absorption band at 565 and 605 cm-1. The relative retention of organic material and the incorporation of carbonate, relative to phosphate were determined by comparing the heights of amide and the phosphate peaks (1640/1035 cm^{-1}) and the carbonate and phosphate ones (1420/1035 cm^{-1})

FTIR spectra were collected and described that the amide I peak (1650–1620 cm^{-1}) and the phosphate peak (PO_3^{-4}), centered at approximately 1035 cm^{-1}, were used as the respective reference absorptions for the organic and mineral components of ivory,

while the peak centered at 1420 cm^{-1} was used as the carbonate (CO_2^{-3}) reference peak. The intensity ratios *I*1640/*I*1035 and *I*1420/*I*1035 were calculated for all duplicate samples to quantify the relative retention of organic material and the incorporation of carbonate, relative to phosphate, in the inorganic matrix respectively. Absorptions at approximately 1035 and 960 cm^{-1}, typical of phosphate and at 1460, 1420 and 873 cm^{-1}, typical of carbonate in un-degraded biological apatites, indicate that the carbonate-containing hydroxyapatite structure has been substantially retained in these materials. Interestingly, high carbonate/phosphate ratios (*I*1420/*I*1035) for all samples indicate that carbonate substitution for phosphate has been a significant part of the overall digenesis of the ivory found off Goa (Sila and Ian, 2007)

Nuclear magnetic resonance, scanning and transmission electron microscopy, and Fourier Transform Infrared (FTIR) spectroscopy can be used to assess the chemistry, substitutions, and crystallinity of extant material. In FTIR spectroscopy, the functional groups in biological apatites (e.g. $HPO^{2-}4$), $PO^{3-}4$), $CO^{2}2$) absorb infrared energy at specific frequencies, which alter according to their properties and positions in the structure. FTIR spectra distinguish between enamel and bone or dentine apatites and also between major animal groups (Botha *et al*., 2004).

Recent studies (Michel *et al*., 1995) have shown that FTIR can also be used for assessing the integrity of fossil biological apatite, including enamel. It is a quick technique, which also makes minimal demands on valuable fossil material. The proportions of ‘‘type A’’ and ‘‘B’’ carbonate may alter to some extent due to fossilization resulting in another form of apatite (e.g., fluorapatite;). However, as the absorption

spectra of biological apatites differ from that of other carbonate minerals such as calcite, diagenetic minerals in fossil material can be detected (Botha *et al*., 2004).

When comparing the extant mammalian and reptilian enamel spectra, the reptilian spectra exhibit a lower overall absorbance in peak height, which is not due to sample mass as this was kept constant. In addition, the reptilian spectra have a higher (1657-cm^1) peak compared to the mammalian enamel. The (1657-cm^1) peak is thought to correspond to the N—H/O–H peak.

Botha *et al*. (2004) studied the Cynognathus and Diademodon enamel, spectra taken were indistinguishable from each other and were similar in appearance to the extant *Crocodylus niloticus* spectra. A notable feature of the Cynognathus and Diademodon spectra is are the (565-cm^1) phosphate peak in the v4 phosphate domain which has a higher absorbance than the (605-cm^1) phosphate peak, whereas the converse applies to the extant *Crocodylus niloticus* and Varanus enamel spectra.

The enamel spectra of Crocodylus niloticus and Varanus were easily distinguishable from their respective dentine spectra as the peaks in the enamel spectra are generally higher than the dentine peaks. Furthermore, the dentine (1657-cm^1) absorbance peaks were proportionately higher than the rest of the peaks in the v3 carbonate domain compared with the respective enamel peaks.

2.3 DNA Analysis

2.3.1 Markers for species characterization

A genetic marker is defined as any stable and inherited variation which is measurable or detectable by using a suitable method and subsequently be used to detect the presence of a specific genotype or phenotype other than itself which otherwise not measurable or difficult to detect (Beckman and Soller, 1987). A genetic marker may be a short DNA sequence, such as a sequence surrounding a single base-pair change (single nucleotide polymorphism, SNP), or a long one, like minisatellites.

Species characterization requires knowledge of genetic variation that can be effectively measured within and between populations. Such variations may be of morphological or anatomical origin and are called 'classical markers'. Besides these, certain chromosomal abnormalities (numerical or structural) may also serve as markers, termed as 'chromosomal markers'. In addition, the variations in macromolecules present in body fluids and tissues that are detectable by immunological (e.g., blood groups, MHC, etc.) and electrophoretic (e.g. isozymes, milk proteins, blood proteins, etc.) methods may also serve as markers, referred to as 'biochemical markers'. Classical and chromosomal markers usually have low degree of polymorphism and/or heterozygosity and are therefore not very useful for genome analysis.

Some commonly used types of genetic markers are, RFLP (Restriction fragment length polymorphism), SSLP (Simple sequence length polymorphism), AFLP (Amplified fragment length polymorphism), RAPD (Random amplification of polymorphic DNA),

VNTR (Variable number tandem repeat), Microsatellite polymorphism, SSR (Simple sequence repeat), SNP (Single nucleotide polymorphism), STR (Short tandem repeat), SFP (Single feature polymorphism), DArT (Diversity Arrays Technology) and RAD markers (Restriction site associated DNA markers).

One of the most important advances in the field of forensic science has been the use of genetic markers to identify the source of biological materials. The same technologies are used in human forensics which may also be applied to crimes involving the trade of endangered species.

2.3.2 Molecular markers

Due to the tremendous progress in the field of molecular biology, a new class of markers called 'molecular markers' or 'genomic markers' have originated during the last two decades. It is apparent that almost unlimited number of genetic polymorphism at the DNA sequence level have provided a number of markers for effective species characterization, such as traditional restriction fragment length polymorphism (RFLP) (Foran *et al.,* 1997), minisatellites or variable number of tandem repeats (VNTR), microsatellites (Shankaranarayanan *et al.*,1997), mitochondrial analysis (Shankaranarayanan and Singh, 1998), PCR-RFLP (Saiki *et al.*, 1988) and random amplified polymorphic DNA (RAPD) (Williams *et al.*, 1990; Welsh and McClelland, 1990).

2.3.3 DNA isolation

In wild animals, the ideal sources of nucleated cells for the isolation of genomic DNA are blood (Jean *et al.*, 2005), old tissue samples (Qiu-Hong and Sheng-guo, 2003),

hair and scat (Foran *et al.*, 1997). Sambrook *et al.* (1989) opined that the primary objective of the isolation process is to recover the maximum yield of high molecular DNA devoid of protein and other enzyme inhibitors. Phenol-chloroform method is the common method for the isolation of genomic DNA from nucleated cells (Blin and Stafford, 1976; Beckmann and Soller, 1987; Andersson *et al.*, 1986; Montgomery and Sise, 1990 and Gutierrez-Ada *et al.*, 1997). However, phenol is corrosive and toxic and the extraction steps are time consuming, limiting the number of samples that can be processed at a time (Montgomery and Sise, 1990). Huges and Goroscope (1991) described a procedure to isolate DNA from skin samples.

Clinical specimens are often formalin-fixed and paraffin-embedded before histological evaluation. With the increasing significance of molecular markers in the prognosis and selection of therapies, molecular gene analysis of these formalin-fixed, paraffin-embedded tissues (PET) may become routine clinical practice. However, isolating high-quality genomic DNA from formalin-fixed PET can be difficult because only minimal amounts of intact DNA may be present in the sample. Because of this, analysis of the recovered DNA is generally limited to polymerase chain reaction (PCR). In fact, it is challenging to amplify long DNA fragments [larger than 300 base pairs (bp)] because of the poor quality of extracted genomic DNA. The success of PCR amplification of genomic DNA from formalin-fixed PET is critically dependent on a multitude of factors including the handling of specimen before tissue fixation, type of fixative, fixation time, storage time and temperature, histological stains, and PCR conditions sample (Wu *et al., 2002*).

2.3.4 Random Amplified Polymorphic DNA (RAPD)

Williams *et al.* (1990) described a method for identifying genetic polymorphism called RAPD, which is based on PCR amplification of genomic regions using short primers of arbitrary sequence. They observed that RAPD markers, simply detected as DNA segments of the same length amplified from one individual but not from another, are inherited in Mendelian fashion and can be used to construct genetic maps in a variety of species. Williams *et al.* (1990) reported the principle of the RAPD technique. The technique requires only small amount of DNA and no prior knowledge of the genome in question is required. This technique is based on random amplification by a single, shorter primer (9 or 10 bases) of arbitrary sequence at lower annealing temperature than the average PCR reaction. Reaction products are analysed by electrophoresis in agarose gels and ethidium bromide staining. A DNA-based method of species identification uses random amplification of polymorphic DNA (RAPD) (Lee & Chang 1994; Martinez & Yman 1998). This method allows a certain "fingerprint" to be created for each animal.

2.3.5 Nature of polymorphism

RAPD polymorphisms result from sequence differences in one or both of the priming sites, which prevent primer annealing. Williams *et al.* (1990) demonstrated the sensitivity of the assay for detecting single base mismatches between the primer and template. RAPD polymorphisms can also result from mutations (eg. deletions, insertions and inversions) that affect the presence and/or orientation of the primer binding sites, alter the size of the region between these sites or prevent amplification.

They may also result if secondary structures form around the primer annealing sites during the relatively low annealing temperatures (Bowditch *et al.*, 1993).

RAPD polymorphisms are typically detected as the presence or absence of particular fragments after gel electrophoresis. However, other types of polymorphisms (e.g. length and brightness) have also been identified (Williams *et al.*, 1990; Echt *et al.*, 1992; Hunt and Page, 1992; Williams *et al.*, 1993 and Horvat & Medrano, 1994). The polymorphisms may be a result of amplification of a tandem repeat locus that is polymorphic for copy number or differential amplification due to sequence difference in the priming sites (Caetano-Anolles *et al.*, 1991; Hunt and Page, 1992).

2.3.6 Genome distribution

The distribution of RAPD markers throughout the genome is an important consideration when evaluating the usefulness of these markers.

Wardell *et al.* (1993) reported that the RAPD markers were dispersed throughout the mouse genome, with at least one marker localized on each autosome, while a group of eight RAPD markers was also been assigned to the Y-chromosome.

Cushwa *et al.* (1996) reported that among 45 RAPD markers in sheep, forty were distributed among 17 of the 26 autosomes, while the remaining five markers were assigned to the sex chromosomes.

2.3.7 Factors influencing the assay reproducibility

The consistent reproducibility of any genetic marker is an important characteristic. Since the outcome is very sensitive to the amplification conditions,

there are potential problems with the reproducibility of the pattern (Yu and Pauls, 1992). RAPD assay is often used to identify individuals or populations. Bowditch *et al.* (1993) opined that the reproducibility of an individual RAPD reaction should be high. A number of factors have been shown to influence the reproducibility of RAPD markers.

2.3.8 Components of PCR

2.3.8.1 DNA polymerase

The outcome of a RAPD band pattern may depend on the type of polymerase used. The most commonly used Taq DNA polymerase is isolated from *Thermus aquaticus*. A recommended concentration of Taq DNA polymerase varied between 1 and 2.5 units (Lawyer *et al.*, 1989) per 100 µl reaction mixture when other parameters are optimum. While optimizing a PCR, Innis and Gelfand (1990) recommended the testing of enzyme concentration ranging from 0.5 to 5.0 units per 100µl and assaying the result by gel electrophoresis. Too high enzyme concentration resulted in the accumulation of nonspecific background products, while at too low concentration of enzyme, the yield was insufficient.

Schierwater and Ender (1993) did not observe any substantial variation due to commercial preparation of the same enzyme, while significant variation in the observed RAPD amplification patterns resulted from the use of five different types of DNA polymerases (*T. aquaticus, T. flavus, T. thermophilus, Thermococcus litoralis* and *Pyrococcus sp.*).

Meunier and Grimont (1993) reported that variability in commercial preparations of Taq DNA polymerase was a major source of variation in RAPD reactions.

Jayasankar and Dharmalingam (1997) reported that the same DNA template amplified with two different commercial brands of Taq DNA polymerases generated different bands.

2.3.8.2 Deoxyribonucleoside triphosphates (dNTPs)

High purity deoxyribonucleoside triphosphates (dNTPs) are supplied by several manufacturers either as four individual stock solutions or as a mixture of all four dNTPs.

Many stock solutions now supplied are already adjusted to pH 7.5 with NaOH. PCR is normally performed with dNTP concentrations around 100μM, although at lower dNTP concentrations (10-100μM) Taq DNA polymerase has a higher fidelity (Innis *et al.*, 1988). The four dNTPs have to be used at equivalent concentrations to minimize misincorporation errors (Innis and Gelfand, 1990). The optimal concentration of dNTPs depends on several factors including $MgCl_2$ concentrations, reaction stringency, primer concentration, length of the amplified product and number of cycles of PCR (Eckert and Kunkel, 1990).

2.3.8.3 RAPD primers

In the RAPD assay, a single oligonucleotide primer of arbitrary sequence is used for the PCR reaction.

Williams *et al.* (1990) suggested that the minimum useful primer length was an oligonucleotide of nine bases and that the G + C content in an oligonucleotide of 10-mer should be 40 per cent or greater to generate detectable levels of amplification products. Caetano-Anolles *et al.* (1991) also suggested that the number of amplified products may be related to the G + C content of primers and template DNA sequence rather than to the primer length.

If two of the primers anneal to the template on opposite strands, in the appropriate orientation and within amplifiable distance, then a discrete fragment will be amplified. Each RAPD primer is potentially capable of amplifying a number of fragments (1 to 10 or more) from different loci during the same PCR reaction (Waugh and Powell, 1992).

Yu and Pauls (1992) and Ellsworth *et al.* (1993) opined that RAPD primers might not consistently produce scorable banding patterns.

Differences among random primers in the estimation of intra and interpopulation relationships by RAPD may be due to minor changes in the PCR reaction conditions (Hedrick, 1992; Bardakeri and Skibinski, 1994).

The primer design is usually constrained by three factors, viz., G + C percentage (50-70per cent), no palindromes greater than 6 bases and no complementarity at the 3’ end (Williams *et al.*, 1993).

Rothuizen and Wolferen (1994) identified that reactions with two different primers tended to produce more different amplification products than single primer reactions.

According to Smith *et al.* (1996), the level of intra and interpopulation differences varied with the type of random primers used in the RAPD analysis.

Gu *et al.* (1997) concluded that by selecting primers with high GC content, RAPD analysis could be successfully applied to identify polymorphic markers even in inbred populations.

2.3.8.4 Template DNA

Optimal concentration of template DNA per reaction may vary substantially from typical conditions (25 ng per reaction) depending on the primer-template combination used (Carlson *et al.*, 1991).

Micheli *et al.* (1994) stated that ethanol perceptible contaminants in DNA extracted by standard techniques were a major source of variability in RAPD reactions.

Jayasankar and Dharmalingam (1997) did not find the DNA template concentration to be a decisive factor within a wide range of 1-200 ng. Total genomic DNA extracted from frozen, buffered and frozen or alcohol preserved and frozen tissues yielded uniform results in RAPD-PCR.

DNA with OD ratio of A260nm/A280nm ranging from 1.6 to 2.0 was found to be sufficiently pure for PCR reaction (Sambrook *et al*, 1989; Koh *et al*, 1998)

2.3.9 Conditions of PCR

The polymerase chain reaction (PCR) program commonly used for RAPD analysis with random 10-mers included a one min template denaturing step at 94°C, a

one min primer annealing step at 36°C and a two min primer extension step at 72°C (Williams *et al.*, 1990).

A PCR program with a denaturing time of 10 sec was found to give better PCR product yields than programs with 30 sec or 60 sec denaturation times (Nagaraja, 1998). Yu and Pauls (1992) found that it is better to use shortest possible denaturation temperature. These authors also observed an interaction between the time required for primer annealing and the GC content of the primers. For the primers containing 50 to 80 per cent GC, 30 sec of annealing time appeared to be sufficient to obtain a complete RAPD pattern. They also observed a direct correspondence between the extension time and the maximum size of fragment that was amplified. For amplification of PCR products shorter than 1.5 kb, 30 sec of extension time was sufficient but longer PCR products required a longer extension time. Fragments as large as 3 kb were amplified with 1 min extension time. Further, these workers also noticed that no large differences in band intensity were found among PCR products obtained from programs run for 35, 55 or 75 cycles. This result was attributed to Taq DNA polymerase inactivation overtime or be indicative that some other components in the reaction mixture become limiting at high cycle numbers.

2.3.10 Applications of RAPD

2.3.10.1 Identification of breed or species specific markers

Bardakeri and Skibinski (1994) used RAPD for species and subspecies identification of tilapia fish. Rossetto *et al*. (1995) used RAPD analysis in devising conservation strategies for the rare and endangered *Grevillea scapigera* (Proteaceae). Lee

and Chang (1994) used RAPD PCR fingerprints in identification of different livestock species for forensic purpose.

Rao *et al*. (1996) used RAPD analysis to detect species-specific genetic markers in farm animals.

Shankaranarayanan *et al.* (1997) conducted RAPD analysis of Asiatic lions and tigers. Randomly amplified polymorphic DNA (RAPD) analysis of 38 Asiatic lions which existed as single population in the Gir forest sanctuary, showed an average heterozygosity of 25.82 per cent with four primers. Based on these results they concluded that low genetic variability might be the characteristic feature of these species and not the result of intensive inbreeding. DNA fingerprinting studies of Asiatic lion and tigers have helped in identifying individuals with high genetic variability, which can be used for conservation breeding programs. RAPDs were judged to be an effective method for identifying genetic polymorphisms that were line-specific and species-specific.

Singh *et al*. (2004) successfully used RAPD technique for identification of Morel species. Ilhak and Arslan (2003) identified raw meats from beef, lamb, goat and wild swine using a 10-base primer. Lee and Chang (1994) differentiated muscle samples of beef, goat, pork, dog, rat, rabbit, chicken, duck and man using RAPD technique with two different 10-base primers. Similarly, Martinez and Yman (1998) studied identification of raw and processed meats of horse, donkey, mule, swine, Canada deer, Ren deer, sheep, goat and kangaroo using three different 10-base primers. Partis *et al.* (2000) identified 22 different animal species.

Dong *et al*. (2005) used RAPD analysis in Amur tigers to study the effective population size and effects of genetic drift on tigers and also to know the influence of management strategy (particularly reproductive strategy) on patterns of population genetic variation.

Satheesha (2006) used Primer U3, which produced specific fragments of 745bp and 440bp sizes which were specific for tigers. In case of lions a specific fragment of 296bp was uniquely observed. However, no species specific fragments were amplified with DNA samples of leopard. Primer M13 produced distinct bands of sizes 221 bp and 785 bp in tigers. The same primer also produced 290 bp and 670 bp sized fragments in leopard DNA samples. Primer D1 produced specific fragments of 464, 572, 707 and 806bp size in DNA samples of all tigers. It produced specific fragments of size 557 and 688bp size in lions and fragments of 451, 557, 670 and 785bp size in leopards.

Harini (2009) found that primer ILO 876 generated a total of 41 scorable bands from all the six species (tiger, lion, panthera, dog, cattle and sheep). It amplified DNA fragments ranging from 330bp to 553bp observed only in wild animals and fragments of sizes 383 bp and 503bp only in domestic animals.

In a recent study, Hemalatha (2012) a RAPD primer OPG – 17 and successfully used the technique for differentiating different wildlife species and primer OPG – 17 showed 6 bands in tiger, 7 bands in leopards, 4 bands in spotted deer, 4 bands in black buck and 3 bands in elephants. RAn 5 showed total scorable bands of 5 in tiger, 5 in leopard, 3 in spotted deer, 2 in black buck and 7 in elephant.

Satheesha (2006) used RAPD analysis for identification of tiger, lion and leopard tissue samples out of ten primers used, only three primers showed polymorphic tendency within and between species studied. These three primers, viz., M13, D1 and U3 were used for species characterization.

Materials and Methods

III. MATERIALS AND METHODS

3.1 Morphological studies:

The study of morphological features of the skin of bison, black buck, nilgai, Asian elephant, African elephant, cheetah and wild boar were undertaken in the Department of Anatomy and Histology, Veterinary College, Bangalore. The bison (N=10), black buck (N=10), Nilgai (N=12), Asian elephant (N=6), African elephant (N=1), Cheetah (N=5), and wild boar (N=8) skin specimens were obtained from confiscated skins received from forest and police officials and also from Zoos and National parks of Karnataka. The Asian elephant ivory samples were belonging to the laboratory collections of Department of Anatomy, Veterinary College, Bangalore. The skin samples from the lateral abdominal region and leg region were collected and cut into 2×2 cm size and fixed in 10% Neutral Buffered Formalin for a minimum of 48 hours. Further, they were processed for the routine histological techniques.

Before routine histological technique fixed skin samples were washed in running water for overnight and immersed in 4 % phenol aqueous solution for 3-5 days for thinner skin samples and 6% for thick samples such as bison, African and Asian elephant and wild pig for 8-10 days (modified Lendrum's technique, Culling,1981).

The skin samples were processed for paraffin embedding and 6 µm thick horizontal and vertical sections were cut using Thermo SCIENTIFIC-MICROM HM 325 microtome. The horizontal and vertical sections were stained with H&E Phloxine (Singh & Sulochana, 1996) for morphological studies, Weigerts resorcine fuchsin (Culling,1981) for elastic fibers, Masson's Trichrome (Luna,1968) for Collagen fibers, Ayoub-Shklar method for keratin and prekeratin and Gomori's staining method.

3.2 FT-IR spectral analysis

Hair samples from bison, black buck, Nilgai, Sambar, Asian elephant, African elephant, Indian grey wolf, cheetah and wild boar were used for hair analysis and hoof samples from bison, black buck and nilgai were also used for FTIR spectroscopy. The samples were collected from the Bannerghatta National Park, Shri Jayachamarajendra Zoological Gardens, Mysore Zoo, Police and Forest Departments. All hair and hoof samples were first sonicated for 10 minutes in water followed by 10 minutes in isopropyl alcohol and then samples were allowed to air dry and micro waved for 30 seconds prior to analysis in order to reduce the contamination.

The hair and hoof samples were analyzed and assessed using Nicolet 6700 FTIR spectrometer (Thermo Fisher Scientific Inc., Madison, WI, USA 2009) controlled by OMNIC^{TM} 8.1.11 software with Smart Orbit ^{TM}, a horizontal single reflection ATR accessory with type IIA diamond crystal mounted in a tungsten carbide plate was used. The Spectrometer was consisting of a DTGS KBr detector and KBr beam splitter. After cleaning, the sample was placed on the diamond crystal of Smart Orbit and uniformly pressed by turning pressure knob (45 pounds) of swivel pressure tower connected with a powder tip accessory.

Before recording first sample spectral acquisition, a background scan was recorded. Further for every half an hour time interval, a background scans were recorded during spectral acquisition. All the sample and back ground spectra were acquired by scanning 32 times with the resolution of 4.0 cm^{-1} and data spacing of 1.928 cm^{-1}. All spectra were acquired by setting the instrument for automatic atmosphere suppression. No other corrections were applied during spectral acquisition. The final format of the

spectra was absorbance vs. wave number (cm^{-1}) with the spectral range from 400 to 4000 cm^{-1}. The acquired spectra were subjected to automatic base line correction. The auto base line corrected spectra were used for further analysis. Each standard was properly named and minimum of 5 spectra for each standard was acquired.

Different spectral measurements were calculated by using TQ Analyst EZ^{TM} 8.0 Edition (Thermo Fisher Scientific Inc., Madison, WI, USA 2009). The spectral measurements of keratinous tissues calculated were

1. Area under curve at 11 different regions of the spectra – 3400-3100 cm^{-1}, 3100-3000 cm^{-1}, 3000-2800 cm^{-1}, 1770-1585 cm^{-1}, 1585-1480 cm^{-1}, 1480-1423 cm^{-1}, 1423-1360 cm^{-1}, 1360-1205 cm^{-1}, 1205-1140 cm^{-1}, 1140-970 cm^{-1}, 970-900 cm^{-1}.

2. Maximal height measurements at 12 different regions – 940-955 cm^{-1}, 1060-1080 cm^{-1}, 1090-1105 cm^{-1}, 1158-1172 cm^{-1}, 1185-1200 cm^{-1}, 1225-1245 cm^{-1}, 1268-1278 cm^{-1}, 1305-1327 cm^{-1}, 1385-1405 cm^{-1}, 1440-1460 cm^{-1}, 1515-1535 cm^{-1} and 1625-1645 cm^{-1}.

3. Fixed location height measurements at 28 fixed wave numbers of the spectra – 832, 876, 1009, 1043, 1076, 1101, 1126, 1156, 1173, 1230, 1311, 1343, 1368, 1386, 1402, 1450, 1497, , 1512, 1534, 1548, 1609, 1622, 1636, 1641, 1648, 1668, 1678 and 1690 cm^{-1}.

The spectral measurements of tusk calculated were

1. Area under curve at 15 different regions of the spectra – 3100-3000 cm^{-1}, 3000-2850 $cm^{-1,}$ 1700-1590 cm^{-1}, 1590-1485 cm^{-1}, 1485-1430cm^{-1} ,1430-1350cm^{-1},1350-1300

cm^{-1},1300-1260 cm^{-1}, 1260-1215 $cm^{-1,}$ 1215-1180 cm^{-1}, 1150-890 cm^{-1}, 890-825 $cm^{-1,}$ 800-630 cm^{-1}, 630-585 cm^{-1} and 585-450 $cm^{-1.}$

2. Maximal height measurements at 13 different regions – 546-562 cm^{-1}, 588-606 cm^{-1}, 650-669 cm^{-1}, 860-883 cm^{-1}, 999-1022 cm^{-1}, 1190-1211 cm^{-1}, 1230-1255 $cm^{-1,}$ 1271-1296 cm-^{1}, 1330-1348 cm^{-1}, 1396-1423 cm^{-1}, 1441-1462 $cm^{-1,}$ 1535-1560 cm^{-1} and 1620-1651 $cm^{-1.}$

3. Minimal height measurements at 12 different regions – 577-594 cm^{-1},629-660 cm^{-1}, 802-835 cm^{-1}, 879-903 $cm^{-1,}$ 1174-1194 $cm^{-1,}$ 1205-1225 cm^{-1}, 1263-1281 $cm^{-1,}$ 1288-1309 $cm^{-1,}$ 1340-1367 $cm^{-1,}$ 1419-1439 $cm^{-1,}$ 1473-1493 cm^{-1} and 1574-1597 $cm^{-1.}$

4. Fixed location height measurements at 31 fixed wave numbers of the spectra – 467, 521, 556, 583, 599, 655, 667, 827, 874, 890, 958, 1012, 1111, 1181, 1202, 1217, 1240, 1265, 1285, 1300, 1338, 1361, 1401, 1430, 1453, 1485, 1544, 1553, 1590, 1629 and 1674 $cm^{-1.}$

All spectral measurements were made by applying Savitzky-Golay 9 point smoothing filter with polynomial order of 3. All spectral measures were first copied into Microsoft Excel sheet. The Area measurements of each spectrum were first normalized by dividing each area measurement by corresponding spectral area measurement at 1150-890 cm^{-1}. The maximal and minimal height spectral measurements of tusks were normalized by dividing each corresponding spectral data by maximal height measure at 1010 cm^{-1}. The fixed location height measurement data were normalized by dividing each corresponding spectral data by data at 1012 cm^{-1}. The discriminant analysis of spectral

measurements was carried out using Systat 12 for Windows® version 12.02 (Systat Software, Inc., Chicago IL USA, 2007).

In the present analysis, the spectral data of known classes were deduced first into common covariance matrix shared by the groups. The covariance matrix was used to calculate the Mahalanobis distances. These distances were calculated between the cases to be classified and the centre of each group in a multidimensional space. The Mahalanobis distances were used to calculate canonical scores and these canonical scores were used to graphically deduce group classes as canonical score plots (Systat 12, 2007).

3.3 DNA analysis (RAPD- PCR)

3.3.1 Materials

3.3.1.1 Experimental animals

The skin samples of above said species along with sloth bear were used for the RAPD-PCR analysis.

3.3.1.2 Equipments

The major equipments used in the present study are listed in Appendix **I**

3.3.1.3 Molecular biologicals, chemicals and enzymes

The molecular biologicals and chemicals used in the present study are presented in Appendix **II.**

3.3.1.4 Reagents and Buffers

The composition of reagents and buffers used in the present study are presented in Appendix **III.**

3.3.1.5 Primers

RAPD primers were obtained from Eurofins laboratory, Bioserve Biotechnologies and GeNie^{TM} Bangalore. The primers were obtained as freeze dried powder. Stock solution was prepared at a concentration of 100 pmol/µl in Nucleus Free Water (NFW).

3.3.1.6 Glassware and plastic ware

All the glassware were thoroughly cleaned and sterilized as per the standard procedures. Micro-centrifuge tubes and micro tips were autoclaved before use.

3.3.2 Isolation of genomic DNA from skin samples

DNA was isolated from skin samples as per the procedure described by Huges and Gorosope (1991) with some modifications.

About 500 mg to 1g of skin samples without formalin fixation were cut into small pieces and triturated using pestle and mortar by adding little quantity of lysis buffer as and when required. Triturated samples were resuspended in 5ml of pre warmed lysis buffer. Formalin fixed skin samples were cut into small pieces and kept for over night wash in running water and 24 hrs in PBS solution.

Proteinase-K was added at the final concentration of 40µg/ml. Then incubated at 70^0C for overnight. More proteinase K was added whenever the solution was not clear and incubated till it got cleared without any stickiness. The contents were then transfered in to Oakridge tubes, extracted once with equal volumes of Tris saturated phenol (no vortexing, gentle mixing by hand) and left for 10 minutes. Samples were mixed gently and centrifuged at 8,000 rpm for 10 minutes at room temperature. Supernatant was

transferred to another Oakridge tube and then extracted twice with phenol: chloroform (1:1). Samples were mixed gently and centrifuged at 8,000 rpm for 10 minutes at room temperature. Supernatant was transferred to another Oakridge tube, and extracted once with chloroform: isoamyl alcohol (49:1). The samples were then gently mixed and centrifuged at 8,000 rpm for 10 minutes at room temperature. Supernatant was transferred to another Oakridge tube. The aqueous phase was pooled in a single tube and added 1/10 volumes of 3M sodium acetate and 2.5 volumes of ice cold 100 per cent ethanol and refrigerated overnight for the DNA to get precipitated completely. The DNA was palletized at 4^0C, at 10,000 rpm for 10 minutes, washed with 1-5 ml ice cold 80 per cent ethanol by spinning for 15 minutes, at 10,000 rpm at 4^0C. The ethanol was then discarded and the DNA pellet was air dried (not more than 3 – 5minutes). The DNA was resuspended in 50µl NFW and kept at -20^0C till further use.

3.3.3 Determination of the yield and purity of DNA samples

From the resuspended DNA solution, 60 µl of sample was dissolved in 1,940 µl of sterile distilled water, giving a dilution of 50 times. Optical densities (OD) were measured at 260nm and at 280nm, using a 2 ml silica cuvette in a UV spectrophotometer against sterile distilled water as blank. The yield and purity of DNA samples were estimated as follows:

Concentration of DNA stock solution (µg/ml) = OD260nm x Dilution factor x 50

(An OD value of 1.00 at 260 nm is equivalent to 50 µg/ml of double stranded DNA).

Purity of DNA stock solution = OD_{260nm} / OD_{280nm}

A ratio between 1.70 and 1.90 was considered as pure DNA sample.

From the concentration of DNA stock solution, the total yield of DNA from each sample was calculated and recorded.

3.3.4 Testing of DNA samples

The quality of the DNA samples isolated was tested by electrophoresis on 2 per cent agarose gel where a bright streak of genomic DNA was observed. A uniform final concentration of 100 ng/µl was prepared by further dilution of all the samples in NFW after quantifying each DNA sample by spectrophotometer. The diluted samples were further confirmed to be of good quality by checking them on 0.7 per cent agarose gel. A single band like appearance in 5µl loaded sample indicated sufficient quantity and quality of DNA for PCR analysis.

3.3.5 Working environment for RAPD analysis

As the RAPD method uses a single short primer of arbitrary sequence and a lower annealing temperature than the average PCR reaction, even minute quantities of contaminated DNA from the work area would seriously affect the reproducibility of the analysis. Hence, special precautions were taken to maintain a sterile environment throughout the PCR amplification.

Most of the bench works like dilution of template DNA, preparation of master mix and setting up of PCR reactions were performed under laminar flow bench. The hood supplying filtered air through 0.2 µ HEPA (High Efficiency Particulate Air) filters was always sterilized with ultraviolet rays for 30 minutes before starting PCR work.

3.3.6 RAPD primers

A total of fifteen arbitrary oligonucleotide primers were used separately for amplification of genomic DNA. The GC content of the primers used was between 60 and 80 per cent. The sequence and length of the primers used are presented in Table 17.

3.3.7 Reconstitution and dilution of primers

The selected primers were obtained in lyophilized powder form from the manufacturer and were reconstituted in low TE buffer with a concentration of 100 p. mol/µl as stock solution and 20 p.mol/µl as working solution and stored at -80^{0}C and -20^{0}C, respectively.

3.3.8 PCR- RAPD analysis

The RAPD technique was standardized by varying annealing temperatures, cycle numbers and primer concentrations. Different annealing temperatures ranging from 35 to 37^{0}C were tested for reproducible amplification of DNA fragments.

To ascertain the appropriate concentration of primer, primer concentration ranging from 5 p.mol to 20 p.mol per reaction mix of 20 µl, were tested with other parameters kept constant. Various denaturing, annealing and extension durations were also tried to test the possibility of reducing the length of PCR programme.

3.3.9 PCR amplification

The amplification reaction was carried out in 0.5ml micro centrifuge tubes using programmable thermal cycler (Eppendorf). Each 20 µl reaction mix comprised of 100 ng of template DNA, one µl of primer (20 p.mol/µl), 100mM of dNTP mix, 0.33 unit of Taq

DNA polymerase, 25mM Magnesium chloride and 10x PCR buffer (Bangalore Genei). The content was mixed thoroughly by spinning for five seconds at 5000 rpm.

3.3.10 Cycling Conditions for OPG 17 and D1

The DNA was denatured initially at 94^0C for two minutes. The amplification was carried out for 35 cycles with following thermal cycling conditions.

Process	**Temperature**	**Duration**
Denaturation	94^0C	1 minute
Annealing	35^0C	1 minute
Extension	72^0C	1 minute

One final extension at 72^0C for ten minutes was included in the programme.

3.3.11 Cycling Conditions for RAn 5 and U3

94˚ C	94˚ C	35˚ C	72˚ C	94˚ C	37˚ C	72˚ C	72˚ C
5.0 min	45 sec	1 min	1.5 min	45 sec	45 sec	1 min	10 min
Initial Denaturation	X 10 cycles			X 30 cycles			Final extension

3.3.12 Agarose gel electrophoresis

After completion of PCR reaction, amplified products of DNA were separated out using 2 per cent agarose gel in a horizontal submarine gel electrophoresis unit (Bangalore Genei). Agarose was mixed in 1X Tris-borate EDTA buffer and was heated until it was

completely dissolved and was cooled to 60^0C and ethidium bromide (8µl/100ml of 1X TBE buffer) was added to the mixture and mixed thoroughly. After keeping the comb in proper position in gel casting tray, the molten agarose mixture was poured carefully on it avoiding air bubbles. After completion of gel formation in about 15 minutes, the comb was removed carefully and the gel tray was immersed in buffer tank filled with 1X TBE. The 10µl of PCR products were mixed with one-sixth volume of 6X gel loading dye and loaded into the wells. The 100 bp molecular size marker (1µl) mixed with gel loading dye (2µl) was also loaded in one of the wells. Electrophoresis was carried out at 50V till the tracing dye reached the edge of the gel. After the end of electrophoresis, RAPD bands were visualized and documented in gel documentation unit 2000 (BioRad).

3.3.13 Data analysis

All reproducible bright bands were scored for presence or absence. Further, RAPD bands were compared only on samples run in the same gel. Polymorphism was analysed for individual sample in each species and for pooled samples in each species.

Results

IV. RESULTS

4.1 Skin Morphology

4.1.1 Indian Bison:

The epidermis was stratified squamous keratinized epithelium and thicker epidermis characterized the epidermal pegs which comprised of thicker stratum corneum with 4-5 layers (Plate.1). The stratum granulosum was made up of 1 or 2 layers with keratohyaline granules. The stratum spinosum was 4-5 cell layers with a single layer of stratum basale presented melanin pigments (Plate.2). In the other areas without epidermal pegs, was thin layer of stratum corneum with 2-3 layers. The stratum granulosum was only one cell layer with keratohyaline granules (Plate.3). The stratum spinosum was consisted of 2-3 layers and stratum basale was single layer with melanin pigments. Just below the epithelium at places there was adipose tissue and also blood capillaries. The papillary zone was made up of dense fibrous connective tissue with many connective tissue cells. In the middle of reticulare zone large number of transversely cut hair follicles along with sebaceous and sweat glands and blood vessel were observed (Plate.4). The elastic fibers were more in this zone particularly surrounding the hair follicles (Plate.5).

The Compound hair follicles were uniformly distributed and were rectangular in shape (Plate.6) comprising of primary hair follicle associated with 3-4 secondary hair follicles together with their sebaceous glands (Plate.7). In addition uniformly distributed coiled tubular sweat glands were noticed which were lined by simple cuboidal epithelium. The lining cell exhibited secretory blebs on their surface suggesting apocrine mode of secretion (Plate.8). The collagen fibers were abundant as compared to smooth

muscle fiber distribution in the dermis. The capillary plexus and fine arterioles and venules comprising the vascular component of the dermis (Plate.9). Evenly distributed fine elastic fibers were present and reticular fibers were not observed within the connective tissue.

4.1.2 Black buck:

The epidermis was stratified squamous keratinized epithelium with thicker stratum corneum at the epidermal pegs than other region. The stratum granulosum was single cell layer with keratohyaline granules. The stratum spinosum was made up of 3-4 layers of cells and single layer of stratum basale both showed melanin pigments (Plate.10). The stratum papillare of the dermis consisted of loose connective tissue with large number of blood vessels and ducts of sweat glands, number of cross sections of hair follicles associated with single sided opening of sebaceous glands and erector pili muscles (Plate.11, 12). There was even distribution of elastic fibers in between the collagen fiber bundles and around the hair follicles (Plate.13). In the stratum reticulare densely packed thick bundles of collagen fibers were seen along with few muscle fibers. At the base of the stratum reticulare the collagen bundles were loosely arranged with large number of blood vessels, nerve fiber bundles and elastic fibers (Plate.14).

The compound hair follicles were densely distributed and were arranged linearly in the dermis of skin. Within the compound hair follicle there was linear arrangement of primary and secondary follicle observed (Plate.15). Each primary hair follicle was supported by 2-4 secondary hair follicles and at few places within compound hair follicle primary hair follicle was surrounded by secondary hair follicle in a semicircular shape when it was with more than 2 secondary hair follicles (Plate.16). The primary hair follicle

was always present at the center when it was present with 2 secondary hair follicles (Plate.17). Sebaceous glands were associated with each hair follicle and numerous coiled tubular sweat glands were present at few places in the dermis of skin (Plate.18). Elastic fibers were uniformly distributed among the collagen fibers and also around the hair follicles. The smooth muscle fibers were sparsely distributed between the collagen fibers and the reticular fibers were absent.

4.1.3 Nilgai:

The vertical section of skin showed that the epidermis was stratified squamous keratinized type of epithelium. The stratum corneum was made up of 2-3 cell layers thicknes. The stratum granulosum was made up of 2-3 cell layers with melanin pigments and flat nucleus. The stratum spinosum was made up of 5-7 cell layers, nuclei were more vertical and oblique in position. The stratum basale was single cell layer with vertical and obliquely positioned nucleus and had melanin pigments (Plate.19). The superficial layer of dermis, stratum papillare was made up of dense fibrous connective tissue, blood vessels and connective tissue cells were also present. The arrector pili muscles were also seen along with obliquely oriented primary hair follicles. Nerve fibers were observed running in the papillary layer which were approaching towards the basale layer of the epidermis (Plate.20). The sebaceous glands were present at one side of the primary hair follicle which was opening directly into the hair follicle. Sparsely distributed sweat glands were observed in papillary layer of the dermis (Plate.21). The deeper layer of the dermis, stratum reticulare was consisted of loose connective tissue with large blood vessels and parallelly running nerve fiber bundles.

The Compound hair follicles were densely distributed in the dermis of skin (Plate.22). The primary hair follicles were bilaterally surrounded by 2-3 secondary hair follicles. Each primary and secondary hair follicle was associated with sebaceous glands (Plate.23). The dermal connective tissue comprised of bundles of collagen and smooth muscle fibers separating the hair follicle. The fine strands of elastic fibers were present in the connective tissue and the reticular fibers were present surrounding the hair follicle bundles and blood vessels (Plate.24).

4.1.4 Wild boar:

The epidermis was stratified squamous keratinized type of epithelium. The stratum corneum was thicker and presented melanin pigments in their cells. The stratum granulosum was made up of 1-2 layers with keratohyaline granules. The stratum spinosum consisted of 4-5 layers and single layered stratum basale both demonstrated melanin pigments (Plate.25). The flattened or spindle shaped nuclei of cells of stratum corneum overlied by well defined prekeratin and keratin (Plate.26). In the dermis, stratum papillare presented loose connective tissue with large number of adipose tissue, more particularly in between the epidermal pegs (Plate.27). The stratum reticulare was mainly collagenous with sparse muscle fiber bundles and of elastic fibers (Plate.28). The bundles were arranged longitudinally, transversely and obliquely and at the base of the reticulare layer nerve fiber bundles along with blood vessels were observed. The adipose tissue was abundantly present underlying the dermis.

The compound hair follicles were sparsely distributed in the dermis of skin. Each compound hair follicle has linearly arranged three primary hair follicle and larger in size at the center (Plate.29). Each hair follicle was supported by thick layer of collagen fiber

bundles where as dermis is musculo- collagenous in nature, muscle fibres were oriented longitudinally and vertically. Elastic fibers were surrounded the hair follicles and scarcely distributed in the connective tissue (Plate.30). The reticular fibers were absent with the hair follicles and surrounding connective tissue in the dermis of skin. The uniform distributions of blood vessels were seen in the dermis. The nerve fiber entering into the hair follicle was also observed (Plate.31). No sebaceous and sweat glands were observed in the dermis of skin.

4.1.5 Asian elephant:

The vertical section of the skin of Asian elephant was lined by stratified squamous keratinized epithelium with many layers of thin stratum corneum (Plate.32). The stratum basale was made up of single layer of cells with melanin pigments. The stratum spinosum was 4-5 cell layers followed by 8-10 layers of stratum granulosum. The thickness of stratum granulosum was more around the papillary bodies (Plate.33). The stratum corneum was comparatively thin. The epidermal pegs present at various places, which were quite thin and irregular in shape causing haphazard arrangement of dermal papillary bodies (Plate.34). The papillary bodies consisted of loose connective tissue with blood capillaries in abundance than the collagen fibers. In the deeper part of the dermis the collagen fiber bundles along with muscle fibers were horizontally as well as vertically oriented (Plate.35). There was no sweat or sebaceous glands in the dermis and muscle fiber bundles were separated by interfascicular connective tissue.

The horizontal section of skin in Asian elephant showed single isolated hair follicles surrounded by loose connective tissue with collagen fibers and sparsely distributed elastic fibers in the dermis (Plate.36). A few cross sectioned muscle fiber

bundles were also sparsely distributed amongst the loose connective tissue around the hair follicles. Blood vessels seen at the periphery of the loose connective tissue around the hair follicle. Thick bundles of skeletal muscles running in different directions were found in the deeper part of the dermis.

4.1.6 African elephant:

The vertical section of the skin of African elephant was lined by stratified squamous keratinized type of epithelium with a thick keratin and prekeratin layers (Plate.37). The dermal papillae evaginated between surface epidermal interdigitations (Plate.38). The dermis consisted of dense collagenous fiber bundles with few muscle fibers. The muscle fibers were parallel to the epidermal invaginations (Plate.39).

The epithelium was made of single layer of stratum basale with 4-5 layers of stratum spinosum showed spindle or oval shaped cells with hallow space around the nucleus resembling hyaline cartilaginous cells with the presence of melanin pigment granules (Plate.40). The 7-8 layers of stratum granulosum showed keratohyaline granules followed by a thin layer of prekeratin and thick layer of keratin. The granulosum layers were thick at the zone of papillary bodies (Plate.41). The short and thick dome shaped dermal papillae were present. The papillary layer was highly vascular in nature with an indistinct reticular layer. However, muscle fiber bundles along with collagen fibers were oriented horizontally and vertically in the dermis. In the dermis just below the papillary layer collagen fibers interspersed between thick zone of muscle fiber bundles. Below this layer the collagen fibers were abundant with longitudinal and vertical orientation of muscle fibers. In the deeper part of dermis and beginning of hypodermis thick bundles of

muscle fibers were seen. A single hair follicle was also observed in the dermis below the papillary layer. There was absence of sebaceous and sweat glands surrounding the primary hair follicle in the dermis (Plate.42). The deeper dermis consisted of longitudinal and transverse orientation of muscle fibers. The loose connective tissue was present in between the muscle fiber bundles.

The Horizontal section of African elephant skin showed single isolated primary hair follicles in the dermis. The hair follicle was surrounded by vascular loose connective tissue surrounded by densely packed collagen fibers and sparse muscle fibers and then followed by a thick layer of skeletal muscle fiber bundles (Plate.43). The blood vessels and nerve fibers were visible in between the muscle fibers (Plate.44). In between the muscle fasciculi vascular loose connective tissue was noticed. A few elastic fibers and nerve bundles were found in the dermis.

In the horizontal section of the epidermo-dermal junction, the dermis of the skin was associated with surrounding epidermis as epidermal pegs due interdigitation of the skin fold which was a characteristic feature to African elephant (Plate.45). The shapes of the skin folding were hexagonal as well as oval (Plate.46). The epidermal pegs comprised peripherally corneum layer with keratin and prekeratin and followed by other epidermal layers, in the middle there was dense collagen fiber bundle along with muscle fibers and blood vessels (Plate.47).

4.1.7 Cheetah:

The surface epithelium was stratified squamous keratinized with keratin zones and at few places prekeratin zone was also observed (Plate.48). The epidermis consisted

of many epidermal pegs. The surface of epidermis was irregular. The stratum granulosum was 1-2 cell layers with keratohyaline granules and followed by the stratum spinosum with 2-4 layers and the stratum basale was single cell layer with melanin pigments (Plate.49, 50).

The vertical section of the cheetah skin presented perpendicularly oriented hair follicles in the papillary and reticular layer of the dermis (Plate.51).This cross sectional appearance of the hair follicles observed in the vertical sections of the skin can be attributed to almost oblique or parallel orientation of the hair with respect to the surface of skin. This is exemplified by the fact that the cross sectional appearance of the hair follicles were also noticed amongst the epidermal folds (Plate.52). Further, in the horizontal sections of the skin the hair follicles appeared oblique and vertical in their orientation (Plate.53). This type of arrangement of the hair follicles were observed only in the cheetah which is peculiar. It appears that the hairs emerge out of the skin almost parallel to the surface. Because of this orientation the hair coat appears to be very smooth and soft in this species. This finding is a characteristic to cheetah and not observed in any of the animal species studied and also not recorded in the literature.

The dermis consisted of stratum papillare and stratum reticulare, stratum papillare had loose connective tissue of collagen fibers and sparsely distributed elastic fibers (Plate.54). The capillaries were seen running parallel to the epidermis and also in cross section. The large number of blood vessels and connective tissue fibroblast cells were also observed. At places where there were hair follicles present showed the presence of sweat glands lined by simple cuboidal epithelium with their secretions on their surface and sebaceous glands were also opening in to the hair follicles (Plate.55). The arrector

pili muscles were also seen close to the primary hair follicles. Many histiocytes were found in the papillary zone.

In the dermis reticulare zone presented dense fibrous connective tissue and longitudinally arranged muscle fiber bundles along with nerve fiber bundles and blood vessels. There were hair follicles running longitudinal to the epidermal layer (Plate.56). The hypodermis consisted of cross cut and longitudinally oriented skeletal muscle fibers with large number of blood vessels and nerve fibers surrounded by adipose tissue (Plate.57). The hair follicles were running parallel to the epidermal layer but at places they were also running perpendicular to the epidermis (Plate.58).

The horizontal section of skin of cheetah showed uniformly distributed compound hair follicle throughout the dermis. Each compound hair follicle consisted of a primary hair follicle with 3-7 secondary hair follicles on either side of it. At the base of the primary hair follicle coiled tubular sweat glands lined by simple cuboidal epithelium with secretory blebs observed on the surface were seen along with blood vessels in between them (Plate.59). All the primary and secondary hair follicles were surrounded by loose connective tissue with peripherally arranged dense collagenous fiber bundles. All the compound hair follicles were always associated with one or two sweat glands (Plate.60). The nerve fibers were also associated with large blood vessels in the dermis. The collagen fibers were abundant compared to muscle fibers. There were no sebaceous glands observed in horizontal section of the skin.

4.2 FTIR Spectral analysis

4.2.1 FTIR Spectral analysis of Hair

Figures 1, 2, 3, 4, 5, 6, 7, 8 and 9 are the average ATR FTIR spectra of Asian elephant, Bison, Black buck, Cheetah, Indian Grey Wolf, Nilgai, Sambar, wild boar and sloth bear hair, respectively. The FTIR spectra from 400 cm^{-1} to 4000 cm^{-1} are divided into 3 spectral regions for detailed analysis viz, Spectral Region 500cm^{-1} to 1200cm^{-1}, 1200 cm^{-1} to 2000 cm^{-1} and 2000 cm^{-1} to 4000 cm^{-1}. The spectral band assignments were made according to literature on biological materials.

Spectral Region 500cm^{-1} to 1200cm^{-1}:

In hair spectral (Fig.1to 9) region 500 cm^{-1} to 1200 cm^{-1} was less conspicuous. The peaks between 600 cm^{-1} to 900 cm^{-1} were mostly due to C-H out of bending vibrations. The peak at 1069cm^{-1}, 1075 $cm^{-1,}$ and 1073 cm^{-1}, 1072 cm^{-1} in Asian elephant, black buck, Nilgai and wild boar hair, respectively and 1076 cm^{-1} cheetah and sloth bear hair were assigned to S-O symmetric stretching vibrations of cysteine monoxide residues (Espinoza *et al.* 2008). But this peak was not observed in bison, Indian grey wolf and sambar. Weak band at 1157 cm^{-1} in Asian elephant, 1175 cm^{-1} bison, cheetah and Nilgai, 1173 cm^{-1} in black buck and sambar hair, 1172 cm^{-1} and 1151 cm^{-1} in Indian grey wolf and wild boar hair, respectively and 1154 cm^{-1} in sloth bear hair were assigned to C-O stretching vibrations of C-OH group.

Spectral Region 1200 cm^{-1} to 2000 cm^{-1}:

This spectral region was mostly composed of characteristic peaks of protein amide bands. The medium Amide III band peak was observed at 1239cm^{-1} in Asian

elephant hair, 1238cm^{-1} in bison and Nilgai hair, 1235 cm^{-1} in Black buck, Indian Grey Wolf and wild boar hair, 1237 cm^{-1} in cheetah and sloth bear hair and 1236 cm^{-1} in and Sambar hair, respectively. A weak amide III band component peak was also observed at 1319cm^{-1} in Asian elephant and wild boar hair, 1313 cm^{-1}, 1312 cm^{-1}, 1303cm^{-1}, 1308cm^{-1} in bison, Black buck, cheetah, Nilgai hair respectively and 1315cm^{-1} in Indian Grey Wolf, Sambar hair and sloth bear hair.

A strong amide II band with peak at 1536 cm^{-1} in Asian elephant and wild boar hair, in addition 1540 cm^{-1}, 1522 cm^{-1} peaks were also observed in wild boar.hair. 1515 cm^{-1}, 1517 cm^{-1}, 1522 cm^{-1} and 1524 cm^{-1} was observed in Black buck, Indian Grey Wolf, Nilgai and Sambar hair respectively and 1525 cm^{-1} in bison and cheetah hair and 1530 cm^{-1} in sloth bear hair. The most intense peak in entire region of spectra of hair was Amide I band peak and was observed at 1630 cm^{-1} in Asian elephant and sloth bear hair, 1631 cm^{-1} and 1627 cm^{-1} in, wild boar (1637 cm^{-1} also observed) and cheetah hair, respectively. 1626 cm^{-1} in bison and nilgai hair**,** 1628 cm^{-1} in black buck, Indian grey wolf and sambar hair.

The medium peak at 1390 cm^{-1} in bison, black buck and nilgai hair, 1391 cm^{-1} in wild boar, 1396 cm^{-1} in, Indian grey wolf and sambar hair and 1397 cm^{-1} in Asian elephant and cheetah hair observed due to symmetric -CH_3 bending vibrations of aliphatic side chains of amino acid residues. But this peak was not observed in sloth bear.

The peak at 1449cm^{-1} in Asian elephant, Indian Grey Wolf and sloth bear hair, 1450 cm^{-1} in bison, Black buck, Nilgai and sambar hair, 1451 cm^{-1} only in cheetah hair

were assigned to asymmetric $–CH_3$ bending of proteins. This peak was absent in wild boar hair.

Spectral Region 2000 cm^{-1} to 4000 cm^{-1}

The intensity of peaks was comparatively weak in this region. The peak at 2873 cm^{-1} in wild boar, 2874 cm^{-1} in Black buck hair, 2875 cm^{-1} cheetah and Indian Grey Wolf hair and 2876 cm^{-1} found in Asian elephant, bison, Nilgai and Sambar and sloth bear hair was assigned to symmetric C-H stretching of $–CH_3$ groups.

The peak at 2917 cm^{-1} in wild boar hair which was highest peak observed in whole spectra in wild boar, 2921 cm^{-1} and 2923 cm^{-1} in Indian Grey Wolf and Black buck hair, respectively, 2922 cm^{-1} in sloth bear hair, 2926 cm^{-1} in bison and cheetah hair, 2929 cm^{-1} in Nilgai and Sambar hair and 2931cm^{-1} in Asian elephant hair, were assigned to asymmetric C-H stretching vibrations of $–CH_2$ groups.

Peaks at 2957 cm^{-1} in Indian Grey Wolf and wild boar, 2958 cm^{-1} in Black buck and sloth bear hair, 2959 cm^{-1} in cheetah hair, 2960 cm^{-1} in bison hair, Nilgai and Sambar hair and 2961 cm^{-1} in Asian elephant hair were assigned to asymmetric C-H stretching of $–CH_3$ groups.

Amide A band was observed at 3271cm^{-1} in Asian elephant, wild boar, sloth bear, bison, Indian Grey Wolf, Nilgai and Sambar hair, 3272 cm^{-1} and 3274 cm^{-1} in Black buck and cheetah hair, respectively.

Amide B band peak due to Fermi enhanced overtone of amide II was observed at 3089 cm^{-1}, 3068cm^{-1}, 3085 cm^{-1}, 3072 cm^{-1}, bison, Black buck, cheetah, Indian Grey

Wolf hair respectively, 3081 cm^{-1} in Nilgai, Sambar and Wild boar hair and 3090 cm^{-1} in sloth bear. This band peak was not found in Asian elephant.

4.2.2 FTIR Spectral analysis of Hoof

Figures 10, 11 and 12 are the average ATR FTIR spectra of Black buck, Bison and Nilgai hoof, respectively. The FTIR spectra from 400 cm^{-1} to 4000 cm^{-1} are divided into 3 spectral regions for detailed analysis viz, Spectral Region 500cm^{-1} to 1200cm^{-1}, 1200 cm^{-1} to 2000 cm^{-1} and 2000 cm^{-1} to 4000 cm^{-1}. The spectral band assignments were made according to literature on biological materials.

Spectral Region 500cm^{-1} to 1200cm^{-1}:

In hoof spectral (Fig.1to 3) region 500 cm^{-1} to 1200 cm^{-1} was less conspicuous. The peaks between 600 cm^{-1} to 900 cm^{-1} were mostly due to C-H out of bending vibrations. The peak at 1078cm^{-1} in black buck, bison and Nilgai hooves were assigned to S-O symmetric stretching vibrations of cysteine monoxide residues. Weak band at 1173 cm^{-1} in black buck, bison and nilgai were assigned to C-O stretching vibrations of C-OH group of serine, threonine and tyrosine residues.

Spectral Region 1200 cm^{-1} to 2000 cm^{-1}:

This spectral region was mostly composed of characteristic peaks of protein amide bands. The medium Amide III band peak was observed at 1238cm^{-1} in black buck and bison hoof and 1239 cm^{-1} in Nilgai hoof. A weak amide III band component peak was also observed at 1309cm^{-1} in black buck hoof, 1310cm^{-1} in bison and Nilgai hooves.

A strong amide II band with peak at 1515 cm^{-1} black buck and bison hooves and 1516 cm^{-1} nilgai hoof. The most intense peak in entire region of spectra of hair was Amide I band peak and was observed at 1632 cm^{-1} in black buck and 1633 cm^{-1} in bison and Nilgai hooves.

The medium peak at 1390 cm^{-1} in black buck, bison and Nilgai hooves observed were due to symmetric -CH_3 bending vibrations of aliphatic side chains of amino acid residues. The peak at 1450 cm^{-1} black buck, bison and Nilgai hooves were assigned to asymmetric –CH_3 bending of proteins.

Spectral Region 2000 cm^{-1} to 4000 cm^{-1}

The intensity of peaks was comparatively weak in this region. The peak at 2876cm^{-1} black buck, bison and Nilgai hooves was assigned to symmetric C-H stretching of –CH_3 groups. The peak at 2934cm^{-1} black buck, bison and Nilgai hooves was assigned to asymmetric C-H stretching vibrations of –CH_2 groups. Peaks at 2961 cm^{-1}, black buck, bison and Nilgai hooves were assigned to asymmetric C-H stretching of –CH_3 groups.

Amide A band was observed at 3273cm^{-1} in black buck, 3274 cm^{-1} bison and Nilgai hooves. Amide B band peak due to Fermi enhanced overtone of amide II was observed at 3069 cm^{-1} black buck, bison and Nilgai hooves.

4.2.3 FTIR Spectral analysis of African elephant tusk

Fig.13. represents the average primary spectrum of African elephant ivory. The results showed that Amide A peak observed at 3274cm^{-1}wave number due to O-H stretching vibration. Amide B peak was found at 3087 cm^{-1}. Very weak CH_3 stretching band peak was observed at 2980cm^{-1}. Amide I peak observed at 1633cm^{-1}. Amide II

peak was found at 1541cm^{-1}. The prominent peak at 1450 cm^{-1}was assigned to asymmetric CH_3bending mode of proteins. The weak peak at 1419 cm^{-1} was assigned C-H deformation. The medium peak at 1242 cm^{-1}was assigned to amide III. The highest peak at 1010 cm^{-1} was assigned to PO_4^{3-} III stretching. The medium peak at 872 cm^{-1}was assigned to CO_3^{2-}II stretching vibration. The broad peak at 683cm^{-1} was assigned to CO_3^{2-} IV band. The peaks at 597 cm^{-1} and 555cm^{-1} were assigned to PO_4^{3-}IV.

4.2.4 Spectral analysis of artifacts

Fig 14, represents the average primary spectra of artifacts showed that there was no O-H stretching vibration absorption peak between 3500-3000cm^{-1} the functional group responsible for this peak was amide A band. Amide I and amide II bands stretching were not visible at 1632cm^{-1} and 1515 cm^{-1}. More prominent peak found at 1720cm^{-1}, 1412cm^{-1}, 1263cm^{-1}, 1118cm^{-1}, and 872cm^{-1}. The functional responsible group is due to M-H stretching, and M-O bending of inorganic metal and halogen ions.

4.2.5 Discriminant analysis

Discriminant analysis is a multivariate statistical method that assists in the classification of data into distinct groups. In the present study, the discriminant function was used to classify keratin materials of uncertain origin. Spectral data was utilized for the discriminant analysis. Each known standard is validated by determining the mahalanobis distance of the sample from the average spectrum. The closer a sample is to a particular centroid class, the higher the likelihood that it will be classified with that particular sample. The performance index is a measure of how well a discriminant analysis method can categories spectrum from calibration standard. When the

performance index exceeds more than 90% and the wilks's lambda lies closer to zero indicates that the unknown samples were correctly assessed against a normal distribution of known samples.

4.2.5.1 Discriminant analysis of Hair

The canonical score plot of Asian elephant hair, Black buck hair, Nilgai hair were depicted in the Fig.15.The plot clearly shows segregation of individual class members into distinct 3 clusters without any overlapping of class members. The observation was further confirmed by CVA classification matrix with 100% correct class distribution of all individual class members (Table 1). Further, CVA test statistic assigns score was 0.003 for Wilks's Lambda.

The canonical score plot of Asian Elephant, Black Buck, Sambar hairs were depicted in the Fig.16. The plot clearly shows segregation of individual class members into distinct 3 clusters without any overlapping of class members. The observation was further confirmed by CVA classification matrix with 100% correct class distribution of all individual class members (Table 2). Further, CVA test statistic assigns score was 0.001 for Wilks's Lambda.

The canonical score plot of Bison, Black Buck, Nilgai hairs were depicted in the Fig.17. The plot clearly shows segregation of individual class members into distinct 3 clusters without any overlapping of class members. The observation was further confirmed by CVA classification matrix with 100% correct class distribution of all individual class members (Table 3). Further, CVA test statistic assigns score 0.023 for Wilks's Lambda.

The canonical score plot of Bison, Black Buck and Sambar hairs were depicted in the Fig.18. The plot clearly shows segregation of individual class members into distinct 3 clusters without any overlapping of class members. The observation was further confirmed by CVA classification matrix with 100% correct class distribution of all individual class members (Table 4). Further, CVA test statistic assigns score 0.015 for Wilks's Lambda.

The canonical score plot of Asian Elephant, Nilgai and Sambar hairs were depicted in the Fig.19. The plot clearly shows segregation of individual class members into distinct 3 clusters without any overlapping of class members. The observation was further confirmed by CVA classification matrix with 100% correct class distribution of all individual class members (Table 5). Further, CVA test statistic assigns score 0.003 for Wilks's Lambda.

The canonical score plot of Black Buck, Nilgai and Sambar hairs were depicted in the Fig.20. The plot clearly shows segregation of individual class members into distinct 3 clusters without any overlapping of class members. The observation was further confirmed by CVA classification matrix with 100% correct class distribution of all individual class members (Table 6). Further, CVA test statistic assigns score 0.006 for Wilks's Lambda.

The canonical score plot of bison, Nilgai and Sambar hairs were depicted in the Fig.21. The plot clearly shows segregation of individual class members into distinct 3 clusters. There was a slight overlap of clusters between Nilgai and bison and bison scored

96% accuracy in classification matrix. The overall accuracy was 96% (Table 7). Further CVA test statistic assigns score 0.021 for Wilks's Lambda.

The canonical score plot of Asian elephant, bison and sloth bear hairs were depicted in the Fig.22. The plot clearly shows segregation of individual class members into distinct 3 clusters without any overlapping of class members. The observation was further confirmed by CVA classification matrix with 100% correct class distribution of all individual class members (Table 8). Further, CVA test statistic assigns score 0.014 for Wilks's Lambda.

The canonical score plot of Asian elepant, sloth bear and wild boar hairs were depicted in the Fig.23. The plot clearly shows segregation of individual class members into distinct 3 clusters without any overlapping of class members. The observation was further confirmed by CVA classification matrix with 100% correct class distribution of all individual class members (Table 9). Further, CVA test statistic assigns score 0.002 for Wilks's Lambda.

The canonical score plot of Cheetah, leopard and tiger hairs were depicted in the Fig.24. The plot clearly shows segregation of individual class members into distinct 3 clusters without any overlapping of class members. The observation was further confirmed by CVA classification matrix with 100% correct class distribution of all individual class members (Table 10). Further CVA test statistic assigns score 0.004 for Wilks's Lambda.

The canonical score plot of cheetah, Indian grey wolf and leopard hairs were depicted in the Fig.25. The plot clearly shows segregation of individual class members into distinct 3 clusters without any overlapping of class members. The observation was further confirmed by CVA classification matrix with 100% correct class distribution of all individual class members (Table 11). Further, CVA test statistic assigns score 0.000 for Wilks's Lambda.

4.2.5.2 Discriminant analysis of Hoof

The canonical score plot of bison, black buck and nilgai hooves were depicted in the Fig.26. The plot clearly shows segregation of individual class members into distinct 3 clusters without any overlapping of class members. The observation was further confirmed by CVA classification matrix with 100% correct class distribution of bison and black buck hooves whereas, 97 % in nilgai hoof (Table 12). Further, CVA test statistic assigns score 0.007 for Wilks's Lambda.

4.2.5.3 Discriminant analysis of Tusk

To compare African elephant tusk, Asian elephant and wild boar tusk were used in discriminant analysis. The canonical score plot of African elephant tusk, Asian elephant and wild boar tusk were depicted in the Fig.27. The plot clearly shows segregation of individual class members into distinct 3 clusters without any overlapping of class members. The observation was further confirmed by CVA classification matrix with 100% correct class distribution of all individual class members (Table 13). Further CVA test statistic assigns score 0.001 for Wilks's Lambda.

4.3 DNA Analysis

4.3.1 DNA Isolation:

In the present study, DNA was isolated from skin samples. About 300-350 μg of pure genomic DNA could be isolated from each skin sample. The purity of most of the DNA samples extracted was good as indicated by the OD 260/280 ratio which ranged between 1.7 and 1.9. However, some samples where DNA extracted from skin had OD ratio of below 1.7 were further subjected to purification before use. Overall, fifty two DNA samples were isolated from skin samples.

The quality of DNA isolated was also tested by electrophoresis on 0.8 per cent agarose gel where a bright streak of genomic DNA was observed (Fig 28). A uniform final concentration of 100 ng/μl of DNA was prepared by further dilution of all the samples in TE buffer after quantifying each DNA samples by Spectrophotometer (thermo scientific) by nano drop method (Fig.29, 30). The diluted samples were further confirmed to be of good quality by checking them on 0.7 per cent agarose gel. A streak like appearance indicated sufficient quantity and quality of DNA for PCR analysis.

4.3.2 PCR-RAPD:

RAPD analysis was carried out with 15 different oligonucleotide random primers. The RAPD technique was standardized by adopting various annealing temperatures, cycle numbers and primer concentrations. Three annealing temperatures of 35, 36 and 37^0C were tested for reproducible amplification of DNA fragments. Out of these three annealing temperatures, 35^0C was found to be ideal for OPG 17 & DI and 37^0C for RAn

5 & U3 which gave a consistent result on all the samples, while higher temperatures resulted in amplification with very few fragments.

The appropriate primer concentration was also tested ranging from 5 pmol to 20 p.mol per reaction mix of 20µl. Higher concentration of primer sometimes did not produce distinct bands, and a streak of DNA also appeared along with the bands. A primer concentration of 20 pmol per reaction volume of 20µl was found to be ideal for optimum result.

Another parameter of PCR programme tested was the number of cycles. No significant variation in the band intensity was found among PCR products obtained when the reaction was run for 35 and 40 cycles.

The PCR product was electrophoresed on two per cent agarose gel and high contrast bands were visible and documented in Geldoc unit (BioRad 2000).

4.3.3 Screening of RAPD primers:

Out of the fifteen random primers tested for DNA polymorphism in wild animals, eight primers, namely RAn1 to RAn4 and RAn6 to RAn9 could not amplify any sample. Among the six primers which amplified the DNA, three primers namely ILO 876, ILO 526 and RAn10 were found to produce non polymorphic fragments and hence were not used for further analysis.

In all, four primers namely U3, D1, OPG 17 & RAn5 were used for polymorphic studies within and between different wild animal species. These primers produced consistent polymorphic banding patterns.

4.3.4 RAPD-PCR variation:

Random primers U3, D1, OPG 17 & RAn5 amplified polymorphic fragments on DNA isolated from skin samples of wild animals. These four primers generated a total of 12 scorable bands in sloth bear, OPG 17, RAn5, and D1 primers generated 19 scorable bands in bison and 11 scorable bands in black buck and 14 scorable bands in cattle, OPG 17, D1 and U3 primers generated 12 scorable bands in black buck and OPG 17 alone generated 3 scorable bands in cheetah. All scorable bands mentioned above were ranging in size from approximately 110 to 1400 base pairs (bp). All the four random primers yielded amplified fragments that were consistently polymorphic and specific between the species (Table 18).

4.3.4.1 Primer OPG 17:

Primer OPG 17 was found to produce high polymorphic fingerprints among DNA pools of different types of wild animals (Figs 31). It generated a total of 31 scorable bands from all seven wild animals (Tables 18). Fragments of 550 bp, 600 bp, 690 bp (brightest), 800 bp and 950 bp were amplified in bison, 400 bp, 500 bp (brightest), 700 bp and 850 bp fragments recorded in black buck, 320 bp, 700 bp and 800 bp (brightest) observed in nilgai, fragments of 550 bp, 700 bp (brightest), 800 bp, 820 bp and 1400 bp were amplified in cattle, 390 bp and 600 bp (brightest) seen in wild boar, 280 bp, 300 bp, 400 bp (brightest), 500 bp and 700 bp were amplified in sloth bear, 400 bp, 500 bp and 800 bp (brightest) were amplified in cheetah. There was not much variation in banding patterns among individuals within species.

4.3.4.2 Primer RAn5:

The primer RAn5 produced moderate polymorphic fingerprints. It generated a total of 22 scorable bands from Bison, Black buck, Nilgai, Cattle and Wild boar. The fragments ranged from approximately 150 bp to 1000bp. A high percentage of polymorphism (Fig 32) was observed in different wild animal species. Fragments of 300bp, 390 bp, 450 bp, 550 bp (brightest), 800 bp and 900 bp were amplified in bison, 300 bp (brightest), 400 bp and 750 bp observed in black busk, 250 bp, 550 bp, 600 bp, 800 bp and 1000 bp (brightest) recorded in nilgai, 280 bp, 400 bp (brightest) and 900 bp were amplified in cattle and in wild boar fragments amplified were 200 bp, 400 bp (brightest) and 600 bp.

4.3.4.3 Primer D1

Primer D1 generated a total of 19 scorable bands from bison, black buck, cattle, wild boar and sloth bear (Figs. 33). Fragments of approximately 120 bp, 450 bp, 550 bp (brightest), 650 bp , 750 bp and 950 bp were amplified in case of bison, 110 bp, 150 bp (brightest) and 290 bp were amplified in black buck, in case of cattle 300 bp, 450 bp, 550 bp and 720 bp (brightest) fragments were observed, 120 bp, 190 bp (brightest) and 300 bp recorded in wild boar and 180 bp, 200 bp (brightest) and 250 bp found in sloth bear.

4.3.4.4 Primer U_3:

The primer U3 produced polymorphic fingerprints only in wild boar and sloth bear (Figs. 34). It generated a total of 5 scorable bands from these two animals. The fragments ranged from approximately 210bp to 450bp. Fragments of approximately 220bp and 450bp (brightest) were amplified in case of wild boar and in sloth bear fragments were amplified at 100bp, 210bp (brightest) and 320bp.

Plate 1. Photomicrograph showing epidermis with epidermal pegs (Arrows) in the vertical section of skin of Indian bison. H & E- Phloxine X 100.

Plate 2. Photomicrograph showing epidermis with epidermal layers in the vertical section of skin of Indian bison.(SB-Stratum Basale, SS-Stratum Spinosum, SG-Stratum Granulosum, SC-Stratum Corneum) H & E- Phloxine X 400.

Plate3. Photomicrograph showing epidermis with only one cell layer of stratum granulosum with keratohyaline granules (Arrow) in the vertical section of skin of Indian bison. H & E- Phloxine X 200.

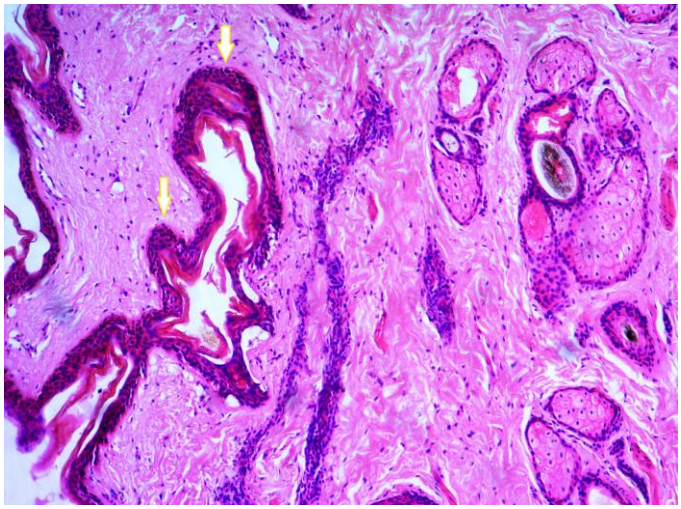

Plate 1.

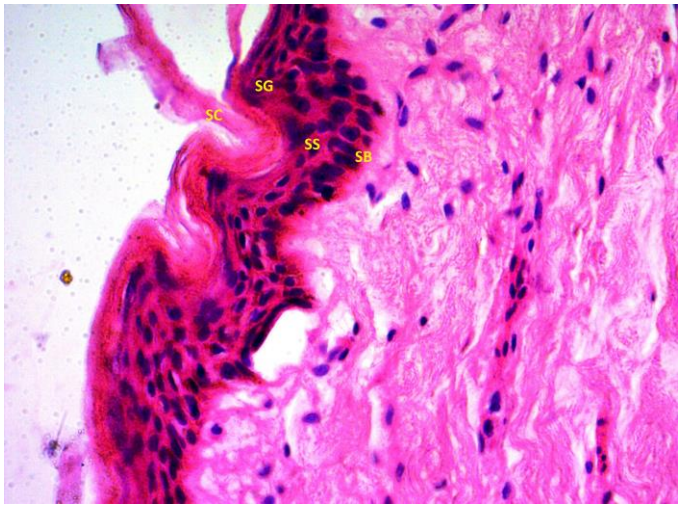

Plate 2.

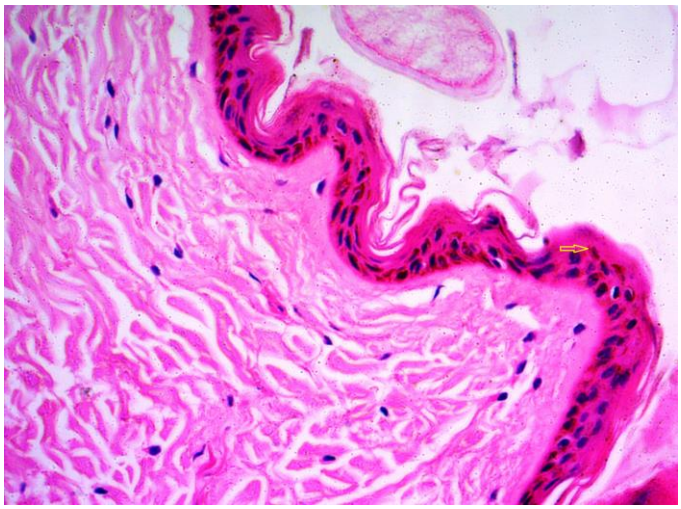

Plate 3.

Plate 4. Photomicrograph showing transversely cut hair follicles along with sebaceous (Sb) and sweat glands (Swt) and blood vessel (BV) in the middle of reticulare zone in the vertical section of skin of Indian bison. H & E- Phloxine X 100.

Plate 5. Photomicrograph showing the elastic fibers (Arrows) surrounding the hair follicles in the vertical section of skin of Indian bison. Weigert's X 200.

Plate 6. Photomicrograph showing uniformly distributed rectangular shape Compound hair follicles in the horizontal section of skin of Indian bison. Masson's Trichrome X 40.

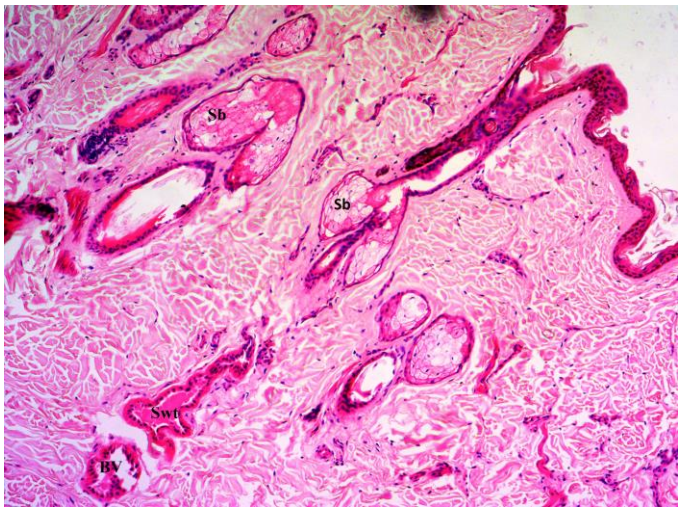

Plate 4.

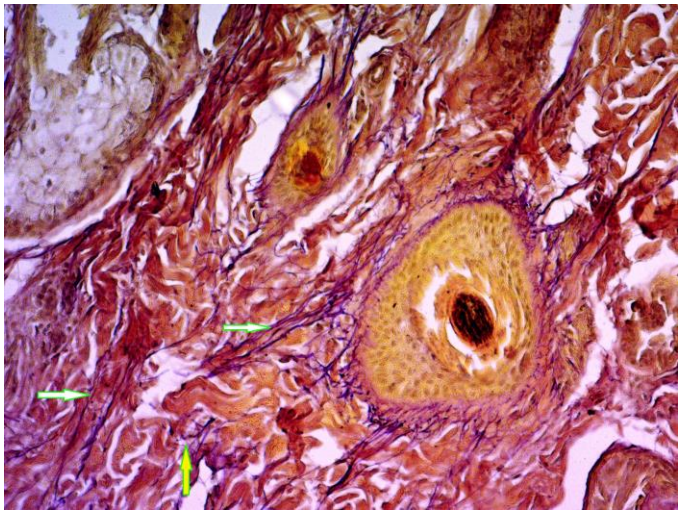

Plate 5.

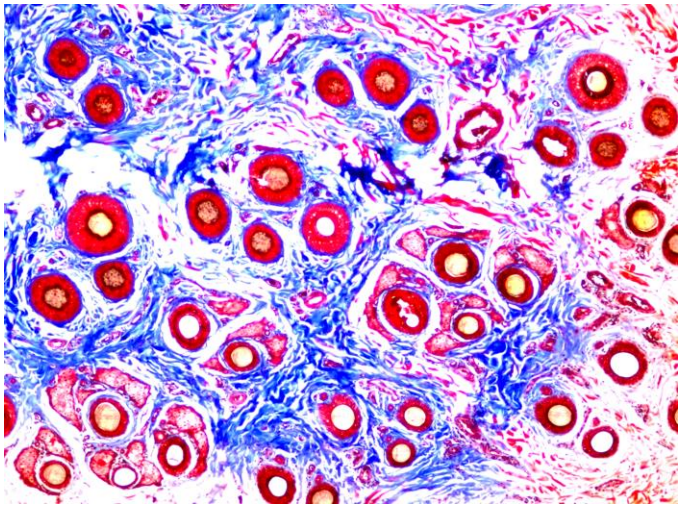

Plate 6.

Plate 7. Photomicrograph showing primary hair follicle (P) associated with 3-4 secondary hair follicles (S) together with their sebaceous glands (Sb) in the horizontal section of skin of Indian bison. Masson's Trichromem X 100.

Plate 8. Photomicrograph showing uniformly distributed coiled tubular sweat glands (Swt) with secretary blebs on their surface (Arrow) in the horizontal section of skin of Indian bison. H & E- Phloxine X 400.

Plate 9. Photomicrograph showing the capillary plexus and fine arterioles (a) and venules (v) comprising the vascular component of the dermis in the horizontal section of skin of Indian bison. Masson's Trichrome X 400.

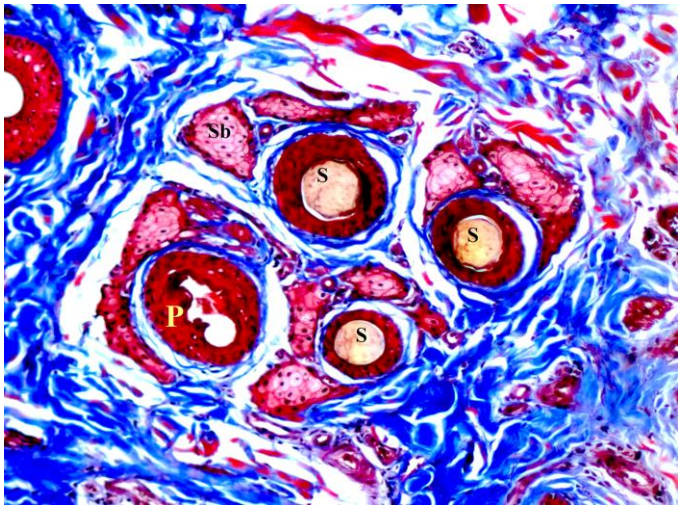

Plate 7.

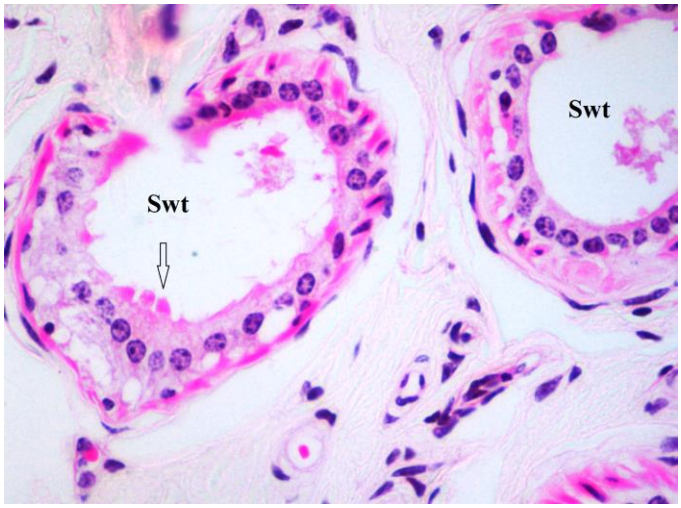

Plate 8.

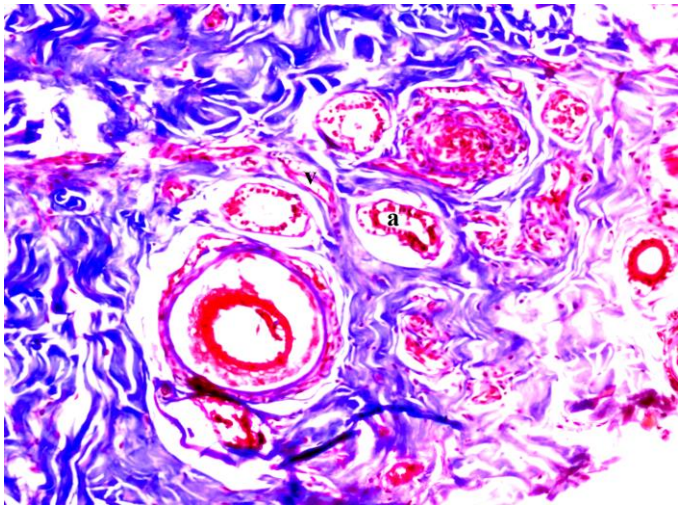

Plate 9.

Plate 10. Photomicrograph showing epidermis with epidermal layers in the vertical section of skin of black buck. H & E- Phloxine X 1000.

Plate 11. Photomicrograph showing ducts of sweat glands (d), cross sections of hair follicles (Arrow) associated with single sided opening of sebaceous glands (Sb) and erector pili muscles (Er) in the vertical section of skin of black buck. H & E- Phloxine X 100.

Plate 12. Photomicrograph showing blood vessels (BV), cross sections of hair follicles associated with single sided opening of sebaceous glands (Sb) and erector pili muscles (Er) in the vertical section of skin of black buck. Ayoub Shklar X 100.

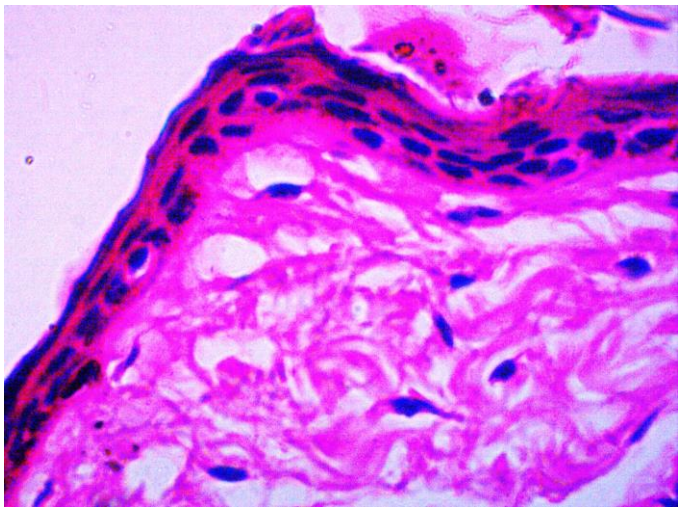

Plate 10.

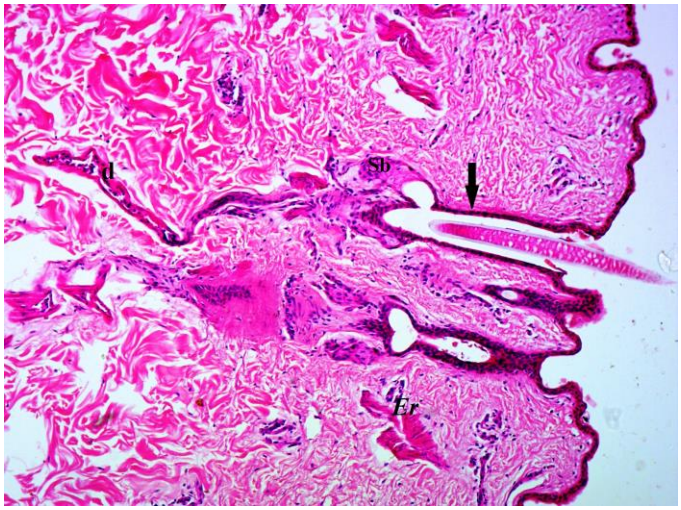

Plate 11.

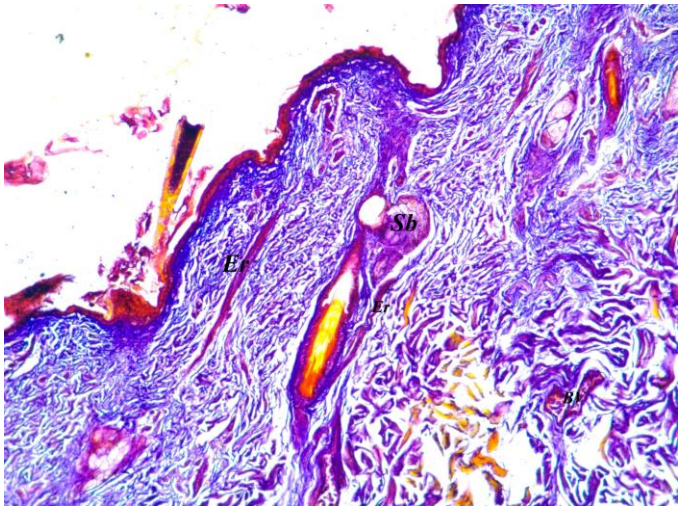

Plate 12.

Plate 13. Photomicrograph showing even distribution of elastic fibers (Arrows) in between the collagen fiber bundles and around the hair follicles in the dermis in the vertical section of skin of black buck. Weigert's X 200.

Plate 14. Photomicrograph showing the stratum reticulare (SR) with densely packed collagen fibers and few muscle fibers, loosely arranged collagen bundles, large number of blood vessels, nerve fiber bundles (NF) and elastic fibers at the base of the stratum reticulare in the vertical section of skin of black buck. H & E- Phloxine X 50.

Plate 15. Photomicrograph showing densely distributed linearly arranged compound hair follicles with primary (P) and secondary follicle (S) observed in the horizontal section of skin of black buck. Masson's Trichrome X 40.

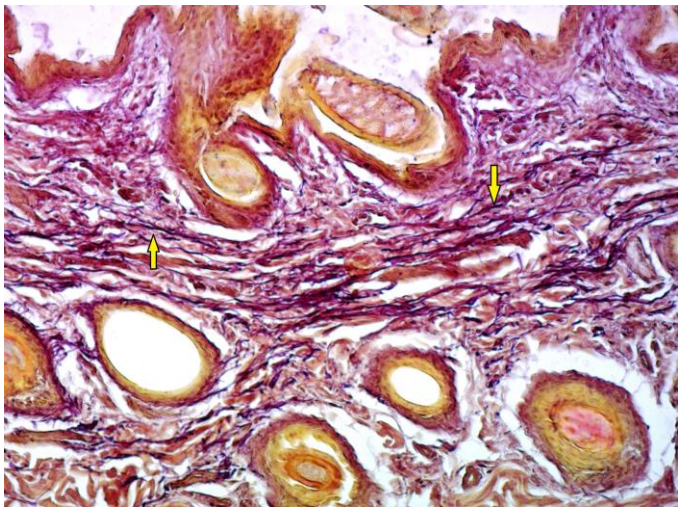

Plate 13.

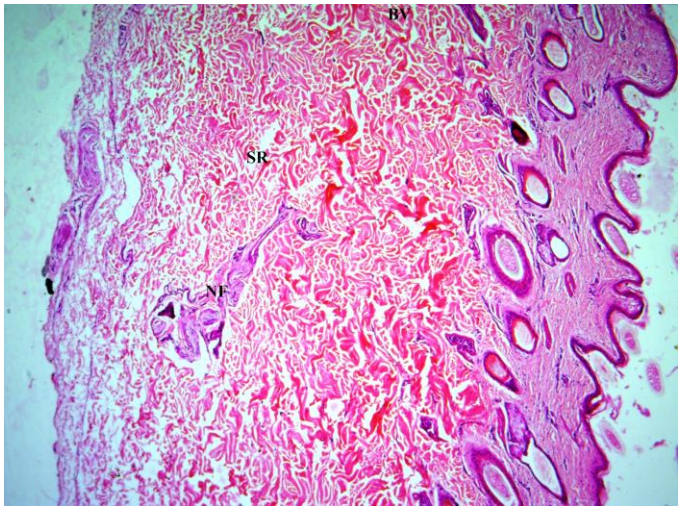

Plate 14.

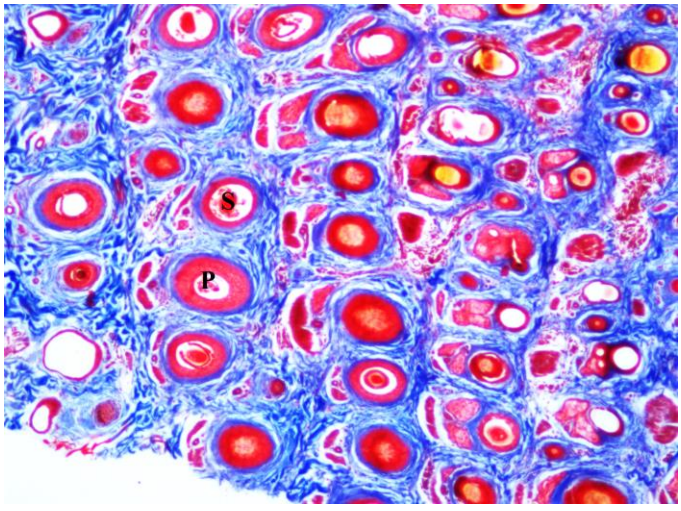

Plate 15.

Plate 16. Photomicrograph showing compound hair follicle within which semicircular arrangement of secondary hair follicles (S) with primary hair follicle (P) in the horizontal section of skin of black buck. Weigert's X 100.

Plate 17. Photomicrograph showing centrally placed primary hair follicle (P) when it is present with 2 secondary hair follicles (S) in the horizontal section of skin of black buck. Masson's Trichrome X 100.

Plate 18. Photomicrograph showing (Arrows) hair follicle with Sebaceous glands (Sb) in the horizontal section of skin of black buck. Masson's Trichrome X 200.

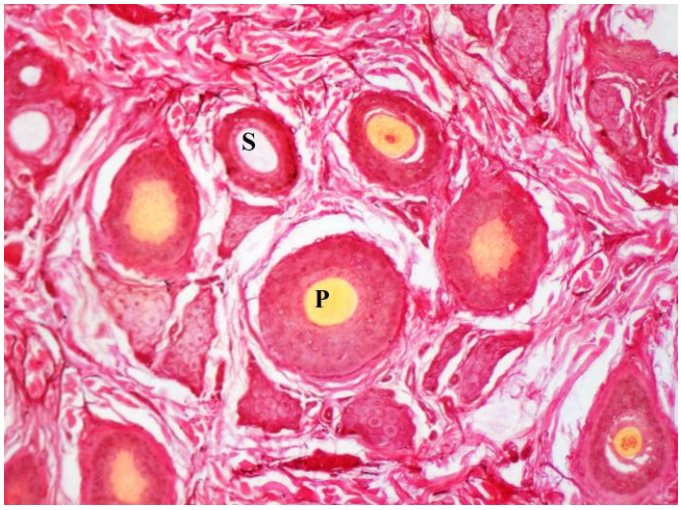

Plate 16.

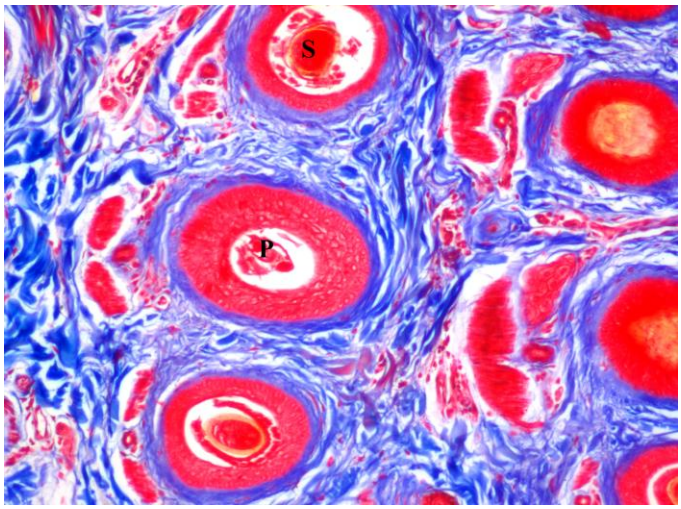

Plate 17.

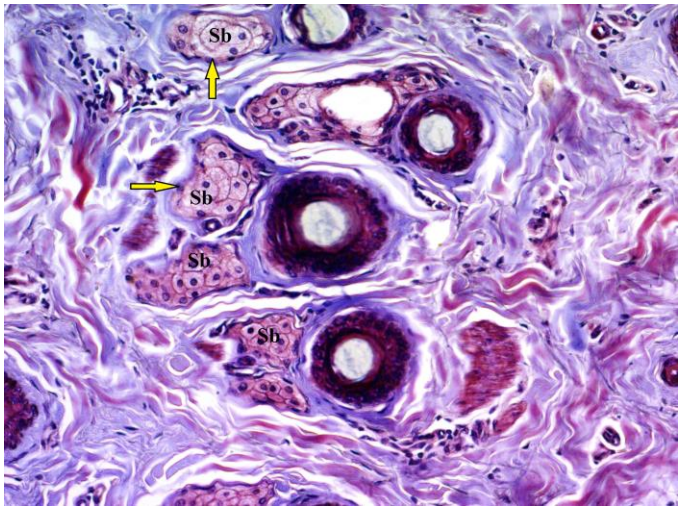

Plate 18.

Plate 19. Photomicrograph showing epidermis with epidermal layers (SB, SS, SG, SC) in the vertical section of skin of Nilgai. H & E- Phloxine X 1000.

Plate 20. Photomicrograph showing Nerve fibers (Arrows) running in the papillary layer and approaching towards the basale layer of the epidermis in the vertical section of skin of Nilgai. H & E- Phloxine X 100

Plate 21. Photomicrograph showing direct opening of the sebaceous glands (Arrow) at one side of the primary hair follicle and Sparsely distributed sweat glands (Swt) in papillary layer of the dermis in the vertical section of skin of Nilgai. Masson's Trichrome X 100.

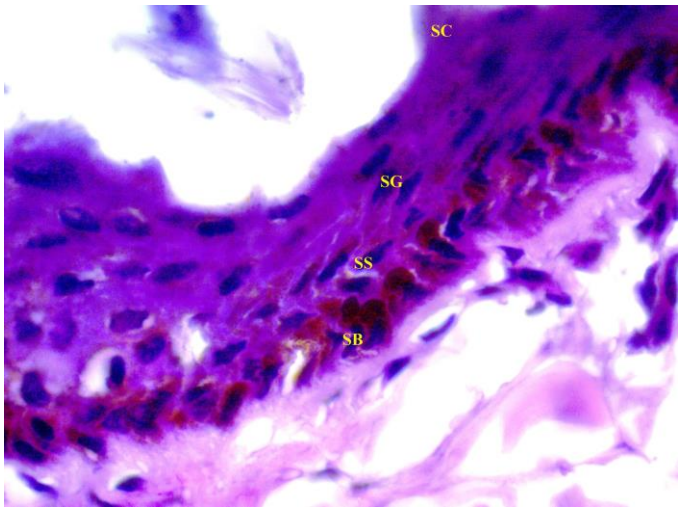

Plate 19.

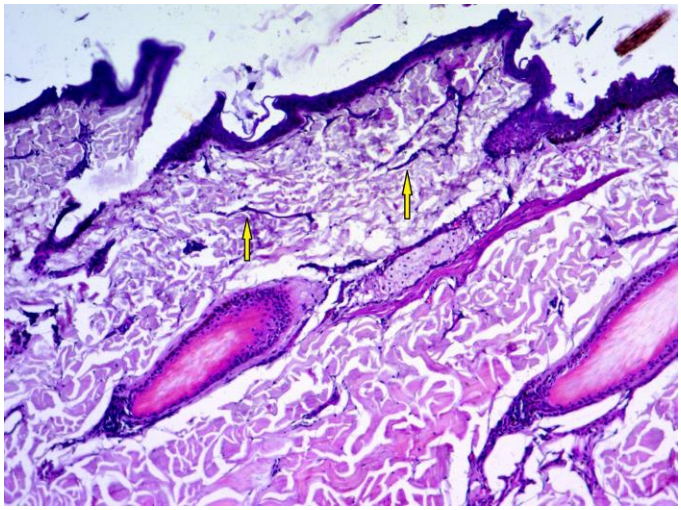

Plate 20.

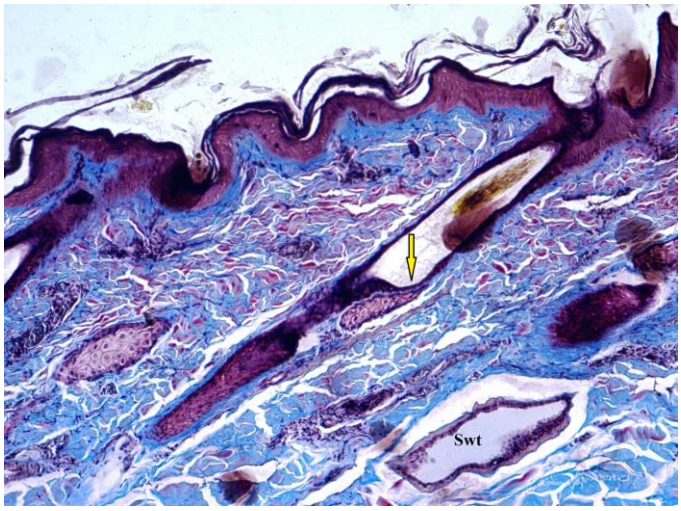

Plate 21.

Plate 22. Photomicrograph showing densely distributed Compound hair follicles in the dermis of nilgai skin in the horizontal section. Masson's Trichrome X 40

Plate 23. Photomicrograph showing the primary hair follicles (p) with bilaterally surrounded 2 secondary hair follicles (S) along with sebaceous glands in horizontal section of nilgai skin. Masson's Trichrome X 100

Plate 24. Photomicrograph showing the reticular fibers (Arrow) surrounding the hair follicle bundles in horizontal section of Nilgai skin. Gomori's X 100

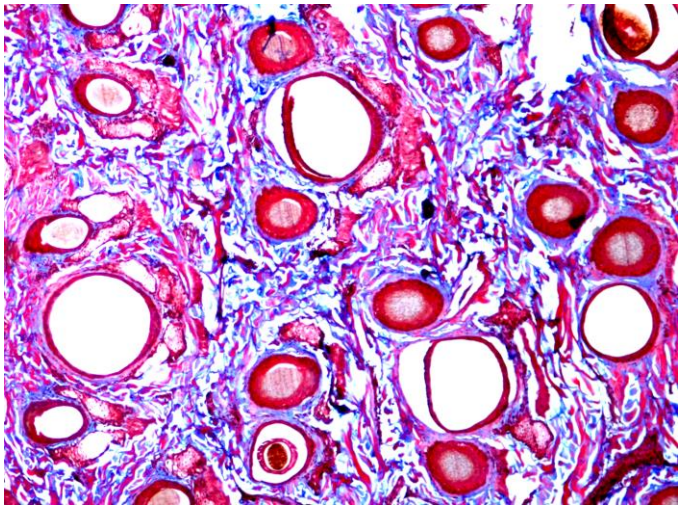

Plate 22.

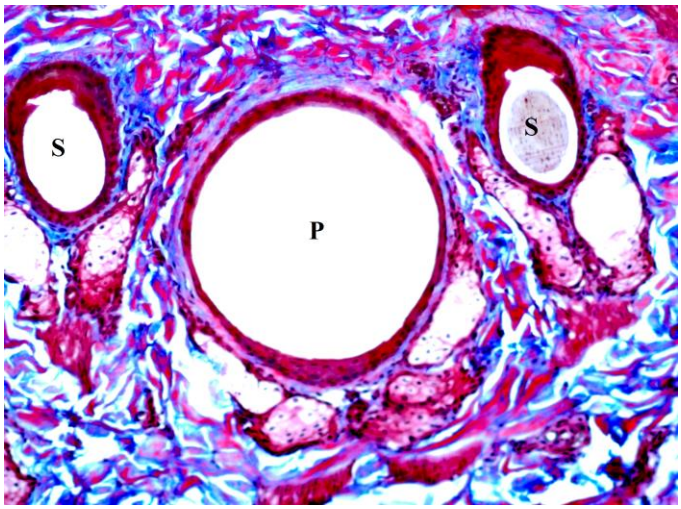

Plate 23.

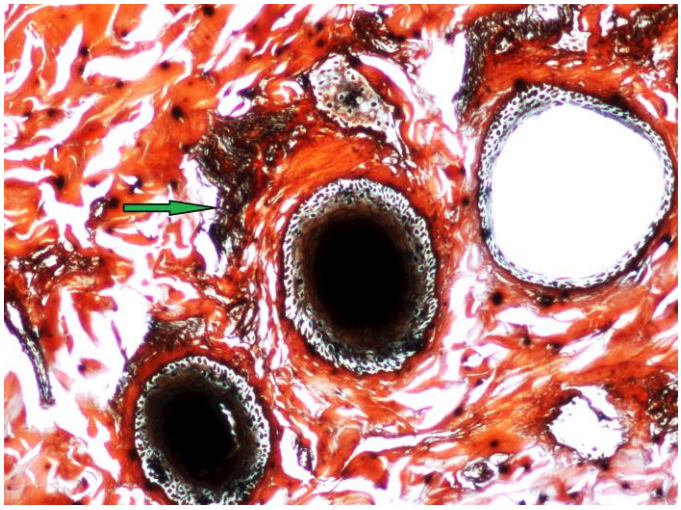

Plate 24.

Plate 25. Photomicrograph showing 1-2 layers of stratum granulosum (SG) with keratohyaline granules, 4-5 layers of stratum spinosum (SS) and single layered stratum basale (SB) with melanin pigments (Arrow) in vertical section of wild boar skin. H & E-Phloxine X 400

Plate 26. Photomicrograph showing well defined prekeratin (Green arrow) and keratin (yellow arrow) with thicker stratum corneum presented melanin pigments in vertical section of wild boar skin. Ayoub Shklar X 200

Plate 27. Photomicrograph showing loose connective tissue with large number of adipose tissue (Ad), particularly in between the epidermal pegs (Arrow) at stratum papillare in vertical section of wild boar skin. H & E- Phloxine X 400

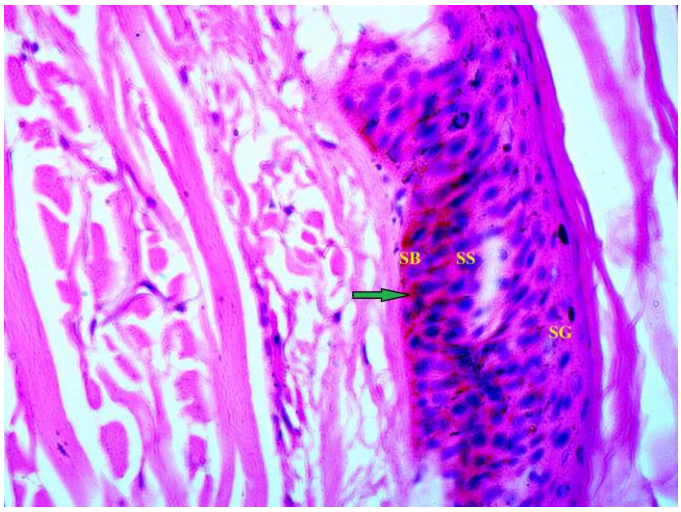

Plate 25.

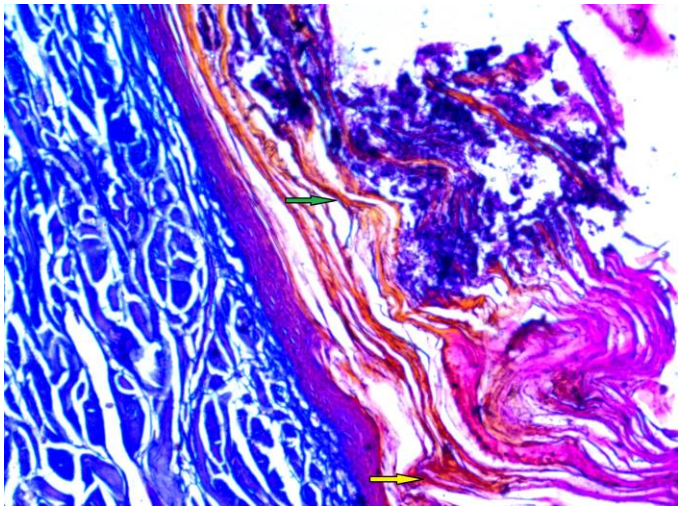

Plate 26.

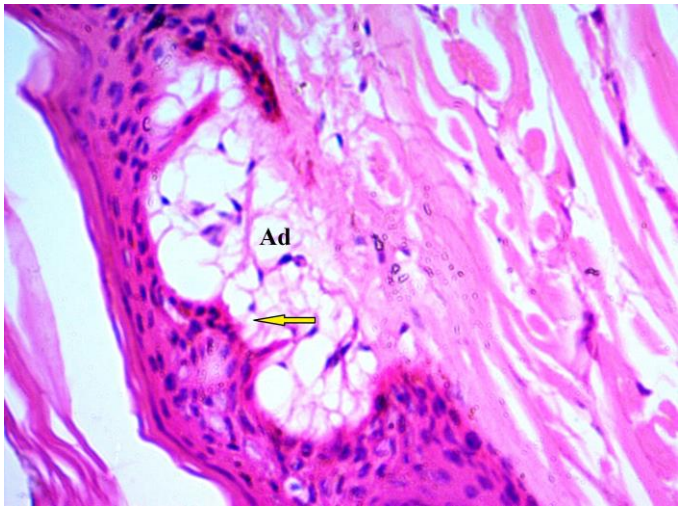

Plate 27.

Plate 28. Photomicrograph showing more of collagenous stratum reticulare (SR) with sparsely distributed muscle fiber bundles and elastic fibers in vertical section of wild boar skin. Masson's Trichrome X 50.

Plate 29. Photomicrograph showing sparsely distributed compound hair follicles with linearly arranged three primary hair follicle (P) and larger in size at the center in horizontal section of wild boar skin. Masson's Trichrome X 50.

Plate 30. Photomicrograph showing the Elastic fibers (Arrows) surrounded the hair follicles and scarcely distributed in the connective tissue in horizontal section of wild boar skin. Weigert's X 200

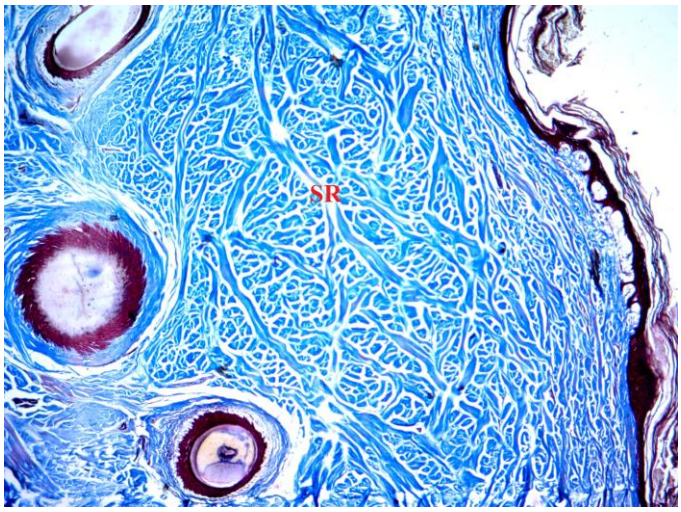

Plate 28.

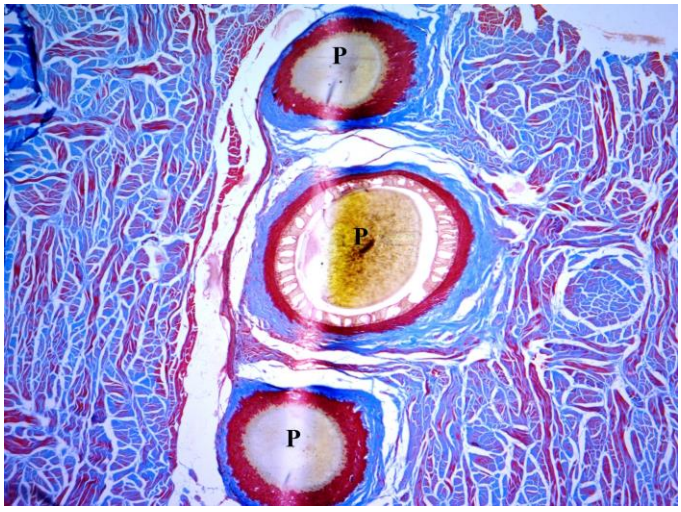

Plate 29.

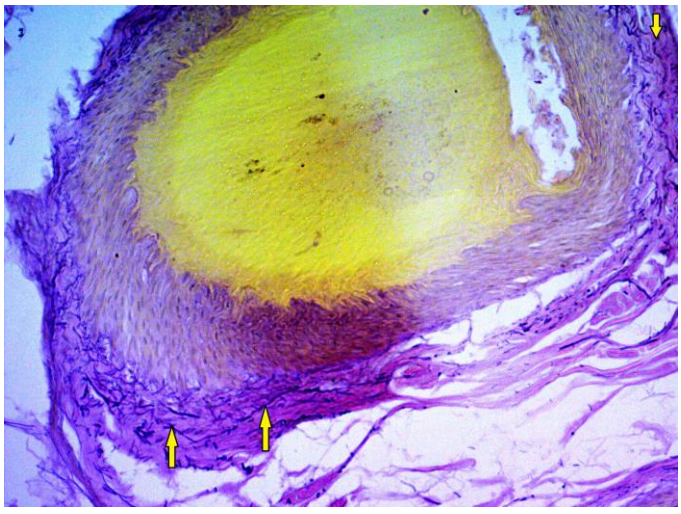

Plate 30.

Plate 31. Photomicrograph showing the nerve fiber (NF) entering into the hair follicle (HF) in the connective tissue in horizontal section of wild boar skin. Gomori's X 100

Plate 32. Photomicrograph showing multiple layers of stratum corneum (SC) and other epidermal layers with well defined prekeratin (Green arrow) and keratin (Yellow arrow) in vertical section of Asian elephant skin. Ayoub Shklar X 100.

Plate 33. Photomicrograph showing the stratum basale (SB), stratum spinosum (SS), thicker stratum granulosum (SG) and stratum corneum (SC) around the papillary bodies (Arrow) in vertical section of Asian elephant skin. Masson's Trichrome X 400.

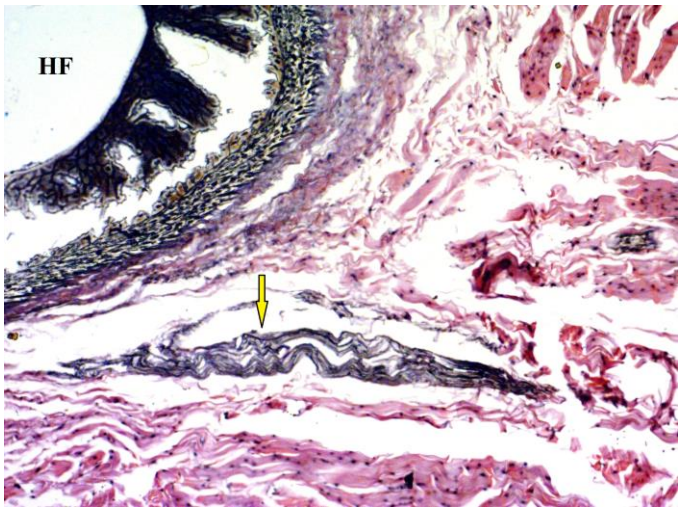

Plate 31.

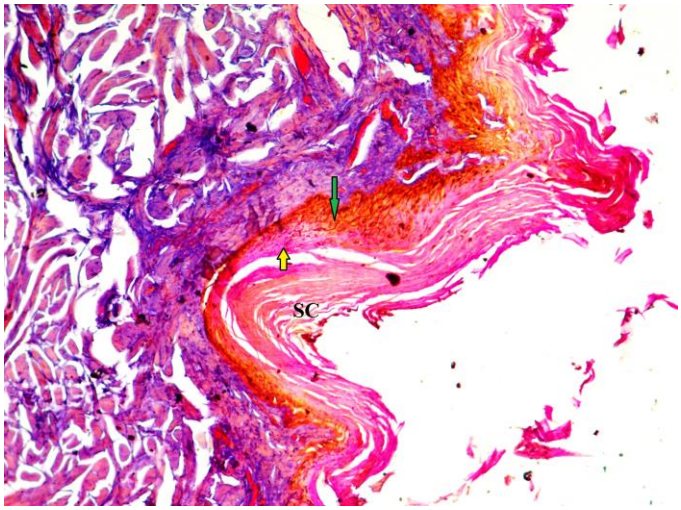

Plate 32.

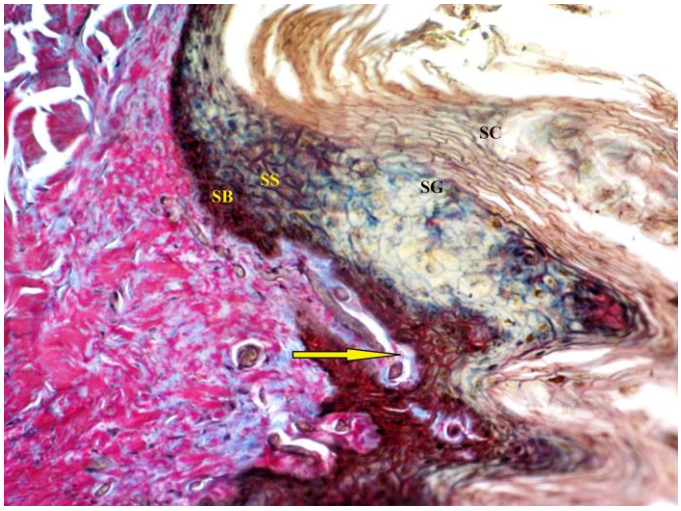

Plate 33.

Plate 34. Photomicrograph showing thin irregular shaped epidermal pegs (Arrows) causing haphazard arrangement of dermal papillary bodies in vertical section of Asian elephant skin. H & E- Phloxine X 100.

Plate 35. Photomicrograph showing horizontally as well as vertically oriented collagen fiber bundles (Yellow arrow) along with muscle fibers (Green arrow) in the deeper part of the dermis in vertical section of Asian elephant skin. Masson's Trichrome X 50.

Plate 36. Photomicrograph showing single isolated hair follicles surrounded by loose connective tissue with collagen fibers with sparsely distributed elastic fibers (Arrows) in the horizontal section of skin of Asian elephant. H & E- Phloxine X 100

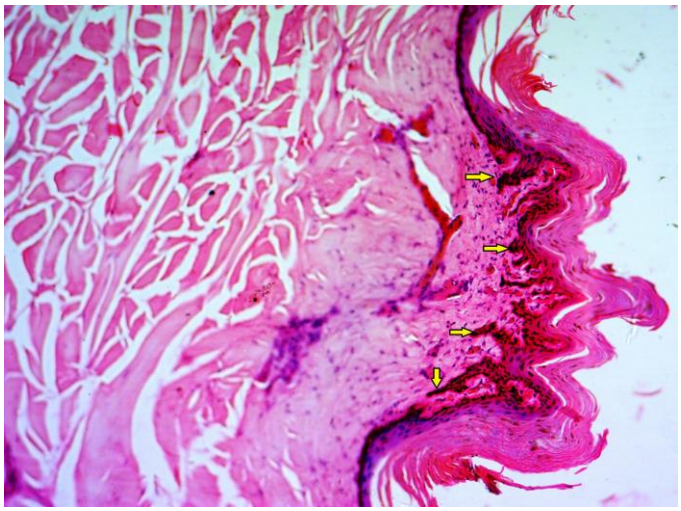

Plate 34.

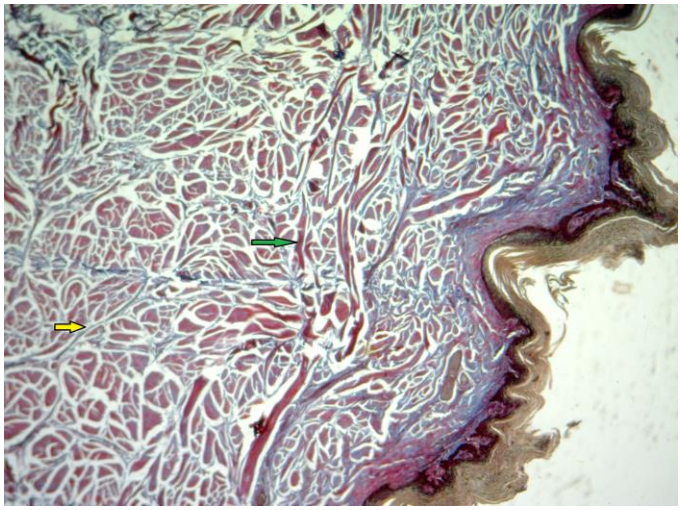

Plate 35.

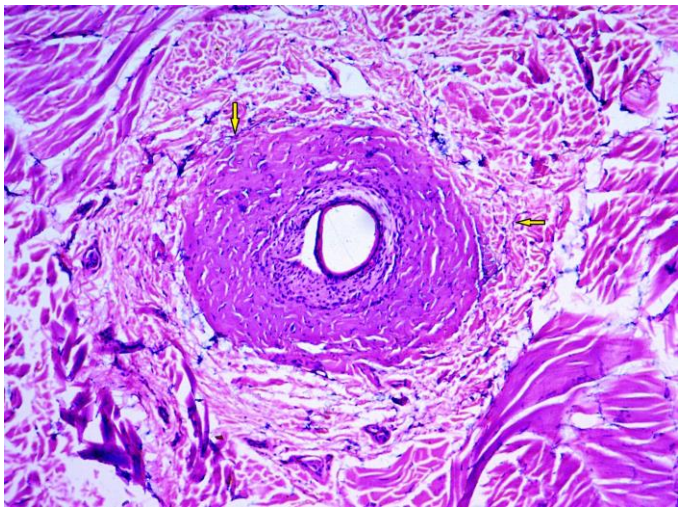

Plate 36.

Plate 37. Photomicrograph showing epidermis with epidermal layers and thick keratin (Yellow arrow) and prekeratin (Green arrow) layers in vertical section of African elephant skin. Ayoub Shklar X 100.

Plate 38. Photomicrograph showing the dermal papillae evaginated between surface epidermal interdigitations (Arrows) in vertical section of African elephant skin. H & E- Phloxine X 50.

Plate 39. Photomicrograph showing dense collagenous fiber bundles with few muscle fibers and are running parallel (Arrow) to the epidermal invaginations in the dermis in vertical section of African elephant skin. H & E- Phloxine X 50.

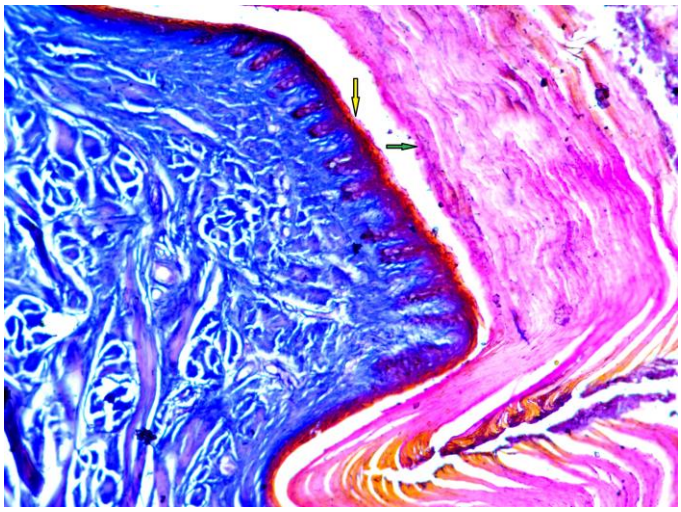

Plate 37.

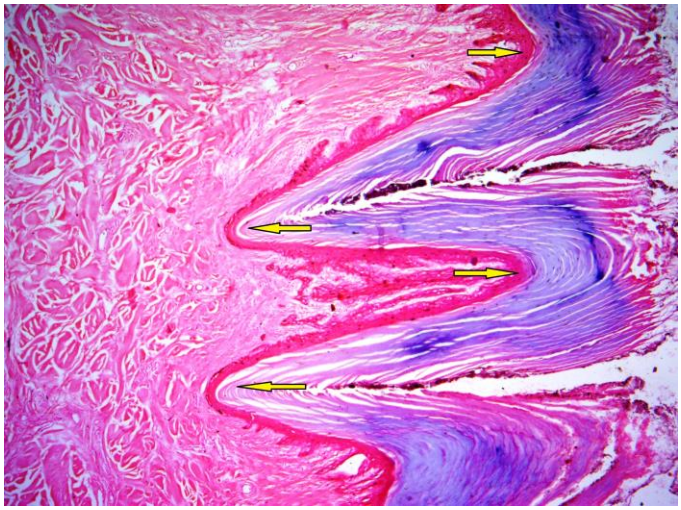

Plate 38.

Plate 39.

Plate 40. Photomicrograph showing the stratum basale (SB) and stratum spinosum (SS) with spindle or oval shaped cells with hallow space around the nucleus resembling hyaline cartilaginous cells (Arrows) with the presence of melanin pigment granules in vertical section of African elephant skin. Ayoub Shklar X 400

Plate 41. Photomicrograph showing thick stratum granulosum (SG) layer at the zone of papillary bodies in vertical section of African elephant skin. H & E- Phloxine X 400

Plate 42. Photomicrograph showing single hair follicle in the dermis below the papillary layer and absence of sebaceous and sweat glands surrounding the primary hair follicle (P) in the dermis in vertical section of African elephant skin. Masson's Trichrome X 50

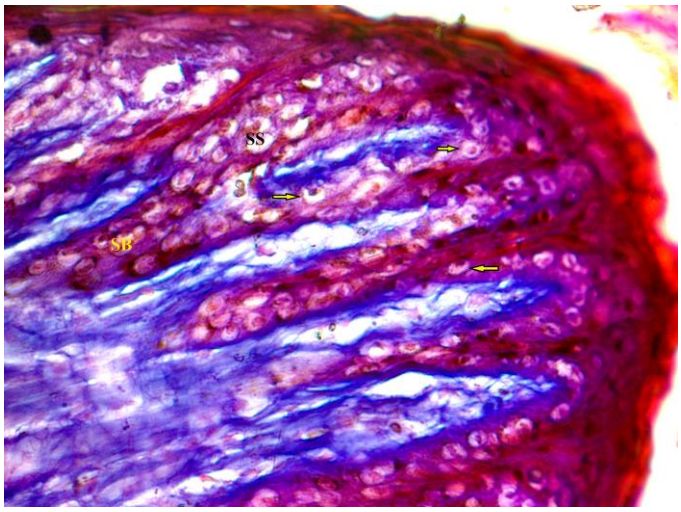

Plate 40.

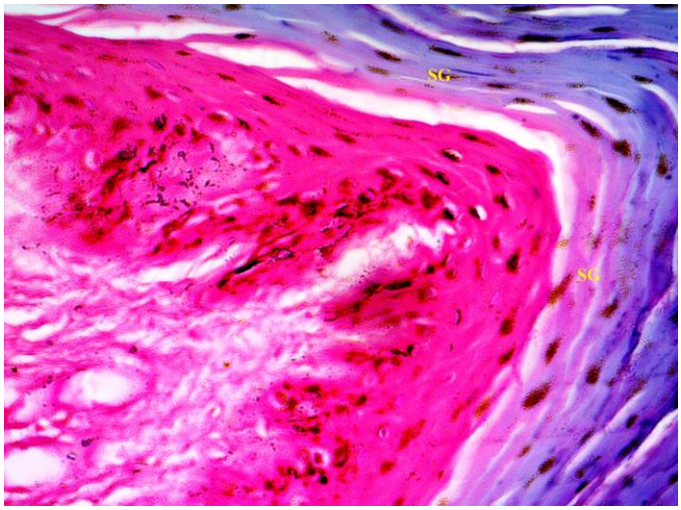

Plate 41.

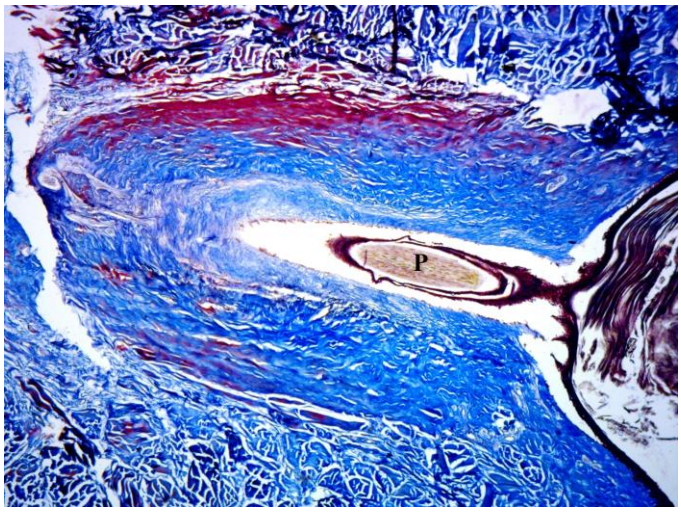

Plate 42.

Plate 43. Photomicrograph showing single isolated primary hair follicles surrounded by vascular loose connective tissue (CT), densely packed collagen fibers (C), sparse muscle fibers and then followed by a thick layer of skeletal muscle fiber bundles (Arrows) in vertical section of African elephant skin. Masson's Trichrome X 100

Plate 44. Photomicrograph showing the presence of blood vessels (Yellow arrows) and nerve fibers (Green arrows) in between the muscle fibers surrounding primary hair follicles (P) in vertical section of African elephant skin. H & E- Phloxine X 100

Plate 45. Photomicrograph showing the epidermo-dermal junction (Arrows), association of dermis with surrounding epidermis as epidermal pegs due interdigitation of the skin fold in the horizontal section of African elephant skin. Ayoub Shklar X 50

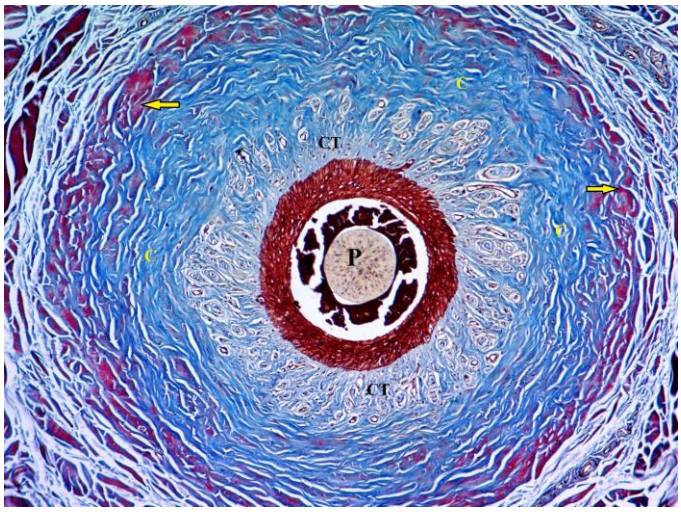

Plate 43.

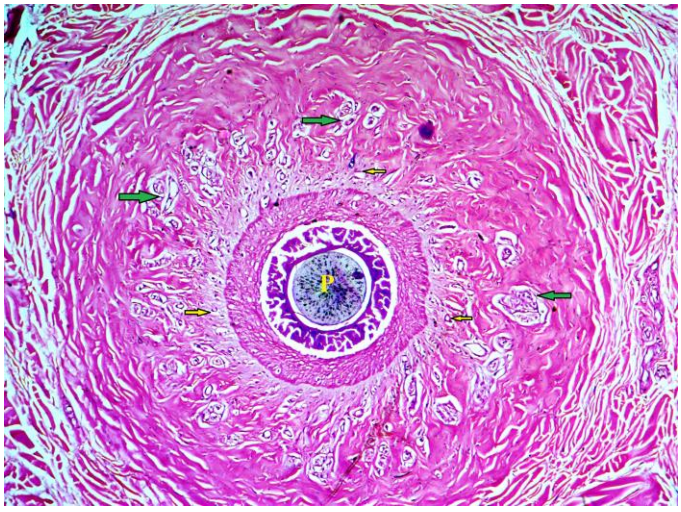

Plate 44.

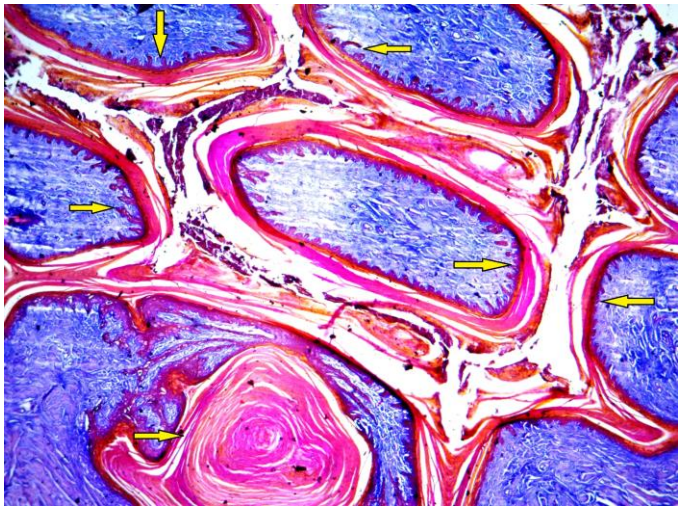

Plate 45.

Plate 46. Photomicrograph showing hexagonal as well as oval shapes of the skin folding in the epidermo-dermal junction in the horizontal section of African elephant skin. Ayoub Shklar X 50

Plate 47. Photomicrograph showing the epidermal pegs, peripherally corneum layer with keratin and prekeratin and followed by other epidermal layers, in the middle dense collagen fiber bundle (Yellow arrows) along with muscle fibers and blood vessels (Red arrow) in the horizontal section of African elephant skin. Ayoub Shklar X 100

Plate 48. Photomicrograph showing epidermal layers with keratin zones (Yellow arrow) and at few places prekeratin zones (Blank arrow) in the vertical section of cheetah skin. Ayoub Shklar X 400

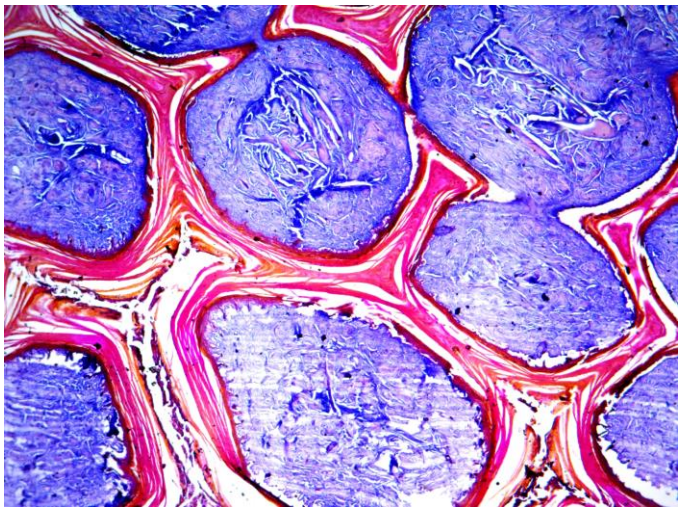

Plate 46.

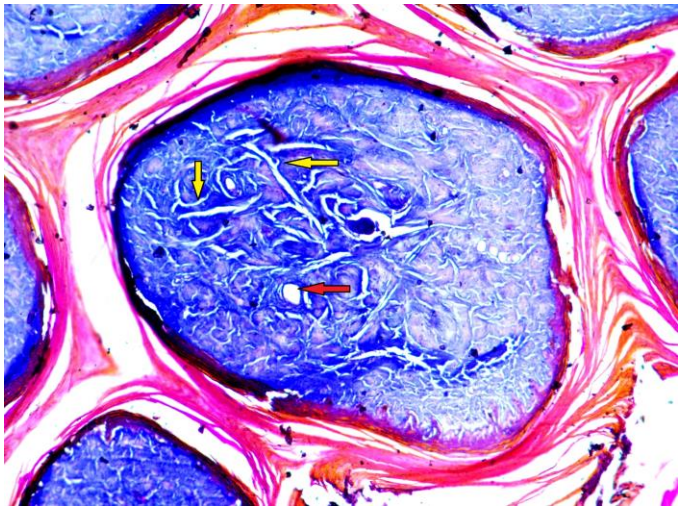

Plate 47.

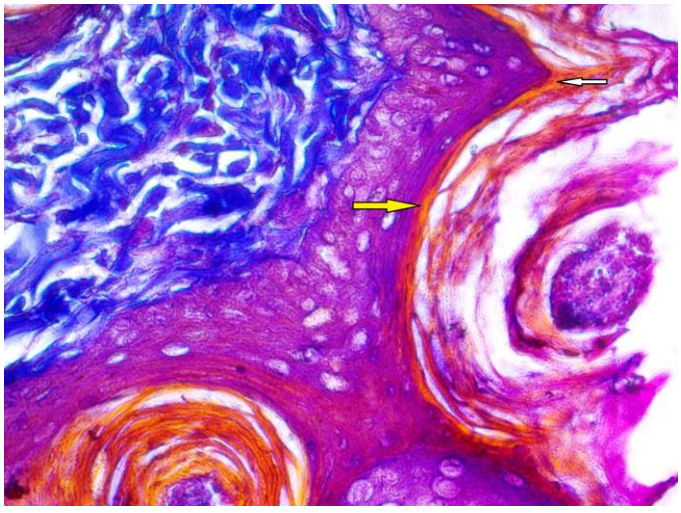

Plate 48.

Plate 49. Photomicrograph showing The stratum granulosum (SG) with keratohyaline granules (Arrow) and followed by the stratum spinosum (SS) and the stratum basale (SB) with melanin pigments in the vertical section of cheetah skin. H & E- Phloxine X 400

Plate 50. Photomicrograph showing stratum basale (SB) with melanin pigments (Arrows) in the vertical section of cheetah skin. Methyl green pyronin X 1000

Plate 51. Photomicrograph showing perpendicularly oriented hair follicles (Arrows) in the papillary (SP) and reticular (SR) layer of the dermis in the vertical section of cheetah skin. H & E- Phloxine X 200

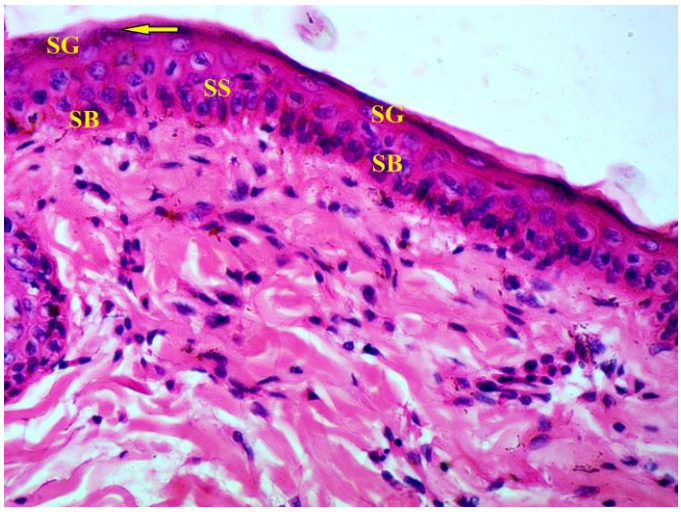

Plate 49.

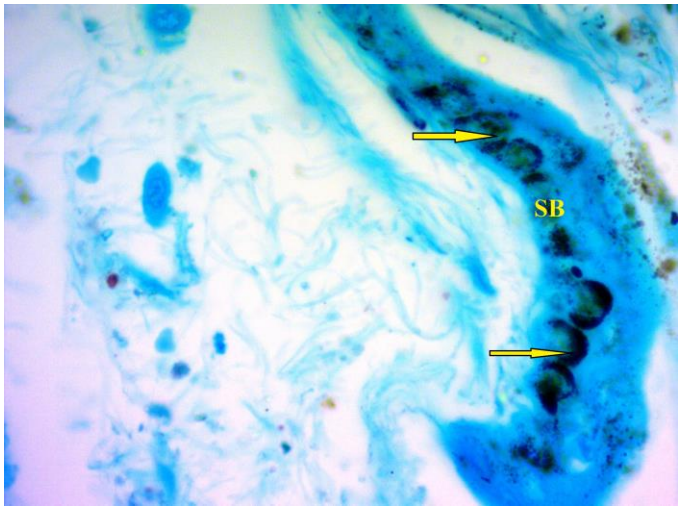

Plate 50.

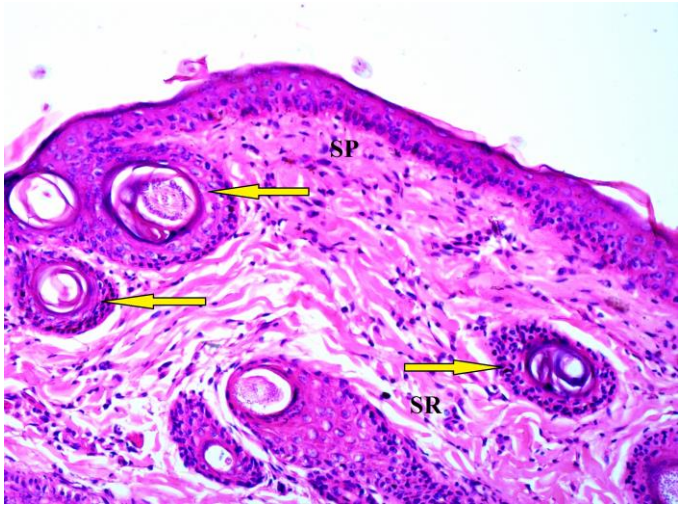

Plate 51.

Plate 52. Photomicrograph showing the cross sectional appearance of the hair follicles (HF) amongst the epidermal folds (Arrows) in the vertical section of cheetah skin. Ayoub Shklar X 200

Plate 53. Photomicrograph showing oblique and vertical orientation of hair follicles (Arrows) in the horizontal section of cheetah skin. H & E- Phloxine X 50

Plate 54. Photomicrograph showing loose connective tissue of collagen fibers and sparsely distributed elastic fibers (Arrows) in the stratum papillare of dermis in the horizontal section of cheetah skin. Weigert's X 100

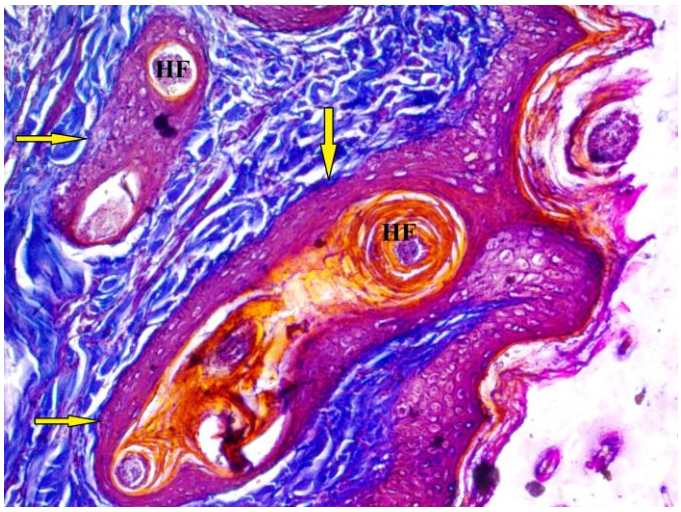

Plate 52.

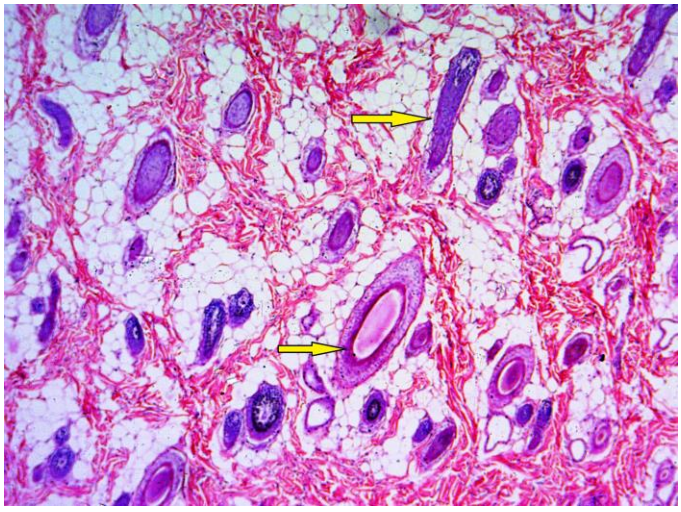

Plate 53.

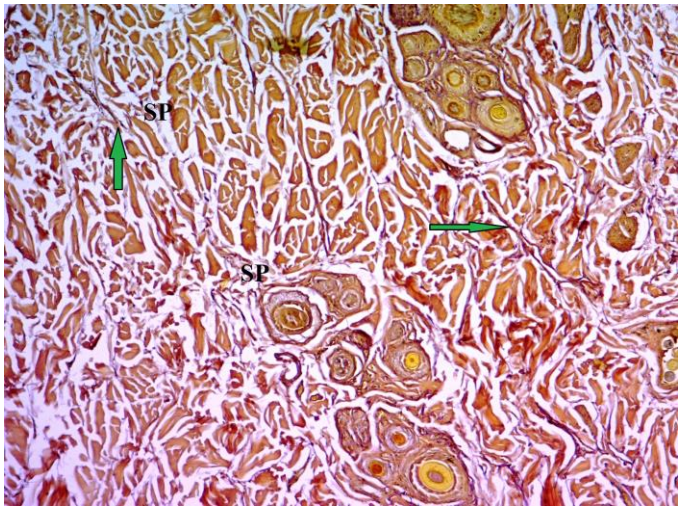

Plate 54.

Plate 55. Photomicrograph showing the presence of sweat glands (Swt) lined by simple cuboidal epithelium with their secretions on their surface and sebaceous glands (Arrow) opening in to the hair follicles in the horizontal section of cheetah skin. Ayoub Shklar X 200

Plate 56. Photomicrograph showing the hair follicles (Arrow) running longitudinal to the epidermal layer in the vertical section of cheetah skin. Masson's Trichrome X 100

Plate 57. Photomicrograph showing cross cut and longitudinally oriented skeletal muscle fibers (Yellow arrows) with large number of blood vessels (Blank arrow) and nerve fibers (NF) surrounded by adipose tissue (Green arrow) in the hypodermis in the vertical section of cheetah skin. Masson's Trichrome X 100

Plate 55.

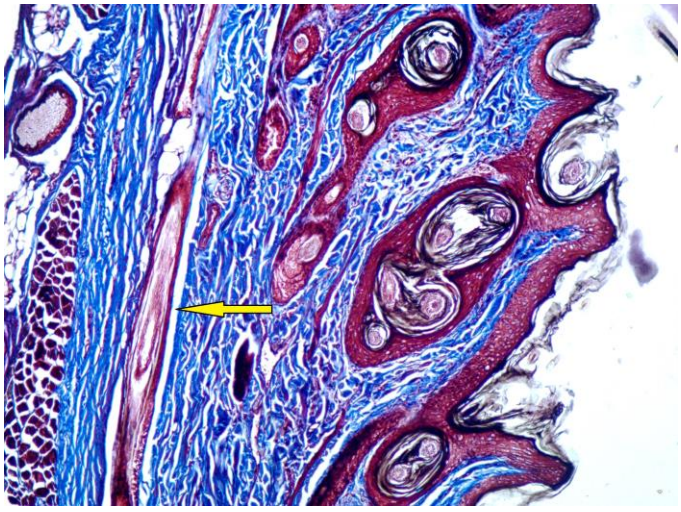

Plate 56.

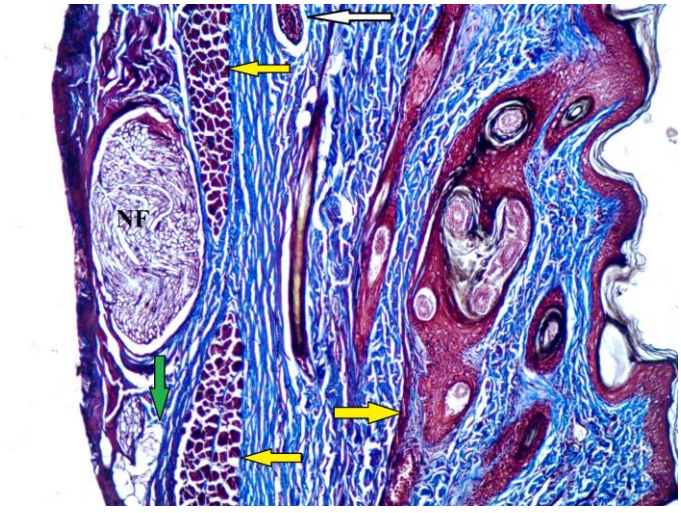

Plate 57.

Plate 58. Photomicrograph showing the hair follicles (Arrows) running perpendicular to the epidermis in the vertical section of cheetah skin. H & E- Phloxine X 50

Plate 59. Photomicrograph showing coiled tubular sweat glands (Arrow) lined by simple cuboidal epithelium with secretory blebs on the surface at the base of the primary hair follicle (P) in the horizontal section of cheetah skin. H & E- Phloxine X 100

Plate 60. Photomicrograph showing the compound hair follicles always associated with one or two sweat glands (Arrows) in the horizontal section of cheetah skin. H & E- Phloxine X 50

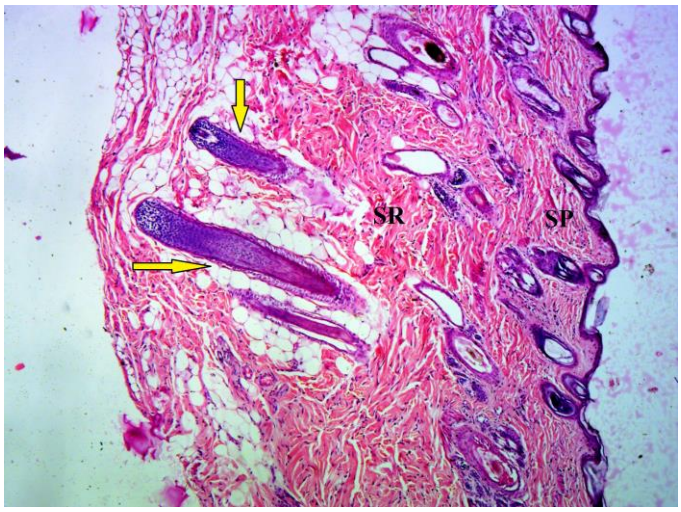

Plate 58.

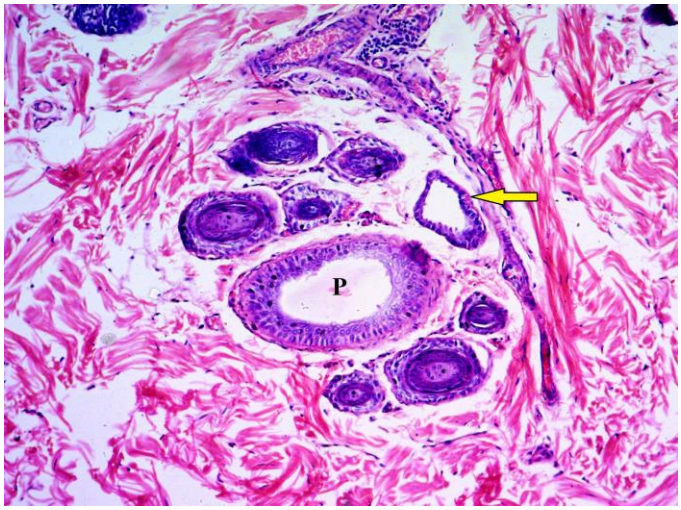

Plate 59.

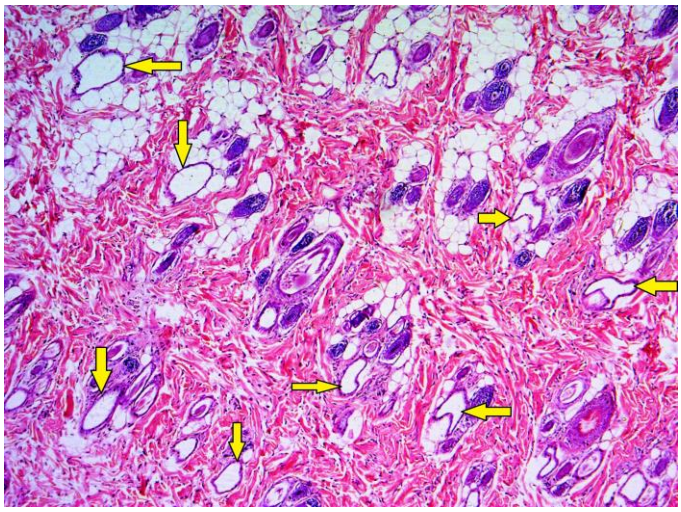

Plate 60.

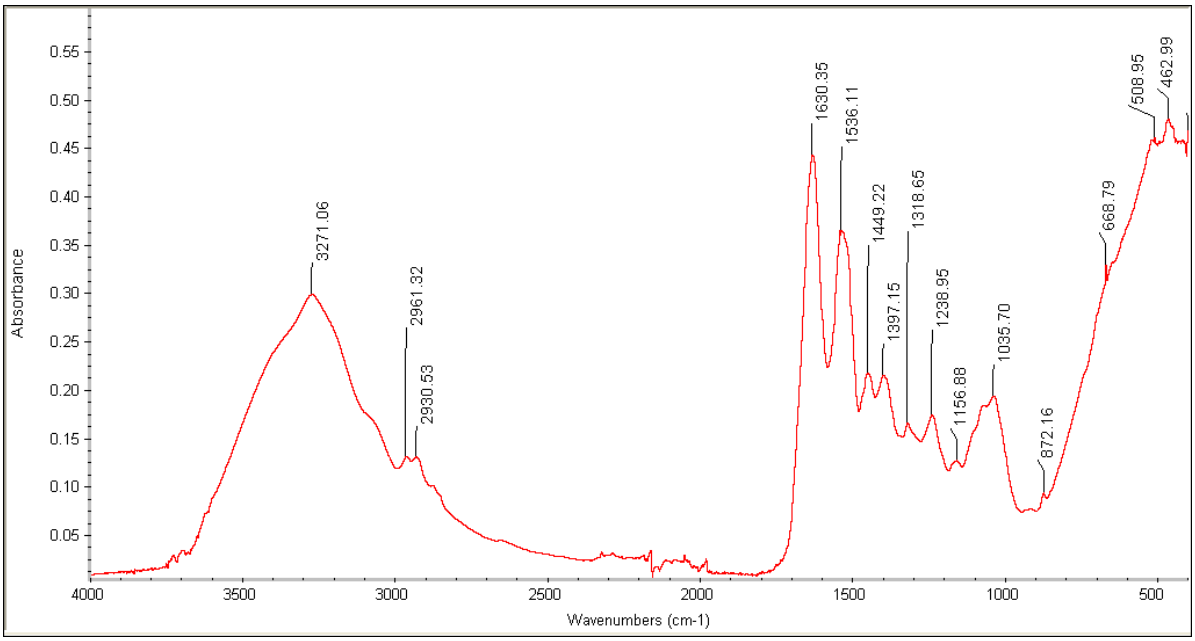

Fig.1Average primary spectrum of Asian Elephant hair

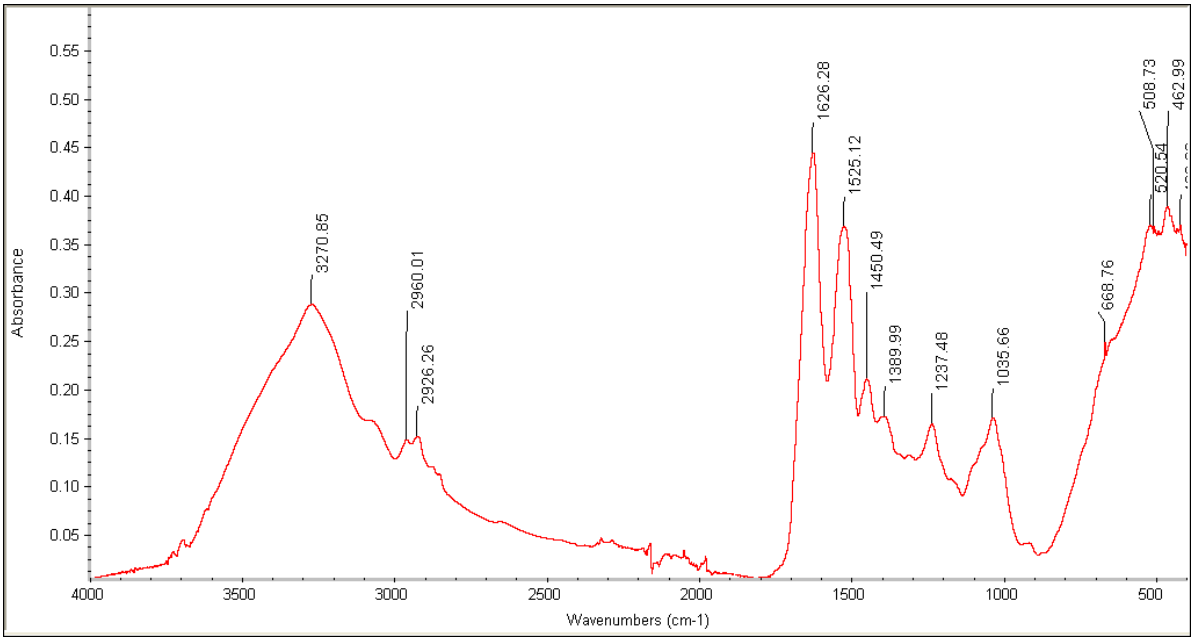

Fig.2 Average primary spectrum of Bison hair

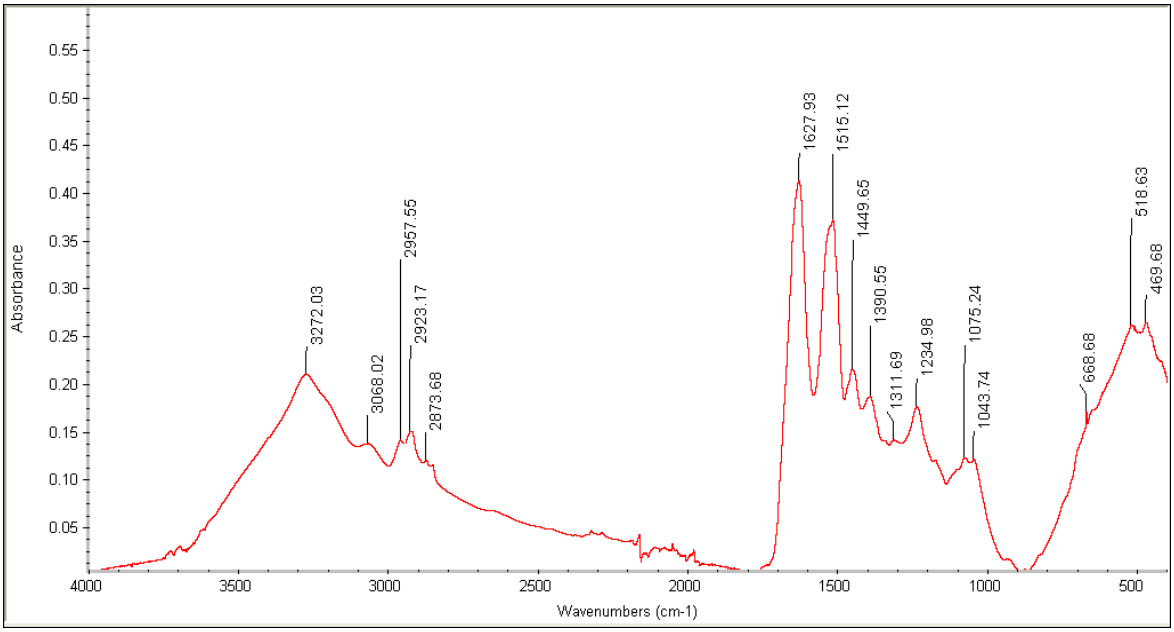

Fig.3 Average primary spectrum of Black buck hair

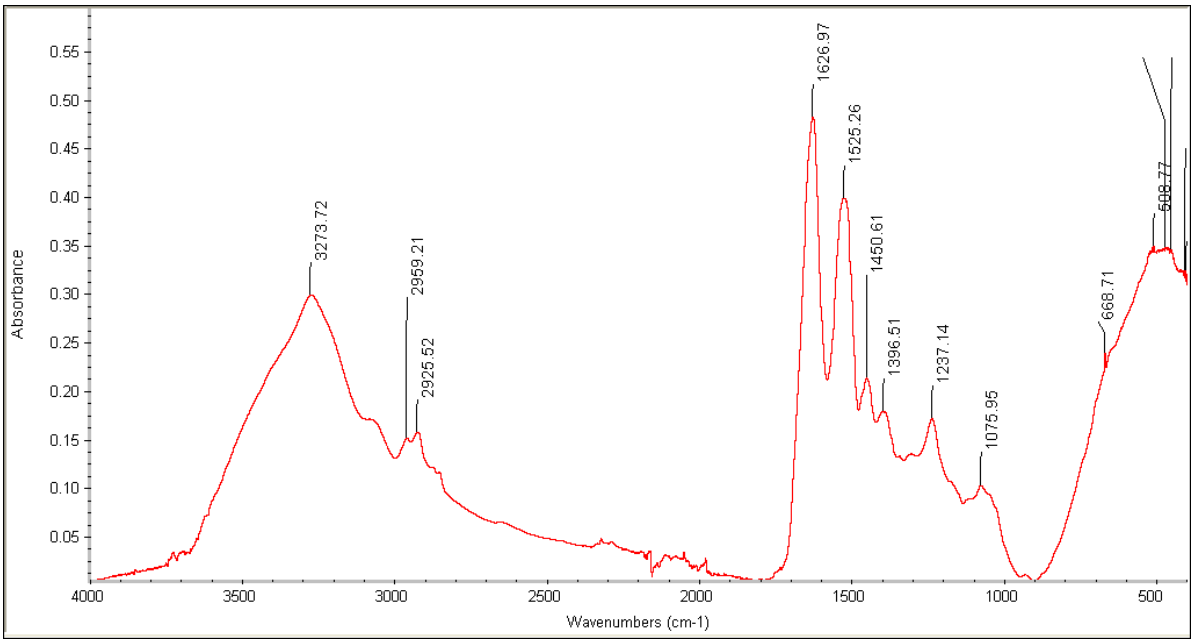

Fig.4 Average primary spectrum of Cheetah hair.

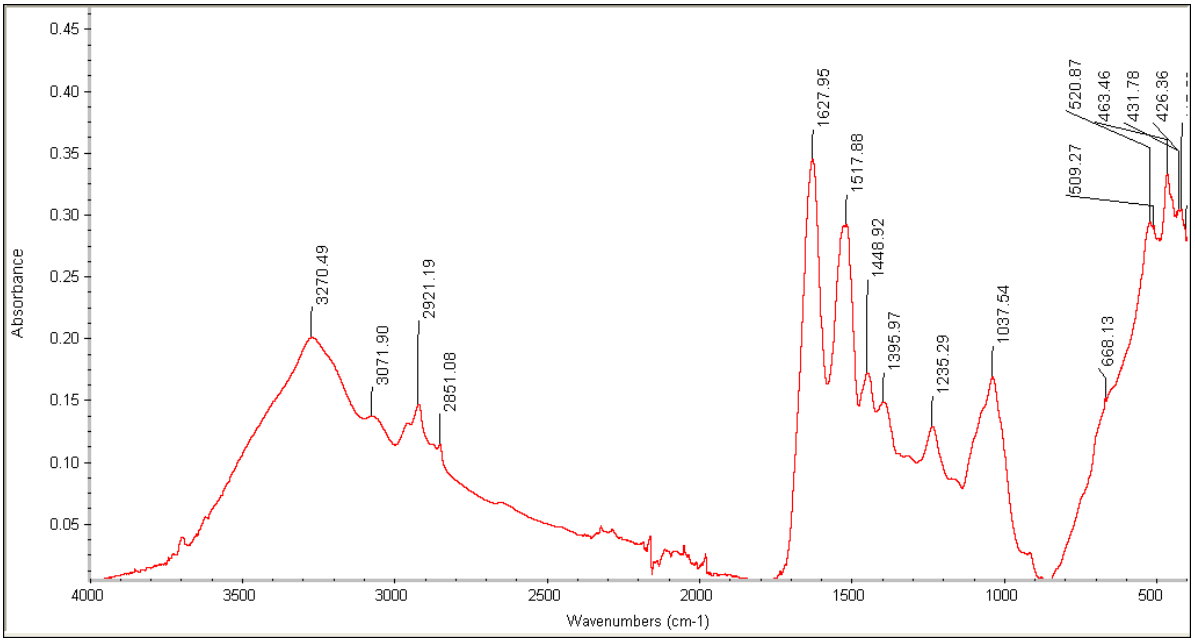

Fig.5 Average primary spectrum of Indian grey wolf hair

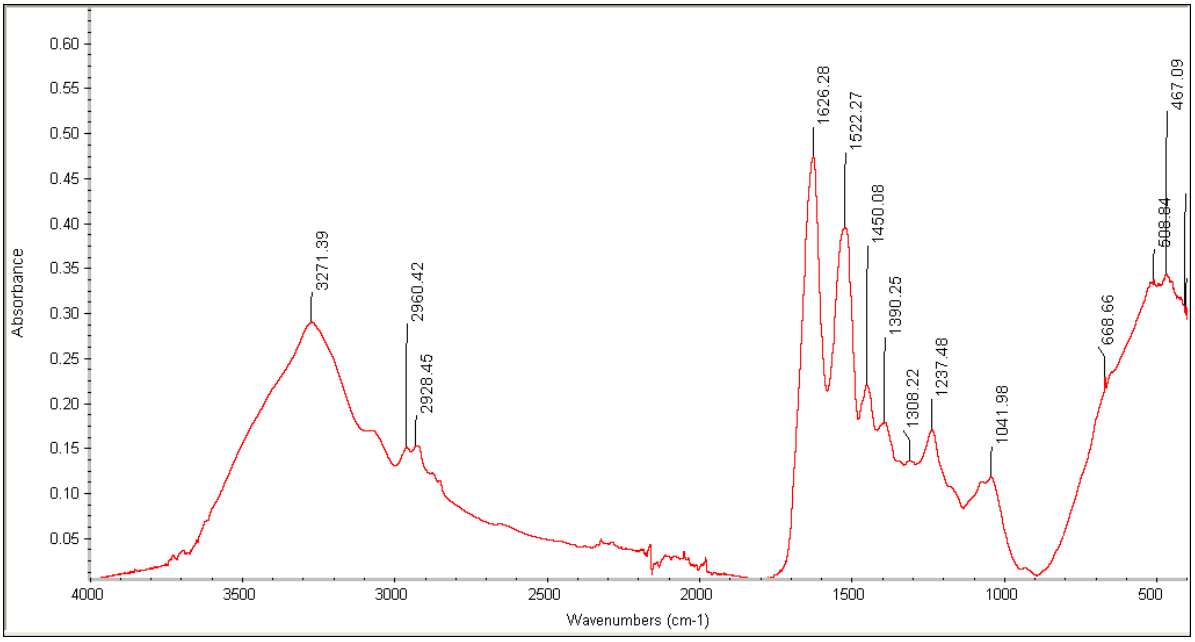

Fig.6 Average primary spectrum of Nilgai hair

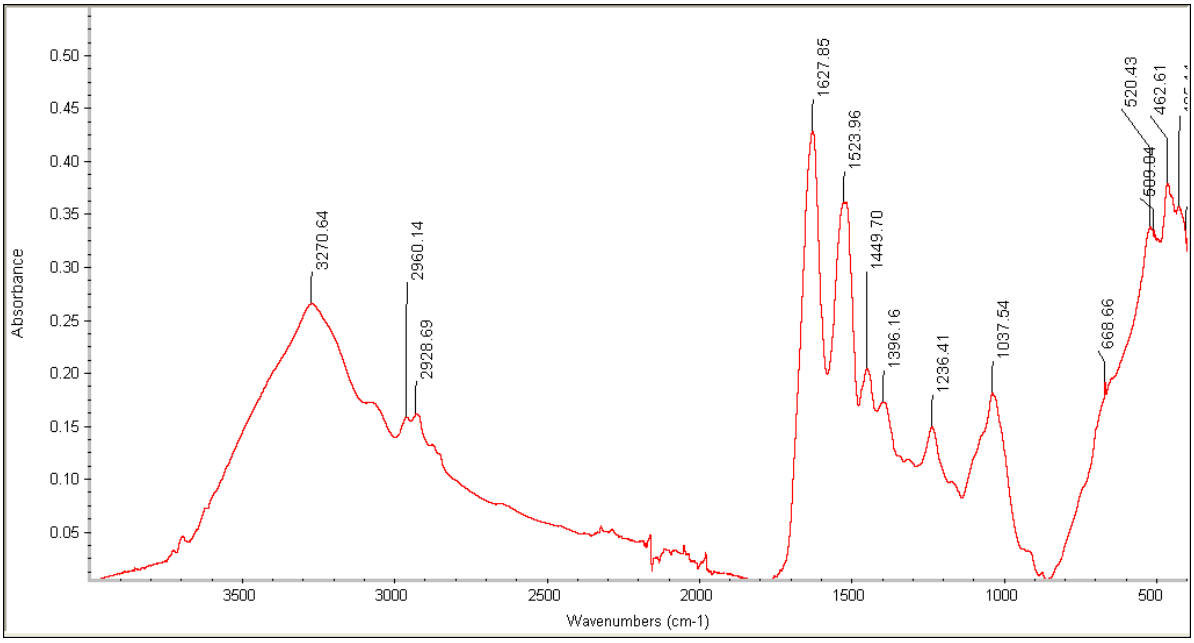

Fig.7 Average primary spectrum of Sambar hair

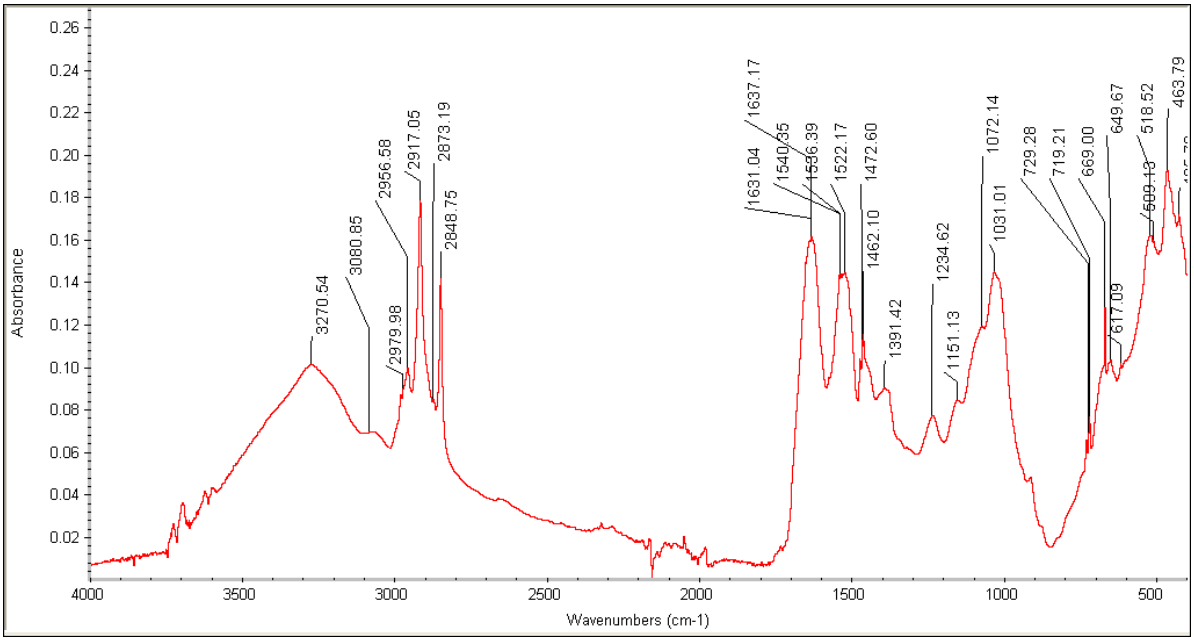

Fig.8 Average primary spectrum of Wild boar hair

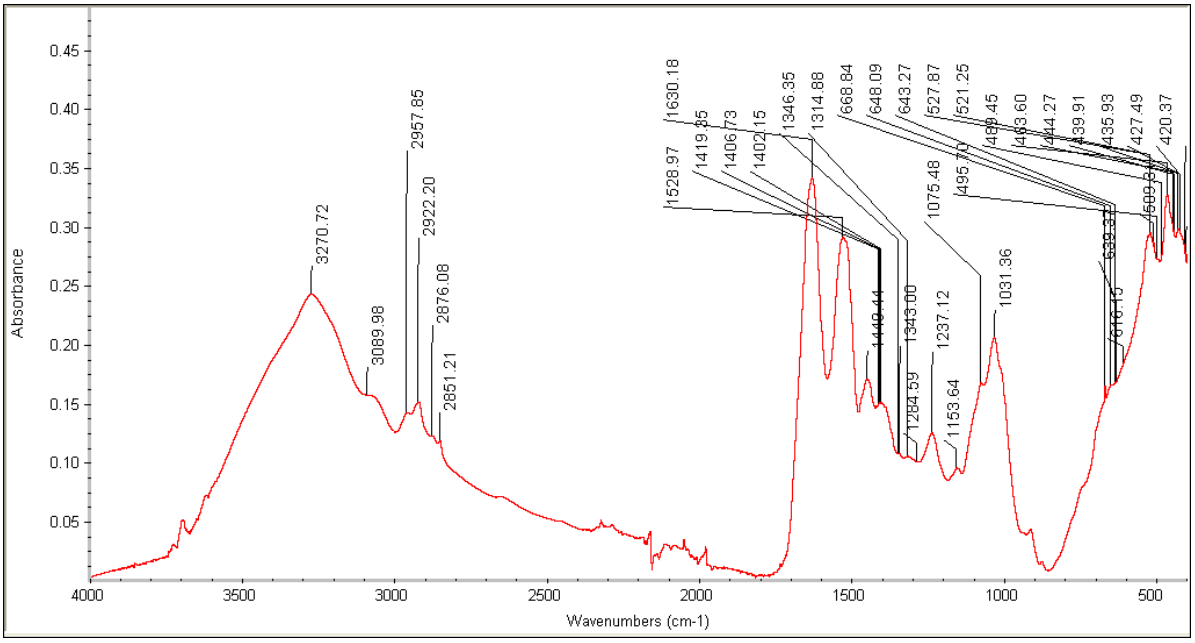

Fig.9 Average primary spectrum of Sloth bear hair

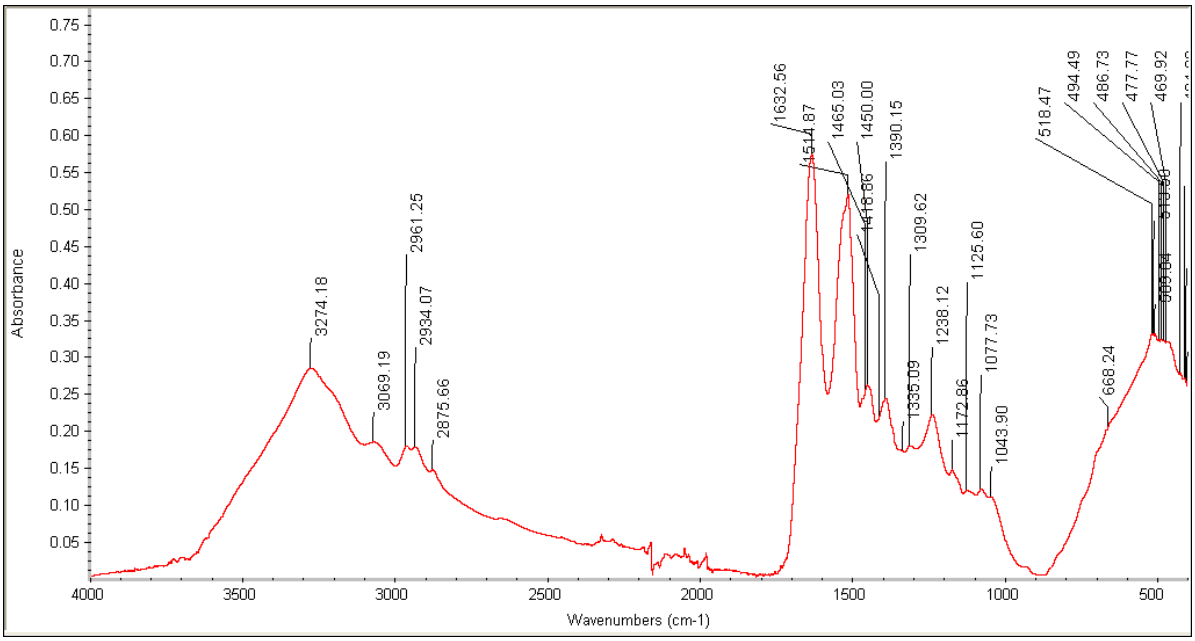

Fig.10 Average primary spectrum of Bison hoof

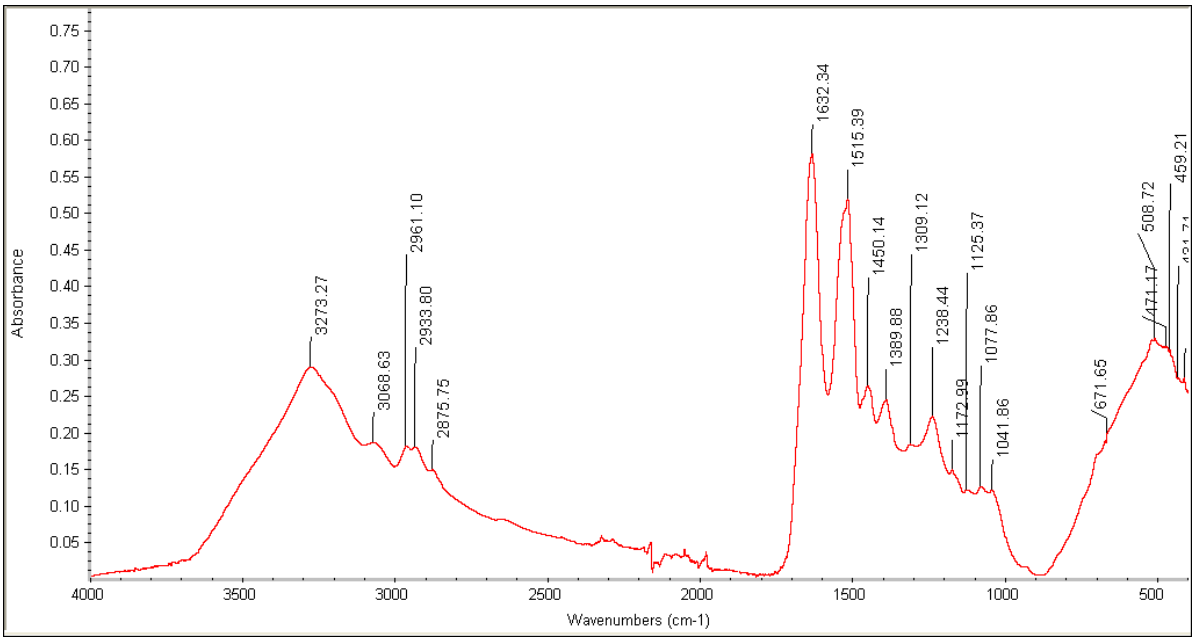

Fig.11 Average primary spectrum of Black buck hoof

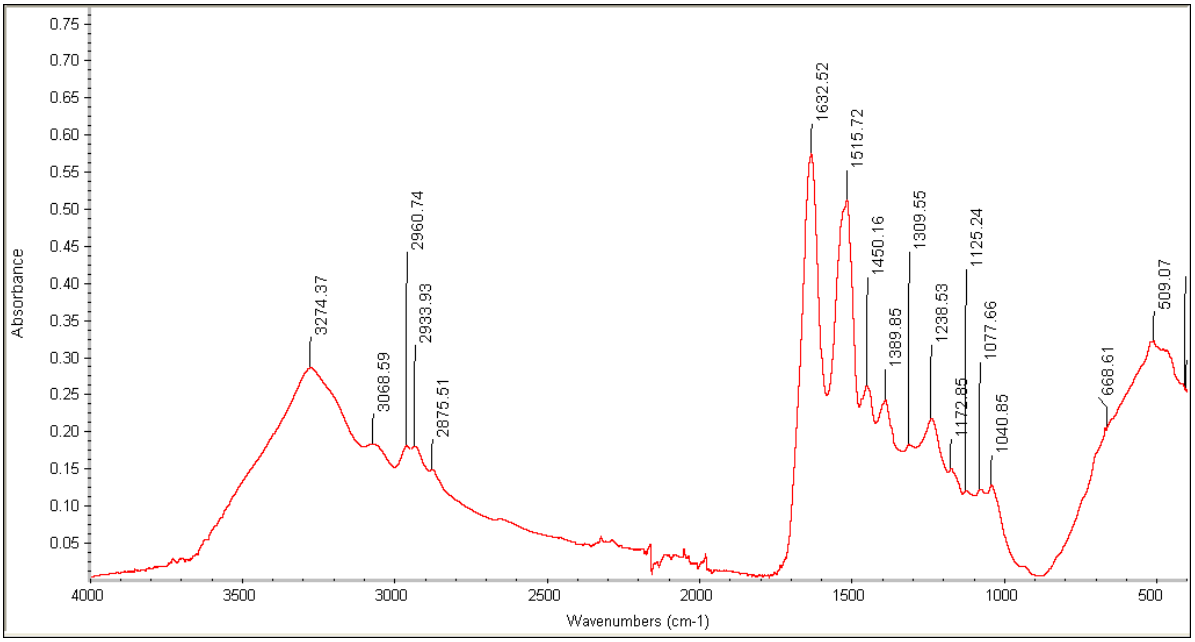

Fig.12 Average primary spectrum of Nilgai hoof

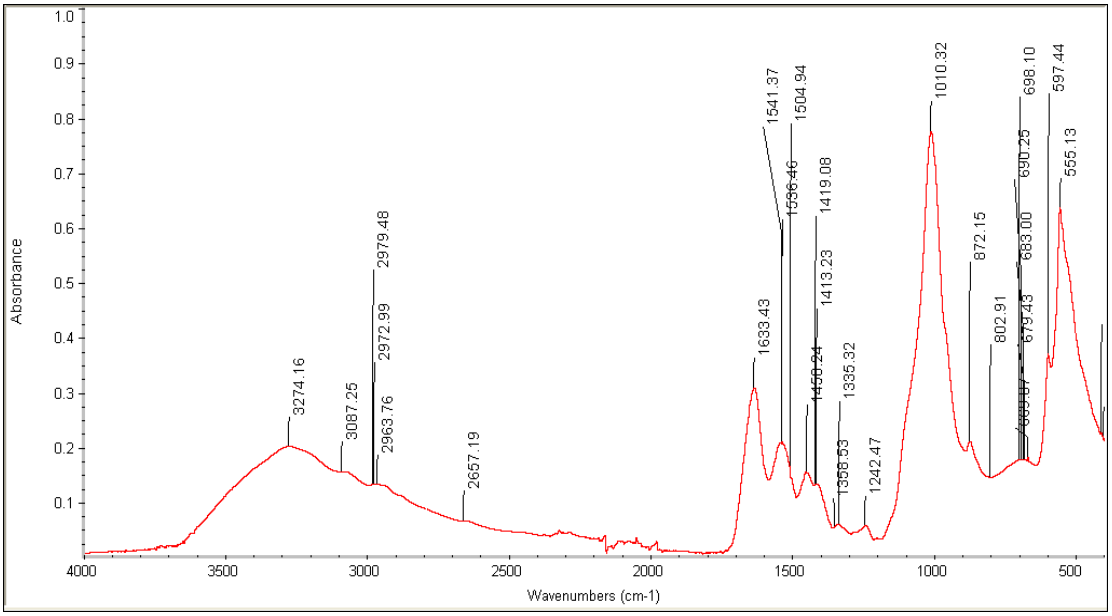

Fig.13 Average primary spectrum of African Elephant tusk

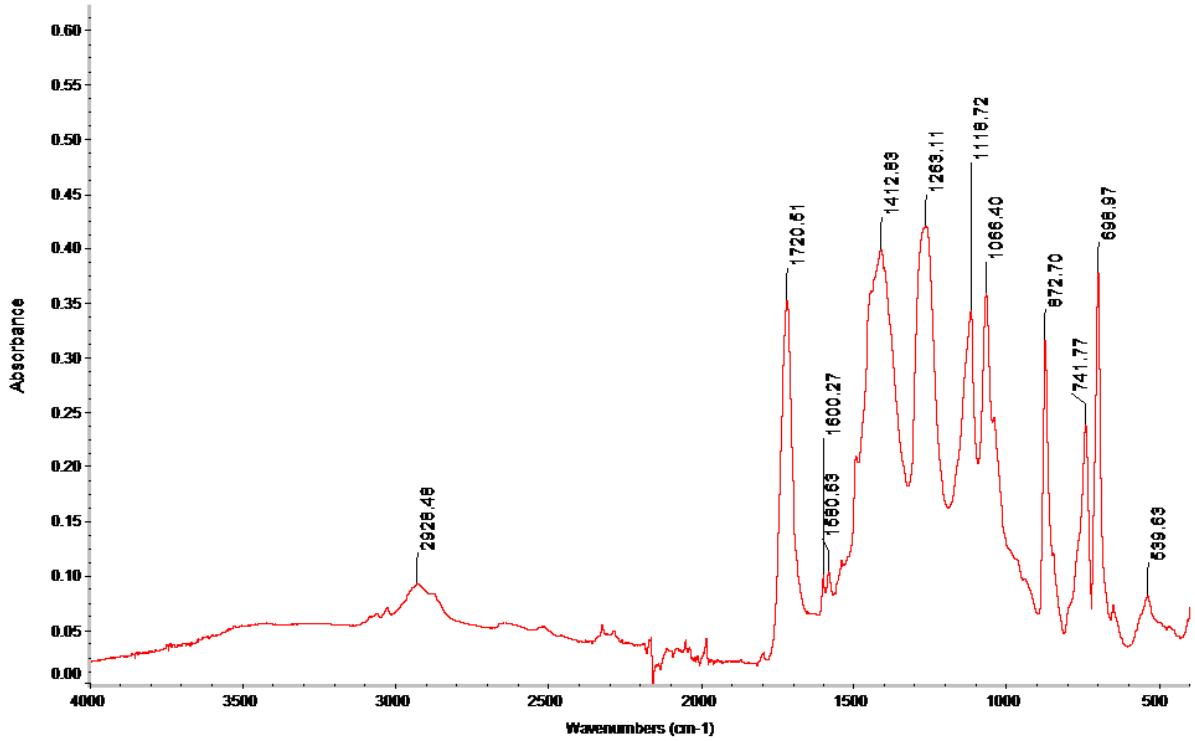

Fig 14: Showing average primary FTIR Spectrum of artifacts.

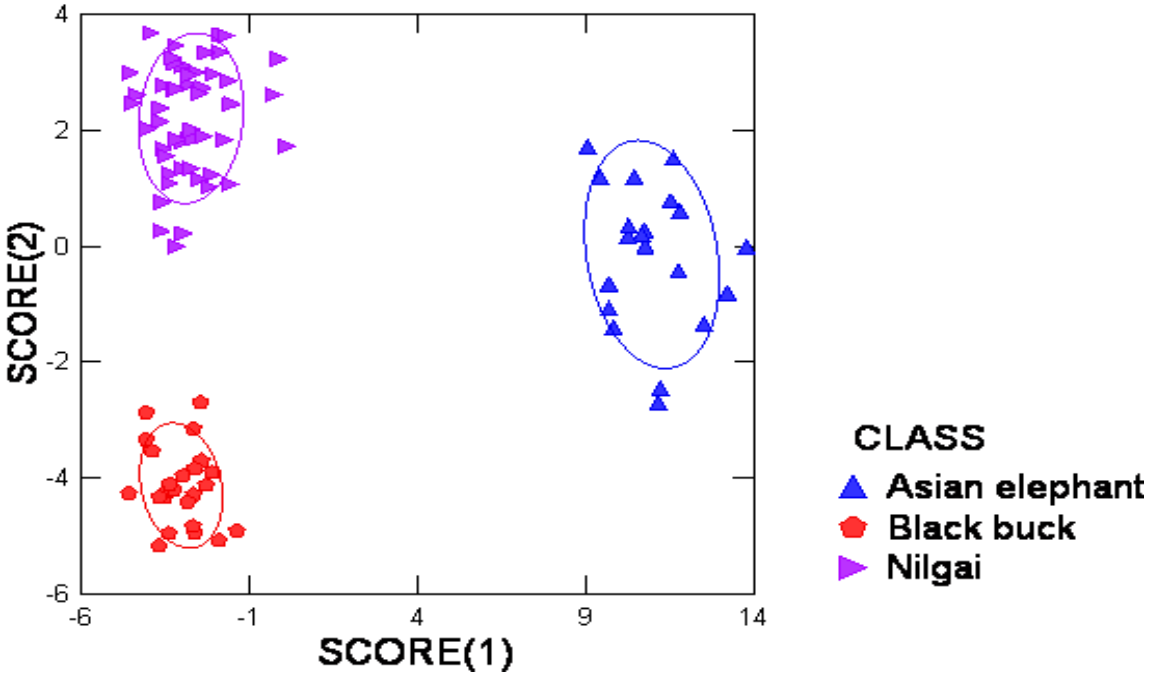

Fig.15 Canonical Score Plot of Asian elephant, Black buck and Nilgai hairs

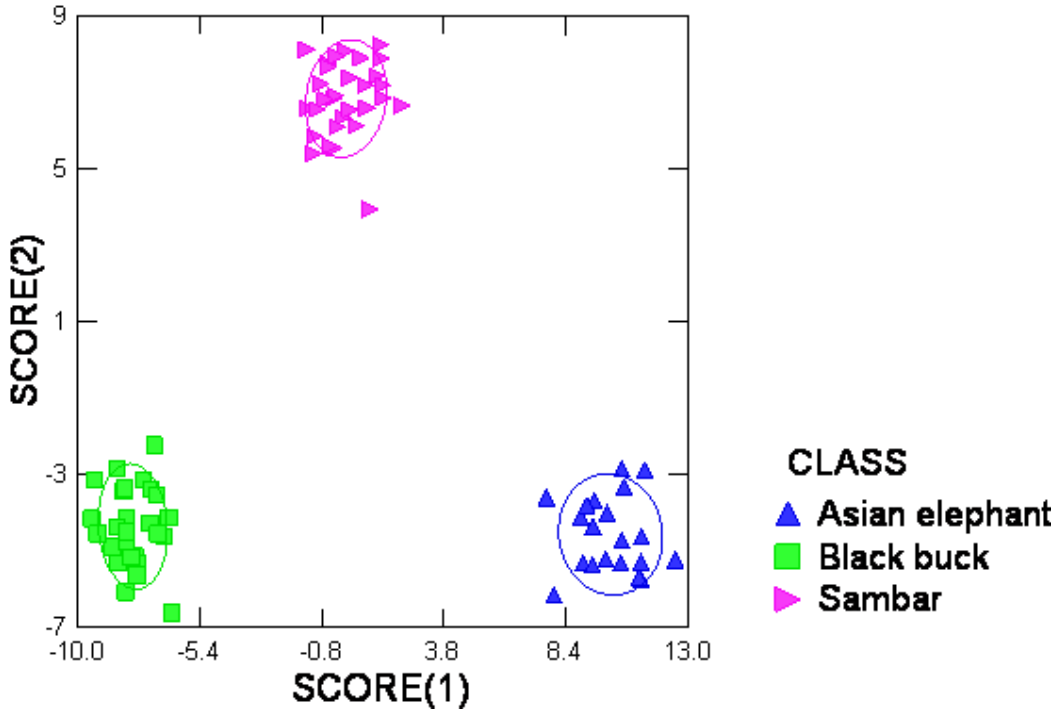

Fig.16 Canonical Score Plot of Asian elephant, Black buck and Sambar hairs

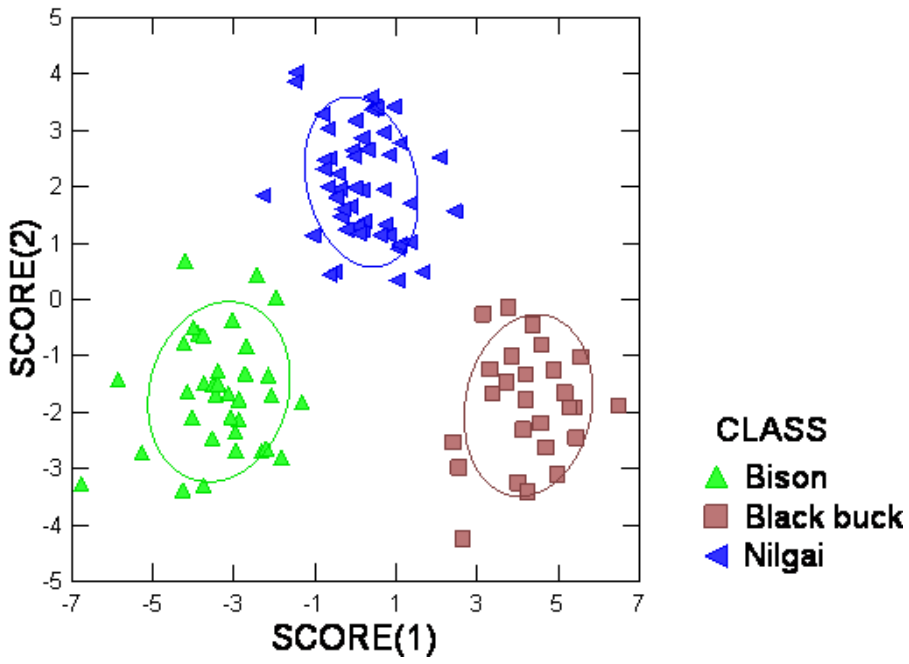

Fig.17 Canonical Score Plot of Bison, Black buck and Nilgai hairs

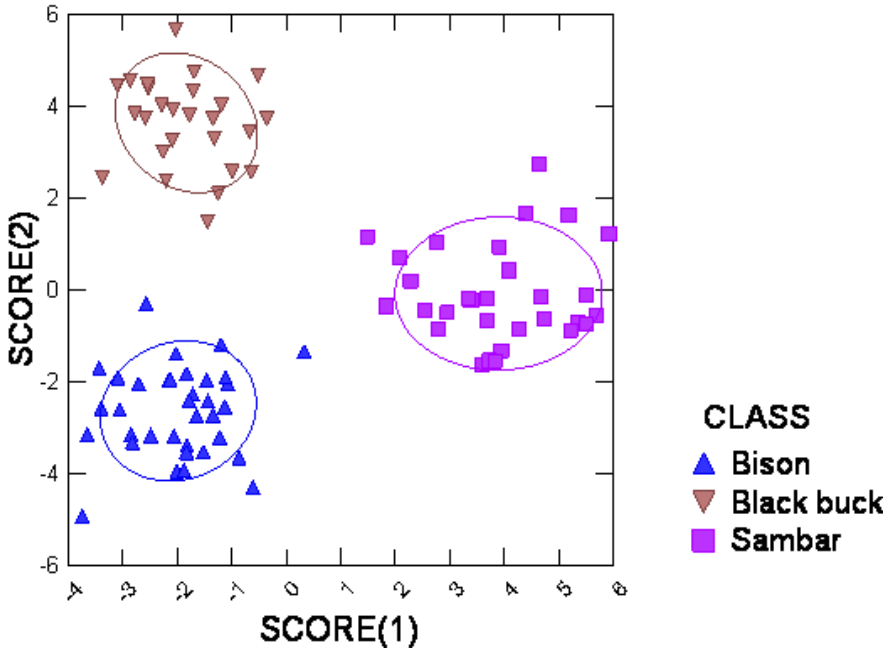

Fig.18 Canonical Score Plot of Bison, Black buck and Sambar hairs

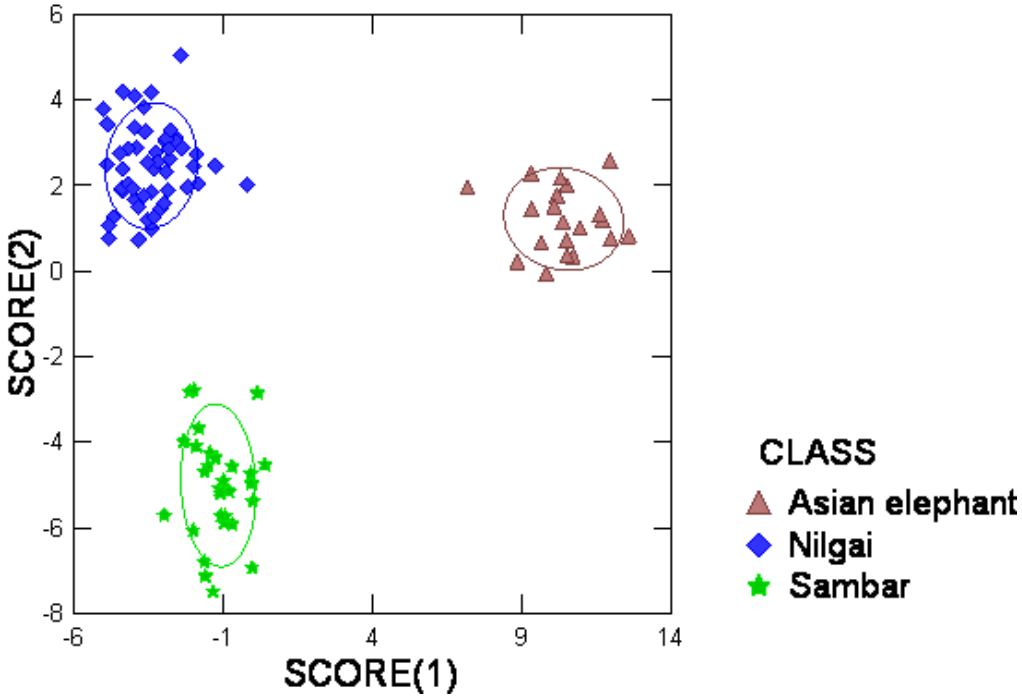

Fig.19 Canonical Score Plot of Asian elephant, Nilgai and Sambar hairs

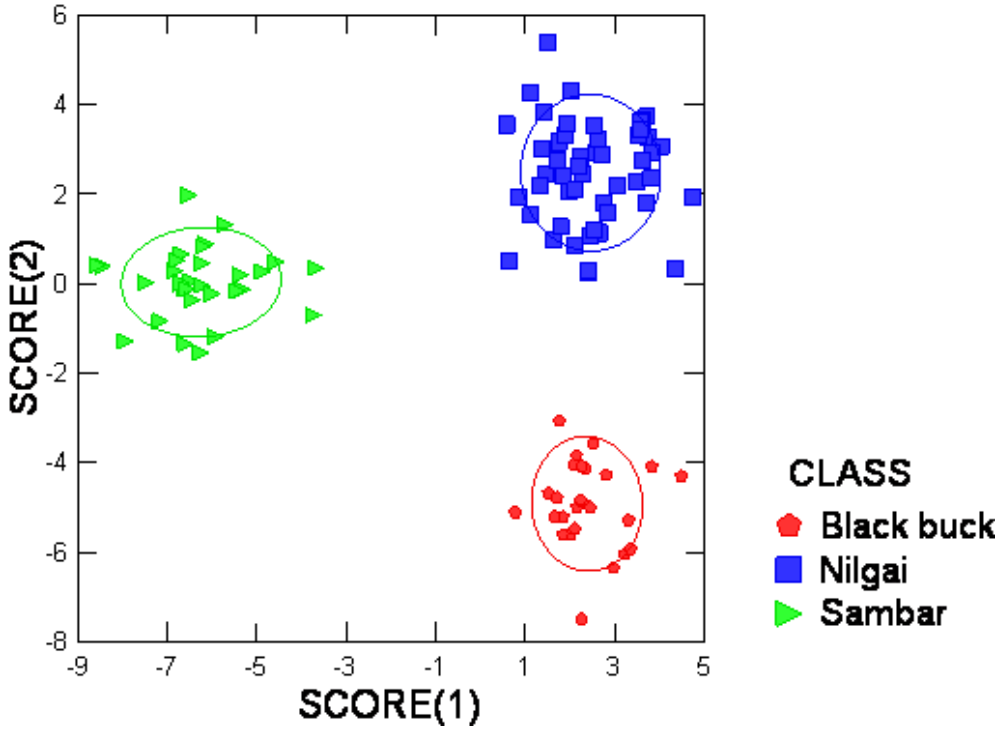

Fig.20 Canonical Score Plot of Black buck, Nilgai and Sambar hairs

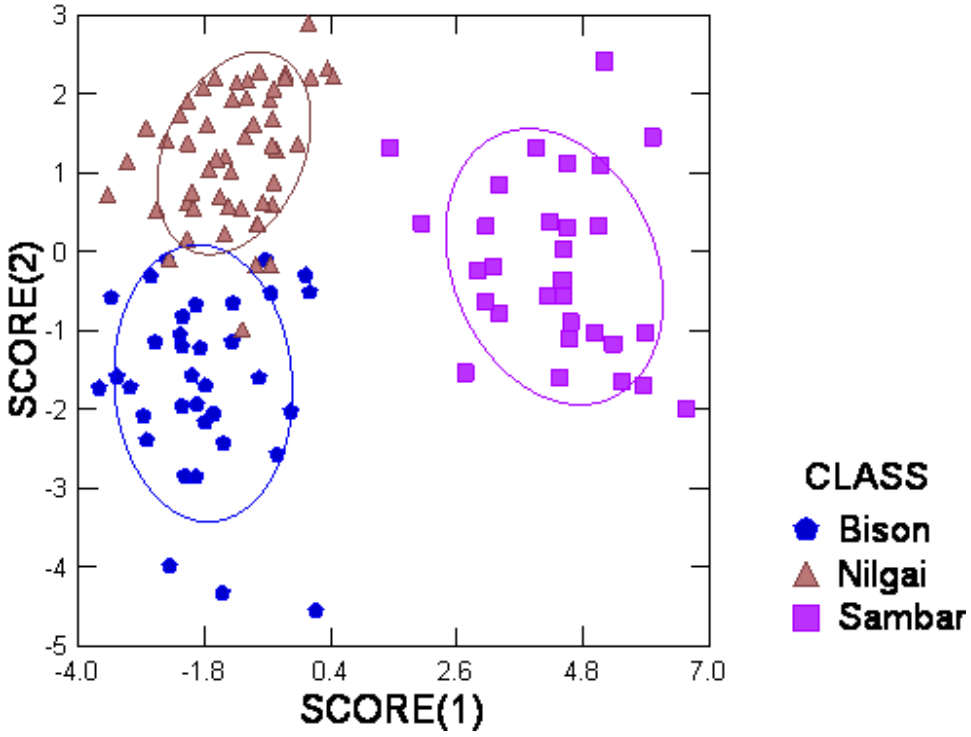

Fig.21 Canonical Score Plot of Bison, Nilgai and Sambar hairs

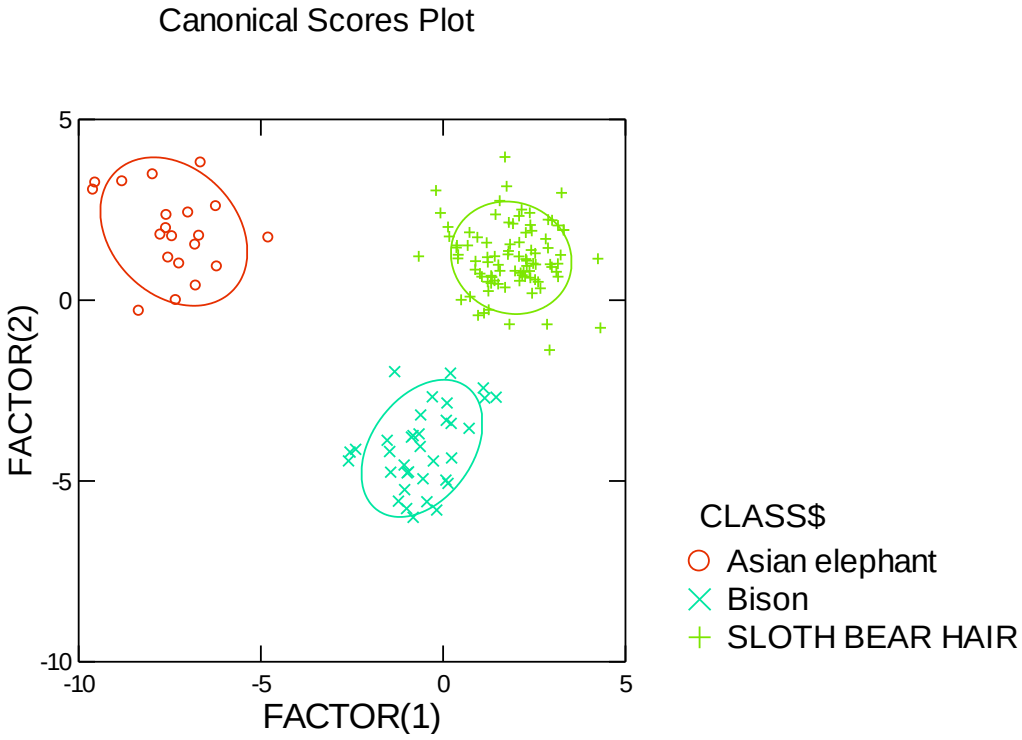

Fig.22 Canonical Score Plot of Asian elephant, Bison and Sloth bear hairs

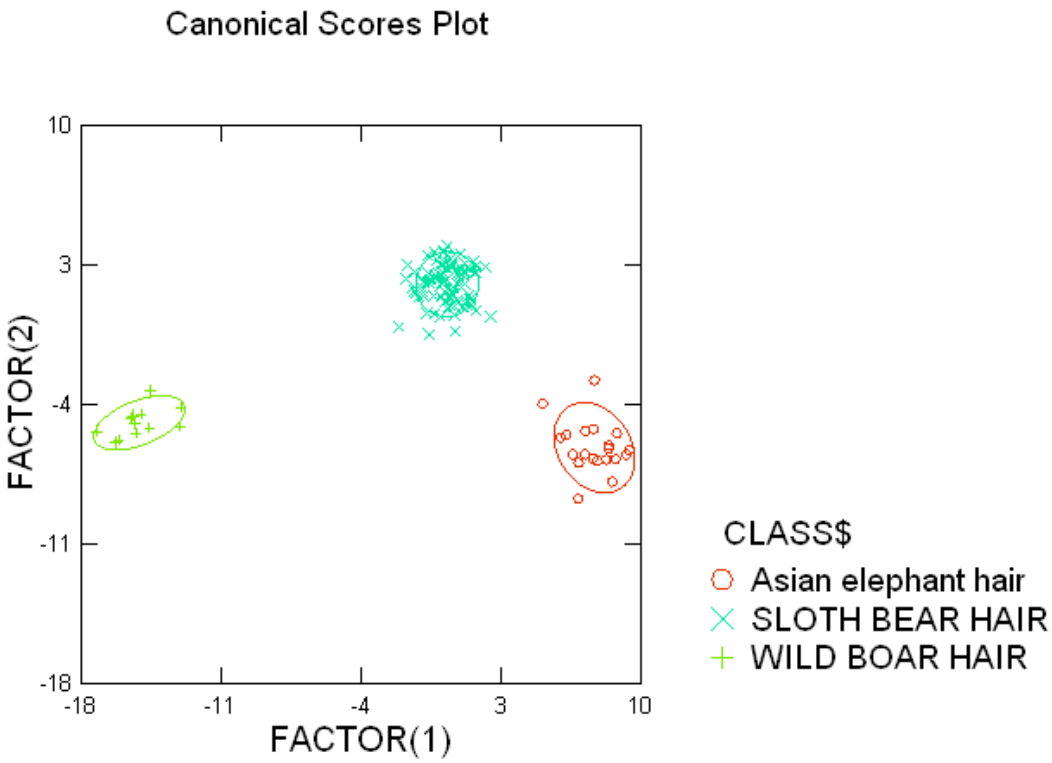

Fig.23 Canonical Score Plot of Asian elephant, Sloth bear and Wild boar hairs

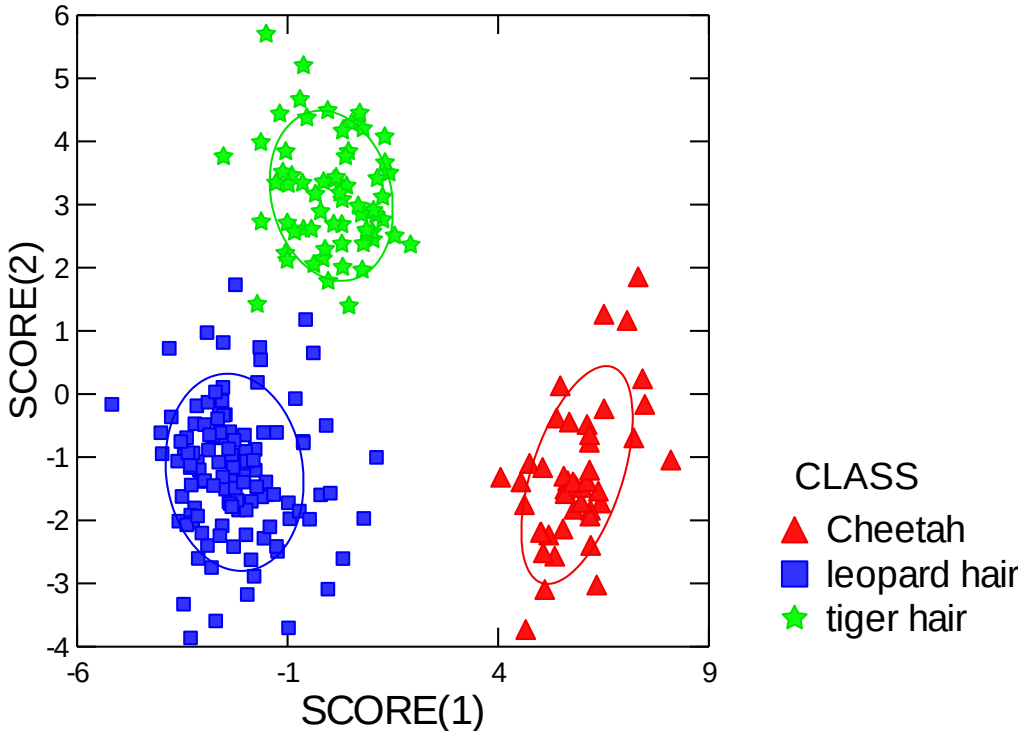

Fig. 24 Canonical Score Plot of Cheetah, Leopard and Tiger hairs

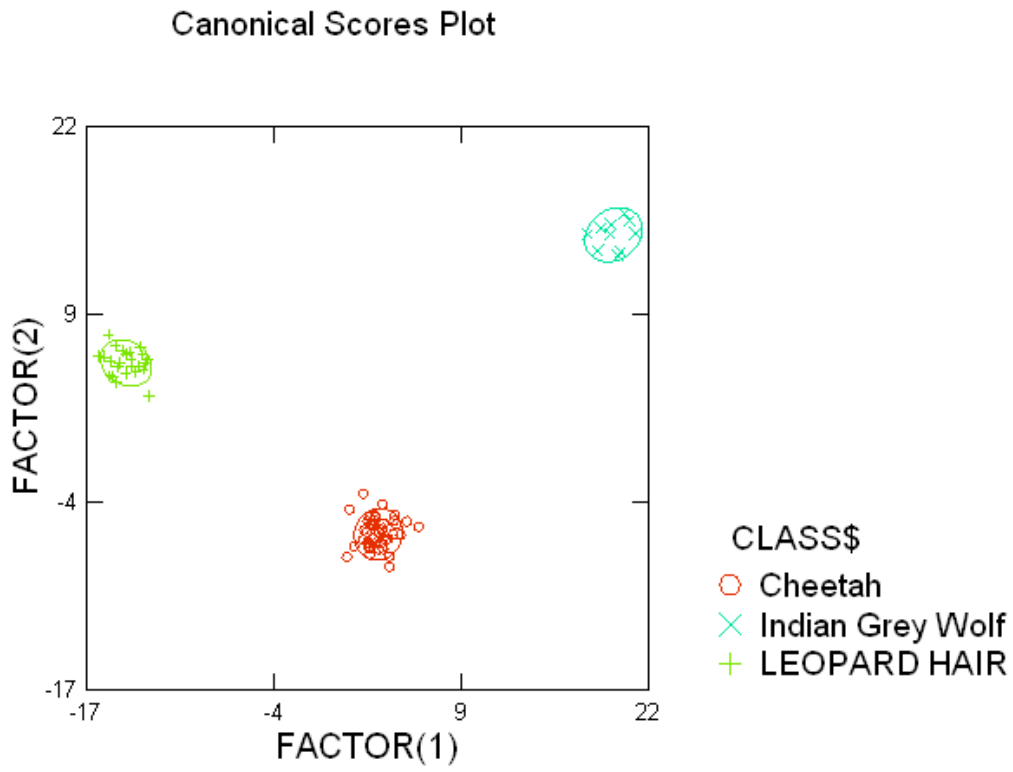

Fig.25 Canonical Score Plot of Cheetah, Indain grey wolf and Leopard hairs

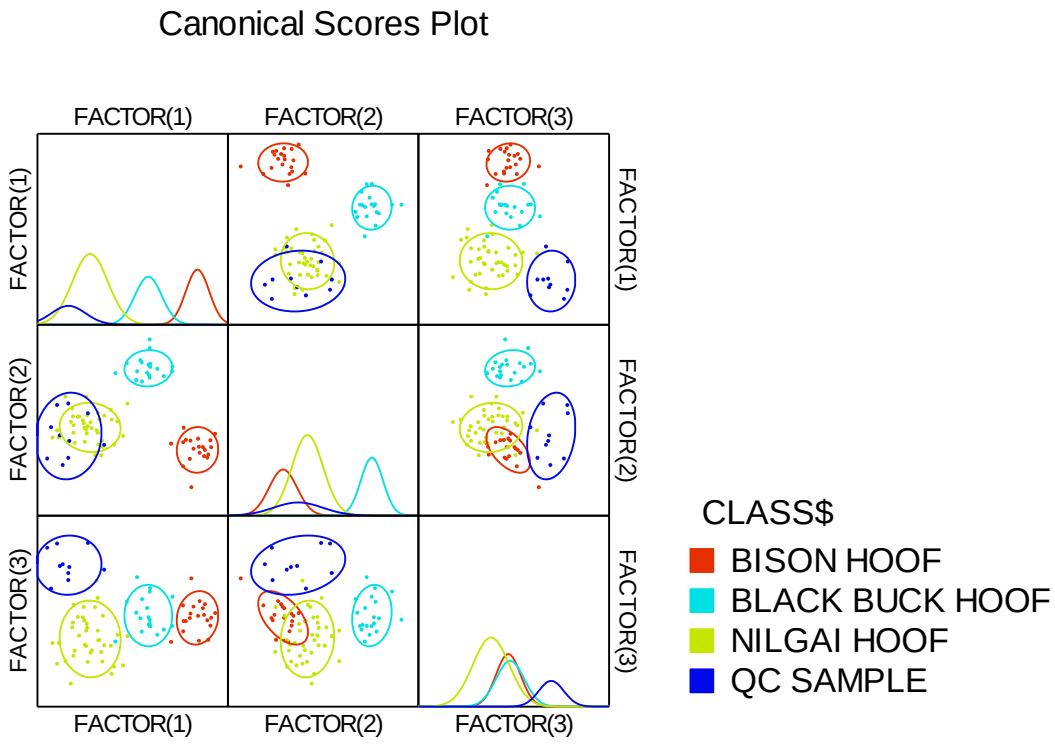

Fig.26 Canonical Score Plot of Bison, Black buck and Nilgai hooves along with QC sample

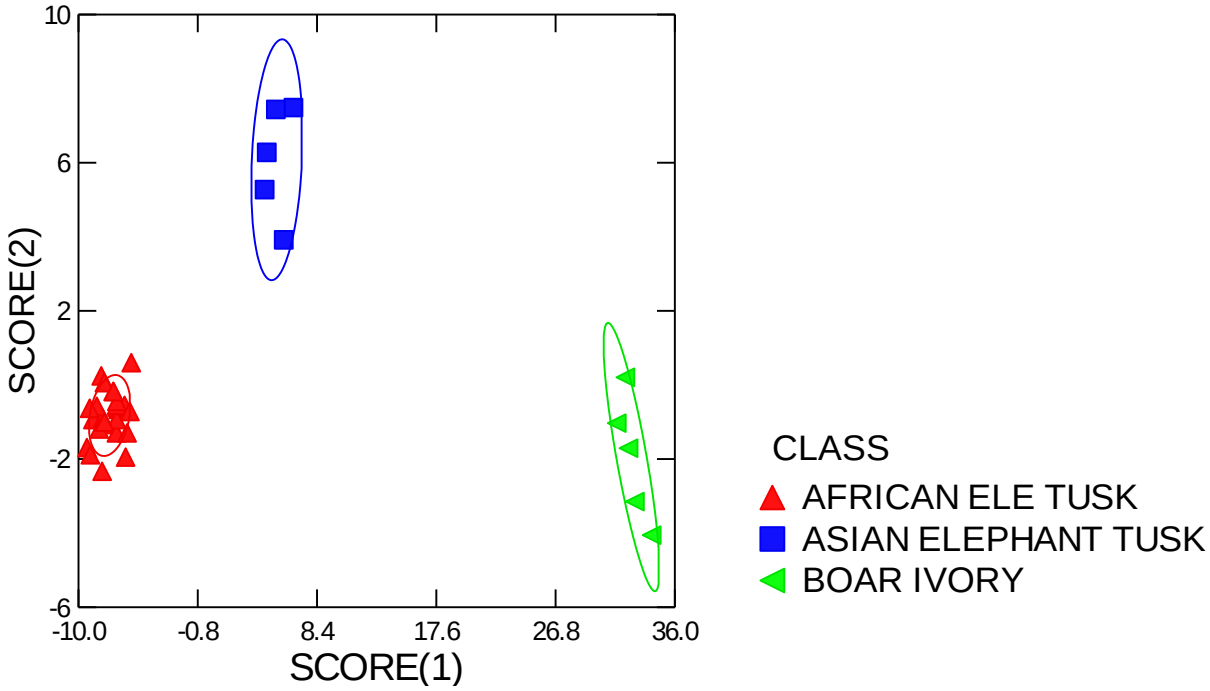

Fig. 27 Canonical Score Plot of African elephant, Asian elephant and wild boar tusks

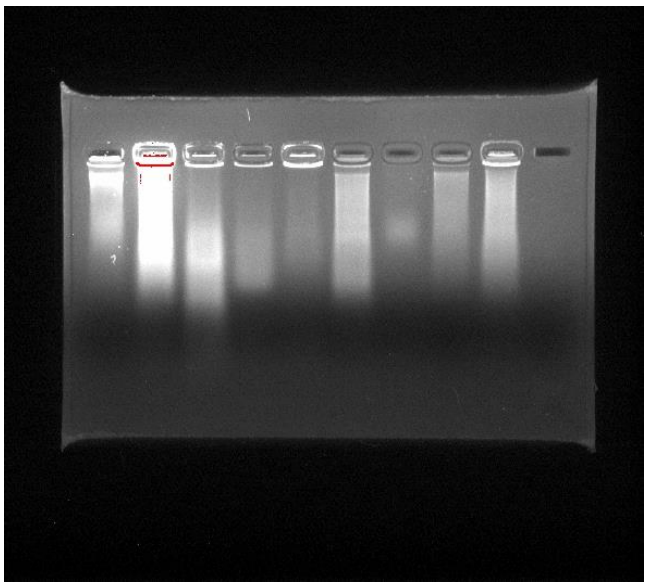

Fig. 28. 0.8 % agarose gel- tested for presence of bright streak of genomic DNA.

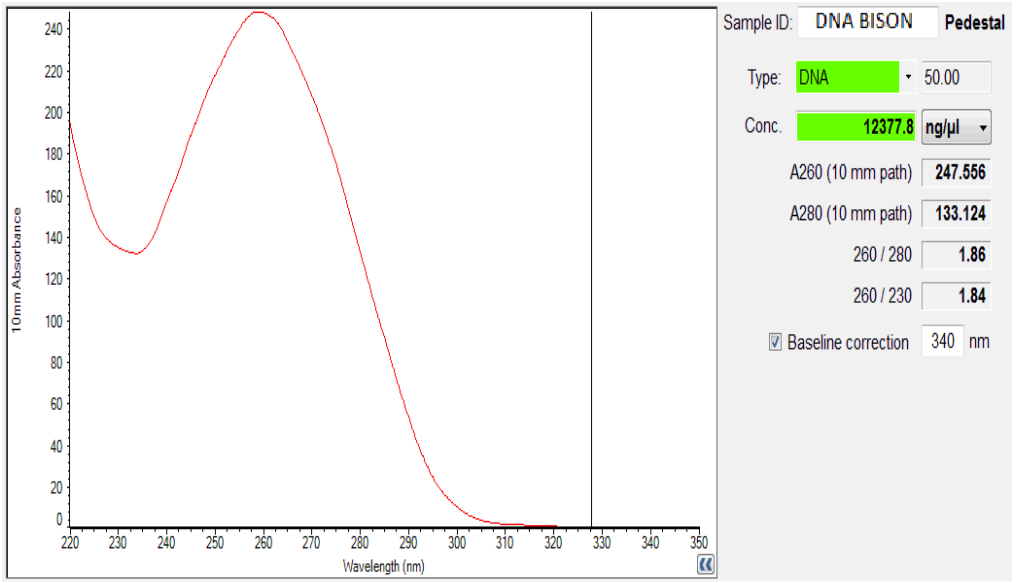

Fig. 29. Quantification of DNA samples by Spectrophotometer (thermo scientific) by nano drop method (bison skin sample).

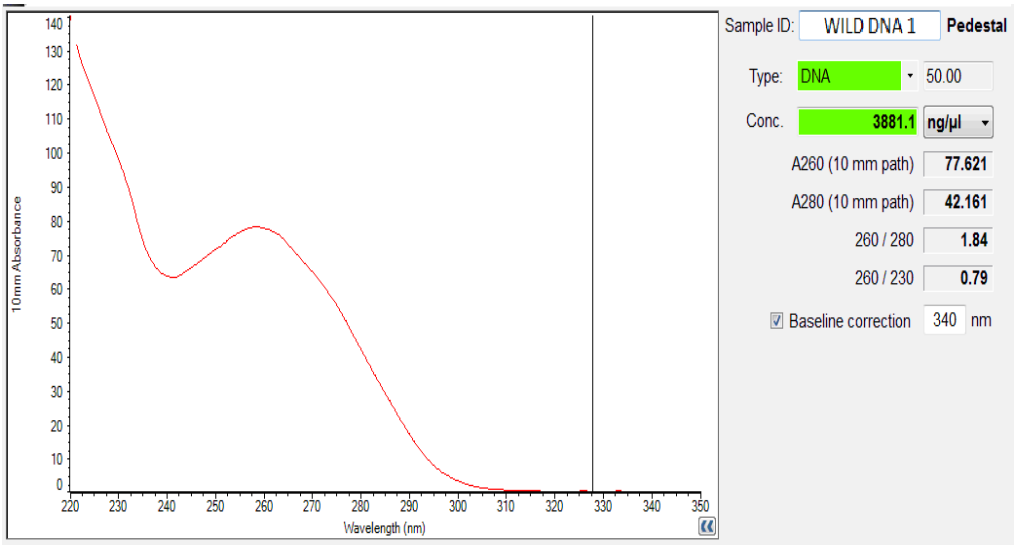

Fig. 30. Quantification of DNA samples by Spectrophotometer (thermo scientific) by nano drop method (nilgai skin sample).

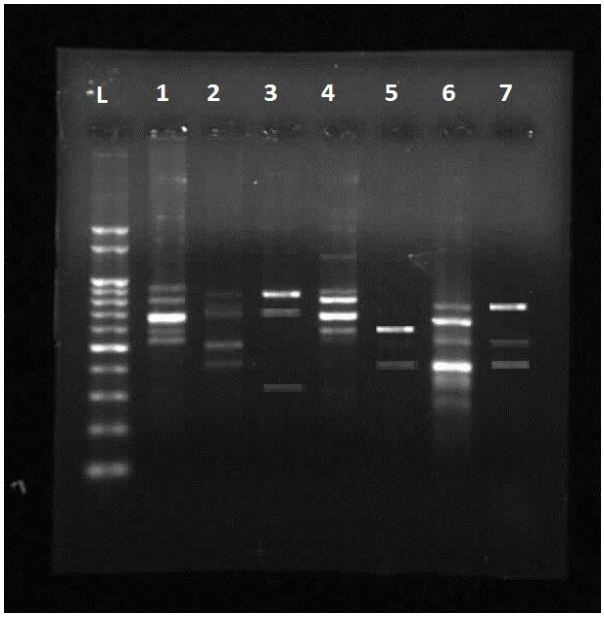

Fig.31 . Agarose gel electrophoresis showing band patterns of amplified DNA products with random primer OPG of 17 for all 7 species.
[L-1000bp ladder; 1- Indian bison DNA; 2- Black buck DNA; 3- Nilgai DNA; 4- Cattle DNA; 5- Wild boar DNA; 6- Sloth bear DNA; 7- Cheetah DNA]

Fig. 32. Agarose gel electrophoresis showing band patterns of amplified DNA products with random primer RAn 5 for 5 species.
[L-1000bp ladder; 1- Indian bison DNA; 2- Black buck DNA; 3- Nilgai DNA; 4- Cattle DNA; 5- Wild boar DNA]

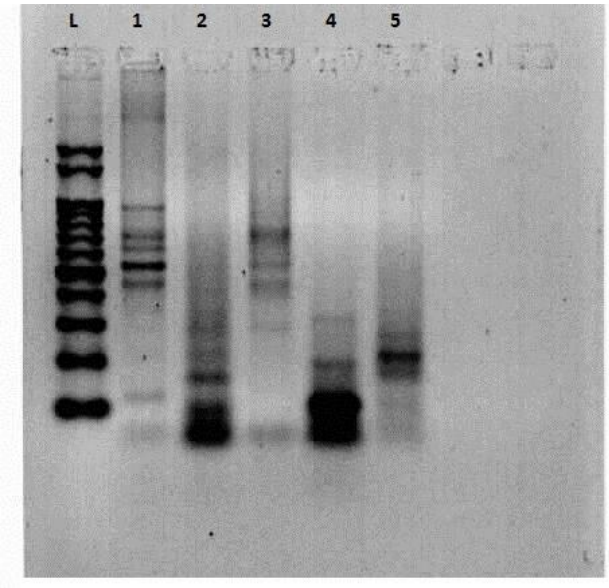

Fig. 33. Agarose gel electrophoresis showing band patterns of amplified DNA products with random primer D1 for 5 species
[L-1000bp ladder; 1- Indian bison DNA; 2- Black buck DNA; 3- Cattle DNA; 4- Wild boar DNA; 5- Sloth bear DNA]

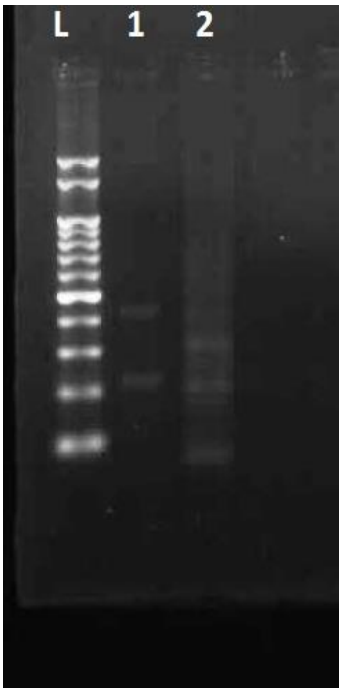

Fig. 34. Agarose gel electrophoresis showing band patterns of amplified DNA products with random primer U3 for 2 species.
[L-1000bp ladder; 1- Wild boar DNA; 2- Sloth bear DNA]

Classification Matrix (Cases in row categories classified into columns)				
	Asian elephant	**Black buck**	**Nilgai**	**%correct**
Asian elephant hair	52	0	0	100
Black buck hair	0	80	0	100
Nilgai hair	0	0	92	100
Total	52	80	92	100

TABLE 1

Classification Matrix (Cases in row categories classified into columns)				
	Asian elephant	**Black buck**	**Sambar**	**%correct**
Asian elephant hair	52	0	0	100
Black buck hair	0	80	0	100
Sambar hair	0	0	38	100
Total	52	80	38	100

TABLE 2

Classification Matrix (Cases in row categories classified into columns)				
	Bison	**Black buck**	**Nilgai**	**%correct**
Bison hair	110	0	0	100
Black buck hair	0	80	0	100
Nilgai hair	0	0	92	100
Total	110	80	92	100

TABLE 3

Classification Matrix (Cases in row categories classified into columns)				
	Bison	**Black buck**	**Sambar**	**%correct**
Bison hair	110	0	0	100
Black buck hair	0	80	0	100
Sambar hair	0	0	38	100
Total	110	80	38	100

TABLE 4

Classification Matrix (Cases in row categories classified into columns)				
	Asian elephant	**Nilgai**	**Sambar**	**%correct**
Asian elephant hair	52	0	0	100
Nilgai hair	0	92	0	100
Sambar hair	0	0	38	100
Total	52	92	38	100

TABLE 5

Classification Matrix (Cases in row categories classified into columns)				
	Black buck	**Nilgai**	**Sambar**	**%correct**
Black buck hair	80	0	0	100
Nilgai hair	0	92	0	100
Sambar hair	0	0	38	100
Total	80	92	38	100

TABLE 6

Classification Matrix (Cases in row categories classified into columns)				
	Bison	**Nilgai**	**Sambar**	**%correct**
Bison hair	110	0	0	89
Nilgai hair	0	92	0	98
Sambar hair	0	0	38	97
Total	110	92	38	95

TABLE 7

Classification Matrix (Cases in row categories classified into columns)				
	Asian elephant	**Bison**	**Sloth bear**	**%correct**
Asian elephant hair	52	0	0	100
Bison hair	0	110	0	100
Sloth bear hair	0	0	195	100
Total	52	110	195	100

TABLE 8

Classification Matrix (Cases in row categories classified into columns)				
	Asian elephant	**Sloth bear**	**Wild boar**	**%correct**
Asian elephant hair	52	0	0	100
Sloth bear hair	0	195	0	100
Wild boar hair	0	0	40	100
Total	52	195	40	100

TABLE 9

Classification Matrix (Cases in row categories classified into columns)				
	Cheetah	**Leopard**	**Tiger**	**%correct**
Cheetah hair	45	0	0	100
Leopard hair	0	24	0	100
Tiger hair	0	0	65	100
Total	45	24	65	100

TABLE 10

Classification Matrix (Cases in row categories classified into columns)				
	Cheetah	**Indian Grey Wolf**	**Leopard**	**%correct**
Cheetah hair	45	0	0	100
Indian Grey Wolf hair	0	30	0	100
Leopard Hair	0	0	24	100
Total	45	30	24	100

TABLE 11

Classification Matrix (Cases in row categories classified into columns)					
	Bison	**Black buck**	**Nilgai**	**Qc sample**	**%correct**
Bison Hoof	20	0	0	0	100
Black buck hoof	0	32	0	0	100
Nilgai hoof	0	0	48	1	97
QC SAMPLE	0	0	0	10	100
Total	20	32	48	11	99

TABLE 12

Classification Matrix (Cases in row categories classified into columns)				
	African Elephant	**Asian Elephant**	**Boar ivory**	**%correct**
African Elephant tusk	5	0	0	100
Asian Elephant tusk	0	25	0	100
Boar ivory	0	0	5	100
Total	5	25	5	100

TABLE 13

Table 14. - FTIR Peak assignment for Keratinaceous Appendages resolved by secondary derivative spectra.
(Hopkins et. al., 1991, Joy and Lewis 1991, Akhtar and Edwards 1997).

Mean Peaks	Assignment
3274, 3273, 3272, 3271	Stretching O-H symmetric, N-H stretching, Amide A band
3066, 3065, 3064, 3063, 3062	C_2 aromatic stretching, Amide B band
2667, 2965, 2964, 2963	CH_3 modes
2931, 2930, 2929, 2927	C-H stretching bands
2925	C-H stretching bands
2874, 2873	ν st CH3 , Stretching C-H, N-H
2853, 2852, 2851	Symmetric CH_2 stretch
1693	Antiparallel β-sheet of amide I
1683, 1682, 1681, 1679	Unordered random coils and turns of amide I
1664, 1663	Amide I (disordered structure-solvated), 3 turn Helix
1647,1646, 1645	Amide I Random Coil
1642, 1640, 1637	Amide I β-sheet
1630	Amide I β-sheet
1625, 1623, 1622	Amide I β-sheet
1611, 1610, 1609, 1608	Amide I Unordered
1568, 1567	Amide II Ring base
1553	CO stretching Predominately a-sheet of amide II (Amide II band mainly stems from the C-N stretching and C-N-H bending vibrations weakly coupled to the C=O stretching Ring base
1552, 1551, 1550, 1549	Amide II Ring base (an N-H bending vibration coupled to C-N stretching)
1539, 1538, 1537, 1536	Amide II β-sheet, Stretching C=N, C=C (an N-H bending vibration coupled to C-N stretching
1519, 1518, 1517, 1516, 1515	Amide II (tyrosine side chain)

1513, 1512	ν(C=C)pigment , Amide II (an N-H bending vibration coupled to C-N stretching)
1498, 1497	CH in-plane bending
1451, 1450	Asymmetric CH_3 bending modes of the methyl groups of proteins, Methylene Deformation
1400	COO- symmetric stretching of acidic amino acids aspartate and glutamate Aliphatic side groups of the amino acid residues
1397	CH3 symmetric deformation
1395, 1393, 1392, 1391, 1390, 1389	Aliphatic side groups of the amino acid residues
1380, 1379, 1378, 1377, 1376	δCH_3, Stretching C-O, deformation C-H, deformation N-H
1371, 1369, 1368	Deformation N-H, C-H, δ(CH2), ν(CC)
1341, 1340	CH_2 wagging
1316, 1315, 1314, 1313, 1312	Amide III band components of proteins
1308, 1307, 1306, 1305	Amide III
1303, 1302	Amide III
1290, 1289	Amide III
1286, 1285, 1284	Amide III, Deformation N-H
1273, 1271, 1270	CHα' rocking
1269, 1268, 1266, 1265	Amide III, CHα' rocking
1236, 1235, 1234, 1233	Amide III
1209, 1207, 1205, 1204, 1203, 1202	C-O-C , Ring vibrations, PO_2^- asymmetric (phosphate I), proteins-amide III
1200	Protein
1166	C-O stretching mode of C-OH groups of serine, threosine, & tyrosine of proteins), ν(CC), δ(COH), ν(CO) stretching
1163	CH'_9, , CH_7, $CH'7$ deformations, C-O stretching
1161, 1160, 1159, 1158, 1156, 1155	νC-O of proteins,
1127, 1126	ν(C-O)
1108, 1107, 1106, 1105, 1104	ν asym(SO) Cystein dioxide, ν(CO), ν(CC)
1102, 1100	SO stretch (cysteine residue)
1078, 1077, 1076	ν sym(SO) Cysteine monoxide
1048, 1047, 1046, 1045	ν sym(SO) Cysteine monoxide
1043, 1042	ν st(SO) Cysteine monoxide
950, 948	Pigments
944, 942, 940, 939, 938	Pigments

Table 15: FTIR Peak Assignment for Antler or Ivory (Boney appendages)
(Miller and Wilkins 1952; Espinoza E.O. *et al.,* 2008; Movasaghi, Z., 2007; Kourkoumelis and Tzaphlidou, 2010)

Wave umber (Mean)	Assignment
3279	– OH stretch symmetric
2875	νs Stretch C-H
2847	Symmetric stretch Methoxy, C-H stretch , Cholesterol, Phospholipids
1693,1694	Anti parallel β- sheet of Amide I
1680, 1681, 1683	C=O Guanine deformation N-H in plane
1680	Unordered random coil turns Amide I
1668	Amide I - Anti parallel β- sheet, inorganic Sulfate
1663, 62	C = O Cytosine, Uracyl
1654	Amide I, C2 = O Cytosine / C = O, C = N, N - H of Adenine, Thiamine, Guanine and Cytosine
1648, 1647	Amide I
1633, 34, 36	β- sheet – Amide I
1630, 1629	Amide I / C = C Uracyl C = O, Inorganic Sulfate
1567, 1566	Ring base
1563, 1560, 1557	Ring base
1548, 49, 50	Amide II
1528, 1531	C = N modified Guanine C = N Adenine, Cytosine Stretching C=N, C=C
1526, 1525, 1524	C = N Guanine, Stretching C=N, C=C
1522, 1521, 1519	Amide II ?
1513, 1512	CH in-plane bend.
1499, 1498	C = C, deformation C-H
1472, 1470	CH2 bending of the methylene chain in lipids
1453, 1452, 1451	Asymmetric CH3 bending of methyl groups of proteins, Inorganic carbonate
1379,1378, 1377	δ CH3, C – O stretching, deformation - C – H, deformation N – H .
1338	CH2 wagging / Collagen
1317	Amide III proteins / Collagen
1284, 1283	Amide III proteins – Collagen
1240	ν_{as} PO_2^- , Collagen, Amide III
1202, 1201	PO_2^- (Phosphate I) asymmetric
1162, 1161, 1160	CO stretching, Stretching vibrations of hydrogen-bonding C-OH groups, n(CC), d(COH), n(CO) stretching, Stretching modes of the C-OH groups of serine, threonine, and tyrosine residues of cellular proteins
1111	Symmetric Stretching P-O-C ?, Inorganic Phosphate
1097	Phosphate II stretching PO_2 symmetric
1085,1084	νs PO_2^-, DNA (PO_2^- vibrations), νs PO_2^- of nucleic acids, PO_2 symmetric (phosphate II)

1079	νs PO_2
1059, 1058	Stretching C-O deoxyribose, Oligosaccharide C-OH stretching band
1012, 1011	$CH_{\alpha\,\alpha'}$ out of plane and $C_\alpha = C_\alpha$ out of plane bending, Stretching C-O deoxyribose
1010	Stretching deoxyribose
958	Inorganic Phosphate, CH out of plane bending vibrations (700 – 1000)
872	CO_3^{-2} (carbonate), CH out of plane bending vibrations (600 – 900)
668, 666, 664	Inorganic sulfate, CH out of plane bending vibrations (600 – 900)
599, 600	CH out of plane bending vibrations (600 – 900)
576,557,522, 21	$C_\alpha = C_{\alpha'}$ torsion and C-OH_3 torsion of Methoxy group

Table 16: FTIR Peaks Assignments for Artifacts

Mean peaks	SD	Peak Assignment
469.41	2.705565	
539.5856	0.464384	
651.8533	0.079057	C-S Stretching
698.9856	0.094089	C-H Out of Plane Bending
741.7689	0.187779	C_H Out of Plane Bending
847.87	0.080178	
872.7089	0.108218	
1041.928	0.240936	S=O Stretching
1066.411	0.148277	S=O Stretching
1118.741	0.239867	C=O Stretching and Bending
1263.138	0.656521	C-O Stretching; C=O Stretching and Bending
1413.316	1.977885	C-H Bending
1491.918	0.300574	C-H Bending - Aromatic
1541.093	0.028702	C-H Bending - Aromatic
1580.627	0.18775	C-H Bending - Aromatic
1600.282	0.211174	C=C Stretching
1720.581	0.347291	C=O Stretching
2287.053	0.661784	
2324.148	0.071375	
2517.214	1.898145	S-H Stretching
2642.486	4.093984	
2927.879	1.219851	CH Stretching -CH2 Group
3027.326	0.352353	
3061.061	0.546064	CH Stretching
3423.977	4.71418	

Table. 17. Details of primers used for RAPD analysis

Primer	Oligo Name	Sequence (5'-3')	Length	Manufacturer
1	U-3	GCATGCATGT	10 mer	Eurofins
2	D-1	CAGCTATGACCA G	13 mer	Eurofins
3	OPG17	ACGACCGACA	10 mer	Bioserve Biotechnologies
4	ILO526	GCCGTCCGAG	10 mer	Bioserve Biotechnologies
5	ILO 876	GGGACGTCTC	10 mer	Eurofins
6	RAn 1	GAT GAC CGC C	10 mer	GeNie™
7	RAn 2	GGC ACC ATT C	10 mer	GeNie™
8	RAn 3	GGC ACG TAA C	10 mer	GeNie™
9	RAn 4	GGC ATG ACC T	10 mer	GeNie™
10	Ran 5	GGG TAA CGC C	10 mer	GeNie™
11	RAn 6	GGT GCG CCT T	10 mer	GeNie™
12	RAn 7	GTC AGA GTC G	10 mer	GeNie™
13	RAn 8	GTC GCC GTC T	10 mer	GeNie™
14	RAn 9	GTG CCA AAT G	10 mer	GeNie™
15	RAn 10	GTG CCC GAT G	10 mer	GeNie™

Table 18: Number of RAPD bands amplified and number of species specific bands for all primers.

ANIMALS	OPG 17		Ran 5		D1		U3	
	No. of bands amplified	No. of species specific bands	No. of bands amplified	No. of species specific bands	No. of bands amplified	No. of species specific bands	No. of bands amplified	No. of species specific bands
Bison	6	2	7	2	6	3	_	_
Black buck	4	1	3	2	4	1	_	_
Nilgai	3	2	5	3	_	_	_	_
Cattle	5	2	4	1	4	2	_	_
Wild boar	3	1	3	2	3	1	2	1
Sloth bear	6	1	_	_	3	1	3	2
Cheetah	3	1	_	_	_	_	_	_

Table 19: Primer species Specific RAPD Patterns in Different Wild animals.

Animals	Primer OPG 17 Species specific bands	Primer RAn5 Species specific bands	Primer D1 Species specific bands	Primer U_3 Species specific bands
Bison	600bp, 950bp	800bp, 900bp	650bp, 750bp, 950bp	_
Black buck	400bp	450bp 750bp	150bp	_
Nilgai	320bp	550bp, 1000bp	_	_
Cattle	1400bp	900bp	720bp	_
Wild boar	580bp	200bp	190bp	220bp
Sloth bear	650bp	_	250bp	320bp
Cheetah	550bp	_	_	

Discussion

V. DISCUSSION

5.1 Skin morphology

5.1.1 Bison, Black Buck and Nilgai (Family: *Bovidae*)

In the present study, epidermis was stratified squamous keratinized type of epithelium, consisted of stratum basale, stratum spinosum; stratum granulosum and stratum corneum were constantly present in bison, black buck and nilgai. Similar findings were observed by Talukdar *et al.* (1972) in the horse, Sharma and Bharadwaj (1993) in yak, Bacha and Bacha (1990) and Dellmann and Eurell (1998) in domestic animals, Bhattacharya *et al.* (2003a) in buffalo, Pfeiffier *et al*. (2006) in one humped camel, More *et al.* (2007) in spotted deer, but Nagaraju *et al*. (2012) in spotted deer observed only three layers namely stratum corneum, stratum granulosum and stratum basale and all the five layers in cattle. On the contrary, Atlee *et al*. (1997) in addition to layers mentioned above, reported the presence of stratum lucidum in llama skin.

The epidermis was irregularly arranged with large number of epidermal pegs with thick stratum corneum in bison and black buck; stratum corneum was thicker with 4-6 layers in epidermal peg region but 2-3 cell layers in non epidermal peg region in bison and 4-5 cell layers in black buck, but in Nilgai only 2-3 cell layer thickness was observed in stratum corneum. However, Banks (1993) observed several layers of non-nucleated cornified cells in domestic animals. Atlee *et al*. (1997) found in llama basket weave appearance of stratum corneum, Mugale and Bhosle (2002) studied in young Deoni cattle and observed thinner stratum corneum, Bhattacharya *et al.* (2003a) found dead cells without nuclei and cellular architecture in non-descriptive buffalo. However, the stratum

corneum consisted of smooth, thin epithelial layer in spotted deer and it was prominent with absence of nuclei in cattle (Nagaraju *et al*., 2012).

The stratum granulosum was made up of single cell layer with keratohyaline granules in bison and black buck, and it was made up of 2-3 cell layers with melanin pigments and flat nucleus in nilgai. This observation is in accordance with the findings of Atlee *et al*. (1997) in llama, Dellmann and Eurell, (1998) in domestic animals, Hole *et al*. (2008a) in Red Kandhari cows and Nagaraju *et al*. (2012) in spotted deer and cattle. However, Singh *et al*. (1975) reported the absence of this layer in paralumbar region of Indian buffalo calf.

The stratum spinosum was 4-5 cell layers in bison, 3-4 layers of cells in black buck and 5-7 cell layers in nilgai with melanin pigments of the present study. Atlee *et al.* (1997) found 1-3 layers of stratum spinosum in the skin of llama and four to five layers of polyhedral cells with rounded nuclei in Red Kandhari cows (Hole *et al*., 2008a) and which was comparable to the present study. The stratum basale was single cell layer; nuclei were more vertical and oblique in position and showed melanin pigments in all bovidae species of the present study. A similar observation was made by Atlee *et al*. (1997) in llama and Hole *et al.* (2008a) in Red Kandhari cows.

Except for some variations in the species studied generally, the dermis consisted primarily dense irregular connective tissue with a feltwork of collagen, elastic and reticular fibres, nerve components, cross sections of hair follicles, ducts of sweat and sebaceous glands, blood vessels and arrector pili muscle. The dermis was divisible into superficial papillary layer and deep reticular layer. In bison, just below the epithelium

places there was adipose tissue and both in bison and nilgai the papillary zone was made up of dense fibrous connective tissue with many connective tissue cells while in Black buck it consisted of loose connective tissue. The sebaceous glands were attached at both side of the hair follicle in bison and black buck but in nilgai, they were attached at one side of the hair follicle which was opening directly into the hair follicle. There was even distribution of elastic fibers in between the collagen fiber bundles and also around the hair follicle in black buck. The present observations are in accordance with the findings in horse (Talukdar *et al*., 1972), in domesticated mammals (Meyer *et al*., 1994; Dellmann and Eurell, 1998), in llama (Atlee *et al*., 1997), in one humped camel (Pfeiffier *et al*., 2006), in Red Kandhari cows (Hole *et al*., 2007b) and in spotted deer and cattle (Nagaraju *et al*., 2012). Nilgai skin showed obliquely oriented or acuteness orientation of primary hair follicles which was peculiar feature observed only in this animal and nerve fibers were observed running in the papillary layer which was approaching towards the basale layer of the epidermis. On the contrary, in bison large number of transversely cut hair follicle along with sebaceous glands were observed in the middle of the reticular zone. However, Nagaraju *et al*. (2012) studied and inferred that the sweat glands were predominantly innervated than the sebaceous glands in spotted deer. The stratum reticulare consisted of loose connective tissue with large blood vessels and parallelly running nerve fiber bundles in all the bovidae species studied.

Nagaraju, *et al*., (2012) reported that in spotted deer the compound hair follicle with a primary hair follicle associated with two to three secondary hair follicles that were arranged in parallel fashion to each other. The sebaceous glands surrounding the primary hair follicle alone were seen in spotted deer, cattle and goat. However, in the present

study the primary hair follicle was associated with 3-4 secondary follicles in bison and bilaterally surrounded by 2-3 secondary hair follicles in nilgai which were uniformly distributed in the skin but not arranged in parallel fashion as observed in the spotted deer. All the hair follicles were associated with sebaceous glands. In black buck, the compound hair follicles were densely distributed and were arranged linearly as observed in spotted deer and each primary hair follicle was surrounded by 2-4 secondary hair follicles with sebaceous glands. The primary hair follicle was always present at the centre when present with 2 secondary hair follicles in black buck. However, Raheem and Al-hety (1997) observed in Iraqi goats that the sebaceous glands were associated with mainly primary follicles and some secondary follicles.

Atlee *et al*. (1997) found high density of hair follicles with one or two primary hair follicles surrounded by multiple smaller secondary follicles oriented at a sharp oblique angle in llama skin but there was no oblique orientation of the hair follicles observed in skin of wild ruminants' skin in the present study. In the present study there was only one primary hair follicle situated in the compound hair follicle. Jenkinson and Nay (1972) on the contrary reported primary hair follicle with no secondary hair follicles in European cattle. The Presence of primary hair follicle, secondary hair follicle, sebaceous glands were reported in non-woolly Indian goats (Koul *et al*., 1990). The coiled tubular sweat glands lined by simple cuboidal epithelium with secretory blebs observed on their surface suggested apocrine mode of secretion in the bison and black buck in the present study. Adib and sheibani, (2000) recorded both bilobed sebaceous glands and sweat glands in the skin of Raini goats. The simple tubular sweat glands in the spotted deer, cattle and goat located at the junction of dermis and hypodermis with

merocrine mode of secretion have been described by Nagaraju, *et al*. (2012). However, Kapadnis, *et al*. (2004) found sebaceous glands associated with secondary hair follicle deep in the dermis of goat skin but both sebaceous and sweat glands associated with hair follicle in red kandhari cows have been reported by Hole *et al*. (2008b). However, there were no sweat glands noticed in horizontal sections of nilgai skin in the present study. The dermal connective tissue comprised of bundles of collagen, elastic and smooth muscle fibres in all the wild animals studied in the present study but reticular fibres were not observed in all the animals except nilgai. However, in skin of hippopotamus reticular dermis showed very thick bundles of coarse collagen fibres arranged in a more regular pattern and the presence of sub dermal glands were also reprted (Lucy *et al*., 2014).

5.1.2 Elephant (Family: *Elephantidae*)

The vertical sections of Asian and African elephant skin showed stratified squamous keratinized type of epithelium with a thick prekeratin and keratin layers. The stratum basale was made up of single layer of cells with melanin pigments. Smith, (1890) also mentioned the presence of pigment in this layer in the elephant skin. The stratum spinosum with 4-5 cell layers showed spindle or oval shaped cells with hallow space around the nucleus resembling hyaline cartilaginous cells, a feature also reported by Smith, (1890). The stratum granulosum was made up of 8-10 cell layers. Adjacent to papillary bodies the stratum granulosum was thicker as opposed to the thinner stratum corneum.

The dermal papillae interdigitated with surface epidermis. The thinner and irregular epidermal pegs accounted for the haphazard arrangement of papillary bodies in Asian elephant. This feature was also observed by smith, (1890) who described them as

finger like projections which branching into primary and secondary divisions. The papillary bodies consisted of loose connective tissue embedded in ground substance with distributed amongst blood capillaries and the collagen fibers. The dermis consisted of dense collagenous fiber bundles with few muscle fibers. The muscle fibers were oriented in a parallel fashion along the length of epidermis.

In the present study short and thick dome shaped papillae were present, Smith, (1890) termed these structures as primary papillary bodies. These papillary bodies were highly vascular in nature and there was no distinct reticular layer seen. In the dermis just below the papillary layer there was thick zone of muscle fiber bundles with collagen fibers arranged horizontally and vertically. Further, in the deeper part of dermis and beginning of hypodermis thick bundles of muscle fibers were seen. A single hair follicle was also observed in the dermis below the papillary layer. Though earlier observations (Evans, 1910) expressed that the elephants must have sweat glands over their backs looking at the dampness under their harness when working in warm weather, the presence or absence of sweat glands in elephant have been a long time topic of debate (Munmun *et al*., 2009). There were neither sebaceous glands nor sweat glands observed along with hair follicles and in the entire dermis of skin in both the species studied. On the contrary to this Mariappa (1986) found only sebaceous glands in the elephant fetus but no sweat glands. However, Munmun *et al*. (2009) observed the presence of sweat glands in the skin of adult Asian elephants. The present observation is in accordance with Shoshani *et al*. (1982) and Lilly white and Stein (1987) who suggested that elephants have other mechanisms for their thermoregulation. Elephant skin is wrinkled in appearance, with African elephants more wrinkled than Asian elephants. Wrinkles act as a cooling

mechanism by increasing the skin's surface area. The additional skin and wrinkles trap moisture, which then takes longer to evaporate and also elephants are recognized as water dependent. Elephants are able to dissipate heat using a variety of non-evaporative strategies, including ears that are adapted for maximum heat transfer and a low surface density of hair, which likely enhances heat loss especially at low wind speeds and through behavioral strategies such as shade seeking (Myhrvold *et al.,* 2012; Sukumar, 2003). Therefore, wrinkles keep elephants cooler, for longer, than if they had smooth skin. Some authors observed that the elephants have sweat glands only over their toenails, just above the coronary bands. The deeper dermis consisted of longitudinally and transversely oriented muscle fibers. The loose connective tissue was present in between the muscle fiber bundles. The reticular zone did not show the reticular fibers. However there was a demarcation with a thick band of collagen fibers. In the dermal part the muscle fiber bundles were separated by interfascicular connective tissue fibers. No nerve terminals penetrating into the papillary bodies were observed in the present study contrary to this Smith, (1890) described nerve endings and fibers entering into the primary and secondary papillary bodies. There was nerve fiber bundles located at the base of dermis.

The horizontal section of Asian elephant and African elephant skin showed single isolated hair follicle surrounded by loosely arranged collagen fibers with more vascularity in between them. It was followed by densely packed collagen fibers with sparse muscle fibers and then followed by a thick layer of muscle fiber bundles giving cart wheel appearance but in Asian elephant it was observed to be thin layers around the hair follicle as compared to African elephant skin. Hair follicle appeared like sinus hair

follicle in dog, even though it is different family, it is comparable with sinus hair follicle in dog mentioned by dellman and brown (1981) where hair follicle is surrounded by external root sheath followed by glassy membrane, inner layer of dermal sheath, cavernous blood sinus with trabeculae and outer layer of the dermal sheath. In the dermis sparsely distributed elastic fibers were found. Few cross cut muscle fiber bundles were also sparsely distributed amongst the loose connective tissue around the hair follicle. Thick muscle fiber bundles were oriented in different directions in the dermis. The connective tissue stroma contained more of muscle fibers compared to collagen and elastic fibers. Smith, (1890) also described the presence of white fibrous tissue with elastic fibers in the corium of elephant skin but there were no mention of muscle fibers in the corium. Nerve bundles and blood vessels were also seen in between the muscle fibers in African elephant. Between the inter fasciculi of the muscle loose connective tissue was vascular in nature. As observed by Smith, (1890) there were canal system with collection of pigment cells in the medulla of bristle hair follicle. In the present study no such canals were found but there were pigmented cells found in the medulla of the cross section of hair follicle of both the species of elephants.

Usually African elephant skin is more wrinkled compared to Asian elephant and looked like interdigitation of the epidermis and dermis in vertical section of the skin. To support this, horizontal section of the skin showed epidermo-dermal junction, the epidermis of the skin was surrounding dermis appearing as epidermal pegs due interdigitation of the skin fold which was a characteristic feature of African elephant. The epidermal pegs comprised of highly keratinized stratified squamous type of epithelium. The papillary body surrounding the epidermal peg showed dense collagen fiber bundle along with

muscle fibers and blood vessels. The shapes of the skin folding were hexagonal as well as oval.

5.1.3 Wild boar (Family: *Suidae*)

Both sloth bear and wild boar are snout bearing animals and omnivores, sharing common food habitat. Although the skin histomorphology resembles in these two species certain differences in the arrangement of hair follicles were noticed.

Llyod and Garth Waite (1982) observed that in the canine, the epidermis of skin was composed of 3-6 cell layers where as 3-4 cell layers with well defined stratum basale, stratum spinosum and stratum corneum was observed in the sloth bear epidermis (Baddi, 2009). The melanin pigments were observed in the stratum germinativum. The melanin pigments were seen in the cells of stratum corneum in addition to cells of stratum basale and stratum spinosum, keratohyaline granules observed in the stratum granulosum in wild boar which is in accordance with earlier report of the author in sloth bear skin, where as Trautmann and Fiebiger (1957) recorded melanin pigments in higher concentration in the stratum basale only in the carnivores. The musculo collagenous nature of dermis observed in wild boar was differentiated from the dermis of sloth bear in that it was mainly collagenous in the latter species (Baddi, 2009). The well defined dermal papillae between the epidermal pegs observed in the species of wild boar studied concurs with similar findings in Yorkshire pigs (Sumena, 2010), in dog (Evans and Christensen, 1967) and in tiger (Baddi, 2009). The loose connective tissue with adipose tissue observed between epidermal pegs observed in the wild boar is comparable to loose areolar connective tissue of the dermal papillae observed in Indian crested porcupine (Archana *et al*., 2006). The predominant collagenous bundles over muscular fibers and

elastic bundles observed in the reticular layer of dermis in wild boar finds agreement with the observation of reticular layer of dermis in the horse (Talukdar *et al.*, 1972). The elastic fibers observed around the hair follicles and their sparse distribution in connective tissue of dermis of wild boar which correlates well with the findings of Mowafy and Cassens (1975) in pig. The massive three dimensional networks of collagen bundles were observed in dermis of wild boar agreed with the results of Meyer *et al*. (1982) in different body regions of wild boars, domestic pigs and miniature pigs. The blood vessels and nerve fiber bundles of various sizes observed in the reticular layer of dermis in wild boar are comparable to the findings of Pfeiffier *et al*. (2006) in one humped camel.

Delmann and Brown (1981) reported the presence of a single primary hair follicle surrounded by clusters of secondary follicles in the carnivore. This is in contrast to the observations of carnivorous sloth bear where in three to four primary hair follicles arranged in elliptical outline surrounded by connective tissue were noticed by Shambhulingappa *et al*. (2013) and this feature was not noted among the many of the carnivorous species studied (Shambhulingappa *et al*., 2013). However, the clusters of two to four primary hair follicles surrounded by connective tissue is the feature in the domestic pig (Delmann and Brown, 1981). This feature resembles linear arrangement of hair follicles in wild boar differing from the arrangement of hair follicle clusters described in the sloth bear (Shambhulingappa *et al*., 2013). The linear arrangement of hair follicle with erector pili muscle observed in the wild boar was also observed by Gaykee *et al*., (2008) in wild pig. The absence of sebaceous glands in the wild boar observed in this study contradicts the sparsely distributed sebaceous glands found in the dermis of sloth bear (Shambhulingappa *et al*., 2013) and yalk skin (Sharma *et al*., 1996).

The skeletal muscle fiber and nerve bundles with high vascularity and adipose tissue observed in the deep part of the dermis of wild boar. Similar findings were observed in the sloth bear and leopard skin (Baddi, 2009). By this the morphology of the skin of wild boar and sloth bear can be differentiated and it is also useful in the study of normal architecture of the skin for pathologists, dermatology researchers and forensic researchers.

5.1.4 Cheetah (Family: *Felidae*)

Nickel *et al*. (1981) have described that the epidermis consisted of reduced cell layers with stratum basale, stratum spinosum and stratum corneum with stratum granulosum and stratum lucidum being absent in some of the domestic animals. Strickland and Calhoun (1963) have reported decreased skin thickness dorsal to ventral on the trunk and proximal to distal on the limbs of cat. Baddi, (2009) described all the four layers of epidermis except stratum lucidum in the lateral abdominal wall of leopard, lion, Bengal tiger and sloth bear. In the present study the stratum granulosum was 1-2 cell layers with keratohyaline granules in cheetah which was in accordance with the findings of Baddi, (2009) in leopard and melanin pigment granules in Bengal tiger.

. Lloyd and Garthwaite (1982) observed that in the canine, the epidermis of skin was composed of three to six cell layers. In sloth bear skin the epidermis was made up of 3-4 cell layers with well defined stratum basale, stratum spinosum and stratum corneum with melanin pigments in stratum basale (Baddi, 2009). Trautmann and Fiebiger (1957) have also mentioned that the pigment granules were in highest concentration in the stratum basale in domestic animals. In the present study cheetah presented melanin pigments in the stratum basale. In the present study epidermis consisted of many

epidermal pegs and similar observation was observed by Baddi, (2009) in Bengal tiger and Evans and Christensen (1967) in dog.

The dermis of cheetah skin consisted of both stratum papillare and stratum reticulare. The stratum papillare had loose connective tissue of collagen fibers with sparsely distributed elastic fibers. Whereas in leopard dermis was dense irregular connective tissue comprising of bundles of collagen fibers were seen in stratum papillare (Baddi, 2009). Trautmann and Fiebiger (1957) reported in ox, sheep, and dog a feltwork of delicate reticular fibers with an admixture of fibroelastic elements in superficial layers of the dermis. Presence of sweat glands lined by simple cuboidal epithelium with their secretions on their surface and at places sebaceous glands with opening in to the hair follicles were observed in the present study. However in contrast to this, Baddi, (2009) mentioned branched alveolar sebaceous glands surrounding the bundles of hair follicles in leopard with no sweat glands and Bhayani *et al*. (1995) and Baddi, (2009) reported sweat glands in lion. In the reticulare zone dense fibrous connective tissue and longitudinally arranged muscle fiber bundles along with nerve fiber bundles and blood vessels were observed with hair follicles running parallel to the epidermal layer. The hypodermis consisted of cross cut and longitudinally oriented skeletal muscle fibers with large number of blood vessels and nerve fibers surrounded by adipose tissue. The collagen fibers were abundant as compared to muscle fibers. Similar features were found in the leopard, lion, Bengal tiger and sloth bear skin (Baddi, 2009).

The vertical section of the cheetah skin presented perpendicularly oriented hair follicles in the papillary and reticular layer of the dermis. This cross sectional appearance of the hair follicles observed in the vertical sections of the skin can be attributed to almost

oblique or parallel orientation of the hair with respect to the surface of skin. This is exemplified by the fact that the cross sectional appearance of the hair follicles were also noticed amongst the epidermal folds. Further in the horizontal sections of the skin the hair follicles appeared oblique and vertical in their orientation. This type of arrangement of the hair follicles were observed only in the cheetah which was quite peculiar. It appears that the hairs emerge out of the skin almost parallel to the surface. Because of this orientation the hair coat appears to be very smooth and soft in this species. This finding could be a characteristic feature to cheetah and as such feature were not observed in any of the wild animal species studied and also recorded in the literature.

Shambhulingappa *et al*. (2013) found compound hair follicles in leopard, lion, Bengal tiger and sloth bear skin comparable to similar feature observed in cheetah of present study. The skin of cheetah showed uniformly distributed compound hair follicle consisting of a primary hair follicle with 3-7 secondary hair follicles on either side of it. However, Shambhulingappa *et al*. (2013) described hair follicle pattern as a single primary hair follicle surrounded by circumferentially arranged groups of compound follicles, each compound follicle consisted of 6-8 fine secondary hair follicles interspersed with fine connective tissue fibers in Leopard skin; sparsely distributed compound follicles with a primary hair follicle located at one end underneath which 6-8 secondary hair follicles were observed in Bengal tiger skin. The clusters of compound hair follicles surrounding a primary hair follicle and within each compound follicle a primary hair follicle was always noticed in Lion skin. In sloth bear sparsely distributed elliptical shaped compound hair follicles were recorded each compound follicle had 2-4 primary hair follicles, irregularly arranged. The pattern of hair follicle arrangement in the

present study was similar to the findings of Delmann and Brown (1981) and Baddi, (2009) in dog. At the base of the primary hair follicle coiled tubular sweat glands which were lined by simple cuboidal epithelium with secretory blebs on their surface were seen along with blood vessels in between them and all the compound hair follicles were always associated with one or two sweat glands. Contrary to this Shambhulingappa *et al*. (2013) found only sebaceous glands in leopard and sloth bear and absence of the same in the Bengal tiger. The presence of sweat glands which serve to remove excess heat in the form of sweat, a function true in the non panting animals was surprisingly observed in the skin of cheetah. These features were also reported in lion and hyena by Bhayani *et al.* (1995, 1999) and Shambhulingappa *et al*. (2013) in lion. However, Trautmann and Fiebiger (1957) reported absence of both sebaceous and sweat glands in dog and cat.

The present finding and previous observations (Baddi, 2009; Shambhulingappa *et al*., 2013) in the big cats about the presence of sweat glands necessitates one to investigate the heat loss mechanism in these species. This is in light of the physiological knowledge that the panting is the mechanism involved in excess heat loss amongst carnivorous species.

5.2 FTIR Analysis

5.2.1 Spectral analysis

The present study was conducted on representative hair samples from wild herbivores and carnivores animals namely bison, black buck, Nilgai, Sambar, Asian elephant, Indian grey wolf, wild boar, cheetah and sloth bear and hoof from Bison, Black buck and Nilgai, tusk samples from African elephant and artifacts were taken. For

comparison, previous study (Nagaraju, 2012) on Asian elephant, wild boar tusk's FTIR spectra, hair spectra of leopard and tiger were used.

These representative samples of different tissues collected from wild animals, which were subjected to FTIR analysis and FTIR spectra were obtained. The natural keratin fibers, hoof and tusk were investigated through the use of FTIR followed by Linear Discriminant Analysis or Canonical Score Variate Analysis.

The infrared spectra of proteins exhibit absorption bands associated with their characteristic amide group. In-plane modes are due to C=O stretching, C–N stretching, N–H stretching and O–C–N bending, while an out-of-plane mode is due to C–N torsion. The characteristic bands of the amide groups of protein chains are similar to the absorption bands exhibited by secondary amides in general, and are labelled as amide bands. There are nine such bands, called amide A, amide B and amides I–VII, in order of decreasing wavenumber. Some of the bands are more useful for conformation studies than others and the amide I and amide II bands have been the most frequently used (Stuart, 2004).

5.2.2 Spectral analysis of hairs

All samples studied in this work showed similar vibration spectra in the spectral region between 4000-400 cm^{-1}.

Spectral Region 500cm^{-1} to 1200cm^{-1}:

In hair spectral region between 500 cm^{-1} to 1200 cm^{-1} was less conspicuous. Some peaks observed between 600 cm^{-1} to 900 cm^{-1} were mostly due to C-H out of bending vibrations. The region of S-O stretching vibration related to the cystine monoxide, which

was exhibited peak at 1076 cm^{-1} in cheetah and sloth bear, where as in Asian elephant, black buck, Nilgai and wild boar hairs these peaks were observed at 1069cm^{-1}, 1075 $cm^{-1,}$ and 1073 cm^{-1}, 1072 cm^{-1} respectively. Surprisingly this peak was not observed in bison, Indian grey wolf and Sambar. Weak band at 1157 cm^{-1} in Asian elephant, 1175 cm^{-1} bison, cheetah and Nilgai, 1173 cm^{-1} in black buck and sambar hair, 1172 cm^{-1} and 1151 cm^{-1} in Indian grey wolf and wild boar hair respectively and 1154 cm^{-1} in sloth bear hair were assigned to C-O stretching vibrations of C-OH group according peak assignment made by Akhtar and Edward (1997) and Edward *et al.* (1998). However Nagaraju, (2012) found additional peaks in tiger hairs at 1125cm^{-1} and 1102cm^{-1} which was due to rocking of methylene group according peak assignment made by Akhtar and Edward (1997) and Edward *et al.* (1998). Panayiotou (2004) reported in cow, goat, horse, human hair and cat fur, the amide III band was found at 1040cm^{-1} where as in the parrot feather this band was attributed to a cystic acid.

Spectral Region 1200 cm^{-1} to 2000 cm^{-1}:

Generally Amide I absorption occurs in the region between 1600-1700cm^{-1}. Major contribution for this peak could be attributed to C=O stretching and minor contributions from C-N stretching and N-H bending. This band has been most widely studied for assignment of secondary structure of the protein and polypeptide (Stuart, 2004). In the study made by Nagaraju, (2012), the peak for Amide I band was recoded at 1638 cm^{-1} in cattle hair, at 1629cm^{-1} in goat hair, at 1626cm^{-1} in spotted deer hair, at 1628cm^{-1} in leopard hair, at 1626cm^{-1} in tiger hairs. The study on the hairs of bison and Nilgai were in accordance with Nagraju, (2012) findings in spotted deer and Bengal tiger. The peak at 1628cm^{-1} was observed in the black buck, Indian grey wolf and sambar in the

present study and the same peak was found in leopards (Nagraju, 2012). In contrary to this amide- I band peak was observed at 1630 cm^{-1} in Asian elephant and sloth bear hair, 1631 cm^{-1} and 1627 cm^{-1} in wild boar and cheetah hair respectively, with additional peak at 1637 cm^{-1} in wild boar hair. Elliot (1956) reported that folded forms of amide I band occurred at 1655cm^{-1}. Whereas extended form of amide I peak observed at 1630cm^{-1}. Pielesz and Wesełucha-birczynska (2000) reported that amide I band found at 1652cm-1 and this peaks was similar to that of β chitin at 1630cm-1 (Bruner et. al.,2009). The shift in amide I band to lower wave number may be due to use of diamond ATR techniques.

Amide II band occurred due to C-N stretching and C-N-H bending vibration coupled with C=O stretching was observed 1536 cm^{-1} in Asian elephant and wild boar hair , along with this peak wild boar also has additional peaks at 1540 cm^{-1}, 1522 cm^{-1}, the peaks at 1515 cm^{-1}, 1517 cm^{-1}, 1522 cm^{-1} and 1524 cm^{-1} were observed in Black buck, Indian Grey Wolf, Nilgai and Sambar hair respectively and 1530 cm^{-1} in sloth bear hair, 1525 cm^{-1} in bison and cheetah hair. Nagaraju, (2012) also observed same peak in cattle like that of bison and cheetah in the present study. Whereas, in goat and leopard hair the peaks were at 1521cm^{-1} and 1519cm^{-1} respectively, at 1520cm^{-1} in spotted deer and tiger. All animals exhibited almost similar spectral peaks positions with little variations. Panayiotou (2004) observed amide I and amide II bands at 1657cm^{-1} and at 1537cm^{-1} respectively in cattle, sheep, cat, horse and human hair which could be attributed to refractive index of Kbr (potassium bromide) used for pelleting in her spectral collections.

Amide II absorption resulted from both N-H bending vibration and from C-N stretching vibration. The absorption for this band occurred in the region between 1500

to1600cm^{-1}. Similar observations were found at 1630cm^{-1} for amide I peak and at 1515cm^{-1} for amide II peak in the spectra of wool fiber according to Griebenow *et al,* (1992). Elliot (1956) reported that amide II band occurred at 1540cm^{-1} and Pielesz and Wesełucha-birczynska (2000) reported at 1541cm^{-1}, these peaks were similar to that α chitin at 1562cm^{-1} (Bruner et. al.,2009). Espinoza *et al.* (2007) studied sea turtle and bovidae keratin using DRIFT method where amide II peak was recorded at 1516cm^{-1} in the sea turtle. The region between 1700-750cm^{-1} contains vibration from the CONH stretching primarily from protein structure with amide I and amide II bands occurring at 1647cm^{-1} and 1547cm^{-1} respectively (Baddiel, 1968). Panayiotou (2004) reported strong band at 1652cm^{-1} for all keratin except feather.

Asymmetric CH_3 bending modes of the methyl groups of proteins, methylene deformation were observed at 1450cm^{-1} in cattle, goat, spotted deer, leopard and tiger hairs (Nagaraju, 2012). Same observation found in bison, Black buck, Nilgai and sambar hair in the present study. However, the peak at 1449cm^{-1} in Asian elephant, Indian Grey Wolf and sloth bear hair, peak at 1451 cm^{-1} only in cheetah hair were assigned to asymmetric –CH_3 bending of proteins and this peak was not observed in wild boar in the present study.

Symmetric -CH_3 bending vibrations of aliphatic side chains of amino acid residues were observed at medium peak at 1390 cm^{-1} in bison, black buck and nilgai hair. The present observation was correlates with Nagaraju, (2012) in spotted deer hair. However, this peak was not observed in sloth bear hair. In the present study peaks observed at 1391 cm^{-1} in wild boar, 1396 cm^{-1} in Indian grey wolf and sambar hair and 1397 cm^{-1} in Asian elephant and cheetah hair. In contrary to this, Nagaraju, (2012) found

the peaks at 1394cm^{-1} in cattle, at 1399cm^{-1} in goat, while flat peak was recorded in tiger at 1399cm^{-1}.

Amide III band attributed to C=O stretching was observed at 1239cm^{-1} in Asian elephant hair, 1238cm^{-1} in bison and Nilgai hair and the peak at 1236 cm^{-1} seen in Sambar hair. 1235 cm^{-1} in Black buck, Indian Grey Wolf and wild boar hair was assigned for amide III band, same findings observed by Nagaraju, (2012) in spotted deer and Bengal tiger hair. Nagaraju, (2012) found the peak at 1237 cm^{-1} in cattle hair, same observations made in the present study in cheetah and sloth bear hair. Whereas, the same band was observed at 1241cm^{-1}and 1234cm^{-1} in goat and leopard hair respectively (Nagaraju, 2012). However, Panayiotou (2004) reported that amide III band was seen at 1244cm^{-1} in cattle, cat, horse, goat and human hair. Cattle and spotted deer exhibited shoulder at 1158cm^{-1}, leopard exhibited shoulder at 1159cm^{-1}, whereas tiger and goat exhibited prominent peaks at 1160cm^{-1} and 1161cm^{-1} respectively (Nagaraju, 2012).

The present findings were in accordance with Stuart, (2004) where he conferred the occurrence of Amide III absorption band in the region 1220-1330 cm^{-1}. The amide III absorption band mainly arise due to C-N stretching vibration as well as N-H in plane bending vibration with weak contributions from C-C stretching and C=O in plane bending vibration. Generally alpha helix structure occurs in the region 1293 and 1328cm^{-1}, beta sheet in the region 1225, 1250cm^{-1} and unordered structures in the region 1257 and 1288cm^{-1} (Stuart, 2004). This observation was almost consistent with the comments made by Griebenow *et al.* (1992); he opined that absorption bands of protein at 1230cm^{-1} was due to amide III peak which occurred because of heavily mixed vibration modes.

In the present study a weak amide III band component peak was also observed at 1319cm^{-1} in Asian elephant and wild boar hair, 1313 cm^{-1}, 1312 cm^{-1}, 1303cm^{-1}, 1308cm^{-1} in bison, Black buck, cheetah, Nilgai hair respectively and 1315cm^{-1} in Indian Grey Wolf, Sambar hair and sloth bear hair.

Spectral Region 2000 cm^{-1} to 4000 cm^{-1}

Amide A band due to N–H stretching in resonance with overtone was observed at 3271cm^{-1} in Asian elephant, wild boar, sloth bear, bison, Indian Grey Wolf, Nilgai and Sambar hair, 3272 cm^{-1} and 3274 cm^{-1} in Black buck and cheetah hair respectively. This band peak recorded was correlates with the study made by Nagaraju, (2012) in Bengal tiger, leopard, spotted deer, cattle, goat hair. Compared to bony horn core and antlers, hair had prominent amide-A band (Nagaraju, 2012).

Differences were observed in the Amide B band 3089 cm^{-1} and 3085 cm^{-1} in bison and cheetah respectively, 3081 cm^{-1} in Nilgai, Sambar and Wild boar hair and 3090 cm^{-1} in sloth bear. 3068cm^{-1} in Black buck, 3072 cm^{-1} Indian Grey Wolf hair. Nagaraju, (2012) also observed the differences in this band which were at 3080cm^{-1} in cattle and goat, in spotted deer exhibited at 3076cm^{-1}, in tiger at 3070cm^{-1} and in leopard hair at 3069cm^{-1}. These results showed that the Black buck and Indian Grey Wolf hair exhibited almost at same positions, except in bison, cheetah, Nilgai, Sambar, Wild boar hair and sloth bear hair which were due to over toning of Fermi resonance doublet of N-H stretching and O-H stretching between 3400-3300cm^{-1} (Stuart 2004). Similar observations were made by Panayiotou (2004) in cat, cattle, horse, human hair where spectra were found between 3300-3050cm^{-1}. However, amide-B band was not recorded in the Asian elephant hair in the present study.

CH_3 mode vibrations were observed Peaks at 2960 cm^{-1} in Bison hair, Nilgai and Sambar hair and 2961 cm^{-1} in Asian elephant hair. This observation was in accordance with Nagaraju, (2012) in cattle, leopard, goat, tiger and spotted deer. In the present study Peaks at 2957 cm^{-1} in Indian Grey Wolf and Wild boar, 2958 cm^{-1} in Black buck and sloth bear hair, and 2959 cm^{-1} in Cheetah hair. Similar observations were made by Panayiotou, (2004) in cow, cat, horse, human hair exhibited CH_3 modes of vibration at 2955cm^{-1}. Whereas, in wool fiber these CH_3 modes of vibration of protein was not observed (Griebenow et. al., 1992). Fabian, (2000) observed symmetric stretching vibration at 2956cm^{-1} and asymmetric stretching of CH_2 of acyl chain at 2922cm^{-1}.

The peak at 2917 cm^{-1} in wild boar hair which was highest peak observed in whole spectra in wild boar, 2921 cm^{-1} and 2923 cm^{-1} in Indian Grey Wolf and Black buck hair respectively, 2922 cm^{-1} in sloth bear hair, 2926 cm^{-1} in bison and cheetah hair, 2929 cm^{-1} in Nilgai and Sambar hair and 2931cm^{-1} in Asian elephant hair, were assigned to asymmetric C-H stretching vibrations of $–CH_2$ groups. Fabian, (2000) also observed asymmetric stretching vibration at CH_2 of acyl chain at 2922cm^{-1}.

The peak at 2873 cm^{-1} in wild boar, 2874 cm^{-1} in Black buck hair, 2875 cm^{-1} cheetah and Indian Grey Wolf hair and 2876 cm^{-1} found in Asian elephant, bison, Nilgai and Sambar and sloth bear hair was assigned to symmetric C-H stretching of $–CH_3$ groups.

5.2.3 Spectral analysis of hooves

Hoofs, claws and horns are made up of the fibrous structural protein called keratin, the two major class of keratin are alpha-keratins and beta-keratins. Alpha keratins are characterized by helical structure, whereas beta keratins have a pleated structure.

The hoofs represented the harder tissue where as claws represented the intermediate tissues. All samples showed similar vibrational modes in the spectral region between 4000-400cm^{-1}. The amide A, B and amide I display similar characteristic band in all animals hoofs and claws. The amide II and III are very important bands because from their position and shape, information about protein structure (keratin) and conformation can be described.

Spectral Region 500cm^{-1} to 1200cm^{-1}:

In hoof spectral (Fig.1to 3) region 500 cm^{-1} to 1200 cm^{-1} was less conspicuous. The peaks between 600 cm^{-1} to 900 cm^{-1} were mostly due to C-H out of bending vibrations. Nagaraju, (2012) observed the peak due to S-O symmetric stretching vibration of cystine monoxide (Espinoza *et al.*, 2008) at 1078cm^{-1} in cattle hoof, leopard claw and at 1077cm^{-1} in goat horn, cattle horn, which was similar to findings of present study in black buck, bison and Nilgai hooves. Whereas, black buck, bison and nilgai hooves were exhibited additional peak at 1173 cm^{-1} was assigned to C-O stretching vibrations of C-OH group of serine, threonine and tyrosine residues. Nagaraju, (2012) also observed additional peak at 1106cm^{-1} due to asymmetric S-O stretching in tiger claw. However, No S-O stretching was reported by Shengqing *et al.* (2011) in yak, goat and rhinoceros horn except in cattle horn where S-O stretching vibration was reported similar to our finding.

Spectral Region 1200 cm^{-1} to 2000 cm^{-1}:

This spectral region was mostly composed of characteristic peaks of protein amide bands. The most intense peak in entire region of spectra of hair was Amide I band

peak and was observed at 1632 cm^{-1} in black buck and 1633 cm^{-1} in bison and Nilgai hooves. Same observation for amide I band was made by Nagaraju, (2012) in cattle hoof, goat hoof, spotted deer hoof, tiger claw and leopard claw occurred due to C=O stretching vibration.

A strong amide II band with peak at 1515 cm^{-1} black buck and bison hooves. This study was in accordance with the findings of Nagaraju, (2012) in goat hoof, spotted deer hoof and cattle horn. The same peak was recorded in nilgai hoof at 1516 cm^{-1} in the present study, whereas in cattle hoof, leopard claw and tiger claw the same peak was observed at 1514 cm^{-1} (Nagaraju, 2012). Singquing *et al.* (2011) reported that the amide II peak occurred due to C=C stretching vibration at 1540cm^{-1} in rhinoceros horn and 1583cm^{-1} in yak horn. Usually amide II peaks observed between the regions 1580-1500cm^{-1} according to Akhtar and Edward (1997).

In the present study the peak at 1450 cm^{-1} black buck, bison and Nilgai hooves were assigned to asymmetric $–CH_3$ bending of the methyl group of proteins and methylene deformation. Nagaraju, (2012) recorded the same peak at 1451 cm^{-1} as weak peak in cattle hoof, goat hoof, goat horn and a prominent peak at 1450 cm^{-1} in spotted deer hoof, leopard claw, tiger claw and cattle horn. The C-H bending vibration modes at 1446cm^{-1} was stronger in rhinoceros horn compared to cattle horn and this peak was not recorded in sheep, goat, and yak horn as reported by Shengqing *et al.* (2011).

The aliphatic side groups of the amino acid residue stretching vibration observed at the region of 1395-1389cm^{-1} in cattle hoof, goat hoof, cattle horn, spotted deer hoof prominent peaks were observed, whereas in leopard and tiger claws weak aliphatic side

groups of amino acid residue stretching seen at 1403 and 1400cm^{-1} which indicates that the amino acid contents were more in the carnivore's animals. Stronger peak of 1393cm^{-1} was observed in goat horn due to stronger intensity of stretching vibration. Espinoza *et al.* (2007) were not described these peaks in the sea turtle and bovidae keratins , similar observations were not reported in rhinoceros horn, cattle horn, sheep horn and goat horn by Singquing *et al.* (2011). The same peak observed in the present study with medium peak at 1390 cm^{-1} in black buck, bison and Nilgai hooves were due to symmetric -CH_3 bending vibrations of aliphatic side chains of amino acid residues.

A weak Amide III peak occurred at 1312cm^{-1} and medium peak at 1237cm^{-1} and shoulder observed at 1156cm^{-1} in cattle hoof, whereas in goat hoof and spotted deer hoof amide III bands were observed at 1313cm^{-1} and 1238 cm^{-1}.

The medium Amide III band peak was observed at 1238cm^{-1} in black buck and bison hoof and 1239 cm^{-1} in Nilgai hoof. Whereas, the same peak found at 1237cm^{-1} in cattle hoof along with shoulder at 1156cm^{-1} but spotted deer hoof showed the same peak as observed in the present study (Nagaraju, 2012). No such shoulders recorded in the present study. However, the same author observed amide III bands at 1313cm^{-1} in goat hoof. In leopard and tiger claws the amide III peaks were observed at 1236cm^{-1} and shoulder observed at 1163 cm^{-1}, whereas shoulder was observed at 1166cm^{-1} in tiger claw. In cattle horn and goat horn similar observations were made (Nagaraju, 2012).

A weak Amide III peak occurred at 1312cm^{-1} (Nagaraju, 2012). However, in contrary a weak amide III band component peak was observed at 1309cm^{-1} in black buck hoof, 1310cm^{-1} in bison and Nilgai hooves in the present study.

Spectral Region 2000 cm^{-1} to 4000 cm^{-1}

Amide A band and amide B band were due to over toning of N-H stretching and O-H stretching (Stuart, 2004). Amide A peak observed at 3273cm^{-1} in cattle hoof, spotted deer hoof (Nagaraju, 2012), same observation recorded in the present study in black buck. But the same peak observed at 3274 cm^{-1} in bison and Nilgai hooves. Whereas in goat hoof, leopard claw and tiger claw it was found at 3271cm^{-1} (Nagaraju, 2012).

Amide B band was observed at 3069 cm^{-1} black buck, bison and Nilgai hooves. This result holds good with findings of Nagaraju, (2012) in cattle hoof, goat hoof, tiger claw, whereas in spotted deer hoof he observed the same peak at 3073cm^{-1}, in leopard claw at 3068cm^{-1} due to more interaction of vibrational bands. Panayiotou (2004) reported that the region between 3300-3050cm^{-1} corresponded to the O-H stretching. The peak at 2876cm^{-1} black buck, bison and Nilgai hooves was assigned to symmetric C-H stretching of $–CH_3$ groups. The peak at 2934cm^{-1} black buck, bison and Nilgai hooves was assigned to asymmetric C-H stretching vibrations of $–CH_2$ groups. Peaks at 2961 cm^{-1}, black buck, bison and Nilgai hooves were assigned to asymmetric C-H stretching of $–CH_3$ groups.

In the present study the spectral peaks were almost at similar positions as described by Espinoza *et al.* (2006) and Griebenow *et al.* (1992) with their spectral peaks of keratin tissues.

5.2.4 Discriminant analysis

Discriminant analysis is concerned with deriving helpful rules for allocating observations to one or other set of priories defined classes in some optimal way, using the information provided by a series of measurements made of each sample member. The technique is used in situations in which group membership is known with certainity a priori, and a second set, the test sample, consisting of the observation for which group membership is unknown, with which we require to allocate to one of the known groups with a few misclassification as possible. If we know that our classifying variables are normally distributed within groups we can use a classification procedure called linear discriminant analysis (LDA). Another approach is canonical variate analysis. Canonical variate analysis (CVA) separates objects into classes by minimizing the within class variance and maximizing between class variance. The aim of CVA is to find directions (i.e., linear combination of original variables) in the data space, that maximize the ratio of the between class to within class variance. These directions are called discriminant functions or canonical variates (Ballabio and Todeschini. 2009)

5.2.4.1 Discriminant analysis of Hairs

In the present analysis the spectral data of known classes were deduced first into common covariance matrix shared by the groups. The covariance matrix was used to calculate the Mahalanobis distances. These distances were calculated between cases we want to classify and the center of each group in a multidimensional space. The Mahalanobis distances were used to calculate canonical scores. These canonical scores were used to graphically deduce group classes as canonical score plots (Systat 12, 2007, Kimsley, 1998).

We used 110 replicate spectra of bison hairs, 80 replicate spectra of black buck hairs, 92 replicate spectra of nilgai hairs, 28 replicate spectra of sambar hairs, 45 replicate spectra of cheetah hairs, 30 replicate spectra of Indian grey wolf hairs, 195 replicate spectra of sloth bear hairs, 40 replicate spectra of wild boar hairs, 52 replicate spectra of Asian elephant hairs. In this analysis the spectral data of known classes were deduced first into common co-variance matrix shared by the groups, the canonical scores were used to geographically deduce group classes.

The CVA classification matrix with 100% correct class distribution and Wilk's lambda was between 0-1 of all individual class members observed. The performance index of all species lies between 95 to 100%. The results exceeded 90% of the performance index (Espinoza *et al.,* 2007) and Wilks lambda close to 0 indicates the accuracy of the samples (Ballabio and Todeschini, 2009). Our studies can be compared to the results obtained by Espinoza *et al.* (2007) who while analyzing sea turtle and bovidae keratin reported a performance index of 95.5% and in an another study by Espinoza *et al.,* (2008) differentiated elephant hair with giraffe hair with a performance index of 97%.

5.2.4.2 Discriminant analysis of Hoof

There were no major differences observed in the spectrum of bison, black buck and Nilgai hooves. The classification matrix with 100% correct class distribution of bison and black buck hooves. Whereas, 97 % in Nilgai hoof. Further CVA test statistic assigns score 0.007 for Wilks's Lambda. Same observation was made by Nagaraju, (2012) in three grouped animals such as cattle, goat, and tiger were 100%.

5.2.4.3 Discriminant analysis of African Elephant tusk

For the linear discriminant analysis, we used 20 replicate spectra of 4 African elephant tusk samples, 20 replicate spectra of 3 boar ivory samples and 30 replicate spectra of 6 elephant ivory samples. The performance index and classification matrix was 100% for all the 3 test species. The results indicating in excess of 90% of performance index (Espinoza *et al.*, 2007) and the value of Wilks lambda closer to zero (Ballabio and Todeschini 2009) then it can be inferred that the accuracy of the classification as accurate. Further, the value of Wilks lambda was 0.001 and the value close to 0 indicates group means are different and validates the classification. The present result was in accordance with the findings of Nagaraju (2012) on boar ivory, asian elephant tusk and spotted deer antler with the value of Wilks lambda closer to zero and 100% performance index and classification matrix.

We performed the linear discriminant analysis using different spectral measurements rather than direct spectral data points normally being used for the analysis. Still we were able to get correct classification of species. All the spectral measurements were subjected to normalization by dividing with a constant variable from each spectrum and thus minimizing the variation within the spectra of each group and which also helped in correct classification.

The present study was undertaken to develop a standardized procedure to identify different wild animals such as bison, black buck, Nilgai, cattle, wild boar, sloth bear and cheetah. The genetic structure of these animals were studied by using RAPD technique which is simple, cost effective, faster and doesn’t require any sophisticated laboratory to run the technique.

5.3 DNA analysis

5.3.1 DNA isolation:

DNA from skin samples of 10 bison, 10 black buck, 12 Nilgai, 6 cattle, 8 wild boar, 7 sloth bear and 5 cheetah were isolated by using procedure described by Huges and Gorosope (1991) with certain modifications. The yield of DNA ranged from 300-400 µg from approximately 40 to 200 mg of skin. The yield of DNA obtained in this study was consistent and as reported by other workers in wild animals (Satheesha, 2006; Harini, 2009; Hemalatha, 2012).

5.3.2 RAPD technique:

RAPD technique in veterinary field is a method used for identifying species specific DNA fingerprint patterns in various animals (Bardakeri and Skibinski,1994. Rossetto *et al.,* 1995; Lee and Chang, 1994). The RAPD technique is easy to carry out compared to other techniques such as RFLP, AFLP and Microsatellite. The RAPD technique obviates the need of any time consuming and cumbersome procedure (e.g., southern transfer, selection and screening of probes). RAPD being a PCR based technique requires very small amount (in nanograms) of genomic DNA and doesn't require any prior knowledge of genome sequence as primers are chosen arbitrarily.

Bardakeri and Skibinski (1994) used RAPD for species and subspecies identification of tilapia fish. Rossetto *et al.* (1995) used RAPD analysis in devising conservation strategies for the rare and endangered *Grevillea scapigera* (Proteaceae). Lee and Chang (1994) used RAPD PCR fingerprints in forensic species identification of different livestock species. Shankaranarayanan *et al.* (1997) conducted RAPD analysis

of Asiatic lions and tigers which showed high degree polymorphism. Recent studies (Satheesha, 2006; Harini, 2009 and Hemalatha, 2012) also showed high degree polymorphism in wild animals.

5.3.3 Reproducibility of polymorphisms:

The applicability of RAPD technique for molecular genetic studies depends on reproducibility of the reaction protocols (Hedrick, 1992; Riedy *et al.*, 1992; Scott *et al.*, 1992; Meunier and Grimont, 1993). Although the annealing temperature of 35^0C, 36^0C and 37^0C were tried with varied cycle numbers, the reproducibility of PCR was optimized in the present study with a programme having initial denaturation at 94^0C for 2 minute, followed by one minute denaturation at 94^0C, one minute annealing at 35^0C (37^0C for Ran5 & U3) and one minute extension at 72^0C for 35 cycles followed by one cycle of ten minutes for extension. The result was consistent through out the study with this programme. The apprehension about the reproducibility of RAPD banding pattern was raised because this technique is based on low annealing temperature and the absence of amplification at higher temperature indicates that binding of the primers at some sites could be non specific. Inspite of such considerations, it has been shown that RAPD gave highly reproducible results (Welsh and McClelland, 1990; Carlson *et al.*, 1991; Williams *et al.*, 1990; Rothuitzen and Wolferen, 1994). In the present study, the RAPD pattern was consistent with the primers tested and conditions optimized for the reaction. Consistent band pattern was also observed with species specificity.

5.3.4 RAPD primers:

Fifteen random primers were used for amplification of genomic DNA of wild animals. Out of these, only seven could amplify genomic DNA and of these, only four

primers (OPG 17, Ran5 D1 and U3) produced low to high polymorphic finger prints in DNA samples of different wild animals. Hence these four primers which produced polymorphic fingerprints in wild animals were tried to explore the possibility of using them to differentiate the species of wild animals. Each of these primers produced different banding patterns in wild animals studied.

5.3.5 RAPD polymorphic analysis:

Individual RAPD primers were separately used for studying variations in DNA fingerprint patterns. Species wise pooled DNA samples were studied to compare the variation between the species. On finding species specific band/s, individual samples constituting each species were separately amplified with the same primers to examine if the species specific bands are present in all the individuals constituting that particular species.

5.3.5.1 Primer OPG 17:

The primer OPG 17 produced high polymorphic bands in all the wild animals. It produced specific band of sizes 600bp and 950bp in case of bison, 400bp, 330bp, 1400bp, 580bp, 620bp and 550bp in black buck, nilgai, cattle, wild boar, sloth bear and cheetah respectively. Hence primer OPG 17 can be used to differentiate all above wild animals.

For the same primer Hemalatha, (2012) found the fragments ranged from approximately 200 bp to 1000 bp in bengal tiger, leopard and spotted deer. A high percentage of polymorphism was observed in different wild animal species. The primer showed 6 bands in tiger, 7 bands in leopards and 4 bands in spotted deer.

5.3.5.2 Primer RAn5:

The primer RAn5 produced high polymorphic bands in the following wild animals. It produced specific band of sizes 800bp and 900bp in case of bison, 450bp and 750bp in black buck, 550bp and 1000 in nilgai, 900bp and 200bp in cattle and wild boar respectively. There was no amplification in sloth bear and cheetah for this particular primer. Therefore primer RAn5 can be used to differentiate all above wild animals except sloth bear and cheetah. Whereas, the same primer showed total scorable bands of 5 in tiger, 5 in leopard and 3 in spotted deer and it showed the brightest band for tiger at 310 bp, for leopard at 330 bp, for spotted deer at 350bp (Hemalatha, 2012)

5.3.5.3 Primer D1

The primer D1 produced specific bands at 650bp, 750bp and 950bp in case of bison, 150bp, 720bp, 190bp and 250bp in black buck, cattle, wild boar and sloth bear respectively. There were no bands found in nilgai and cheetah from this particular primer. Therefore primer D1 can be used to differentiate all above wild animals except nilgai and cheetah.

5.3.5.4 Primer U_3:

The primer U3 produced specific bands of sizes 220bp and 320bp in wild boar and sloth bear only. There were no amplification found in rest of the wild animals studied in this primer. Hence primer D1 can be used to differentiate wild boar and sloth bear.

The RAPD technique is a fast and relatively simple process for marker identification in animals, especially in species for which DNA sequence information is

not readily available. Other advantages of this technique are that large number of samples can be processed quickly and that no radioactive reagents are handled in the assay.

5.4 Evaluation of above methods (Morphology, FTIR Spectroscopy and DNA analysis) from the point of identification of the animal species.

The methods followed in this study can be successfully used from the point of identification of species. The tissue from the same sample was subjected to all the three methods used wherever applicable and the concurrent results were obtained without errors in the identification of the species. Thus each method evaluates itself to be used for identification and they are mutually complimentary to each other rather than contradictory. Depending upon the facilities available any one of the methods can be followed for the identification of species.

Summary

VI. SUMMARY

The epidermis of Indian bison was stratified squamous keratinized epithelium and thicker epidermis characterized the epidermal pegs which comprised of thicker stratum corneum with 4-5 layers. The stratum granulosum was made up of 1 or 2 layers with keratohyaline granules. The stratum spinosum was 4-5 cell layers with a single layer of stratum basale presented melanin pigments. Just below the epithelium at places there was adipose tissue and also blood capillaries. The papillary zone was made up of dense fibrous connective tissue with many connective tissue cells. In the middle of reticulare zone large number of transversely cut hair follicles along with sebaceous and sweat glands and blood vessel were observed. The elastic fibers were more in this zone particularly surrounding the hair follicles. The Compound hair follicles were uniformly distributed and were rectangular in shape. comprising of primary hair follicle associated with 3-4 secondary hair follicles together with their sebaceous glands. In addition uniformly distributed coiled tubular sweat glands were noticed which were lined by simple cuboidal epithelium. The lining cell exhibited secretary blebs on their surface suggesting apocrine mode of secretion. Evenly distributed fine elastic fibers were present and reticular fibers were not observed within the connective tissue.

The epidermis of black buck skin was stratified squamous keratinized epithelium with thicker stratum corneum at the epidermal pegs than other region. The stratum granulosum was single cell layer with keratohyaline granules. The stratum spinosum was made up of 3-4 layers of cells and single layer of stratum basale both showed melanin pigments. The ducts of sweat glands were presented in papillary zone, number of cross sections of hair follicles associated with single sided opening of sebaceous glands and

erector pili muscles. Densely distributed compound hair follicles were arranged linearly in the dermis. Within the compound hair follicle there was linear arrangement of primary and secondary follicle observed. Each primary hair follicle was supported by 2-4 secondary hair follicles and at few places within compound hair follicle primary hair follicle was surrounded by secondary hair follicle in a semicircular shape when it was with more than 2 secondary hair follicles. The primary hair follicle was always present at the center when it was present with 2 secondary hair follicles. The Sebaceous glands were associated with each hair follicle and numerous coiled tubular sweat glands.

The epidermis of Nilgai was stratified squamous keratinized type of epithelium. The stratum corneum was made up of 2-3 cell layers thicknes. The stratum granulosum was made up of 2-3 cell layers with melanin pigments and flat nucleus. The stratum spinosum was made up of 5-7 cell layers, nuclei were more vertical and oblique in position. The stratum basale was single cell layer with vertical and obliquely positioned nucleus and had melanin pigments. The arrector pili muscles were also seen along with obliquely oriented primary hair follicles. Nerve fibers were observed running in the papillary layer which were approaching towards the basale layer of the epidermis. The sebaceous glands were present at one side of the primary hair follicle which was opening directly into the hair follicle. Sparsely distributed sweat glands were observed in papillary layer of the dermis. The Compound hair follicles were densely distributed in the dermis of skin. The primary hair follicles were bilaterally surrounded by 2-3 secondary hair follicles. Each primary and secondary hair follicle was associated with sebaceous glands.

The skin of Wild boar showed stratified squamous keratinized type of epithelium. The stratum corneum was thicker and presented melanin pigments. The stratum spinosum

and stratum basale both demonstrated melanin pigments, well defined prekeratin and keratin were seen in stratum corneum and large number of adipose tissue was present in between the epidermal pegs. The compound hair follicles were sparsely distributed in the dermis of skin. Each compound hair follicle has linearly arranged three primary hair follicle and larger in size at the center. The uniform distributions of blood vessels were seen in the dermis. The nerve fiber entering into the hair follicle was also observed. No sebaceous and sweat glands were observed in the dermis of skin.

The skin of Asian elephant was lined by stratified squamous keratinized epithelium; single layer of stratum basale cells with melanin pigments was present. The stratum corneum was comparatively thin. The epidermal pegs present at various places, which were quite thin and irregular in shape. There was no sweat or sebaceous glands in the dermis. Asian elephant showed single isolated hair follicles surrounded by loose connective tissue with collagen fibers and sparsely distributed elastic fibers in the dermis. A few cross sectioned muscle fiber bundles were also sparsely distributed around the hair follicles.

The epidermis Skin of African elephant was lined by stratified squamous keratinized type of epithelium with a thick keratin and prekeratin layers. The dermal papillae evaginated between surface epidermal interdigitations. The stratum spinosum showed spindle or oval shaped cells with hallow space around the nucleus resembling hyaline cartilaginous cells with the presence of melanin pigment granules. The short and thick dome shaped dermal papillae were present. There was absence of sebaceous and sweat glands surrounding the primary hair follicle in the dermis. The Horizontal section of African elephant skin showed single isolated primary hair follicles and a few elastic

fibers and nerve bundles were found in the dermis. At the epidermo-dermal junction, the dermis of the skin was associated with surrounding epidermis as epidermal pegs due interdigitation of the skin fold which was a characteristic feature to African elephant. The shapes of the skin folding were hexagonal as well as oval.

The cheetah skin surface epithelium was stratified squamous keratinized with keratin zones and at few places prekeratin zone was also observed. The epidermis consisted of many epidermal pegs. The surface of epidermis was irregular. The cheetah skin presented perpendicularly oriented hair follicles in the papillary and reticular layer of the dermis. This cross sectional appearance of the hair follicles observed in the vertical sections of the skin can be attributed to almost oblique or parallel orientation of the hair with respect to the surface of skin. This is exemplified by the fact that the cross sectional appearance of the hair follicles were also noticed amongst the epidermal folds. Further in the horizontal sections of the skin the hair follicles appeared oblique and vertical in their orientation. This type of arrangement of the hair follicles were observed only in the cheetah which is peculiar. Because of this orientation the hair coat appears to be very smooth and soft in this species. This finding is a characteristic to cheetah and not observed in any of the animal species studied and also not recorded in the literature. At places where there were hair follicles present showed the presence of sweat glands lined by simple cuboidal epithelium with their secretions on their surface and sebaceous glands were also opening in to the hair follicles. The arrector pili muscles were also seen close to the primary hair follicles. The hair follicles were running parallel to the epidermal layer but at places they were also running perpendicular to the epidermis. The skin of cheetah showed uniformly distributed compound hair follicle throughout the dermis. Each

compound hair follicle consisted of a primary hair follicle with 3-7 secondary hair follicles on either side of it. At the base of the primary hair follicle coiled tubular sweat glands lined by simple cuboidal epithelium with secretory blebs observed on the surface were seen along with blood vessels in between them. All the compound hair follicles were always associated with one or two sweat glands. The nerve fibers were also associated with large blood vessels in the dermis.

The average ATR - FTIR spectra of Asian elephant, Bison, Black buck, Cheetah, Indian Grey Wolf, Nilgai, Sambar, wild boar and sloth bear hair were taken for the analysis. The FTIR spectra from 400 cm^{-1} to 4000 cm^{-1} are divided into 3 spectral regions for detailed analysis viz, Spectral Region 500cm^{-1} to 1200cm^{-1}, 1200 cm^{-1} to 2000 cm^{-1} and 2000 cm^{-1} to 4000 cm^{-1}. The spectral band assignments were made according to literature on biological materials.

In hair spectral region 500 cm^{-1} to 1200 cm^{-1} was less conspicuous. The peaks between 600 cm^{-1} to 900 cm^{-1} were mostly due to C-H out of bending vibrations. The peak at 1069cm^{-1}, 1075 $cm^{-1,}$ and 1073 cm^{-1}, 1072 cm^{-1} in Asian elephant, black buck, Nilgai and wild boar hair respectively and 1076 cm^{-1} cheetah and sloth bear hair were assigned to S-O symmetric stretching vibrations of cysteine monoxide residues. But this peak was not observed in bison, Indian grey wolf and sambar. Weak band at 1157 cm^{-1} in Asian elephant, 1175 cm^{-1} bison, cheetah and Nilgai, 1173 cm^{-1} in black buck and sambar hair, 1172 cm^{-1} and 1151 cm^{-1} in Indian grey wolf and wild boar hair respectively and 1154 cm^{-1} in sloth bear hair were assigned to C-O stretching vibrations of C-OH group.

Spectral Region 1200 cm^{-1} to 2000 cm^{-1} spectral region was mostly composed of characteristic peaks of protein amide bands. The medium Amide III band peak was observed at 1239cm^{-1} in Asian elephant hair, 1238cm^{-1} in bison and Nilgai hair, 1235 cm^{-1} in Black buck, Indian Grey Wolf and wild boar hair, 1237 cm^{-1} in cheetah and sloth bear hair and 1236 cm^{-1} in and Sambar hair respectively. A weak amide III band component peak was also observed at 1319cm^{-1} in Asian elephant and wild boar hair, 1313 cm^{-1}, 1312 cm^{-1}, 1303cm^{-1}, 1308cm^{-1} in bison, Black buck, cheetah, Nilgai hair respectively and 1315cm^{-1} in Indian Grey Wolf, Sambar hair and sloth bear hair. The amide II band with peak at 1536 cm^{-1} in Asian elephant and wild boar hair, in addition 1540 cm^{-1}, 1522 cm^{-1} peaks were also observed in wild boar.hair. 1515 cm^{-1}, 1517 cm^{-1}, 1522 cm^{-1} and 1524 cm^{-1} was observed in Black buck, Indian Grey Wolf, Nilgai and Sambar hair respectively and 1525 cm^{-1} in bison and cheetah hair and 1530 cm^{-1} in sloth bear hair. The Amide I band peak and was observed at 1630 cm^{-1} in Asian elephant and sloth bear hair, 1631 cm^{-1} and 1627 cm^{-1} in, wild boar (1637 cm^{-1} also observed) and cheetah hair respectively. 1626 cm^{-1} in bison and nilgai hair**,** 1628 cm^{-1} in black buck, Indian grey wolf and sambar hair.

In the Spectral Region 2000 cm^{-1} to 4000 cm^{-1}, the intensity of peaks was comparatively weak in this region. Amide A band was observed at 3271cm^{-1} in Asian elephant, wild boar, sloth bear, bison, Indian Grey Wolf, Nilgai and Sambar hair, 3272 cm^{-1} and 3274 cm^{-1} in Black buck and cheetah hair respectively. Amide B band peak due to Fermi enhanced overtone of amide II was observed at 3089 cm^{-1}, 3068cm^{-1}, 3085 cm^{-1}, 3072 cm^{-1}, bison, Black buck, cheetah, Indian Grey Wolf hair respectively, 3081 cm^{-1}

in Nilgai, Sambar and Wild boar hair and 3090 cm^{-1} in sloth bear. This band peak was not found in Asian elephant.

The average ATR FTIR spectra of Black buck, Bison and Nilgai hoof were taken for the analysis. The FTIR analysis of hooves showed Amide A band between 3273cm^{-1} to 3274 cm^{-1} Amide B band peak was observed at 3069 cm^{-1} in all animals studied. The Amide I band peak was observed between 1632 cm^{-1} to 1633 cm^{-1} and Amide II band with peak between 1515 cm^{-1} to 1516 cm^{-1}. The medium Amide III band peak between 1238 cm^{-1} to 1239 cm^{-1} and weak Amide III band peak between 1309 cm^{-1} to 1310 cm^{-1}.

The FTIR analysis of African elephant tusk showed Amide A, Amide B, Amide I, Amide II bands at 3274 cm^{-1}, 3087 cm^{-1}, 1633 cm^{-1} and 1541 cm^{-1} respectively. The medium amide III band at 1242 cm^{-1}, weak amide III at 1419 observed in African elephant tusk.

Discriminant analysis is a multivariate statistical method that assists in the classification of data into distinct groups. In the present study the discriminant function was used to classify keratin materials of uncertain origin. Spectral data was utilized for the discriminant analysis. The canonical score plot of all wild animal hairs, hooves and tusk shows segregation of individual class members into distinct 3 clusters without any overlapping of class members. The observation was further confirmed by CVA classification matrix with 100% correct class distribution of all individual class members. Further, CVA test statistic assigns score range was between 0-1 for Wilks's Lambda.

In the present study, DNA was isolated from skin samples for RAPD analysis. The quality and quantity of the samples were checked by Spectrophotometer (thermo

scientific) by nano drop method. RAPD analysis was carried out with 15 different oligonucleotide random primers. Out of these three annealing temperatures, 35^0C was found to be ideal for OPG 17 & DI and 37^0C for RAn 5 & U3 which gave a consistent result on all the samples, while higher temperatures resulted in amplification with very few fragments. In all, four primers namely U3, D1, OPG 17 & RAn5 were used for polymorphic studies within and between different wild animal species. These primers produced consistent polymorphic banding patterns. Random primers U3, D1, OPG 17 & RAn5 amplified polymorphic fragments on DNA isolated from skin samples of wild animals. These four primers generated a total of 12 scorable bands in sloth bear, OPG 17, RAn5, and D1 primers generated 19 scorable bands in bison and 11 scorable bands in black buck and 14 scorable bands in cattle, OPG 17, D1 and U3 primers generated 12 scorable bands in black buck and OPG 17 alone generated 3 scorable bands in cheetah. All scorable bands mentioned above were ranging in size from approximately 110 to 1400 base pairs (bp). All the four random primers yielded amplified fragments that were consistently polymorphic and specific between the species.

Primer OPG 17 was found to produce high polymorphic fingerprints among DNA pools of different types of wild animals. It generated a total of 31 scorable bands from all seven wild animals. Fragments of 550 bp, 600 bp, 690 bp (brightest), 800 bp and 950 bp were amplified in bison, 400 bp, 500 bp (brightest), 700 bp and 850 bp fragments recorded in black buck, 320 bp, 700 bp and 800 bp (brightest) observed in nilgai, fragments of 550 bp, 700 bp (brightest), 800 bp, 820 bp and 1400 bp were amplified in cattle, 390 bp and 600 bp (brightest) seen in wild boar, 280 bp, 300 bp, 400 bp (brightest), 500 bp and 700 bp were amplified in sloth bear, 400 bp, 500 bp and 800 bp

(brightest) were amplified in cheetah. There was not much variation in banding patterns among individuals within species.

The primer RAn5 produced moderate polymorphic fingerprints. It generated a total of 22 scorable bands from Bison, Black buck, Nilgai, Cattle and Wild boar. The fragments ranged from approximately 150 bp to 1000bp. A high percentage of polymorphism was observed in different wild animal species. Fragments of 300bp, 390 bp, 450 bp, 550 bp (brightest), 800 bp and 900 bp were amplified in bison, 300 bp (brightest), 400 bp and 750 bp observed in black busk, 250 bp, 550 bp, 600 bp, 800 bp and 1000 bp (brightest) recorded in nilgai, 280 bp, 400 bp (brightest) and 900 bp were amplified in cattle and in wild boar fragments amplified were 200 bp, 400 bp (brightest) and 600 bp.

Primer D1 generated a total of 19 scorable bands from bison, black buck, cattle, wild boar and sloth bear. Fragments of approximately 120 bp, 450 bp, 550 bp (brightest), 650 bp , 750 bp and 950 bp were amplified in case of bison, 110 bp, 150 bp (brightest) and 290 bp were amplified in black buck, in case of cattle 300 bp, 450 bp, 550 bp and 720 bp (brightest) fragments were observed, 120 bp, 190 bp (brightest) and 300 bp recorded in wild boar and 180 bp, 200 bp (brightest) and 250 bp found in sloth bear.

The primer U3 produced polymorphic fingerprints only in wild boar and sloth bear. It generated a total of 5 scorable bands from these two animals. The fragments ranged from approximately 210bp to 450bp. Fragments of approximately 220bp and 450bp (brightest) were amplified in case of wild boar and in sloth bear fragments were amplified at 100bp, 210bp (brightest) and 320bp.

Bibliography

VII. BIBLIOGRAPHY

ABDUL-RAHEEM, M. H., AHMED, N. S. and AL-HAAIK, A. G., 2009. Histological and topographical study of the skin of native buffalo. Iraqi Journal of Veterinary Sciences 01/2009: [DOI:http://www.doaj.org/doaj?func=openurl &genre=article&issn=16073894&date=2009&volume=23+(Arabic)&issue=2& spage=65]

ADIB, M. M. and SHEIBANI, M. T., 2000. Histological study of hair follicles of Raini goat skin. *J. Faculty Vet. Med.*, **55**(2): 75-78.

AKHTAR, W. and EDWARDS, H. G., 1997. Fourier-Transform Raman Spectroscopy of Mammalian and Avian Keratotic Biopolymers. *Spectrochimica Acta Mol. Biomol. Spectrosc*., **53A**: 81–90

ALEXANDER, N. J. and PARAKKAL P. F., 1969. Formation of α- and β-type keratin in lizard epidermis during the molting cycle. *Cell Tissue Res*., **101**:72–87

ALIBARDI, L., 2003a. Immunocytochemistry and keratinization in the epidermis of crocodilians. Zoological Studies., **42**(2): 346–56

ALIBARDI, L., 2003b. Adaptation to the land: the skin of reptiles in comparison to that of amphibians and endoderm amniotes. *Journal of Experimental Zoology Part B: Molecular and Developmental Evolution*., **298** (1): 12– 41

ALIBARDI, L., 2003c. Proliferation in the epidermis of chelonians and growth of the horny scutes. *J Morphol*., **265**:52–69

AMBROSE, E. J. and ELLIOTT, A., 1951a. Infra-red spectra and structure of fibrous proteins, *Proceedings of the Royal Society of London, Series A, Mathematical and Physical Sciences.,* **206** (1085): 206–19

AMBROSE, E.J. and ELLIOT, A., 1951b. Infra-red spectra and structure of fibrous proteins. *Proc R Soc Lond A Math Phys Sci*., **206**: 206–219

AMIEL, C., MARIEY, L., DENIS, C., PICHON, P. and TRAVERT, J., 2001. FTIR spectroscopy and taxonomic purpose: contribution to the classification of lactic acid bacteria. *Le Lait*, **81**(1–2): 249–255.

ANDERSSON, L., BOHME, J., RASK, L. and PETERSON, P.A., 1986. Genomic hybridization of bovine class II major histocompatibility genes I. extensive polymorphism of DQ alpha and DQ beta genes. *Anim. Genet.*, **17** : 95-112

ANINDO, D., 2009. Rajasthan to be home for cheetahs. TNN, Times of India.

ARCHANA, D. N., SHARMA, R. S., KISHTWARIA. and BHARDWAJ, R. L., 2006. Anatomical studies on the skin of Indian Crested Porcupine *(Hystrix cristata var indicd). Indian J. Vet. Anat.,* **18**(1): 16-22

ATLEE, B. A., STANNARD, A. A., FOWLER, M. E., WILLEMSE, T., IHRKE, P. J. and OLIVRY, T., 1997. The histology of normal llama skin. *Vet. Dermatol.,* **8** (3): 165-176

BABA, M. A., PRASAD. G., PRASAD, R. and PRASAD, J., 1998. Histology and histochemistry of the palpebral epidermis and dermis of Chotanagpuri sheep. *Indian Vet. J.,* **75**: 934-936

BACHA, W. J. and BACHA, J. L. M., 1990. Integument, color atlas of Veterinary Histology, *Edn 2nd*, Lippincott Williams and Wilkins, Philadelphia., *pp* 85-86

BACHA, W. J. and BACHA, L. M., 2000. In Atlas of Veterinary Histology, *Edn 2nd*, Blackwell Publishing, Philadelphia. *pp*: 85-118

BADDI, S. Y., 2009. Morphological studies on the skin of carnivorous wild animals. M.V.Sc. Thesis, Karnataka Veterinary, Animal and Fisheries Sciences University. Bidar. Karnataka. India

BADDIEL, C. B., 1968. Structure and Reaction of Human Hair: an Analysis of by infrared spectroscopy. *J. Mol. Biol.,* **38:** 181-199

BAETEN, V. and APARICIO, R., 2000. Edible oils and fat authentication by Fourier transform Raman spectrometry. *Biotechnology, Agronomy, Society and Environment.*, **4**(4): 196–203

BALLABIO, D. and TODESCHINI, R., 2009. Multivariate Classification for Qualitative Analysis in Infrared Spectroscopy for Food Quality Analysis and Control. Edn.1 Sun D.Academic Press Burlington

BANARJEE, A., BORTOLASO. G. and DINDORF. W., 2008. Distinction between African and Asian Ivory in Ivory and Species Conservation Proceedings of INCENTIVS –Meetings (2004-2007) Bundesamt fur Natuschutz Bonn. 37-50

BANDEKAR, J., 1992. *Biophys. Acta.*, **1120**: 123–143

BANERJEE, A. and BORTOLASO, G., 2004. Digenetic changes of collagen in mammoth ivory as revealed by Isotopic Ratio Mass spectrometry (IRMS) and FTIR spectroscopy, *Geobiology , p*. 53

BANKS, W. J., 1993. Applied Veterinary Histology, Edn 3rd, Williams and Wilkins, London, *pp*: 298-325

BARARI, S. K., BISWAS, D., PAL, R. N. and BASAK, D.K., 1994. Histology of sebaceous glands of yak *(Poephaguspoephagus). Intl. J. Anim. Sci.,* **9**(2): 273-274

BARDAKERI, F. and SKIBINSKI, D. O. F., 1994. Application of the RAPD technique in tilapia fish: species and subspecies identification. *Heredity.*, **73**: 117-123

BARTH, A., 2000. *Prog. Biophys. Mol. Biol.*, **74**:141–173

BECKMANN, J.S. and SOLLER, M., 1987. Molecular markers in the genetic improvement of farm animals. *Biol. Technology.*, **5**: 573-576

BHATTACHARYA, M.K., BANERJEE, R., SINGH, K. S., GUHA, R. K. and GHOSH, R.K., 2003a. Histological and bio-metrical study on epidermis of non-descriptive buffalo *(Bubalus bubalis). Indian J. Anim. Hlth.,* **42**(2): 151-155

BHAYANI, D. M., VYAS, K. N., VYAS, Y. L. and PANDYA, S. P., 1995. Histomorphological study on the skin of lion *(Felis led). Indian J. Vet. Anat.*, **7**(1/2): 44-51

BHAYANI, D. M., VYAS, K. N., PARSAMIA, R. R. and VYAS, Y.L., 1999. Histomorphological study on the skin of the hyaena. *Indian Vet. J.,* **76**: 417-420

BHAYANI, D. M., VYAS, K. N., VYAS, Y. L. and PANDYA, S. P., 2005. Post-natal study on the distribution of mucopolysaccharides, mast cells, lipids and elastic fibers in the skin of sheep. *Indian J. Vet. Anat.,* **17**(1/2): 6-10

BLIN, N. and STAFFORD, D.W., 1976. Isolation of high molecular weight DNA. *Nucleic Acids Res*., **3**: 2303-2308

BOTHA., LEE-THORP, J. and SPONHEIMER, M., 2004. An Examination of Triassic Cynodont Tooth Enamel Chemistry Using Fourier Transform Infrared Spectroscopy. *Calcif Tissue Int.* **74**:162–169

BOWDITCH, B. M., ALBRIGHT, D. G., WILLIAMS, J. G. K. and BRAUN, M. J., 1993. Use of randomly amplified polymorphic DNA markers in comparative genome studies. *Methods Enzymol*., **224** : 294-309

BRUNNER, E., EHRLICH, H., SCHUPP, P., HEDRICH, R., HUNOLDT, S., KAMMER, M., MACHILL, S., PAASCH, S., BAZHENOV, V. V., KUREK, D.V., ARNOLD, T., BROCKMANN, S., RUHNOW, M. and BORN, R., 2009. Chitin based scaffolds are an integral part of the skeleton of the marine demo sponge Ianthella *basta*. *J. Struct. Biol.,* **168**: 539–547

CAETANO-ANOLLES, G., BASSAM, B.J. and GRESHOFF, P.M., 1991. DNA amplification fingerprint using very short arbitrary primers. *Biol. Technology.*, **9**: 553-557

CAMILLA, R. K. L., ANDREW, C. and SERGEI, G. K., 2006. Combining the Tape-Lift Method and Fourier Transform Infrared Spectroscopic Imaging for Forensic Applications. *Applied Spectroscopy.*, **60**: 1013-1021

CARDEN, A. and MORRIS, M. D., 2000. Application of vibrational spectroscopy to the study of mineralized tissues. *J Biomed Opt*., **5**:259–68

CARLSON, J. E., TULSIERAM, I. K., GLAUBITZ, J. C., LUK, V. W. K., KAUFFELDT, C. and RUTTEDGE, R., 1991. Segregation of random amplified DNA markers in F1 progeny of conifers. *Theor. Appl. Genet*., **83**: 194-200

CHANDRA, G. and BHARADWAJ, M. B., 1969. Epidermal pigment distribution in buffaloes. *J. Agric. Sci*., **72**:149-153

CHARLES S., 2009. African elephants: surviving by the skin of their teeth. *Current science.*, **97**(7): 10

CULLING, C. F. A., 1981. Hand Book of Histological and Histochemical Techniques. Edn, 3rd ., Butterworth's, London., *pp*. 422-438

CUSHWA, W. T., DODDS, K. G., CRAWFORD, A. M. and MEDRANO, J. M., 1996. Identification and genetic mapping of random amplified polymorphic DNA (RAPD) markers to the sheep genome. *Mamm. Genome*., **7**:580-585

DELLMAN, H. D. and BROWN, E. M., 1981. *Text Book of Veterinary Histology*. Lea and Febieger, Philodolphia., p382-388.

DELLMANN, H. D. and EURELL, J. A., 1998. Text Book of Veterinary Histology. Edn, 5th ., Williams and Wilkins, London., pp: 303-332.

DHARMARAJ, S., JAMALUDIN, A. S., RAZAK, H. M., VALLIAPPAN, R., AHMAD, N. A., HARN, G. L. and ISMAIL, Z., 2006. The classification of *Phyllanthus niruri* Linn. According to location by infrared spectroscopy, *Vibrational Spectroscopy.*, **41**(1): 68–72.

DIMOND, R. L. and MONTAGNA, W., 1975. The skin of the giraffe. *Anat. ttec*, **1(5)** 63-75.

DONG, Z., XUEDONG, L. I. U. and JIANZHANG, M. A., 2005. Patterns of genetic variation within a captive population of Amur tiger *Panthera tigris altaica*. *Acta Theriologica.*, **50** (1): 23-30

ECHT, C., ERDAHL, L. and MCCOY, T., 1992. Genetic segregation of random amplified polymorphic DNA in diploid cultivated alfalfa. *Genome.*, **35**: 84-87

ECKERT, K. A. and KUNKEL, T. A., 1990. High fidelity DNA synthesis by the *Thermus aquaticus* DNA polymerase. *Nucleic Acids Res*., **18**: 3739-3744.

EDWARD, G. and BATRICK., 2002**.** Applications of Vibrational Spectroscopy in Criminal Forensic Analysis *Handbook of Vibrational Spectroscopy* John M. Chalmers and Peter R. Griffiths (Editors) John Wiley & Sons Ltd, Chishester,

EDWARDS, H. G. M., HUNT, D. E., and SIBLEY, M. G., 1998, FT-Raman spectroscopic study of keratotic materials: horn, hoof and tortoiseshell, *Spectrochimica Acta Part A: Molecular and Biomolecular Spectroscopy*, **54 A**(5), 745–57.

EGAN, W. J., MORGAN, S. L., BATRICK, E. G., MERRILL R. A. and TAYLOR III, H. J., 2003. Forensic discrimination of photocopy and printer toners. II. Discriminant analysis applied to infrared reflection–absorption spectroscopy, *Analytical and Bioanalytical Chemistry*., **376**(8): 1276–85

ELLIOTT, A., 1953. *Proc. Roy. Soc.* A, **221**, 104.

ELLIOTT, A., 1956. *Proc. IIIrd Int. Congr. Biochem. p.* 106. New York: Academic Press.

ELLIOTT, A. and AMBROSE, E. J., 1950. *Nature.*, **165**: 291.

ELLSWORTH, D., RITTENHOUSE, K. and HONEYCUTT, R., 1993. Artifactual variation in randomly amplified polymorphic DNA banding patterns. *Bio Techniques*., **14** : 214-217. Cited by W.T. Cushwa and J.F. Medrano., 1996.

Applications of the Random Amplified Polymorphic DNA (RAPD) assay for genetic analysis of livestock species. *Anim. Biotechnol*., **7**: 11-31

ENLOW, E. M., KENNEDY, J. L., NIEUWLAND, A. A., HENDRIX, J. E. and MORGAN, S. L., 2005. Discrimination of nylon polymers using attenuated total reflection mid-infrared spectra and multivariate statistical techniques. *Applied Spectroscopy.*, **59**(8): 986–992

ESPINOZA, E., PRZYBYLA, J. and COX, R., 2006. Analysis of fiber blends using horizontal attenuate total reflection Fourier transform infrared and discriminant analysis, *Applied Spectroscopy*., **60**(4): 386–91

ESPINOZA, E. O., BAKER, B.W. and BERRY, C.A., 2007. The analysis of sea turtle and bovid keratin artefacts using DRIFT spectroscopy and discriminant analysis. *Archaeometry.,* **49:** 685–698

ESPINOZA, E. O., BAKER, B. W., MOORES, T. D. and VOIN, D., 2008. Forensic identification of Elephant and Girafffe Hair Artifacts Using HATR FTIR Spectroscopy and Discriminant Analysis. *Endanger. Species Res.,* **9**: 239-246

EVANS, G. H., (1910): Elephant and their disease. Government Printing. Rangoon.

EVANS, H. E. and CHRISTENSEN, G. C., 1967. Miller's Anatomy of the dog. *Edn, 2nd*., W.B.Saunders company philadolphia. London, Toronta, Mexico city., *pp.*78-97

FABIAN, H., 2000. 'Fourier Transform Infrared Spectroscopy in Peptide and Protein Analysis', in *Encyclopedia of Analytical Chemistry*, *Edn.2nd*. Vol. 7, Wiley, Chichester, UK, *pp*.5779–5803

FAJARDO, V., GONZAILEZ, I., ROJAS, M., GARCIA, T. and MARTIN, R., 2010. A review of current PCR-based methodologies for the authentication of meats from game animal species. *Trends in Food Science & Technology*., **21**:408-421

FORAN, D. R., KEVIN, R., CROOKS. and STEVEN, C. M., 1997. Species identification from scat: an unambiguous genetic method. *Wild animals society bulletin.*, **25**(4): 835-839

FRASER, R. D. B. and PARRY, D. A. D., 1996. The molecular structure of reptilian keratin. *Int J Biol Macromol.,* **19**: 207–211

FRAZIER, J., 2005. Marine turtles—the ultimate tool kit: a review of worked bones from marine turtles, in From hooves to horns, from mollusc to mammoth: manufacture and use of bone artefacts from prehistoric times to the present (eds. H. Luik, A. M. Choyke, C. E. Batey and L. Lõugas), 359–82, Proceedings of the 4th Meeting of the ICAZ Worked Bone Research Group at Tallinn, 26th–31st of August 2003, International Council for Archaeozoology, Tallinn Book Printers.

GALLAGHER, W. H., TAO, F. and WOODWARD, C., 1992. *Biochemistry.*, **31**: 4673-4680

GAYEN, S., PRASAD, G. and SINHA, R. D., 1989. Comparative histological studies on the skin of Indian buffalo and Black Bengal goats. *Indian J. Anim. Sci.,* **59**(8): 920-924

GAYKEE, D. E., LADUKAR, O. N., ZADE, B. A., MAINDE, U. P. and DALVI, R. S., 2008. Histoarchitecture of skin of wild pig *(Sus scrofa). Indian J. Field Vet.,* **3**(3): 30-31

Gu,W.K., ACLAND, G.M., AGUIRRE, G.D., and RAY, K., 1997. Evaluation of RAPD analysis for identification of polymorphisms in canine genomic DNA. *Anim. Biotechnol.*, **8**: 207-219.

GOSWAMI, S. K., DHINGRA, L. D. and NAGPAL, S. K., 1994. Histological and histochemical studies on sweat glands of camel. *J. Camel Pract. Res.,* **l**(2):63-68

GREG, L., 2004. The Transnational Illegal Wildlife Trade. *Criminal Justice Studies.*, **17**:57-73

GRIEBENOW, K., SANTOS, A. M. and CARRASQUILLO, K. G., 1992. Secondary structure of proteins in the amorphous dehydrated state probed by FTIR spectroscopy, The Internet of Vibrational Spectroscopy. *Edn.1st*. Vol. **3**. pp. 314-318

GUTIERREZ-ADA, A., CUSHWA, W.T., ANDERSON, G.B. and MEDRANO, J.F., 1997. Ovine-specific Y-chromosome RAPD-SCAR marker for embryo sexing. *Anim. Genet*., **28**: 135-138

HARINI. 2009. MVSc thesis. Submitted to Karnataka Veterinary, Animal and Fisheries Sciences University, Bidar, Karnataka. India.

HEDRICK, P., 1992. Shooting the RAPDs. *Nature.*, **355**: 679-680

HEMALATHA, R., 2012. Studies on Molecular Methods for Identification of Skin and other Tissues of wild animals. MVSc thesis. Submitted to Karnataka Veterinary, Animal and Fisheries Sciences University, Bidar, Karnataka. India

HILALUDDIN, R., KAUL, R. and GHOSE, D., 2005. Conservation implications of wild animal biomass extractions in Northeast India. *Anim. Biodivers.Conserv*., **28**: 169–179

HOLE, M. B., BHOSLE, N. S. and KAPADNIS, P. J., 2007a. Micrometrical study of sebaceous gland in skin of Red Kandhari cows. *Indian J. Anim. Res.,* **41**(2): 126-129

HOLE, M. B., BHOSLE, N. S. and KAPADNIS, P. J., 2007b. Connective tissue fiber arrangement of skin in Red Kandhari cows. *Indian J. Anim. Res., **41(2):*** 151-152

HOLE, M. B., BHOSLE, N. S. and KAPADNIS, P. J., 2008a. Histological study of skin epidermis in Red Kandhari cows. *Indian J. Anim. Res.,* **42**(1): 69-70

HOLE, M. B., BHOSLE, N. S. and KAPADNIS, P. J., 2008b. Study of hair follicles in Red Kandhari cows. *Indian J. of Anim. Res.,* **42(**2): 151-152

HOPKINS. J, BRENNER. L. and TUMOSA C. S., 1991. Variation of the amide I and amide II peak absorbance ratio in human hair as measured by Fourier transform infrared spectroscopy. *Forensic Sci. Int.*, **50**: 61–65

HORVAT, S. and MEDRANO, J. F., 1994. Targeting a specific genomic interval to identify RAPD markers linked to the high growth (*hg*) locus in mice. *Proc. 5th World Congress Genet. Appl. Livestock Prod*., **21**: 71-74

HUGES. and GOROSOPE., 1991. Biochemical identification of apoptosis in granulosa cells: evidence for a potential mechanism underlying follicular atresia. *Endocrinology*., **129**: 2415-2422

HUMPHREYS, J. and SMITH, M. L. R., 2011. Protecting endangered species. *Criminal Justice Matters*., **83**:6-7

HUNT, G.J. and PAGE, R.E., 1992. Patterns of inheritance with RAPD molecular markers reveal novel types of polymorphism in the honey bee, *Apis mellifera*, based on RAPD markers. *Genetics*, **139**: 1371-1382

ILHAK. and ARSLAN, A., 2003. Random Amplified Polymorpic DNA. *Sa lık Bil. Derg.*, **17**(1), 59–63

INNIS, M. A. and GELFAND, D. H., 1990. Optimization of PCRs. In: *PCR protocols : A Guide to Methods and Applications.* Academic Press, San Diego. pp. 1-2.

INNIS, M. A., MYAMBO, K. B., GELFAND, D. H. and BROW, M. A. D., 1988. DNA sequencing with *Thermus aquaticus* DNA polymerase chain reaction – amplified DNA. *Proc. Natl. Acad. Sci*., USA., **85**: 9436-9440.

IUCN Red List of Threatened Species [http://www.iucnredlist.org/]

JACKSON, M. and MANTSCH, H. H., 1993. *Spectrochim Acta*:15:53–69

JALKANEN, K. J., WU¨RTZ JU¨R GENSEN, V., CLAUSSEN, A., RAHIM, A., JENSEN, G. M., WADE, R. C., NARDI, F., JUNG, C., DEGTYARENKO, I. M., NIEMINEN, R. M., HERRMANN, F., KNAPP-MOHAMMADY, M., NIEHAUS, T. A., FRIMAND, K., JOY,M. and LEWIS, D. M., 1991. The uses of Fourier transform infrared spectroscopy in the study of the surface chemistry of hair fibers. *Int. J. Cosmetic Sci.,* **13**: 249–261

JAYASANKAR, P. and DHARMALINGAM, K., 1997. Potential application of RAPD and RAHM markers in genome analysis of scombroid fishes. *Current Science*, **72**: 383-390

JEAN, D., PATTERSON, B. D., BRIGGS, M. B., VENZKE, K., FLAMAND, J., STANDER, L., SCHEEPERS, L. and KAYS, R. W., 2005. Molecular genetic variation across the southern and eastern geographic ranges of the African lion, Panthera leo. *Conservation genetics.*, **6**: 15-24

JENKINSON, D. M. and NAY, T., 1972. The sweat glands and hair follicles of Europ cattle. *Aust. J. Boil. Sci.,* **25**: 585-595

KAPADNIS, P. J. and BHOSLE, N. S., 2004. Microscopic anatomy of the integument of Osmanabadi goat. *Indian Vet. J.*, **81**: 912-914

KAPADNIS, P. J., BHOSLE, N. S. and MAMADE, C. S., 2005. Study in connective tissue fibre in neck skin of goat. *Indian J. Anim. Res.*, **39**(1): 60-62

KIMSLEY, E. K., 1998. Discriminant Analysis and Class Modelling of Spectroscopic Data. John Wiley & Sons Chishester

KIRKBRIDE, K. P., TUNGOL, M. W., 1999. Infrared micro spectroscopy of fibers, In: Robertson J, Grieve M (Edn) Forensic examination of fibers, Edn, 2nd., Taylor & Francis Inc., Philadelphia, A., *pp* 179–222

KOH, M. C., LIM, C. H., CHUA, S. B., CHEW, S. T. and PHANG, S.T.W., 1998. Random amplified polymorphic DNA (RAPD) fingerprints for identification of red meat animals species. *Meat Science.*, **48**: 275-285

KOUL, G. L., SOMVANSHI, R. and BISWAS, J. C., 1990. *Follicle* characteristics of non-wooly Indian goats. *Res. Vet. Sci.,* **48**:257-259

KOURKOUMELIS, N. and TZAPHLIDOU, M., 2010. Spectroscopic Assessment of Normal Cortical Bone: Differences in Relation to Bone Site and Sex. *The Scientific World J*., **10**: 402-412

KOZLOWSKI, M. S. G. P. and CALHOUN, M. L., 1969. Microscopic anatomy of the integument of sheep. *Am. J. Vet. Res.,* **30**(8): 1269-1279

LAWYER, F. C., STOFFEL, S., SAIKI, R. K., MYAMBO, K., DRUMMOND, R. and GELFAND, D. H., 1989. Isolation, characterization and expression in *Escherichia coli* of the DNA polymerase gene from *Thermus aquaticus. J. Biol. Chem*., **264**: 6427-6437

LEE, J. C. and CHANG, J.G., 1994. Random amplified polymorphic DNA polymerase chain reaction (RAPD PCR) fingerprints in forensic species identification. *Forensic Sci. Int*., **67**(2):103-7

LEHNINGER, L., 1982. Principles of biochemistry. Worth Publishers.Inc., New York

LLOYD, D. H. and GARTHWAITE, G., 1982. Epidermal structure and surface topography of canine skin. *Res. Vet. Sci.,* **33**(1): 99-104

LLOYD, D. H., DICK, W. D. and JENKINSON, D. M., 1979. Structure of the epidermis in Ayrshire bullocks. *Res. Vet. Sci.,* **26**(2): 172-179

LUNA, L.G., 1968. Manual of Histological Staining Methods of the Armed forces Institute of Pathology. Edn, 3rd ., McGraw-Hill Book co. New York., *pp*.85-95

LYMAN, D. J., MURRAY-WIJELATH, J. and FEUGHLMAN, M., 2001. Effect of temperature on the conformation of extended α-keratin. *Appl Spectroscope***., 55**: 552–554

TAHTOUH, M., KALMAN, J. R., ROUX, C., LENNARD, C. I. and REEDY. B. J., 2005. *J. Forensic Sci*. **50**: 64

MALLON, D. P., 2008. "*Antilope cervicapra*". *IUCN Red List of Threatened Species.* Version 2012.2. International Union for Conservation of Nature.

MANDAGE, S. T., BHOSLE, N.S., KAPADNIS, P. J. and MAMADE, C.S., 2003. Microscopic anatomy of the integument of the Deccani sheep. *Indian J. Vet.Anat.,* **15**(1&2): 68-69

MANDAGE, S. T., BHOSLE, N.S., KAPADNIS, P. J. and MAMADE, C.S., 2006. Age related changes in connective tissue fibres in skin of Deccani sheep. *Indian J. Anim Res.,* **40**(1): 87-88

MARIAPPA, D., (1986). Anatomy and Histology of the Indian elephant. Indira Publishing House, Michigan, USA. pp. 185.

MARSHALL, R. C., ORWIN, D. F. G. and GILLESPIE, J. M., 1991. Structure and biochemistry of mammalian hard keratin. *Electron Microsc Rev*., **4**:47–83

MARTIN, A. L., IRIZARRY-ROVIRA, A. R., BEVIER, D. E., ILICKMAN, L. G., GLICKMAN, N. W. and HULLINGER, R. L., 2007. Histology of ferret skin: preweaning to adulthood. *Vet. Dermatol.,* **18**:401-411

MARTINEZ, I. and YMAN, I. M., 1998. Species identification in meat products by RAPD analysis. *Food Res. Int*. **31**(6/7): 459–466

MEHTA. S., 2002. Comparative morphological studies on the skin of Murrah buffalo and ox. *Indian J. Vet. Anat.,* **14**(1&2): 22-24

MENON. and VIVEK., 2009. Field Guide to Indian Mammals, Christopher Helm Publishers. ISBN 978-1408112137.

MEUNIER, J. R. and GRIMONT, P. A. D., 1993. Factors affecting reproducibility of random amplified polymorphic DNA fingerprinting. *Res. Microbiol*., **144**: 373-379.

MEYER, W., NEURAND, K., SCHWARZ, R., BARTELS, T. and ALTHOFF, H., 1994. Arrangement of elastic fibres in the integument of domesticated mammals. *Scanning Microsc*., **8**(2):375-90

MEYER, W., NEURAND, K. and RADKE, B., 1981. Elastic fibre arrangement in the skin of the pig. *Arch. Dermatol. Res.,* **270**(4): 391-401

MEYER, W., NEURAND, K. and RADKE, B., 1982. *Collagen* fibre arrangement in the skin of the pig. *J. Anat.,* **134**(1): 139-148

MICHEL, V., ILDEFONSE, P. and MORIN, G., 1995. Chemical and structural changes in Cervus elaphus tooth enamels during fossilization (Lazaret cave): a combined IR and XRD *Rietveld analysis. Appl Geochem.,* **10**:145–159

MICHELI, M. R., BOVA, R., PASCALE, E. and D'AMBROSIO, E., 1994. Reproducible DNA fingerprinting with the random amplified polymorphic DNA (RAPD) method. *Nucleic Acids Res.*, **22**: 1921-1922

MILES, A. E. W. and GRIGSON. C., 1990: Colyer's variations and diseases of the teeth of animals, revised edition. Cambridge University Press, Cambridge

MILLER, F. A. and WILKINS, C. H., 1952. Infrared Spectra and Characteristic Frequencies of Inorganic Ions Their Use in Qualitative Analysis. *Anal.Chemistry*., **24**:1253 –1294

MONTE, M. A., COSTA, B. L., GROTTA, R. G., BRAGAGNOLI, M., JACINTO, G. and MEDEIROS, M., 2005. Histological evaluation of goafs hair at different ages. *Brazilian J. Vet. Res.Anim.Sci.,* **42**(1): 12-18

MONTGOMERY, G. W. and SISE, J. A., 1990. Extraction of DNA from sheep white blood cells. *New Zealand J. Agri. Res*., **33**: 437-441

MORE, S. N., KARLE, A. S., LADUKAR, N., SHANKHAPAL, V. D. and LENDE, S., 2007. Microarchitecture of skin of spotted deer *{Axis axis). Indian J. Field Vet.,* **2**(3): 33-35

MOVASAGHI, Z., REHMAN, S., REHMAN, I., 2008. Fourier Transform Infrared (FTIR) Spectroscopy of Bilogical Tissues. *Appl.Spectroscopy Rev.*, **43**: 134-179

MOWAFY, M. and CASSENS, R. G., 1975. Microscopic structure of pig skin. *J. Anim.* Sri., **41**(5): 1281-1290

MUGALE, R. R. and BHOSLE, N. S., 2001a. Melanin pigmentation in the skin of Deoni cattle. *Indian Vet. J.*, **78**: 234-236

MUGALE, R. R. and BHOSLE, N. S., 2001b. Microscopic structure of the sebaceous glands in the skin of Deoni cattle. *Indian Vet. J.*, **78**: 624-626

MUGALE, R. R. and BHOSLE, N. S., 2002. Thickness of epidermis in Deoni cattle. *Indian Vet. J.*, **79**: 368-370

MUNMUN, S., SARMA, K. K., KALITA, S. N. AND CHAKRABORTHY, A., (2009). Revelation on sweat glands in Asian elephants. GAJAMUKTA. National symposium on elephant health care and managerial practices. Guwahati. pp. 189-193

MYHRVOLD, C. L., STONE, H. A. and BOU-ZEID, E., 2012. What Is the Use of Elephant Hair? PLoS ONE 7(10): e47018. doi:10.1371/journal.pone.0047018.

NAGARAJA, C. S., 1998. Studies on breed specific molecular genetic markers in B.*taurus* and B.*indicus* cattle. M.V.Sc. Thesis, submitted to University of Agricultural Sciences, Bangalore, India

NAGARAJU, G. N., 2012. Ph D Thesis.Morphological studies and FTIR analysis of skin and its appandages of wild animals, Submitted to Karnataka Veterinary, Animal and Fisheries Sciences University.Bidar

NAGARAJU, G. N., PRASAD, R. V, JAMUNA, K. V. and RAMKRISHNA, V., 2012. Histological features in the differentiation of skin of spotted deer (*Axis axis*), cattle (*Bos indicus*) and goat (*Capra hircus*). *Ind.J. Vet.Anatomy*., **24** (1): 10-12

NATIONAL RESEARCH COUNCIL. 1983. Little known Asian animals with a Promising Economic Future. Washington, D.C: National Academy Press

NICKEL, R., SCHUMMER, A. and SEIFERLE, E., 1981. The Anatomy of the Domestic Animals. **3**: 487-505

NIKUNJ, G. and NISHITH, D., 2011. Status, Occurrence, Distribution of Some Mammals of North Gujarath, India. *Proce Zool Soc.* **64**(1): 46-53

NOWAK, R. M., 1999. Blackbuck. *Walker's Mammals of the World.* The Johns Hopkins University Press, Baltimore, USA and London, UK. 1:1193–1194

PANAYIOUTOU, H., 2004. Vibrational Spectroscopy of Keratin Fibbers, A Forensic Approach. Ph D thesis submitted to the School of Physical and Chemical Sciences, Queensland University of Technology

PARIS, C., LECOMTE, S. and COUPRY, C., 2005. ATR–FTIR spectroscopy as a way to identify natural protein-based materials, tortoiseshell and horn, from their protein-based imitation, galalith, *Spectrochimica Acta Part A: Molecular and Biomolecular Spectroscopy.*, **62**(1–3): 532–38

PARTIS, L., CROAN, D., GUO, Z., CLARK, R., COLDHAM, T. and MURBY, J., 2000. Evaluation of a DNA fingerprinting method for determining the species origin of meats. *Meat Sci.*, **54**: 369–376

PFEIFFIER, C. J., OSMAN, A. H. K. and PFEIFFIER, D. C., 2006. Ultrastructural analysis of the integument of a desert-adapted mammal, the one humped camel *(Camelus dromedaries). Anat. Histol. Embryol.*, **35:** 97-103

PIELESZ, A. and WESEŁUCHA-BIRCZYNSKA., 2000. The identification of structural changes in the keratin of wool fiber dyed with an azo dye using the Raman and Fourier transform infrared spectroscopy methods. *Journal of Molecular Structure.*, **555:** 325–334

QIU-HONG, W. and SHENG-GUO, F., 2003. Application of species specific polymerase chain reaction in the forensic identification of tiger species. *Forensic International.,* **31**: 75-78

RAHEEM, M. H. A. and Al-HETY, M. S., 1997. Histological and morphometrical study of the skin of black goat. *Iraqi J. Vet. Sci.,* **10**(2): 59-71

RAO, K. B., BHAT, K.V. and TOTEY, S. M., 1996. Detection of species-specific genetic markers in farm animals through random amplified polymorphic DNA(RAPD). *Genet.Anal*., **13**:135-138

RENATA, Ž., VAIDA, J., RIMVYDAS, M., SIGITAS, S. and REGINA, U., 2006. Analysis and Identification of Fiber Constitution of Archaeological Textiles**.** *ISSN 1392–1320 materials science (medžiagotyra).,* **12:**3

RIEDY, M. F., HAMILTON, W.J. and AQUODRO, C. F., 1992. Excess of non-parental bands in offspring from known primate pedigrees assayed using RAPD PCR. *Nucleic Acids Res*., **20**: 918

RINTOUL, L., PANAYIOTOU, H., KOKOT, S., GEORGE. G. and OTHERS, 1998. Fourier transforms infrared spectrometry: a versatile technique for real world samples. *Analyst (Lond).,* **123**: 571–577

ROSSETTO, M., WEAVER, P. K. and DIXON, K. W., 1995. Use of RAPD analysis in devising conservation strategies for the rare and endangered *Grevillea scapigera*. *Mol. Ecol.,* **4**(3):321-9

ROTHUIZEN, J. and VAN WOLFEREN, M., 1994. Randomly amplified DNA polymorphisms in dogs are reproducible and display Mendelian transmission. *Anim. Genet*., **25** : 13-18.

SAIKI, R. K., GELFAND, D. H., STOFFEL, S., SCHARF, S. J., HIGUCHI, R., HORN, G. T., MULLIS, K. B. and ERLICH, H. A., 1988. Primer-directed amplification of DNA with a thermostable DNA polymerase. *Science.*, **239**: 487-491

SAMBROOK, J., FRITSCH, E. F. and MANIATIS, T., 1989. Molecular Cloning: A Laboratory Manual. Edn, 2nd., Cold Spring Harbor Laboratory Press.

SANKAR, K. PABLA, H. S., PATIL C. K., NIGAM P., QURESHI, Q., NAVANEETHAN, B., MANJREKAR, M., VIRKAR, P. S. and MONDAL, K., 2013. Home range, habitat use and food habits of re-introduced gaur (Bos gaurus gaurus) in Bandhavgarh Tiger Reserve, Central India. *Tropical Conservation Science.*, **6**(1):50-69

SAR, M. and CALHOUN, M. L., 1966. Microscopic anatomy of the integument of the common American goat. *Am. J. Vet. Res.*, **27**(117):*444-456*

SATHEESHA, G. M., 2006. DNA Fingerprinting Method for Identification of Wild Cats. MVSc thesis. Submitted to Karnataka Veterinary, Animal and Fisheries Sciences University, Bidar, Karnataka. India

SAXENA, S. K., MALIK, M.R. and PAREKH, H. K. B., 1994a. Histological character of skin in crossbred cattle. *Indian J. Vet. Anat.*, **6**(1): 8-11

SCHIERWATER, B. and ENDER, A., 1993. Different thermostable DNA polymerases may amplify different RAPD products. *Nucleic Acids Res*., **21**: 4647

SCOTT, M. P., HAYMES, K. M. and WILLIAMS, S. C., 1992. Parentage analysis using RAPD PCR. *Nucleic Acids Res*., **20**: 593

SHAMBHULINGAPPA, Y. B., PRASAD, R. V., JAMUNA, K. V. and RAMKRISHNA, V., 2013. Histomorphology of hair follicle pattern in wild big cats and sloth bear skin: a tool for forensic identification. *J. Cell and Tissue Research.*, **13**(2): 3679-3682

SHANKARANARAYANAN, P and LALJI SINGH., 1998. A rapid and simplified procedure for isolating DNA from scat samples. *Current science.*, **75**(9): 321

SHANKARANARAYANAN, P., BANERJEE, M., KACKER, R. K., AGGARWAL, R. K. and SINGH, L., 1997. Genetic variation in Asiatic lions and Indian tigers. *Electrophoresis.*, **18**(9):1693-700

SHARMA, D. N., BHARADWAJ, R. L. and RE NANA, A., 1996. Histoarchitecture of skin of yak *(Bos grwmiens). Indian J. Vet. Anat.*, **8**(1/2): 7-10

SHARMA. D. N. and BHARADWAJ. R. L., 1993. Regional *variations in* the thickness of the skin of adult yak. *Indian Vet J.*, **70**:437-438

SHENGQING, ZU ENDONG and LIU LIJUN., 2011. Identification of Rhinoceros Horn and its Substitutes. *Advanced Materials Research. Trans Tech Publications, Switzerland.* Vol.1st. ***177.*** *pp 636-63*

SHI-YING, L., DONG-H, Z., YI-WEN, L., QI-RAN, S., KAI-FEI, D., YI-JIU, C. and PING, H., 2014. Characteristics of electrically injured skin from human hand tissue samples using Fourier transform infrared microspectroscopy. *Science and Justice.*, **54**: 98–104

SHOSHANI, J., ALDER, R., ANDREWS, K., BACCALA, M. J., BARVISH, A., BARRY, S., BATTIALA, R., BEDORE, M. P., (1982). On the dissection of female asian elephant (Elephas maximus maximus Linnaeus, 1758) and data from other elephants. Elephant 2(1): 3-93.

SILA, T. and IAN, G., 2007. Studies on elephant tusks and hippopotamus teeth collected from the early 17th century Portuguese shipwreck off Goa, west coast of India: Evidence of maritime trade between Goa, Portugal and African countries. *Current science.*, **92**(3): 333-339

SINGH, L. P., Prasad, J. and Yadava, C. J. P., 1975. Microscopic studies on the epidermis of paralumbar skin of the Indian buffalo calf. *Indian J. Anim. Hlth.*, **14**:117-119

SINGH, U. B. and SULOCHANA, S., 1996. Hand Book of Histological and Histochemical Techniques. Edn. 2nd ., Premier Publishing House, Hyderabad., *pp*.39-41

SINGH, S. K., SHWET, K., MUGDHA, T., YADAV, M. C. and UPADHYAY**,** R. C., 2004. Arbitrary primer based RAPD – a useful genetic marker for species identification in Morels**.** *J. Plant Biochemistry and Biotechnology.,* **13:** 07-12

SMITH, E. J., JONES, C.P., BARLETT, J. and NESTOR, K. E., 1996. Use of Randomly amplified polymorphic DNA markers for the genetic analysis of relatedness and diversity in chickens and turkeys. *Poultry Sci*., **75**: 579-584

SMITH, F., (1890). The histology of the skin of the elephant. *J. Anat and Phy.* 24: 493-503

SOLOMON, S. E., HENDRICKSON, J. R., and HENDRICKSON, L. P., 1986. The structure of the carapace and plastron of juvenile turtles, *Chelonian mydas* (the green turtle) and *Caretta caretta* (the loggerhead turtle), *Journal of Anatomy.*, **145**: 123–31

STRICKLAND, M. S. J. H. and CALHOUN, M. L., 1963. The integumentary system of the cat. *Am. J. Vet.Res., **24:*** 1018-1029

STUART, B., 2004. Infrared Spectroscopy – Fundamentals and Applications. John Wiley & Sons, Ltd

SUKUMAR, R. 2003. The Living Elephants. New York, NY: Oxford University Press.

SUMENA, K.B., LUCY, K.M., CHUNGATH, J.J., ASHOK, N. and HARSHAN, K.R., 2010. Regional histology of the subcutaneous tissue and the sweat glands of large white Yorkshire pigs. *Tamilnadu Journal of Veterinary and Animal Sciences*, 6(3): 128-135.

SYSTAT SOFTWARE, INC., 2007. Chicago IL USA

TALUKDAR, A. H., CALHOUN, M. L. and SIINSON, A. W., 1972. Microscopic Anatomy of the skin of the horse. *Am. J. Vet .Res.*, **33**(12): 2365-2390

THERMO FISHER SCIENTIFIC INC., 2009. Madison, WI, USA

TIMMINS, E. M., HOWELL, S. A., ALSBERG, B. K., NOBLE, W.C. and GOODACRE, R., 1998. Rapid differentiation of closely related *Candida* species and strains by pyrolysis-mass spectrometry and Fourier transform-infrared spectroscopy. *J Clin Microbiol.,* **36**: 367–374

TRAUTMANN and FIBIGER. J., 1957. Fundamentals of the Histology of Domestic Animals. 8th and 9th Edn. Comstock Publishing Associates, A Division of Cornell University Press, Ithaca, New York, *pp.* 334-355

TRAVEL INDIA GUIDE. Binoygupta.com. 2012. Retrieved on 2013-05-16

VELHO, N., KARANTH, K. and LAURANCE, W. F., 2012. Hunting: a serious and understudied threat in India, a globally significant conservation region. *Biol. Conserv.*, **148**: 210–215

VIDYA, T.N., FERNANDO, P., MELNICK, D. J. and SUKUMAR, R., 2005. Population differentiation within and among Asian elephant (Elephas maximus) populations in southern India. 2011. *Heredity. 94*(1): 71-80.

WANG, W. and PALIWAL, J., 2007. Near-infrared spectroscopy and imaging in food quality and safety. *Sens and Instrumen. Food Qual.,* **1**: 193-207

WARDELL, B., SUDWEEKS, J., MEEKER, N., ESTES, S., WOODWARD, S. and TEUSCHER, C.,1993. The identification of Y chromosome-linked markers with random sequence oligonucleotide primers. *Mammalian Genome.,* **4**: 109-112

WAUGH, R. and POWELL, W., 1992. Using RAPD markers for crop improvement. *TIBTECH.*, **10** : 186-191

WELSH, J. and MCCLELLAND, M., 1990. Fingerprinting genomes using PCR with arbitrary primers. *Nucleic Acids Res.*, **18**: 7213-7218

WIDJAJA, E. and SEAH, R. K. H., 2006. Use of Raman spectroscopy and multivariate classification techniques for the differentiation of fingernails and toenails. *Applied Spectroscopy.,* **60** (3): 343–345

WILLIAMS, J. G. K., HANAFEY, M. K., RAFALSKI, J. A. and TINGEY, S. V., 1993. Genetic analysis using random amplified polymorphic DNA markers. *Methods Enzymol*., **218**: 704-740

WILLIAMS, J. G. K., KUBELIK, A., LIVAK, K., RAFALSKI, J. A. and TINGEY, S.V., 1990. DNA polymorphisms amplified by arbitrary primers are useful as genetic markers. *Nucleic Acids Res*., **18**: 6531-6535

WU, L., PATTEN., NANCY, B. S., YAMASHIRO, C. T. and CHUI, B. B. S., 2002. Extraction and Amplification of DNA From Formalin-Fixed, Paraffin-Embedded Tissues. *Applied Immunohistochemistry & Molecular Morphology*. **10** (3): 269-274

YAGCI, A., ZIK, B., UGUZ, C. and ALTUNBAS, K., 2006. Histology and morphometry of White New Zealand rabbit skin. *Indian Vet. J.,* **83**: 876-880

YU, L., JUN-YING, C., HAI-TAO, S., CHANG-E, L., YONG, W., RONG, N., JUN, W. and HONG, W., 2010. Light Microscopic, Electron Microscopic, and Immunohistochemical Comparison of Bama Minipig (Sus scrofa domestica) and Human Skin. *Comp Med*., **60**(2): 142–148

YU, K. and PAULS, K. P., 1992. Optimization of the PCR program for RAPD analysis. *Nucleic Acids Res*., **20**: 2606

ZADE, B. A., LADUKAR, O. N., MAINDE, U. P., GAYKEE, D. E. and GABHANE, H. S., 2007. Micro architectural comparison of skin in goat and sheep. *Indian J. Field Vet.*, **3**(1): 35-36.

Abstract

VIII. ABSTRACT

The present study was undertaken with an objective to study the morphology, FT-IR Spectral analysis and DNA Analysis of animal specimens such as skin, hair, hoof and tusk. These methods were standardized for their species identifications. The present study is taken up for histological studies on the original skin of wild herbivores such as *Bos gaurus* (Indian bison or gaur), *Antilope cervicapra* (Black buck), *Boselaphus tragocamelus* (Nilgai), *Elephas maximus* (Asian elephant), *Loxodonta africana* (African elephant), *Sus scrofa afinis* (Wild boar) and *Acinonyx jubatus* (Cheetah). FTIR spectroscopy study on hairs of these animals along with *Rusa unicolor* (Sambar), *Canis lupus pallipes* (Indian gray wolf) and *Melursus ursinus* (Sloth bear), hooves of Indian bison, Black buck and Nilgai and tusk of African elephant. Further, DNA analysis (RAPD-PCR) of Indian bison, Black buck, Nilgai, Wild boar, Sloth bear, Cheetah and *Bos primigenius* (Cattle) was used for comparison.

In all animals the epidermis was stratified squamous keratinized epithelium with some variations in the thickness of the layers. The epidermis comprised of stratum corneum, stratum granulosum with keratohyaline granules, stratum spinosum and stratum basale presented melanin pigments. The smaller epidermal pegs observed mainly in Indian bison, Asian elephants but larger one found only in African elephants with different shapes when observed in horizontal section of skin. The sebaceous and sweat glands were observed in case of wild herbivores such as Indian bison, black buck and Nilgai skin, whereas there were neither sebaceous nor sweat glands observed in the skin of Asian and African elephants. The cheetah skin was always having only sweat glands in the compound hair follicles. The hair follicle pattern in horizontal section of skin of

Indian bison showed rectangular shaped compound hair follicles with primary hair follicle associated with 3-4 secondary hair follicles together with their sebaceous glands, in case of black buck, Within the compound hair follicle there was linear arrangement of primary and secondary follicle observed, in Nilgai skin, Compound hair follicles with primary hair follicles and bilaterally surrounded 2-3 secondary hair follicles. In case of wild boar compound hair follicle with linearly arranged three primary hair follicle and larger in size at the center, whereas, in asian and African elephant skin sparsely distributed single isolated hair follicles were observed. The cheetah skin presented compound hair follicle consisted of a primary hair follicle with 3-7 secondary hair follicles on either side of it with sweat glands. FTIR spectra were analyzed using OMNIC, TQ Analyst and Systat and results were obtained.

The FTIR analysis of hairs showed Amide A band between 3271cm^{-1} to 3274 cm^{-1}, Amide B band peak was observed between 3068cm^{-1} to 3090 cm^{-1}. The Amide B band peak was not found in Asian elephant. The most intense peak in entire region of spectra of hair was Amide I band peak and was observed between 1626 cm^{-1} to 1637 cm^{-1}. The Amide II band with peak between 1515 cm^{-1} to 1540 cm^{-1}, the medium Amide III band peak between 1235 cm^{-1} to 1239 cm^{-1} and weak Amide III band peak between 1303 cm^{-1} to 1319 cm^{-1}. The FTIR analysis of hooves showed Amide A band between 3273cm^{-1} to 3274 cm^{-1} Amide B band peak was observed at 3069 cm^{-1} in all animals studied. The Amide I band peak was observed between 1632 cm^{-1} to 1633 cm^{-1} and Amide II band with peak between 1515 cm^{-1} to 1516 cm^{-1}. The medium Amide III band peak between 1238 cm^{-1} to 1239 cm^{-1} and weak Amide III band peak between 1309 cm^{-1} to 1310 cm^{-1}. The FTIR analysis of African elephant tusk showed Amide A, Amide B, Amide I, Amide

II bands at 3274 cm^{-1}, 3087 cm^{-1}, 1633 cm^{-1} and 1541 cm^{-1} respectively. The medium amide III band at 1242 cm^{-1}, weak amide III at 1419 observed in African elephant tusk.

Discriminant analysis is a multivariate statistical method that assists in the classification of data into distinct groups. The canonical score plot of all wild animal hairs, hooves and tusk shows segregation of individual class members into distinct 3 clusters without any overlapping of class members. The observation was further confirmed by CVA classification matrix with 100% correct class distribution of all individual class members. Further, CVA test statistic assigns score range was between 0-1 for Wilks's Lambda. RAPD analysis with random primers U3, D1, OPG 17 & RAn5 amplified polymorphic fragments on DNA isolated from skin samples of wild animals. These four primers generated a total of 12 scorable bands in sloth bear, OPG 17, RAn5, and D1 primers generated 19 scorable bands in bison and 11 scorable bands in black buck and 14 scorable bands in cattle, OPG 17, D1 and U3 primers generated 12 scorable bands in black buck and OPG 17 alone generated 3 scorable bands in cheetah. All scorable bands mentioned above were ranging in size from approximately 110 to 1400 base pairs (bp). All the four random primers yielded amplified fragments that were consistently polymorphic and specific between the species.

Appendices

IX. APPENDICES

APPENDIX I

Equipment

Centrifuge	Mini spin , eppendorf, UK
Microcentrifuge	Beckman
Micropipettes	Amersham
pH meter	Global, India
Spectrophotometer	Thermo Scientific, Japan
Submarine Electrophoresis unit	Bangalore Genei
Thermal cycler (for RAPD)	AB, Applied biosystem, USA
Thin walled reaction tubes (0.5ml) for PCR	Axygen
UV Transilluminator	Fotodyne Inc, USA
Water bath	Precision, USA
Weighing balance	Sartorius, Switzerland

APPENDIX II

Sources of important chemicals and enzymes used in this study

A. Chemicals

Agarose (ultrapure)	Bangalore Genei Pvt Ltd
Ammonium chloride	Merck
Bromophenol blue	Sigma chemicals Co, USA
dNTPs	Bangalore Genei Pvt Ltd
EDTA	Qualigens Fine Chemicals, Bombay
Ethanol	Hayman Ltd, England
Ethidium bromide	Sigma Chemical Co, USA
Potassium chloride	Merck
Primers for RAPD	Eurofins, Bioserve, bangalore
Sodium chloride	Merck
Sodium dodecyl sulphate (SDS)	BDH
Sucrose	Sigma Cemical Co, USA
Tris (hydroxyl methyl amino methane)	SRL, Bombay
Xylene cyanol	Sigma chemicals Co, USA

B. Enzymes

Proteinase-K	SRL, Bangalore

C. Molecular size markers

100 base pair DNA ladder Bangalore Genei Pvt Ltd

APPENDIX III

COMPOSITION OF REAGENTS AND BUFFERS USED IN THIS STUDY

EDTA (0.5 M, pH 8.0)

Dissolve 18.61 g of EDTA (disodium, dihydrate) in 80 ml of distilled water. Adjust the pH to 8.0 with NaOH and make up the volume to 100 ml. Filter, autoclave and store at room temperature.

Ethidium bromide (10 mg/ml)

Dissolve 100 mg of ethidium bromide in 10 ml of distilled water. Then store in a dark bottle at 4°C.

Gel loading buffer (6x)

Bromophenol blue	0.25 per cent	50 mg
Xylene cyanol	0.25 per cent	50 mg
Sucrose	40 per cent	8 g

Stir well in 20 ml distilled water and store at 4°C

RBC lysis buffer

Ammonium chloride	150 mM	8.0235 g
Potassium chloride	10 mM	0.7455 g
EDTA	0.1 mM	0.0372 g

Add distilled water up to 1000 ml, stir, filter, autoclave and store at 4°C.

Saturated sodium chloride solution (6 M)

For 100 ml, dissolve 35.06 g of sodium chloride in 80 ml of distilled water, make up the volume to 100 ml, filter and store at room temperature.

Sodium dodecyl sulphate (SDS) 20 per cent

SDS	20 g
Distilled water to make up to	100 ml

Stir on a magnetic stirrer, filter and store at room temperature.

Tris-Borate-EDTA (TBE) buffer (pH 8.3) 10X

Tris base	108.0 g
Boric acid	55.0 g
EDTA	9.3 g

Dissolve in 700 ml of distilled water. Adjust the pH to 8.3. Make up the volume to 1000 ml, autoclave and store at room temperature.

Tris buffered saline (pH 7.4)

Sodium chloride	140 mN	8.18 g
Potassium chloride	0.5 mM	0.0373 g
Tris base	0.25 mM	0.0303 g

Dissolve in 900 ml distilled water and adjust the pH to 7.4. Make up the volume to 1000 ml. Filter, autoclave and store at room temperature.

Tissue lysing buffer

a. 50 mM Tris (pH 8.0)

b. 10 mM EDTA (pH 8.0)

c. 0.5 per cent Triton x 100

Tris-EDTA (TE) buffer, pH 8.0

Tris base	10 mM	1.2114 g
EDTA	0.1 mM	0.3722 g

Dissolve in 900 ml distilled water and adjust the pH to 8.0. Make up the volume to 1000 ml. Filter and autoclave in batches of 100 ml and store at 4°C.

GOVERNMENT OF KARNATAKA

Principal Chief Conservator of
Forests (Wildlife) and Chief
Wildlife Warden,
Karnataka

(Off : 080-23345846
Fax: 080-23346389
E-mail: pccfwl@gmail.com
Aranya Bhavan, II Floor,
18th Cross, Malleswaram,
Bangalore – 560 003

No. C1/WL/CR-147/2012-13

Date: 12-09-2012

To
The Chief Conservator of Forests &
Executive Director,
Bannerghatta Biological Park,
Bangalore.

The Addl. Principal Chief Conservator of Forests &
Member Secretary,
Shri Jayachamarajendra Zoological Gardens,
Mysore.

The Deputy Conservator of Forests,
Wildlife Division,
Shimoga.

Sub: Permission to collect biopsy samples and specimens of dead wild animal and birds samples during post mortem (PM)- reg.

Ref: Letter No. anat/PCCF/2012-13 dated : 16-07-2012 Dr. R.V.Prasad, Professor and Head, Department of Anatomy and Histology, Veterinary College, Hebbal, Bangalore.

* * *

With reference to the above subject, permission is granted to Dr. Shambhulingappa.Y.Baddi, (I.D.No. DVHK 1122), who is pursuing his PhD studies in the Department of Anatomy and Histology, Veterinary College, Hebbal, Bangalore to collect specimens of dead animals during post mortem from captive wild animals from the following places for a period of one year from the date of this letter as per the provisions of the Wildlife (Protection) Act, 1972, subject to the general terms and conditions appended to this letter :

1) Bannerghatta Biological Park, Bengaluru
2) Shri Jayachamarajendra Zoological Gardens, Mysore
3) Tiger and Lion Safari-Tyavarekoppa, Shimoga
4) Children's Park cum Mini Zoo, Binkadakatti, Gadag
5) Children's Park and Mini Zoo, Bellary
6) Pilikola Biological Park, Mangalore
7) Kittur Rani Chennamma Nisargadhama, Belgaum

Principal Chief Conservator of Forests
(Wildlife) & Chief Wildlife Warden,
Bangalore.

Copy to Dr. R.V.Prasad, Professor and Head, Department of Anatomy and Histology, Veterinary College, Hebbal, Bangalore for information and necessary action.